

# Probabilistic methods in exotic option pricing

## PROEFSCHRIFT

ter verkrijging van de graad van doctor  
aan de Technische Universiteit Delft,  
op gezag van de Rector Magnificus prof.dr.ir. J.T. Fokkema,  
voorzitter van het College voor Promoties, in het openbaar te verdedigen  
op maandag 21 mei 2007 om 15:00 uur

door

Jasper Hubert Maria ANDERLUH  
elektrotechnisch ingenieur

geboren te Heerlen

Dit proefschrift is goedgekeurd door de promotor:  
Prof.dr. F.M. Dekking

Samenstelling promotiecommissie:

Rector Magnificus,	voorzitter
Prof.dr. F.M. Dekking,	Technische Universiteit Delft, promotor
Prof.dr. A. Bagchi,	Universiteit Twente
Prof.dr. M. De Ceuster,	Universiteit Antwerpen
Prof.dr. M. Jeanblanc,	Université d'Evry Val d'Essonne
Prof.dr.ir. G. Jongbloed,	Technische Universiteit Delft
Prof.dr.ir. J.G.M. Schoenmakers,	Weierstrass Institute Berlin
Dr. J.A.M. van der Weide,	Technische Universiteit Delft

Dr. J.A.M. van der Weide heeft als begeleider in belangrijke mate aan de totstandkoming van het proefschrift bijgedragen.

Het Stieltjes Instituut heeft bijgedragen in de drukkosten van het proefschrift.

THOMAS STIELTJES INSTITUTE  
FOR MATHEMATICS



Probabilistic methods in exotic option pricing.  
Dissertation at Delft University of Technology.  
Copyright © 2007 by J.H.M. Anderluh

ISBN 978-90-8891-002-9





# Preface

This Ph.D. thesis was written during the period 2002-2007, in which I was a part time Ph.D. student at Delft University of Technology and a part time quantitative analyst at BinckBank (formerly known as AOT). During this period a lot of people contributed in a direct or indirect way to the realization of this thesis. I would like to use this preface to express my thanks to these people.

I would like to thank Hans van der Weide. He has played several roles. First, he introduced me to the field of financial mathematics, as I was a participant of the first course he gave on this subject. Secondly, he got me very enthusiastic for mathematics and probability. I still remember that we spend a significant amount of time of the period that I was writing my master thesis with studying the little book of Williams. Finally, Hans was my supervisor during my Ph.D. period and I have been working with him with a lot of pleasure. Hopefully in the future we will continue working together.

I wish to thank my wife Ellen (she used to be my girlfriend when I started as a Ph.D. student). She recommended me to become a Ph.D. student when I was still hesitating. Later on she encouraged me to take the time I needed for completing the thesis and to get not distracted by job-offers from the banking world. She also listens with interest when I try to explain to her the mathematical problem I am working on, which is maybe not always easy for someone who is specialized in taxation law.

I enjoyed working at Delft University as a Ph.D. student. I would like to thank Michel Dekking for starting the adventure of a part time Ph.D. student on the field of financial mathematics, which was new for the probability group. The people in the probability and statistics department turn out to be very nice colleagues with whom you can discuss mathematics and politics, play tennis and drink coffee.

I also would like to express my thanks to the people at AOT/Binck. The environment of a small trading firm that became a bank turns out to be a rather dynamic one. During the five years I have worked there, the firm was reorganized twice, I have worked for 8 bosses in four different departments and my desk has moved four times. So, it was never boring and it gave me the ability to put academic research into a practical perspective.

Finally I would like to thank my parents, friends and family who all have been showing a lot of interest into the progress of my research and did not bother to listen to the stories I have been telling about it.

Jasper Anderluh  
Delft, April 2007



# Contents

<b>Introduction</b>	<b>1</b>
Outline of the thesis . . . . .	2
Publication details . . . . .	5
<b>1 Preliminaries</b>	<b>7</b>
1.1 Introduction . . . . .	7
1.2 The Parisian Option . . . . .	8
1.2.1 Contracts, pay-offs and path-dependency . . . . .	8
1.2.2 The Parisian pay-off . . . . .	9
1.2.3 Applications of Parisian optionality . . . . .	11
1.3 Key ideas of derivative pricing . . . . .	13
1.3.1 Trading, the bank-account and the market . . . . .	13
1.3.2 No arbitrage assumption . . . . .	15
1.3.3 Pricing and replicating strategies . . . . .	18
1.3.4 The Black-Scholes formula . . . . .	19
1.3.5 Incomplete markets . . . . .	22
1.4 Numerical inversion . . . . .	24
1.4.1 The Fourier and Laplace transform . . . . .	24
1.4.2 Euler summation . . . . .	26
1.4.3 Gaussian quadrature . . . . .	27
<b>2 The implied barrier concept</b>	<b>31</b>
2.1 The Parisian contract . . . . .	31
2.2 Valuation methods for Parisians . . . . .	32
2.3 The implied barrier . . . . .	33
2.4 Approximating the implied barrier . . . . .	34
2.5 Valuing Parisians that are already in the excursion . . . . .	35
2.6 Numerical examples . . . . .	36
2.7 Conclusion . . . . .	38
<b>3 Double-sided Parisian options</b>	<b>39</b>
3.1 Introduction . . . . .	39
3.2 The Parisian contract . . . . .	41

3.3	The Laplace transform of the double-sided hitting times . . .	43
3.4	Calculating the Fourier transform . . . . .	48
3.5	Already in the excursion . . . . .	51
3.6	The Parisian put . . . . .	54
3.7	Other types of Parisian contracts . . . . .	54
3.8	Fourier inversion algorithm . . . . .	56
	3.8.1 General Fourier inversion . . . . .	56
	3.8.2 Remarks on the truncation bound . . . . .	57
3.9	Numerical examples . . . . .	59
	3.9.1 Double-sided Parisian prices . . . . .	59
	3.9.2 Delta . . . . .	60
	3.9.3 Various contract types . . . . .	61
	3.9.4 Theta in the tails . . . . .	62
3.10	Conclusion . . . . .	63
3.11	Appendix . . . . .	65
	3.11.1 Calculation of $\phi_+$ for $k > l_2$ and $\phi_-$ for $k < l_1$ . . . . .	65
	3.11.2 The Laplace Transform of $T_l$ occurring before $d$ . . . . .	66
	3.11.3 UI property of $e^{-\frac{1}{2}\lambda^2(t\wedge\tau)+\lambda W_{t\wedge\tau}}$ . . . . .	67
	3.11.4 Discretization error . . . . .	69
	3.11.5 Truncation error . . . . .	70
<b>4</b>	<b>Pricing Parisians and barriers by hitting time simulation</b>	<b>71</b>
4.1	Introduction . . . . .	71
4.2	Model of the economy . . . . .	73
4.3	Hitting time simulation for the standard barrier option . . . . .	74
4.4	The consecutive Parisian contract . . . . .	79
4.5	The cumulative Parisian contract . . . . .	83
4.6	Numerical remarks . . . . .	85
	4.6.1 The parameter $\epsilon$ . . . . .	86
	4.6.2 Standard barrier versus cumulative and consecutive Parisian . . . . .	89
4.7	Conclusion . . . . .	89
4.8	Appendix . . . . .	91
	4.8.1 The average of $\gamma_{\tau_\delta}$ . . . . .	91
<b>5</b>	<b>Double-sided knock-in calls in an exponential compound Poisson framework</b>	<b>95</b>
5.1	Introduction . . . . .	95
5.2	Description of the model . . . . .	97
5.3	Theoretical background . . . . .	99
5.4	Option Pricing . . . . .	101
5.5	Numerical Examples . . . . .	103
	5.5.1 Calibration of the model . . . . .	104
	5.5.2 Price behavior for double-sided barrier options . . . . .	104

5.5.3	Implied volatility for double-sided barrier options . . .	105
5.6	Conclusions . . . . .	106
5.7	Appendix . . . . .	107
5.7.1	One-boundary characteristics . . . . .	107
5.7.2	Proof of Theorem 5.3.1 . . . . .	108
5.7.3	Proof of Theorem 5.3.4 . . . . .	111
<b>6</b>	<b>Commodity volatility modeling and option pricing with a potential function approach</b>	<b>113</b>
6.1	Introduction . . . . .	114
6.2	Volatility and the potential function model . . . . .	116
6.2.1	The potential function model . . . . .	116
6.2.2	Volatility estimation in the potential function model . . . . .	121
6.3	Option pricing within the potential function framework . . . . .	122
6.3.1	Potential versus Black-Scholes models . . . . .	122
6.3.2	hedge costs . . . . .	124
6.3.3	Options on physical commodity . . . . .	125
6.3.4	Options on futures . . . . .	128
6.4	Applications to oil spot and futures markets . . . . .	130
6.4.1	Option pricing and hedging . . . . .	130
6.4.2	Robustness of option prices in the potential framework . . . . .	131
6.5	Multivariate extension . . . . .	132
6.6	Conclusions and future work . . . . .	134
	<b>Bibliography</b>	<b>135</b>
	<b>Samenvatting</b>	<b>141</b>
	<b>Summary</b>	<b>145</b>
	<b>Curriculum vitae</b>	<b>149</b>



# Introduction

This thesis contains five papers on option pricing; four of them on equity options and one on option pricing for commodities. Each paper should be accessible to both financial mathematicians in academics and quantitative analysts in banks and insurance companies.

Today the area of financial mathematics is rapidly growing, which is a consequence of the increasing complexity of the financial products traded and regulated by the industry and the governments respectively. The majority of these complex products contain optionality, i.e., they can be viewed as derivatives of one or more underlying basic products. Throughout the thesis the terms options, derivatives and products that contain optionality are used as synonyms and the same is true for the terms basic product and underlying. Consider the convertible bond as an example of such a complex product. If certain conditions are satisfied - mostly stated in terms of the price process of the stock of the issuing company - the issuer can decide to convert the nominal value of the bond from a cash amount into a number of stocks. Therefore the value of this bond depends on the development of the stock price and interest rate, i.e., the underlying basic products. Many other financial products ranging from structured products to mortgages and insurances are examples of products containing some kind of optionality and therefore, the issue of option or derivative pricing attracts a lot of interest within the financial mathematics community. Research activity is in the direction of both extending the set of different derivative contract types one can value, and extending the set of models of the underlying basic products that can be used for the derivative valuation. The earliest attempt of modeling such an underlying basic product goes back to Bachelier, see [8], in the year 1900, whereas the actual increase in financial mathematical research activity was triggered by [14], the famous 1973 paper of Black and Scholes. They present the concept of the replicating portfolio for which they obtained the Nobel prize in 1997, see [23] for a short and accessible history.

As usual in the option community, different types of option contracts are labeled by a variety of geographical locations. Examples are European, American, Asian, Russian and Parisian options. The difference is almost always in the pay-off of the option. A pay-off specifies the rule used to calculate the amount of cash the derivative pays out, given a path of the

underlying basic product(s). A typical example is the pay-off of a standard call option with strike  $K$  given by  $(S_T - K)$  in case  $S_T$ , the value of the stock at expiry time, exceeds  $K$  and zero otherwise. There are several standard techniques that one can use to value a derivative, given its pay-off and the model for the underlying. In case of a stock option, geometric Brownian motion (GBM) is the standard way of modeling the underlying stock price process as introduced by Black-Scholes in their famous paper [14]. Using GBM as a model for the stock it is possible to derive closed-form expressions for several types of European options like the plain vanilla put and call and the path-dependent barrier options. For the Parisian option it is not possible to derive a closed-form expression. Moreover, the standard numerical techniques used in option pricing perform badly if applied to the Parisian option. This is why a significant part of this thesis is about Parisian options. Three papers contain three different solutions to this pricing problem using methods based on implied parameter pricing, Fourier transforms and Monte Carlo simulation. Although the solution to the valuation problem of another non-Parisian path-dependent option may need different modifications of one of these methods, the methods presented in the Parisian option papers might be extended to the pricing problem at hand. Research on the topic of Parisian option pricing was mainly initiated by Chesney, Jeanblanc and Yor in their paper [30] of 1997.

The fourth paper is on double-sided barrier option pricing, where the logarithm of the underlying value process follows a compound Poisson process with positive drift and negative exponential jumps. Actual markets exhibit the so-called volatility smile, which in fact reflects that the actual stock price processes do not behave like a GBM. It is nowadays popular to use a Lévy process to model the stock price behavior and calibrate this model to the volatility smile given by the market. The compound Poisson process is an example of such a Lévy process. The reason to consider double-sided barrier options is that these options are a degenerate case of the double-sided Parisian option without losing the ability to derive pricing formulas for the non-GBM underlying in terms of Laplace transforms. The paper shows that if the parameters of the compound Poisson process are calibrated to the market, the prices of the double-sided barrier options also exhibit a volatility smile. This is a motivation to do further research into the direction of Parisian option pricing for non-GBM stock price processes.

The fifth paper is about oil option pricing, where the oil price process follows a different model, i.e., not GBM. The connection between the Parisian papers and this paper is obviously the option pricing part. However, the paper adds the different view needed to price options on commodities. Well-known concepts in the equity world, i.e., the world of stocks, like short selling and replication do not have obvious counterparts in the commodity world. Therefore option pricing in the commodity world is quite a different business as is illustrated by the paper on oil option pricing.

## Outline of the thesis

The thesis consists of five self-contained papers preceded by a first chapter containing the preliminaries. This chapter gives an elaborate introduction on Parisian options. Its second section concerns concepts of option pricing: option pricing is about a fair price, but what is the definition of a fair price and how is this price related to the market price. The concept of no-arbitrage plays a central role, which informally stated comes down to the impossibility of making risk-free profits by trading the derivative or the underlying assets. The first chapter is concluded by a section on numerical Laplace or Fourier inversion, mainly based on the papers of Abate and Whitt [4] and Den Iseger [53].

The chapters two, three and four cover the papers about Parisian option pricing. Chapter two is about the concept of implied parameter pricing. The idea behind this concept is roughly that pricing formulas of slightly different options are used to calculate the value of the derivative of interest. A standard example taken from [52] is the calculation of the value of a forward start call, which can be done using the formula for the plain vanilla call. In practice traders use values of a standard barrier option with a slightly higher barrier for calculation of the Parisian option prices. Chapter two elaborates on what barrier should be taken in order to approximate the Parisian option price.

The paper in chapter three gives a derivation of the Fourier transforms of probabilities which are all one needs to compute the double-sided Parisian option prices. In order to arrive at these Fourier transforms, the Laplace transform of the Parisian stopping time is needed which is obtained by exploring the properties of Brownian meander. The reason for considering double-sided Parisian options is that the double-sided contract type can serve as a general Parisian contract. Many other Parisian contract types, like the one-sided up-and-out call, can be derived from this double-sided contract. The paper concludes with numerical examples comparing the various types of Parisian option contracts. These numerical examples show that Parisian option behave very different from plain vanilla options.

The next chapter considers Monte Carlo simulation of Parisian options. It is justified by experiments that straightforward path-simulating Monte Carlo techniques will converge very slowly. The slow convergence in straightforward path-simulating is a result of the typical behavior of Brownian motion. In this paper a method of simulating hitting times is developed, which cannot only be used for Parisian option pricing, but it is also very useful for simulating standard barrier options in a discrete dividend environment. For the latter type of options closed-form formulas do not exist. The chapter ends with a detailed treatment on tuning the algorithm that translates the simulated hitting times into a value for the Parisian option.

The paper in chapter five is about pricing double-sided barrier options in case the logarithm of the stock price process is modeled by a compound Poisson process with positive drift and negative jumps. The paper applies general results on two-sided exit problems for Lévy processes to the Poisson process and uses these results to derive one and two dimensional Laplace transforms for the double-sided barrier prices. The numerical section of the paper shows that, although the compound Poisson process can be considered as a toy model, it can be calibrated to the actual option market rather well. The calibrated model is used to compute prices for the double-sided barrier options and to show that these prices exhibit their own volatility smile. The actual computation of these prices is done by numerical inversion of a two-dimensional Laplace transform.

The last chapter contains a paper on derivative pricing in the commodity world. The paper starts modeling the underlying oil price process by a stochastic differential equation (SDE), built from a potential function that can be estimated from the data. A discussion on the relevance of the no-arbitrage argument follows and results in the incorporation of storage costs into the option pricing problem. Finally, the commodity pricing problem is connected to the equity world by pricing options on oil futures instead of options on oil itself. As there are no storage issues considering the future contract, the no-arbitrage argument holds again.

## Publication details

The second and third chapter are joint work with J.A.M. van der Weide. The work in the second chapter has been presented in 2004 on the 4th international conference in Computational Science in Krakow, Poland, resulting in a refereed publication in the Springer Lecture Notes on Computational Science (LNCS 3039) as,

- J.H.M. Anderluh and J.A.M. van der Weide, Parisian options, the implied barrier concept.

The work in the third chapter has been initially motivated by a project at Delft University in 2003 which had the primal goal to obtain numerical values for Parisian option prices from the Laplace transforms given in [30]. The paper on double-sided Parisian options as it is in this thesis is a revised version that has been resubmitted to Finance and Stochastics.

- J.H.M. Anderluh and J.A.M. van der Weide, Double-sided Parisian options.

The fourth and sixth chapter are a result of the work presented on the Deloitte Conference on Risk-Management held in Antwerp in 2005 and 2004 respectively. The work in chapter four is as a revised version resubmitted to the 2005 special issue of the European Journal of Finance on Risk Management as,

- J.H.M. Anderluh, Pricing Parisian options by hitting time simulation.

The work on options on oil in chapter six has been done together with S.A. Borovkova and is accepted for publication in the 2004 special issue of the European Journal of Finance on Risk Management.

- J.H.M. Anderluh and S.A. Borovkova, Commodity volatility modeling and option pricing with a potential function approach.

The work in chapter five has been initiated at the 4th actuarial and financial mathematics day in Brussels and is joint work with T. Kadankova of Hasselt University. The paper is still in a working-paper stage.



# Chapter 1

## Preliminaries

As the Parisian option is not daily traded on the exchange, its contract specifications might not be well-known. This preliminary chapter introduces this option contract to the reader by describing the contract specifications and the practical relevance of the contract. The second section treats very briefly the concepts of derivative pricing, which are necessary to appreciate chapter 6 on commodity option pricing. The final section gives a quick overview of numerical Laplace and Fourier inversion procedures, used throughout the thesis.

### 1.1 Introduction

Since this thesis consists of a set of self-contained papers, it is not necessary to read the chapters in a certain order. Readers with a background in financial mathematics will not find anything new in the first two sections of the preliminary chapter. The introduction to the Parisian option can be skipped, because the self-containment of the other chapters guarantees a brief introduction of the Parisian option in each of these chapters. The second section on key ideas of derivative pricing is added to this thesis for people with a background in probability rather than in financial mathematics who want to appreciate the commodity option pricing discussion in chapter 6. In fact it is a brief summary of the concepts as laid out in well-known textbooks as [12], [52] and [57] and therefore it contains nothing new for the financial mathematician. The final preliminary section gives an overview of numerical inversion techniques of Laplace and Fourier transforms. These transforms are almost equal from a numerical point of view, because most of the Laplace inversion algorithms start using a complex continuation of the Laplace transform as input for a Fourier inversion algorithm. This final section is mainly based on [4] and [53].

## 1.2 The Parisian Option

### 1.2.1 Contracts, pay-offs and path-dependency

The most basic options are options on one asset that do have a pay-off that is a function  $\Phi$  of the value of the asset at time  $T$  only, the so-called  $T$ -maturing options. Let  $(\Omega, \mathcal{F}, \mathbb{P})$  be a given probability space with filtration  $\{\mathcal{F}_t\}_{t \geq 0}$  and let  $\{S_t\}_{t \geq 0}$  be a non-negative right continuous stochastic process with left limits (RCLL) with respect to this filtered probability space. Here the process  $S$  represents the asset price evolution in time and the pay-off function  $\Phi : \mathbb{R} \rightarrow \mathbb{R}^+$  is Borel measurable and maps  $S_T$ , the value of the asset price at maturity, into the pay-off of the option. The definition of  $\Phi$  implies that the pay-off  $\Phi(S_T)$  is  $\mathcal{F}_T$ -measurable. The non-negativity of the pay-off is a result from the following: as the option-buyer will only exercise his option in case it is advantageous to him, the final value of the option (i.e., the pay-off of the contract) should have a non-negative value. Although the stock price process can only be positive, the option's pay-off can be defined on a spread, i.e., the difference of two stock prices, which is the reason for allowing for negative numbers in the domain of the pay-off function. Examples of the basic options are European standard<sup>1</sup> calls and puts with strike  $K$ . The pay-offs are given by  $(S_T - K)^+$  and  $(K - S_T)^+$  respectively. The term European is used to indicate that the option can only be exercised at maturity time  $T$ . Option contracts that can be exercised at any time are called American contracts.

So far the option contracts treated are not path-dependent, i.e. the terminal pay-off only depends on the value of the stock price at time  $T$  and not on the behavior of the stock price path up to time  $T$ . Path dependent contract types do incorporate the behavior of the stock price path into their pay-off specification. Pay-off functions of  $S_T$  the value of the asset at maturity then become pay-off functionals of  $\{S_t\}_{0 \leq t \leq T}$  the stock price path up to time  $T$ . A typical example is the barrier option, which is a contract paying off like a call or put in case some barrier is crossed or not. For example the down-and-in call with maturity  $T$ , barrier  $L$  and strike  $K$  has pay-off  $\Phi_{cdi}$ ,

$$\Phi_{cdi}(\{S_t\}_{0 \leq t \leq T}) = (S_T - K)^+ 1_{\{T_L \leq T\}}, \quad (1.1)$$

where  $T_L$  is the first hitting time of  $L$  by the process  $S$ . In the equity world barrier options are almost nowhere exchange traded, although they are used as building blocks in structured products like convertible bonds and guaranteed products. A simplified version of the barrier type contracts are the nowadays very popular Turbos and Speeders<sup>2</sup>. The next paragraph

<sup>1</sup>In the finance industry the standard options are mostly labeled *plain vanilla* after the most basic taste of ice cream.

<sup>2</sup>Turbos are issued by ABN Amro and Speeders by Commerzbank, more information can be found on the respective websites [www.abnamromarkets.com](http://www.abnamromarkets.com) and [www.speeders.commerzbank.com](http://www.speeders.commerzbank.com).

introduces the Parisian contract type, which is in some sense an extended version of the standard barrier contract.

### 1.2.2 The Parisian pay-off

Assume the probability space and the asset price process as given in the previous paragraph. Define the random time  $\gamma_T^{L+}$  by,

$$\gamma_T^{L+} := \sup\{0 \leq t \leq T | S_{t-} \leq L \wedge S_{t+} \geq L\}, \quad (1.2)$$

which corresponds to the last time the process  $S$  crosses the level  $L$  in the upward direction. In order to keep track of crossing the level  $L$  into the downward direction  $\gamma_T^{L-}$  analogously to  $\gamma_T^{L+}$  is defined by,

$$\gamma_T^{L-} := \sup\{0 \leq t \leq T | S_{t-} \geq L \wedge S_{t+} \leq L\}. \quad (1.3)$$

Here the definition of  $\gamma$  is different from that in [30], where the authors consider  $S$  to be a continuous process. For  $S$  continuous the random times  $\gamma_T^{L\pm}$  are equal and correspond to the last time before  $T$  the price process  $S$  equals  $L$ ,

$$\gamma_T^{L\pm} = \gamma_T^L = \sup\{0 \leq t \leq T | S_t = L\}. \quad (1.4)$$

Now define  $T_D^{L+}$  the Parisian upward and  $T_D^{L-}$  the Parisian downward stopping times as follows,

$$T_D^{L+} := \inf\{t > 0 | 1_{\{S_t > L\}}(t - \gamma_t^{L+}) \geq D\}, \quad (1.5)$$

$$T_D^{L-} := \inf\{t > 0 | 1_{\{S_t < L\}}(t - \gamma_t^{L-}) \geq D\}. \quad (1.6)$$

The upward and downward Parisian stopping times correspond to the first time the stock price process consecutively <sup>3</sup> spends time  $D$  above respectively below level  $L$ . It is clear that the  $\gamma$ 's defined in (1.2)-(1.4) are not stopping times as the occurrence of the event  $\{\gamma_T^L \leq t\}$  cannot be determined from  $\mathcal{F}_t$ , the information up to time  $t$ . The following explicit construction of the set  $\{T_D^{L+} \leq t\}$  shows that the random times defined in (1.5) and (1.6) actually are stopping times,

$$\{T_D^{L+} \leq t\} = \bigcap_{N=\lceil \frac{t}{D} \rceil}^{\infty} \bigcup_{i=0}^{N - \lfloor \frac{DN}{t} \rfloor} \bigcap_{j=i}^{\lfloor \frac{DN}{t} \rfloor} \{S_{j \frac{t}{N}} \geq L\},$$

for which the RCLL property of the process  $S$  is essential.

---

<sup>3</sup>In this section the consecutive Parisian contract is introduced. It is also possible to define a Parisian stopping time by looking at the cumulative time a stock price process spends below or above some level. The cumulative Parisian option is treated in chapter 4.

Like in the standard barrier pay-off (1.1), typical Parisian pay-offs are constructed from the standard put and call pay-off multiplied by an indicator function of the Parisian stopping time. Consider as an example  $\Phi_{cpdi}$  the pay-off of a Parisian down-and-in call with strike  $K$ , barrier  $L$ , time to maturity  $T$  and length of period to stay below the barrier  $D$ ,

$$\Phi_{cpdi}(\{S_t\}_{0 \leq t \leq T}) := (S_T - K)^+ 1_{\{T_D^{L-} \leq T\}}.$$

This option pays off like a call option in case the stock price path has been below level  $L$  for a consecutive time period of length  $D$ . Figure 1.1 contains

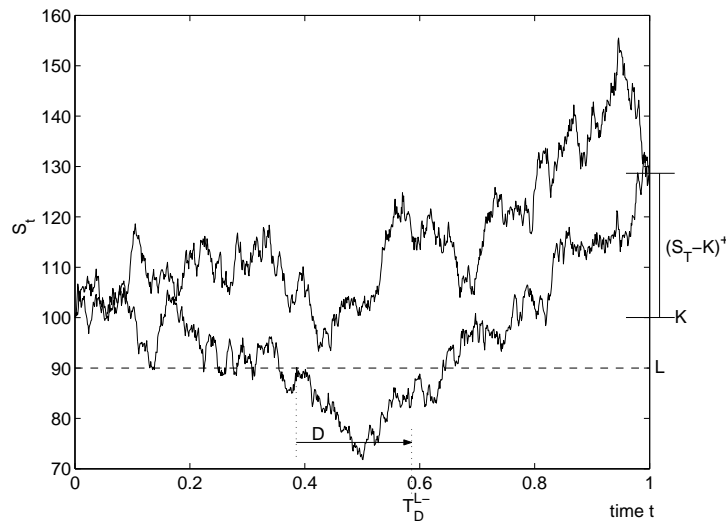


Figure 1.1: Example of Parisian pay-off.

two simulated sample paths of the stock price process  $S$ , both with a terminal value of 125. Consider as a first example the standard European call with time to maturity  $T = 1$  and strike  $K = 100$ . For the sample paths plotted in the graph, this European call is paying off the positive value  $S_T - K = 25$ , regardless of which of the two stock price paths has been realized. Now consider the Parisian down-and-in call with level  $L = 90$ , period to stay below this level  $D = 0.2$  year and same strike and time to maturity as the European standard call. In case the lower sample path is realized, the Parisian option pays off like the European call because the Parisian stopping time  $T_D^{L-}$  occurs before maturity as is marked in the graph. Realizing the upper sample path does not trigger the Parisian option, so in that scenario it will not pay off anything. Suppose now the level  $L$  is lowered to 80, then none of the plotted sample paths would trigger the Parisian option because the lower sample path does not stay long enough below the level 80. A standard barrier down-and-in call option with same strike, time-to-maturity and knock-in level would still pay off like the European call in case the lower

Table 1.1: Parisian contract types.

		Call	
		down-and	up-and
in		$(S_T - K)^+ 1_{\{T_D^{L-} \leq T\}}$	$(S_T - K)^+ 1_{\{T_D^{L+} \leq T\}}$
out		$(S_T - K)^+ 1_{\{T_D^{L-} \geq T\}}$	$(S_T - K)^+ 1_{\{T_D^{L+} \geq T\}}$
		Put	
		down-and	up-and
in		$(K - S_T)^+ 1_{\{T_D^{L-} \leq T\}}$	$(K - S_T)^+ 1_{\{T_D^{L+} \leq T\}}$
out		$(K - S_T)^+ 1_{\{T_D^{L-} \geq T\}}$	$(K - S_T)^+ 1_{\{T_D^{L+} \geq T\}}$

sample path is realized and  $L = 80$ .

Combining standard put and call pay-offs with indicators of the Parisian stopping times (1.5) and (1.6) results in different types of Parisian option contracts. Table 1.1 gives an overview of the various Parisian contract types and their pay-offs.

The Parisian options introduced so far are of the one-sided type. It is a natural extension to consider double-sided Parisian option contracts. This contract will be triggered by the following double-sided Parisian stopping time,

$$T_{D_1, D_2}^{L_1-, L_2+} := \min \left( T_{D_1}^{L_1-}, T_{D_2}^{L_2+} \right).$$

Double-sided Parisian options are triggered by staying long enough below some lower level or long enough above a certain upper level. As a result up and down types of double-sided Parisian contracts do not exist, so there are only four of them given by the combinations of put or call and in or out.

### 1.2.3 Applications of Parisian optionality

The Parisian option as such is not an exchange traded instrument, so, at first glance there is no need to price it for market making purposes. The exchanges serve their investing customers by offering them liquidity. In order to guarantee liquidity in options, i.e., guarantee filled order books such that investors easily can enter into or unwind an option position, the exchanges make agreements with market makers. The market makers should quote almost continuously in their option series. This quoting incorporates a risk for the market makers, for example if markets move fast, and therefore they receive certain privileges like low transaction costs, high bandwidth connections to the exchange or a different priority in the order book. The regula-

tions and privileges vary per exchange, but they are all based on giving the market maker something in return for being visible in the market. Nowadays a lot of derivative exchanges, like EuroNEXT Liffe and EURex, are screen trading environments and the open-outcry systems, like the Chicago Board of Trade (CBOT), are under pressure. For the screen trading market maker it is absolutely necessary that he disposes of a real-time option pricing engine. Therefore theoretical valuation of exchange traded option contracts should be very fast, i.e., pricing techniques with computation times of several minutes are useless in this situation.

Consulting the first papers on Parisian option pricing, [29] and [30], it is suggested that Parisian options have been traded in the over-the-counter-market (OTC) by an Australian and a French bank. Large banks do not trade every derivative through an exchange, instead they trade a huge number of contracts directly with other banks in the OTC market. The OTC market is only accessible to large banks, because the counter party risk is not eliminated by an exchange. The reason for banks to trade the Parisian option instead of the standard barrier option was supposed to be in the difficulty of triggering the option by market manipulation, which is of course an issue in case of an illiquid underlying product.

Real option theory, see [38], is the theory of incorporating option valuation into the field of optimal investment decisions. Especially taking into account the value of postponing the investment, the timing of the investment can be optimized. The resulting strategy can be of the type where the investor starts the investment as soon as some economic quantity exceeds a certain level. Real option theory then uses the standard barrier option to compute the value of this investment strategy. However, as pointed out by [43], after exceeding the level time passes by before the start of the investment is actually made. This can be a result of raising funds, convincing the board or hiring people. Now assume that this process will be interrupted as soon as the economic quantity drops below the level and as soon as the quantity exceeds the level again, the process will be re-initiated. In this case, where there is some delay between the exceeding of the level and the actual investment, from a real option perspective it is necessary to value a Parisian option instead of a standard barrier option.

Another example from practice is given by the convertible bond, see [61] and [48]. A convertible bond is a bond that can be converted by the bondholder into some amount of stock of the issuer at the contractual conversion price. The issuer has usually the possibility to call the bond, upon which the holder can either redeem the bond at the call price or convert it into stocks. To protect the holder's conversion privilege, the convertible bond contract contains a hard and a soft call constraint. The hard call constraint ensures that the issuer cannot call the bond during its early life. The soft call constraint usually requires the stock of the issuer to trade above some trigger level for a consecutive period of time. As a result of this soft call

constraint, the ability to price Parisian options is of great use for pricing convertible bonds.

Finally there are applications of Parisian options in the valuation of corporate liabilities. In [66] and [27] the authors explain that the Parisian behavior is a result of the law. After the default event happens, the court can give a company a so-called grace period. During this grace period a company has the time to recover from default by either reorganizing its activities or negotiating with debt and equity holders. If the company does not succeed in recovering during this grace period liquidation follows. So, the liquidation event will be triggered by a Parisian stopping time which is the first time that the value of the firm spends below the default threshold longer than the grace period. In [26] the authors model the firm's cash position by a standard Brownian motion to obtain a model for the time of default. The time of default occurs as soon as the cash position doubles in magnitude after it has been below zero for some period of time, which is equivalent to the first hitting time of zero after a Parisian stopping time has occurred.

### 1.3 Key ideas of derivative pricing

Option pricing problems in the literature are usually presented as the problem of calculating the expected value of the pay-off under a martingale measure  $\mathbb{Q}$ . This section explains the connection between this expectation and the underlying concepts of derivative pricing. Recall the stock price process  $S$  as defined in paragraph 1.2.1 and make the extra assumption that it is a continuous semi-martingale. The derivative that needs to be priced with pay-off  $\Phi$  lives on the finite time interval  $[0, T]$  and its price at time  $0 \leq t \leq T$  is denoted by  $V_\phi(t)$ .

#### 1.3.1 Trading, the bank-account and the market

During the opening hours of the exchanges a lot of financial instruments are traded almost continuously. For very liquid stocks, like Microsoft, the BBO<sup>4</sup> is updated more than once a second. That is why modeling the stock price and the trading strategy by continuous time stochastic processes is not too far from reality.

If you start trading stocks, it is natural to consider the concept of a strategy,

---

<sup>4</sup>The *Best Bid Offer* line is the top line within the orderbook. Every order that cannot be matched directly is stored in the orderbook on a FIFO bases. The order depth consists of prices for which traders want to buy or sell the stock and the total volume that can be traded on that price. The highest bid price and the lowest ask price together with their respective volumes is called the BBO. The difference between the highest bid price and the lowest ask price is called the spread. The smallest possible price difference is defined by the tick size. A spread of one tick size usually indicates that the stock is very liquid, i.e., very heavily traded.

a stochastic process representing your buy and sell decisions. To put it formally, a strategy  $\{\phi_t; 0 \leq t \leq T\}$  is a predictable stochastic process denoting the number of stocks in your portfolio. For example, the strategy  $\phi_t = H_0/S_0$  for every  $t$  represents the buy and hold strategy, where the amount  $H_0 > 0$  is the initial amount you invest in the strategy. A stochastic process  $\phi$  is predictable if as a mapping  $\phi : [0, T] \times \Omega \mapsto \mathbb{R}$  it is measurable w.r.t. the  $\sigma$ -algebra generated on  $[0, T] \times \Omega$  by all left-continuous processes. Later on, when discussing the no-arbitrage assumption, an example will make clear why a strategy should be a predictable process. Consider the simple strategy,

$$\phi_t(\omega) = \sum_{i=0}^{N-1} C_i(\omega) 1_{(t_i, t_{i+1}]}(t),$$

where  $0 = t_0 < t_1 \dots < t_N = T$  is a partition of  $[0, T]$  and  $C_i \in \mathcal{F}_{t_i}$ . The process  $\phi_t$  is predictable and the profit  $P_\phi$  arising from this strategy can be computed by the sum,

$$P_\phi = \sum_{i=0}^{N-1} \phi_{t_i} (S_{t_{i+1}} - S_{t_i}) = \sum_{i=0}^{N-1} C_i (S_{t_{i+1}} - S_{t_i}), \quad (1.7)$$

which converges to the Itô integral w.r.t.  $S$  for all bounded predictable processes  $\phi$ . Recall that for a continuous integrand  $\phi$  that can be approximated by simple integrands  $\phi^{(n)}$  with decreasing mesh-size of the partition of the time interval  $[0, T]$  sums like (1.7) converge to the Itô integral if the integrand is evaluated at the starting point of the interval. In general the profit  $P_\phi(t)$  generated by stock-trading according to strategy  $\phi$  until time  $t$  is given by

$$P_\phi(t) = \int_0^t \phi_u dS_u \quad \text{for } t \in [0, T].$$

The world consists not only of stocks, but it is also possible to keep a positive or negative amount of money on a bank account. By definition on a bank-account the interest rate for keeping positive and negative amounts on the bank account is equal, deterministic with value  $r$  and continuously compounded. The dynamics of the bank account  $B$  are given by

$$dB_t = rB_t dt, \quad (1.8)$$

and together with the assumption  $B_0 = 1$ , this results in  $B_t = e^{rt}$ . Like  $\phi_t$ , the number of stocks in the portfolio, a strategy also has to specify the number of units bank account in the portfolio, denoted by the stochastic process  $\{\psi_t; 0 \leq t \leq T\}$ . The value of the portfolio at time  $t$  is denoted by  $H_t$  and given by

$$H_t = \psi_t B_t + \phi_t S_t. \quad (1.9)$$

Now consider only the self-financing strategies, i.e., strategies that need no extra investment after the initial amount  $H_0$ . For a self-financing portfolio it is only possible to redistribute its value between the stock and the bank account, which results in the following equation

$$\psi_{t_-} B_t + \phi_{t_-} S_t = \psi_t B_t + \phi_t S_t,$$

where  $t_- = t - \Delta t$  for some small  $\Delta t$ . Now the mutation on the bank-account follows

$$\begin{aligned} B_t(\psi_t - \psi_{t_-}) &= -S_t(\phi_t - \phi_{t_-}) \\ &= -(S_t - S_{t_-})(\phi_t - \phi_{t_-}) - S_{t_-}(\phi_t - \phi_{t_-}). \end{aligned}$$

Adding and subtracting  $S_{t_-}(\phi_t - \phi_{t_-})$  is necessary to get Itô differentials in the limit. Letting  $\Delta t \rightarrow 0$  gives the dynamics of  $\psi_t$  in terms of  $\phi_t$  for a self-financing strategy,

$$d\psi_t = -\frac{1}{B_t} (S_t d\phi_t + dS_t d\phi_t). \quad (1.10)$$

An application of the Itô formula gives the dynamics of  $H_t$ , the value of the portfolio at time  $t$  given in (1.9), and for a self-financing portfolio plugging (1.10) into this dynamics gives the result

$$dH_t = d(\psi_t B_t + \phi_t S_t) = \psi_t dB_t + \phi_t dS_t. \quad (1.11)$$

A self-financing strategy is completely specified by the pair  $(H_0, \{\phi_t\}_{0 \leq t \leq T})$ , where  $H_0$  denotes the initial investment and  $\phi_t$  for  $t \in [0, T]$  the number of stocks the portfolio should contain. The number of units bank account  $\psi_t$  for  $t \in [0, T]$  directly follows from the self-financing property. Note, that in case of an interest rate of zero, the value of the portfolio constructed from the self-financing strategy  $(H_0, \{\phi_t\}_{0 \leq t \leq T})$  at time  $t$  equals the initial investment  $H_0$  plus the profit  $P_\phi(t)$  at time  $t$ ,

$$H_t = H_0 + \int_0^t \phi_u dS_u.$$

So far the market contains two tradable assets: money on the bank-account and stocks. The strategies one can trade on the market need to be of the predictable type, i.e., one can only use information at time  $t$  to make a buy or sell decision at time  $t + \varepsilon$  for any  $\varepsilon > 0$ .

### 1.3.2 No arbitrage assumption

Crucial in the theory of derivative pricing is the no-arbitrage assumption, which states that the market is free of arbitrage possibilities. A market

contains an arbitrage possibility if there exists a self-financing strategy  $(H_0, \{\phi_t\}_{0 \leq t \leq T})$  such that,

$$H_0 = 0, \quad \mathbb{P}[H_T \geq 0] = 1 \quad \text{and} \quad \mathbb{P}[H_T > 0] > 0. \quad (1.12)$$

So an arbitrage possibility is a strategy that needs no initial investment, has zero probability of losing money, and a positive probability of ending up with more than zero. Note that in case the market model contains a bank account, putting money on this account that grows with the risk-free interest rate is not an arbitrage possibility, because although you are sure you end with more money than you initially invested, the initial investment is not zero. A strategy that does require an initial investment is an arbitrage possibility if the value of the corresponding portfolio at time  $T$  is at least the initial investment  $H_0$  plus interest and with positive probability even more.

The no-arbitrage assumption puts restrictions on the assets that can be in the model of the market and on the trading strategies that are allowed. Consider for example a market model with two bank accounts with different risk-free interest rates, then keeping a negative amount  $-H_0$  on the bank account with the lower interest rate and a positive amount  $H_0$  on the account with higher interest rate is an arbitrage possibility. Allowing all stochastic processes  $\phi$  in a strategy also introduces arbitrage possibilities. Recall from the previous section that a strategy should already be a predictable process, so what arbitrage possibility arises for example from a right-continuous strategy, i.e., a strategy that is not predictable? Consider the following model for the stock price process  $S$ ,

$$S_t = \begin{cases} 2 & t \in [0, \frac{T}{2}) \\ X & t \in [\frac{T}{2}, T] \end{cases}, \quad \text{where} \quad \mathbb{P}[X = 3] = p \quad \text{and} \quad \mathbb{P}[X = 1] = 1 - p.$$

The following strategy is adapted and right-continuous,

$$\phi_t = \begin{cases} 0 & t \in [0, \frac{T}{2}) \\ 1 & t \in [\frac{T}{2}, T] \quad \text{and} \quad X > 2 \\ -1 & t \in [\frac{T}{2}, T] \quad \text{and} \quad X < 2 \end{cases},$$

and causes an arbitrage possibility as we have for the profit the following Itô integral, which equals the Stieltjes integral as the process  $X$  is of finite variation (see [75] for details),

$$P_\phi = \int_0^T \phi_t dS_t = \phi_{T/2} \Delta S_{T/2} = 1$$

which is a sure profit generated by foreseeing the jumps of the stock price process. In reality it is of course not possible to anticipate a jump in the stock price process, it is only possible to adjust your strategy just after the

jump, which is adequately represented by a left-continuous process, which is the kind of process that generates the class of predictable processes as described in the previous section. Restricting the strategies to predictable processes is not enough, because it is still possible to create a strategy that is similar to the doubling strategy in the casino. The idea is to invest at times  $t_n = T - T/n, n = 1, 2, \dots$  and increase your investment as long as the gain from the previous investments is not enough, where the investments are financed by a loan on the bank account. This type of strategies are not possible in reality, simply because you will not have an infinite credit line. From now on the only strategies  $(H_0, \{\phi_t\}_{0 \leq t \leq T})$  that are admitted are the strategies for which a real number  $\alpha > 0$  can be specified such that the losses never exceed  $-\alpha$ ,

$$\int_0^t \phi_u dS_u > -\alpha \quad \text{a.s. for } t \in [0, T]. \quad (1.13)$$

It is now a natural question whether it is possible to check whether a market model satisfies the no-arbitrage assumption. The answer involves the concept of an equivalent martingale measure (EMM). A measure  $\mathbb{Q}$  is an EMM on  $[0, T]$  for the bank account  $B$  if  $\mathbb{Q}$  is equivalent with  $\mathbb{P}$  on  $\mathcal{F}_T$ , i.e.,  $\mathbb{P}$  and  $\mathbb{Q}$  assign zero measure to the same sets in  $\mathcal{F}_T$ , and the discounted stock price process  $\tilde{S}_t := S_t/B_t$  is a  $\mathbb{Q}$ -martingale on  $[0, T]$ . The following meta-theorem answers the question,

*The market model  $(B, S)$  essentially satisfies the no-arbitrage assumption if and only if there exists an EMM.*

Arriving from the EMM at the no-arbitrage assumption is the easy part of the theorem. Assume for simplicity that the risk-free rate  $r = 0$ , resulting in  $B_t \equiv 1$  for  $t \in [0, T]$ . Suppose that  $\mathbb{Q}$  is an EMM and  $(H_0, \{\phi_t\}_{0 \leq t \leq T})$  is an arbitrage possibility. Then under  $\mathbb{Q}$  the stock price process is a martingale and therefore a stochastic integral w.r.t. the stock price process also is a martingale, giving the following equation,

$$0 = H_0 = \mathbb{E}_{\mathbb{Q}} \left[ \int_0^T \phi_t dS_t \right]. \quad (1.14)$$

Now from  $\mathbb{Q} \sim \mathbb{P}$  it follows by (1.12), the definition of an arbitrage possibility, that  $H_0 > 0$ , which is a contradiction to (1.14).

The other way around, i.e., proving that there should exist an EMM if the market model satisfies the no-arbitrage assumption is very technical. A more subtle version of the arbitrage possibility is involved, which is the reason for including the word *essentially* in the meta-theorem. A rigorous proof of this result can be found in [37]. In [12] an almost complete picture of the proof is given in a very accessible way.

There are two reasons for the no-arbitrage assumption to be a key concept in derivative pricing. On itself, the no-arbitrage assumption seems quite reasonable in practice. Market participants are not spending money they do not need to spend, so for you, there will be no arbitrage possibility. It is therefore practically relevant to assure that if you have a method to price a derivative that your market model, extended with the derivative as a tradable following the price process you have computed with your method, still satisfies the no-arbitrage assumption. On the other hand, suppose you can find a self-financing strategy  $(H_0, \{\phi_t\}_{0 \leq t \leq T})$  resulting in a portfolio with a terminal value  $H_T$  that equals the pay-off  $\Phi$  of the derivative you want to price. Then, by the no-arbitrage assumption, the price  $V_\Phi(0)$  of the derivative at time 0 should equal  $H_0$ .

### 1.3.3 Pricing and replicating strategies

Assume you extend the tradables in the market model already containing the stock and the bank account by the derivative itself. Pricing the derivative is straightforward once you assume that the extended market models still satisfies the no-arbitrage assumption. By this assumption there exists a measure  $\mathbb{Q}$  such that all discounted tradables are martingales, which should in particular be true for  $V_\Phi(t)/B_t$ , the price process of the derivative. So,  $V_\Phi(t)$  is given by the following conditional expectation,

$$V_\Phi(t) = B_t \mathbb{E}_{\mathbb{Q}} \left[ \frac{\Phi(S_T)}{B_T} \middle| \mathcal{F}_t \right]. \quad (1.15)$$

Pricing the derivative by (1.15) guarantees that there exists no strategy of buying or selling the derivative for this price that generates an arbitrage possibility. Then, what to do when the market price is different from this price? Will that give you an arbitrage possibility? The existence of a so-called replicating strategy is crucial in answering this question. The self-financing strategy  $(H_0, \{\phi_t\}_{0 \leq t \leq T})$  is a replicating strategy for the derivative with pay-off  $\Phi$  at time  $T$  if the following equation holds,

$$H_T = H_0 + \int_0^T \psi_t dB_t + \int_0^T \phi_t dS_t = \Phi(S_T) \quad \text{a.s.}$$

In words this equation states that in all possible scenarios of the stock price process, you know how to redistribute the initial investment  $H_0$  between stocks and the bank-account such that the value of your portfolio at time  $T$  exactly equals the pay-off of the derivative. Suppose such a strategy exists, then in case the market model is arbitrage-free, the price of the derivative  $V_\Phi(t)$  should equal the value of the portfolio  $H_t$  a.s. for all  $t \in [0, T]$ . Suppose there exist two such strategies,  $(H_0^{(1)}, \{\phi_t^{(1)}\}_{0 \leq t \leq T})$  and  $(H_0^{(2)}, \{\phi_t^{(2)}\}_{0 \leq t \leq T})$ , then by the no-arbitrage assumption  $H_t^{(1)} = H_t^{(2)}$  for all  $t \in [0, T]$ . The

remaining question now is whether such a strategy exists. A market model in which there exists a replicating strategy  $(H_0, \{\phi_t\}_{0 \leq t \leq T})$  for every pay-off  $\Phi$  is called complete. It is again a meta-theorem that answers the question:

*A market model  $(B, S)$  that satisfies the no-arbitrage assumption is complete if and only if the EMM is unique.*

Again one direction is easy to show. Suppose there exists a replicating strategy and there are two different EMMs generating two different price processes by (1.15). For at least one of these EMMs, trading the derivative price process against the portfolio value  $H_t$  constructed by the replicating strategy generates an arbitrage possibility which is assumed not to exist. The other way around is more technical and in the zero interest rate case it comes down to showing that for each martingale  $M$  being the price process of the derivative, there exists a stochastic integrand  $\{\phi_t\}_{0 \leq t \leq T}$ , being the replicating strategy, such that the following equation holds,

$$M_t - \mathbb{E}[M_t] = \int_0^t \phi_u dS_u.$$

So showing that the existence of a unique martingale measure ensures the existence of a replicating strategies boils down to using a martingale representation theorem that is suitable for both the class of pay-offs and the model for the stock price process you are considering.

### 1.3.4 The Black-Scholes formula

The famous Black-Scholes formula is a pricing formula for a  $T$ -maturing European call option with strike  $K$  on a single stock, where the stock price process  $S$  is given by a GBM, so its dynamics under the objective measure  $\mathbb{P}$  are given by,

$$dS_t = \mu S_t dt + \sigma S_t dW_t, \quad S_0 = s_0, \quad t \in [0, T]. \quad (1.16)$$

Here  $\mu$  is the drift and  $\sigma$  the volatility of the stock price process. The volatility introduces risk into the future values of the stock price process. Note that the bank account  $B$  as given in (1.8) is governed by the same type of dynamics with zero volatility, i.e., zero risk. The rational investor demands  $\mu > r$  as a compensation for this risk.

By Girsanov's theorem for every real  $\alpha$  there exists an  $\mathcal{F}_T$ -equivalent measure  $\mathbb{Q}$  such that the process  $\{Z_t\}_{0 \leq t \leq T}$  given by  $Z_t = W_t + \alpha t$  is a  $\mathbb{Q}$ -Brownian motion. Together with the equality  $dW_t = dZ_t - \alpha dt$ , equation (1.16) translates for  $\alpha = \frac{\mu-r}{\sigma}$  into

$$dS_t = rS_t dt + \sigma S_t dZ_t. \quad (1.17)$$

Now  $Z$  is a  $\mathbb{Q}$ -Brownian motion and therefore the discounted stock price process  $S_t/B_t$  is a  $\mathbb{Q}$ -martingale on  $[0, T]$ . Under the measure  $\mathbb{Q}$  the process given by (1.17) is not the actual, real-world stock price process anymore, it is artificial and it is a process with uncertain future values and a drift equal to the risk-free rate. Suppose this process represents the stock price evolution in reality, then the only people who are interested are the investors who do not need a compensation for the risk. These investors do not bother about risk, so they are risk-neutral. Therefore the dynamics given by equation (1.17) are denoted by the risk-neutral dynamics,  $\mathbb{Q}$  is called the risk-neutral measure and  $S$  governed by the risk-neutral dynamics is called the risk-neutral stock price process. By the pricing formula (1.15) the price  $V_C(t, S_t)$  of a standard call option at time  $t$  and the corresponding stock price value  $S_t$  is given by

$$V_C(t, S_t) = e^{-r(T-t)} \mathbb{E}_{\mathbb{Q}} \left[ \left( S_t e^{(r-\frac{1}{2})\sigma^2(T-t) + \sigma Z_{T-t}} - K \right)^+ \right]. \quad (1.18)$$

Showing that (1.18) is the fair price, i.e., the only price that does not introduce an arbitrage opportunity, is similar to showing that there exists a replicating strategy  $(H_0, \{\phi_t\}_{0 \leq t \leq T})$ . A replicating strategy assures  $H_t = V_C(t, S_t)$  a.s. for  $t \in [0, T]$ , which is assured by  $dH_t = dV_C(t, S_t)$  and  $H_0 = V_C(0, S_0)$ . From (1.18) it follows that  $V_C(t, S_t)$  is a continuous, twice differentiable function, so by Itô's formula the dynamics of  $V_C(t, S_t)$  are given by

$$dV = \frac{\partial V}{\partial t} dt + \frac{\partial V}{\partial S} dS + \frac{1}{2} \frac{\partial^2 V}{\partial S^2} \sigma^2 S_t^2 dt, \quad (1.19)$$

where the notation is simplified by writing  $V$  instead of  $V_C(t, S_t)$ . By comparing the dynamics of the price in (1.19) with the dynamics of a self-financing strategy (1.11) it follows that computing the number of stocks in the replicating strategy by

$$\phi_t = \left[ \frac{\partial V(t, S)}{\partial S} \right]_{s=S_t}, \quad (1.20)$$

is consistent with (1.19). One can also obtain the number of units bank account  $\psi_t$  at time  $t$  from (1.19). If this  $\psi$  turns out to be the same as the  $\psi$  that follows from the self-financing property given by (1.10) then the self-financing strategy  $(H_0, \{\phi_t\}_{0 \leq t \leq T})$  with  $\phi$  given by (1.20) is a replicating strategy for the  $T$ -maturing European call option. Guessing  $\psi$  directly from (1.19) might not be enough, because (1.19) holds for any twice continuously differentiable  $V$ . More specific information on  $V$  comes from (1.18) and can be exploited by the Feynman-Kac theorem, see [69] for background and [12] for applications, which results in the following equation,

$$\frac{\partial V}{\partial t} dt + \frac{1}{2} \sigma^2 S_t^2 \frac{\partial^2 V}{\partial S^2} = r \left( V - S_t \frac{\partial V}{\partial S} \right), \quad (1.21)$$

and the following guess for  $\psi_t$ ,

$$\psi_t = \frac{1}{B_t} \left( V - S_t \frac{\partial V}{\partial S} \right).$$

Using Itô and another application of (1.21) shows that  $d\phi_t$  satisfies (1.10). Therefore, the self-financing strategy  $(H_0, \{\phi_t\}_{0 \leq t \leq T})$  with  $\phi$  given by (1.20) is the replicating strategy for a European call option and (1.18) gives the fair price of this derivative. The actual formula for the price that follows from

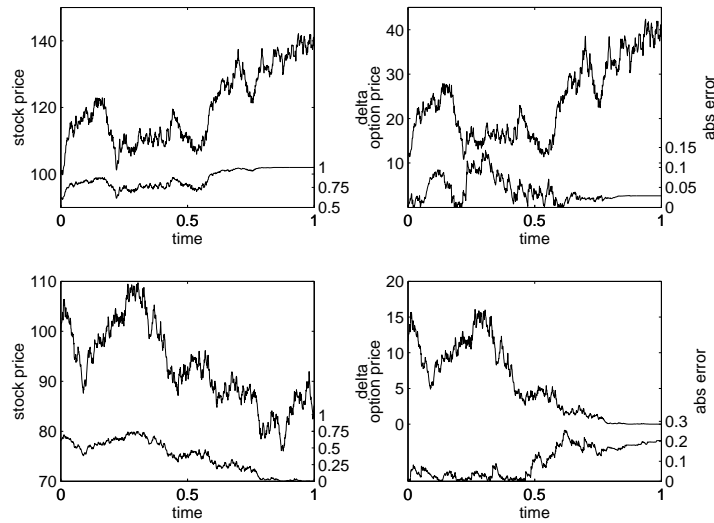


Figure 1.2: Two realizations of the stock and option price process, replicating strategy and absolute error.

computing (1.18) can be found in many textbooks, see for example [52]. In practice the number of stocks in the replicating strategy  $\phi_t$  given by (1.20) is called the delta of the option. Figure 1.2, where the upper and lower part of each subgraph correspond to the right and left hand axis respectively, shows this delta for two simulated paths of stock price process starting at  $S_0 = 100$  with volatility  $\sigma = 0.25$  and drift  $\mu = 0.08$ . The option for which the delta and the option price are computed is a call option with strike  $K = 100$  and time to maturity  $T = 1$ . The risk-free rate on the bank account is set to  $r = 0.035$ . The two simulated stock price paths differ in the sense that the upper one that ends above the strike corresponds to the option ending “in the money”, whereas the lower one ends below the strike and corresponds to the option ending “out of the money”. The left-hand graphs in the figure show that the delta for an in-the-money option approaches one, whereas it approaches zero for the out of the money option. This corresponds to the fact that an option seller only has to deliver one share of stock to the buyer in case the option ends in the money. The right-hand graphs give an idea of the evolution of the option price process and the absolute error

between the option price following from (1.18) and the value of the self-financing portfolio constructed from  $H_0$  the initial option price and  $\phi_t$  given by (1.20). According to the theory the value of the replicating portfolio and the option price should be the same at each point in time, so the absolute error should be zero everywhere. Remember that the replicating strategy  $\phi$  allows to trade continuously, whereas in this simulation the time of one year is divided into 1000 time steps. It is this discretization of time that is responsible for an absolute error different from zero. However, note that a division of one year into 1000 time-steps corresponds to only four trading moments each day. The power of the Black-Scholes formula and the reason that in practice it is used everywhere lies in the fact that you have to trade the stock only four times a day to replicate a one-year option in order to obtain an acceptable final error. So you can act as a market maker because you have a recipe to produce your option and you know your production costs with sufficient certainty. For this to be really true, the stock price process has to follow a GBM in the market. All traders agree that the market does not follow a GBM and that is the reason for numerous modifications of the Black-Scholes framework.

### 1.3.5 Incomplete markets

For the derivation of the Black-Scholes formula, the following assumptions were made:

- The stock price process follows a GBM.
- Borrowing money and saving money goes against the same continuously compounded risk-free interest rate.
- It is possible to trade stocks continuously and in arbitrary fractions.
- Short-selling is allowed without extra costs.
- There are no trading costs.
- The underlying can be stored without costs and without deterioration.

In actual stock markets, only the first assumption is a real issue. The last assumption might even sound trivial as only stocks are considered up to here. However, if the underlying is a perishable commodity this can be a real issue, which is then also the case for the short-selling assumption. In the remainder of this subsection there will be discussion on the GBM assumption. People in practice believe that stock price processes do not follow a GBM. Now, what happens if the underlying process is changed to another process, like a jump-diffusion process?

One approach is to directly model the stock under a martingale measure, i.e., given your model, you choose your parameters in such a way that your

stock price is a martingale and you assume that an equivalent objective measure does exist. Using this approach implies that you have to calibrate your model to option prices, which are determined by the risk-neutral measure. You cannot calibrate your model to historical price information of the underlying stock price process, because then you would be using observations from the physical measure. An arbitrage-free option price can still be obtained by (1.15), but it is no longer ensured that this option price is unique. No unique price means no replicating strategy for the option and you are no longer in a complete market, which is, as explained in the previous paragraph, the real power of the Black-Scholes model.

First it is natural to consider the cheapest self-financing strategy that generates a terminal value that is maybe more, but never less than the option's pay-off. The set-up costs of this strategy is an upper bound for the option price, otherwise it is possible to generate an arbitrage by selling the option. The initial investment of a self-financing strategy with a terminal value maybe less and never more than the option's pay-off is a lower bound for the option price, otherwise buying the option generates an arbitrage possibility. This concept is known as super hedging and results in an interval of possible option prices. For the class of exponential Lévy models, i.e.,  $S_t = S_0 e^{X_t}$  where  $\{X_t\}_{0 \leq t \leq T}$  is a Lévy process the lower bound is at least the Black-Scholes price and the upper bound is  $S_0$ , the stock price at time 0. A detailed discussion for different cases can be found in [40] and [9].

Super hedging gives almost trivial bounds for the option price, so there is a need for another approach, quadratic hedging. This quadratic hedging approach minimizes the variance of the hedging error. Minimizing the variance at the final time  $T$  is called mean variance hedging, whereas minimizing the variance of the one step ahead hedging error is called local risk minimization, see [80] for an overview. In this setting the self-financing strategy defined by (1.20), the partial derivative of the option price at time  $t$  with respect to  $S_t$ , is sub-optimal.

Finally, another approach is to enrich the model with the investor's preferences by introducing a utility function. A general treatment of this concept can be found in [42]. The advantage of this approach is that investors with different preferences assign different values to options, which makes clear why people trade with each other in the markets. The drawback of the method is that it is hard for a trader to specify his utility function and in general this function will depend on his entire position in stock and options. In practice market makers in standard equity options do not like models without hedging strategy. They prefer a modification of the Black-Scholes model where the volatility is given by a function  $\sigma(t, S_t)$  rather than a constant. Parametrization of this function allows the model to be calibrated to the option market, without giving up completeness. The use of the incomplete non-GBM models is that these models can be calibrated to the standard option market and then be used for risk management and pricing

of exotic options. Both areas are growing as a result of increasing regulation and increasing complexity of financial products.

## 1.4 Numerical inversion

In this section the numerical inversion of Laplace and Fourier transforms is discussed. From a probabilistic point of view, it turns out to be convenient to use Fourier or Laplace transforms for the valuation of quantities of interest. In this thesis examples of these quantities are given by pricing formulas for Parisian options and double-sided knock-in calls. The transform needs to be numerically inverted in order that the method has a practical application. This section is mainly based on the papers of Abate and Whitt [4] and Den Iseger [53] describing the use of Euler summation and Gaussian quadrature respectively. The Euler summation method is straightforward and works quite well in case a one dimensional transform needs to be inverted. The Gaussian quadrature method is rather complicated. It has the advantage that it is possible to obtain numerical values for two dimensional transforms within acceptable time. An application of two dimensional Laplace inversion is given in the chapter on double-sided barrier options in a compound Poisson setting. The section starts by a paragraph defining Fourier and Laplace transforms. The second and third paragraph then treat Euler summation and Gaussian quadrature respectively.

### 1.4.1 The Fourier and Laplace transform

For a rigorous treatment of the Fourier transform and its properties see [76]. Assume that the function  $f : \mathbb{R} \rightarrow \mathbb{R}$  is in  $L^1$ , then its Fourier Transform  $\hat{f} : \mathbb{R} \rightarrow \mathbb{C}$  is defined by

$$\hat{f}(t) = \int_{-\infty}^{\infty} f(x)e^{itx} dx. \quad (1.22)$$

Assuming that  $\hat{f} \in L^1$  results in the inversion formula given by

$$f(x) = \frac{1}{2\pi} \int_{-\infty}^{\infty} \hat{f}(t)e^{-ixt} dt \quad \text{a.e.} \quad (1.23)$$

The inversion formula gives an almost everywhere equation because the inversion integral differs from the original  $f$  at points where  $f$  jumps. It follows directly from (1.22) that the real and imaginary parts of  $\hat{f}$  are even and odd respectively. As  $f$  itself is a real function, the inversion formula (1.23) translates into

$$f(x) = \frac{1}{\pi} \int_0^{\infty} \hat{f}(t)e^{-ixt} dt \quad \text{a.e.} \quad (1.24)$$

Let  $g : \mathbb{R}^+ \rightarrow \mathbb{R}$  a function in  $L^1$ . Then its Laplace transform  $\hat{g}$  is defined by

$$\hat{g}(s) = \int_0^\infty e^{-sx} g(x) dx, \quad (1.25)$$

where  $s \in \mathbb{R}^+$  such that (1.25) exists. For the remainder of this section the functions  $f$  and  $g$  are always defined on  $\mathbb{R}$  and  $\mathbb{R}^+$  respectively, where  $\hat{f}$  and  $\hat{g}$  denote their respective Fourier and Laplace transforms. For numerical inversion of the Laplace transform the Fourier inversion formula (1.23) can be used by plugging the complex continuation of the Laplace transform into it. In order to simplify (1.24) the help function  $h : \mathbb{R} \rightarrow \mathbb{R}$  is defined as follows,

$$h(x) := g(|x|).$$

The Fourier transform  $\hat{h}$  of  $h$  is given by

$$\begin{aligned} \hat{h}(t) &= \int_{-\infty}^\infty g(|x|) e^{itx} dx \\ &= 2 \int_0^\infty g(x) \cos(tx) dx = 2\Re\{\hat{g}(-it)\} = 2\Re\{\hat{g}(it)\}. \end{aligned}$$

Plugging  $\hat{h}$  into (1.24) results into the following inversion formula for the Laplace transform  $\hat{g}$  and  $x \geq 0$ ,

$$g(x) = \frac{2}{\pi} \int_0^\infty \Re\{\hat{g}(it)\} \cos(tx) dt \quad \text{a.e.} \quad (1.26)$$

Suppose  $g$  itself is not in  $L^1$ , then the Laplace transform of the damped version  $g_\alpha$  of  $g$  given by  $g_\alpha(x) = e^{-\alpha x} g(x)$  can be used if there exists an  $\alpha > 0$  such that  $g_\alpha$  is in  $L^1$ . By the complex continuation of (1.25) the following equality holds

$$\Re\{\hat{g}_\alpha(-it)\} = \Re\{\hat{g}(\alpha + it)\},$$

translating (1.26) into

$$g(x) = \frac{2e^{\alpha x}}{\pi} \int_0^\infty \Re\{\hat{g}(\alpha + it)\} \cos(tx) dt \quad \text{a.e.} \quad (1.27)$$

One crucial ingredient for both the Euler summation and the Gaussian quadrature method is the Poisson summation formula (PSF). It relates a sum of transformed function values to a sum of function values. Let  $f$  be in  $L^1$  and of bounded variation, then for all  $h > 0$  the Poisson summation formula is given by,

$$\sum_{j=-\infty}^\infty f\left(t + \frac{2\pi j}{h}\right) = \frac{h}{2\pi} \sum_{j=-\infty}^\infty \hat{f}(-jh) e^{ijht}. \quad (1.28)$$

An accessible treatment of the PSF can be found in [36] and a more detailed treatment in [83].

### 1.4.2 Euler summation

The Fast Fourier Transform (FFT) is the most popular numerical inversion method for Fourier transforms. A straightforward way of numerically inverting the Fourier transform is discretization and truncation of the integral in (1.24). The FFT is an efficient algorithm that computes a vector  $\vec{w}$  of length  $N$  from a vector  $\vec{x}$  of length  $N$  such that for each element  $w_k$  of  $\vec{w}$  the following holds,

$$w_k = \sum_{j=1}^N e^{-i\frac{2\pi}{N}(j-1)(k-1)} x_j, \quad \text{where } k = 1, \dots, N.$$

The algorithm is efficient in the sense that it takes order  $N \log N$  time to compute the vector  $w$  instead of order  $N^2$ .

Abate and Whitt propose in [4] a method to invert Laplace transforms. Their method is mainly based on truncation and discretization of (1.26). They obtain a numerical value  $g_{n,h}(x)$  using the trapezoidal rule,

$$g_{n,h}(x) = \frac{he^{\alpha x}}{\pi} \Re\{\hat{g}(\alpha)\} + \frac{2he^{\alpha x}}{\pi} \sum_{j=1}^n \Re\{\hat{g}(\alpha + jhi)\} \cos(jhx). \quad (1.29)$$

Let like in the previous paragraph  $g_\alpha(x) = e^{-\alpha x} g(x)$ . Using  $f(x) = g_\alpha(|x|)$  it again holds that

$$\hat{f}(t) = 2\Re\{\hat{g}(\alpha + it)\} = \hat{f}(-t).$$

Plugging this equation for  $\hat{f}$  into the PSF in (1.28) yields the following alternative Poisson summation formula,

$$\sum_{j=-\infty}^{\infty} g_\alpha \left( \left| x + \frac{2\pi j}{h} \right| \right) = \frac{h}{\pi} \Re\{\hat{g}(\alpha)\} + \frac{2h}{\pi} \sum_{j=1}^{\infty} \Re\{\hat{g}(\alpha + jh)\} \cos(jhx).$$

Comparing this version of the PSF to (1.29) shows that the discretization error can be obtained in the following way,

$$g(x) - \lim_{n \rightarrow \infty} g_{n,h}(x) = e^{\alpha x} \sum_{j=-\infty, j \neq 0}^{\infty} g_\alpha \left( \left| x + \frac{2\pi j}{h} \right| \right). \quad (1.30)$$

The next step is to eliminate the cosine terms in (1.29) by setting  $h = \pi/x$  resulting in

$$g_n(x) = \frac{e^{\alpha x}}{x} \Re\{\hat{g}(\alpha)\} + \frac{2e^{\alpha x}}{x} \sum_{j=1}^n (-1)^j \Re \left\{ \hat{g} \left( \alpha + \frac{j\pi}{x} i \right) \right\}, \quad (1.31)$$

where  $g_n(x)$  is shorthand notation for  $g_{n,\pi/x}(x)$ . If there exists a  $n_0$  such that  $\Re \left\{ \hat{g} \left( \alpha + \frac{j\pi}{x} i \right) \right\}$  is of constant sign for  $j > n_0$ , then  $g_n$  is an alternating

series. Abate, Choudhury and Whitt show in [1] that under some regularity conditions both the real and imaginary parts of a Fourier transform  $\hat{f}(v)$  are of constant sign for  $v > 0$  large enough. Now Abate and Whitt propose the use of Euler summation in order to exploit the alternating series property and speed up the convergence. The Euler summation  $E_{n,m}(x)$  is a binomial average over the partial sums  $g_n(x), g_{n+1}(x), \dots, g_{n+m}(x)$  given by

$$E_{n,m}(x) = \sum_{k=0}^m \binom{m}{k} 2^{-m} g_{n+k}(x). \quad (1.32)$$

More details about Euler summation can be found in [70]. In practice one might want to calculate the partial sums in (1.31) and control the error by first tuning  $\alpha$  resulting in an acceptable discretization error given by (1.30). The second step involves the use of explicit knowledge of  $f$  or  $g$  to obtain an estimate for the truncation bound. Unfortunately this truncation bound is very often too large, i.e., the number of terms that need to be evaluated to get the desired accuracy is huge. A way out might be the use of Euler summation, however, one has to be careful. The error bounds provided by the literature on Euler summation are only valid for alternating series. The series  $\{g_n(x)\}$  of partial sums given by (1.31) is not an alternating series in general, even in case some regularity conditions are satisfied, the series  $\{g_n(x)\}$  becomes alternating for  $n > n_0$  and unknown  $n_0$ . Abate and Valkó argue in [2] that it is not possible to come up with error bounds for general transforms and they recommend to use two algorithms, each with empirical error estimates.

### 1.4.3 Gaussian quadrature

In the previous section the PSF is used to get insight into the discretization error of numerical computation of the integral (1.27). The method of Den Iseger as presented in [53], uses the PSF in a different way and is based on an alternative representation of the PSF. This subsection summarizes the main ideas, for the one dimensional case, with just a few lines on the extension to two dimensions. Details on the multidimensional extension, numerical examples and fine tuning of the algorithm in order to deal with discontinuities are all in the original paper. Let the function  $g$ , defined on  $\mathbb{R}^+$ , be in  $L^1$  and of bounded variation. The Fourier transform of  $f$ , defined by

$$f(x) = 1_{\{x \geq 0\}} e^{-(\alpha + 2\pi i v)x} g(|x|),$$

is related to the complex continued Laplace transform of  $g$  in the following way,

$$\hat{f}(t) = \hat{g}(\alpha + i(2\pi v - t)). \quad (1.33)$$

Now plug (1.33) into (1.28) and choose  $t = 0$  and  $h = 2\pi$  to obtain an alternative form of the Poisson summation formula

$$\sum_{j=0}^{\infty} e^{-(\alpha+2\pi iv)j} g(j) = \sum_{j=-\infty}^{\infty} \hat{g}(\alpha + i2\pi(v + j)). \quad (1.34)$$

The left hand side of this equation represents the discrete Fourier transform. The key idea is now to view the infinite sum as an integral and compute numerical values for this sum by applying Gaussian quadrature to the integral. A more detailed treatment of the summary on Gaussian quadrature than is given here can be found in [70]. For a function  $f$  and a measure  $\mu$  the following approximation of the integral,

$$\int_{\mathcal{I}} f(x)\mu(dx) \approx \sum_{j=1}^n H_j f(a_j), \quad (1.35)$$

is called a Gaussian quadrature of  $\mu$  on the interval  $\mathcal{I}$  if the sets of weights  $H_j$  and evaluation points  $a_j$  are chosen in such a way that the approximation is exact for  $f$  a polynomial of degree  $2n - 1$  or less. Let  $\{q_i\}_{i=0,1,\dots,n}$  be a set of orthogonal polynomials w.r.t. the usual inner product defined on  $\mathcal{I}$  by the measure  $\mu$ . Then the evaluation points  $a_j$  in (1.35) are given by the zeros of  $q_n$  and the weights  $H_j$  are given by

$$H_j = \left( \sum_{k=0}^{n-1} |q_k(a_j)|^2 \right)^{-1}. \quad (1.36)$$

Now the problem is to choose a measure  $\mu$  and an interval  $\mathcal{I}$  to write the right-hand side sum in (1.34) by an integral and, thereafter, to identify the corresponding set of orthogonal polynomials needed to compute the evaluation points and the weights. One needs to be careful choosing the interval and measure, because polynomials of any degree should be integrable. Den Iseger makes in [53] the following choice,

$$\mu(A) = \sum_{k=-\infty}^{\infty} \frac{1}{(\pi(2k-1))^2} 1_A \left( \frac{1}{\pi(2k-1)} \right), \quad (1.37)$$

and with the notation

$$\tilde{g}_{\alpha,v}(x) := \hat{g}(\alpha + i\pi(2v+1) + ix^{-1}),$$

the sum in (1.34) can be written as an integral over  $\mathcal{I} = \mathbb{R}$  in the following way,

$$\sum_{j=-\infty}^{\infty} \hat{g}(\alpha + i2\pi(v+j)) = \int_{-\infty}^{\infty} x^{-2} \tilde{g}_{\alpha,v}(x) \mu(dx).$$

The choice of  $\mu$  in (1.37) might look arbitrarily. The choice of the indicator function argument  $(\pi(2k-1))^{-1}$  is motivated by the necessity of integrating polynomials on the entire interval. The  $(\pi(2k-1))^{-2}$  in front of the indicator is put there to take care of the integrability of the polynomials of degree one and zero. The reason to leave the  $v$  out of the measure, and put it into the function  $\tilde{g}$ , is that one does not need to come up with a different set of orthogonal polynomials for every  $v$ . Therefore, by leaving  $v$  out of the measure it is possible to pre-calculate the weights and evaluation points and reuse them for every  $v$  in the approximation one wants to have of (1.34). Identifying the set of orthogonal polynomials starts from the Legendre polynomials on  $[0, 1]$  denoted by  $p_n$ . By Parseval's equation the Fourier coefficients  $\hat{p}_n(k)$  of the Legendre polynomials  $p_n$  are orthogonal w.r.t. the inner product on the sequence space. Relating the sum representing this inner product to an integral w.r.t. the measure  $\mu$  shows that the set of polynomials  $\{q_i\}_{i=1,2,\dots}$  is orthogonal, where each  $q_n$  is given by

$$q_n(x) = h_n(-ix) + (-1)^n h_n(ix),$$

and  $h_n$  denotes the following polynomial

$$h_n(x) = \sqrt{2n+1} \sum_{k=0}^n \frac{(k+n)!}{(n-k)!} \frac{(-x)^k}{k!}.$$

For some  $N$  the zeros of  $q_N$  are the evaluation points  $a_j$  for  $j = 1, \dots, N$  and the weights  $H_j$  are computed corresponding to (1.36) resulting in the following approximation,

$$G_\alpha(v) = \sum_{j=0}^{\infty} e^{-(\alpha+2\pi iv)j} g(j) \approx \sum_{j=1}^N H_j \frac{\hat{g}\left(\alpha + i\pi(2v+1) + ia_j^{-1}\right)}{a_j^2},$$

where  $G_\alpha$  is the discrete Fourier transform or z-transform of  $e^{-\alpha x} g(x)$ . Den Iseger uses in [53] the results of Abate and Whitt in [3] to obtain values for  $g$  by

$$g(k) \approx \frac{e^{\alpha k}}{M} \sum_{j=0}^{M-1} \cos\left(\frac{2\pi jk}{M}\right) \Re \left\{ G_\alpha\left(\frac{j}{M}\right) \right\}.$$

Tuning the algorithm is equivalent to choosing values for the damping factor  $\alpha$ , the number of points in the Gaussian quadrature  $N$  and the number of points in the discrete Fourier transform inversion  $M$ . Again it is very hard to come forward with error bounds, but for smooth functions the quadrature rule is very accurate. Den Iseger shows that for a specific choice of parameters the algorithm returns numerical values with an accuracy which is near machine precision and the algorithm does it surprisingly quickly. It

is also possible to evaluate  $g$  at the non-integer points  $k\Delta$  for  $k = 0, 1, \dots$  by inverting the Laplace transform  $\hat{g}_\Delta$  given by,

$$\hat{g}_\Delta(s) = \frac{1}{\Delta} \hat{g}\left(\frac{s}{\Delta}\right).$$

The surprising speed of the algorithm in one dimension makes it possible not only theoretically but also practically to extend the algorithm to two dimensions. Starting from a two-dimensional Poisson summation formula and using the same idea of approximating the double sum of two dimensional Laplace transforms via a double integral by Gaussian quadrature one arrives at an algorithm for two dimensional numerical inversion. This two dimensional numerical inversion is applied in the paper on double-sided barriers, which can be found in chapter five.

## Chapter 2

# The implied barrier concept

Research into the direction of specific exotic options - like the Parisians - is often driven by the analysis of structured products. These products contain features that are similar to exotic options. Exchange-trading of the pure exotics is very rare. In the period of rising stock markets, investors were less interested in buying bonds. In order to regain their interest, firms added extra features to the bonds they wanted to issue. One of these features is the right of the bond holder to convert the bond into a given number of stocks under certain conditions. Bonds with this feature are called convertible bonds and are nowadays very common. Most convertible bonds can be re-called by the issuer when the convertible trades above some level for some period. Modeling this feature corresponds to valuation of a Parisian option. In this paper we will point out how we quickly can approximate the Parisian option price by using a standard barrier option with a modified barrier. This is common practice for traders; they increase or decrease the barrier a bit. Here we want to argue what that bit should be. First we will introduce the Parisian contract. Thereafter we list the methods of valuing the Parisian, followed by a section about the implied barrier method. Here we will use concepts from the theory on Brownian excursions and exploit them to derive prices for Parisians that are already in the excursion. We will conclude with a numerical example.

### 2.1 The Parisian contract

Let  $\{S_t, \mathcal{F}_t; t \geq 0\}$  be a process defined on the filtered probability space  $(\Omega, \mathcal{F}, \mathcal{F}_t, \mathbb{P})$ . According to the Black-Scholes model we have for the risk neutral price process

$$S_t = s_0 \exp((r - 0.5\sigma^2)t + \sigma B_t),$$

where  $\{B_t, \mathcal{F}_t; t \geq 0\}$  denotes a standard Brownian motion,  $s_0$  the initial value of the stock,  $r$  the interest rate and  $\sigma$  the volatility. We can use this risk-neutral stock price process to calculate the price of a derivative  $V_\Phi$  with some (path dependent) pay-off  $\Phi((S_t)_{0 \leq t \leq T})$  at time  $T$  by,

$$V_\Phi = e^{-rT} \mathbb{E} [\Phi((S_t)_{0 \leq t \leq T})].$$

Here  $\Phi$  is the contract function. A standard barrier option is a derivative that pays off like a put or a call that knocks in or out as soon as the stock price hits some level. The Parisian option is like a barrier, but we do not only assume the stock price to hit some level, but also to stay above or below that level for a given time. For a given  $t$  let  $\gamma_t$  be the last time before  $t$  that the process was at level  $L$ ,

$$\gamma_t := \sup_{s \leq t} \{S_s = L\}.$$

Now we can use this random time to define  $T_D^-$ , the first time  $(S_t)_{t \geq 0}$  is below  $L$  longer than  $D$  and  $T_D^+$  the equivalent random time for staying above  $L$  by

$$T_D^- := \inf_{t > 0} \{t - \gamma_t > D; S_t < L\} \quad \text{and} \quad T_D^+ := \inf_{t > 0} \{t - \gamma_t > D; S_t > L\}.$$

For an up and down Parisian we use  $T_D^+$  respectively  $T_D^-$ . If it is a knock in we consider the set  $\{T_D^\pm \leq T\}$  otherwise we consider its complement. With this notation we can write pricing formulas for all kinds of Parisian options, e.g. the Parisian down and in call is given by

$$V_{PDIC} = e^{-rT} \mathbb{E} \left[ (S_T - X)^+ 1_{\{T_D^- \leq T\}} \right],$$

where  $X$  denotes the strike of the call. By changing the set of the indicator, we can calculate all variations of down/out and up/in. By changing the left part of the pay-off, we can compute prices for Parisian puts instead of calls.

## 2.2 Valuation methods for Parisians

There are two well-known methods for valuing Parisians. One method [49] uses the Black-Scholes PDE with boundary conditions adapted to the Parisian contract. This modified PDE is then solved by numerical methods. The advantage of this method is, that the pricing framework is flexible, i.e. it is possible to deal with discrete dividends and early exercise. The disadvantage is that the convergence is slow. There are methods using some pre-calculated values [47] to increase this convergence. This method is relatively time-consuming in the sense that it is inappropriate for real-time option pricing.

Another method calculates the Laplace Transforms of these option prices

[30]. There exist quick inversion algorithms [4] to obtain the prices within a given error bound.

Here we propose another method, the so-called implied barrier method. This method consists of coming up with an implied barrier  $L^*$ . Then the standard barrier option with barrier  $L^*$  and the remaining parameters equal to the Parisian has the same price as the Parisian. This method only uses standard barrier formulae for the European case and obtaining prices is neither difficult nor time-consuming.

### 2.3 The implied barrier

Explaining the implied barrier method is threefold. At first we define the implied barrier and give a numerical example. Then we come up with heuristics about what the implied barrier should be and use excursion theory to obtain a formula for it. Finally, we will show for a practical example that prices are quite close. Denoting the first time  $(S_t)$  hits  $L$  by  $T_L$ , the price of a call with barrier  $L^*$  is given by

$$V_{DIC} := e^{-rT} \mathbb{E} [(S_T - X)^+ 1_{\{T_{L^*} \leq T\}}].$$

We know that for  $L = L^*$  the Parisian option should have a value smaller than this standard barrier, but positive. By decreasing  $L^*$  we can have the value of this barrier every value between the  $(L^* = L)$ -case and 0, so for some particular  $L^*$  the standard barrier has the same price as the Parisian. This particular value of  $L^*$  is defined as the implied barrier and can formally be stated as:

#### Definition

Let  $\Phi(S_T)$  the vanilla part of the pay-off of a Parisian Up contract. Then for  $L > S_0$  the implied barrier  $L^*$  is defined by

$$\mathbb{E}[\Phi(S_T) 1_{\{T_{D^+,L} \leq T\}}] = \mathbb{E}[\Phi(S_T) 1_{\{T_{L^*} \leq T\}}].$$

For  $L < S_0$  we define the implied barrier  $L^*$  by

$$\mathbb{E}[\Phi(S_T) 1_{\{T_{D^-,L} \leq T\}}] = \mathbb{E}[\Phi(S_T) 1_{\{T_{L^*} \leq T\}}].$$

By continuity it is clear that  $L^*$  always exists. In the graph in figure 2.1 we show the implied barrier for a down-and-in Parisian call for different times to maturity and different values of  $s_0$ . The Parisian prices we needed for finding this barrier are computed by a numerical inversion of the Laplace Transforms. For this particular option the graph shows that the implied barrier is in the same range for different  $T$  and  $s_0$ . However, by basic monotonicity arguments we have the following proposition.

**Proposition**

Let  $\Phi(S_T)$  be the vanilla part of a Parisian contract. Suppose for a down contract with  $L < S_0$  that for some finite  $T > D > 0$  we have

$$\mathbb{E}[\Phi(S_T)1_{\{T_D^-, L \leq T\}}] > 0.$$

Then  $L^*(t, s)$ , the implied barrier for this contract with maturity  $t$  and initial stock price  $s$  cannot be the same for every  $t \in [D, T]$  and fixed  $s = s_0$ . Moreover  $L^*(t, s)$ , cannot be the same for every  $s > L$  and fixed  $t = T$ .

Considering the scale of the vertical axis figure 2.1, we will try to approximate this implied barrier by a constant. In the next section we arrive intuitively at the approximation. Using this approximation we come up with a numerical example.

## 2.4 Approximating the implied barrier

In order to arrive at the approximation, we argue that the implied barrier should be - whether the contract is of the up or down type - the minimum or maximum we expect  $(S_t)$  to attain, given that the stock follows a path in the Parisian set. For the Parisian

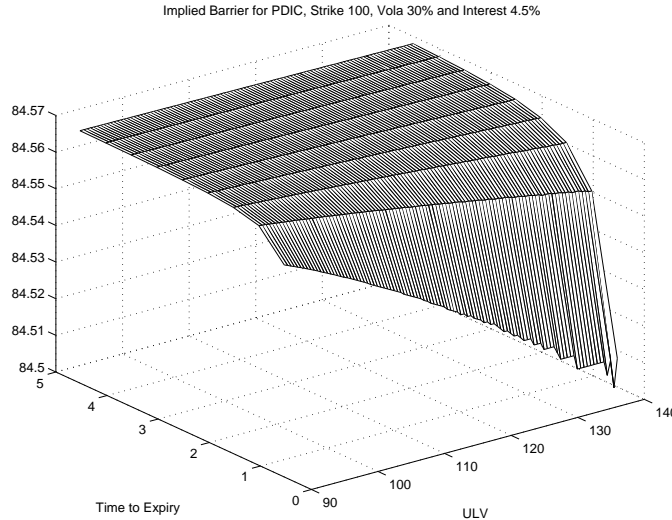


Figure 2.1: Implied Barrier vs  $s_0$  and  $T$

contracts we are interested in the set  $\{T_D^\pm \leq T\}$  and its complement. So, either the realizations of  $(S_t)$  do contain an excursion in the right direction w.r.t. to  $L$  longer than  $D$  or not. If we consider for example the down and in version and divide the stock path into its excursions from  $L$ , we can compute the expected minimum that is attained in each separate excursion

below  $L$ . The minimum the stock path attains up to time  $T$  is the minimum of all these expected minima per excursion. We know from excursion theory that the expected minimum of an excursion decreases when the length of the excursion increases. In this down and in case we know that we need to have at least one excursion longer than  $D$ , so the expected minimum of the knocking-in stock paths should be below the minimum that we expect to attain during an excursion below  $L$  of length  $D$ . Using Brownian excursion theory [31, 39] we have for the expected minimum  $m_D$  of a Brownian excursion with length  $D$

$$\mathbb{E}[m_D] = -\sqrt{\frac{D\pi}{2}}.$$

As we are dealing with geometric Brownian motion, this term will appear within an exponential. Furthermore we are considering an excursion around the level  $L$ , so we find the following approximation  $\tilde{L}^*$  for the implied barrier  $L^*$

$$\tilde{L}^* := L \exp\left(-\sigma\sqrt{D}e^{-\frac{m^2}{2}D}\sqrt{\frac{\pi}{2}}\right) \quad \text{where} \quad m := \frac{r - 0.5\sigma^2}{\sigma}.$$

Here the  $m$  is introduced as a consequence of the Girsanov transformation, that is needed in cases where  $r \neq 0.5\sigma^2$ . The same argumentation holds for the other types of Parisians (up/down, out/in), where the minus sign in the exponent disappears for the up-variant of the Parisian contract. Now we use the  $\tilde{L}^*$  to approximate the value  $V_{PDIC}(L)$  by  $V_{PDIC}(\tilde{L}^*)$ . In the next section we show how we deal with Parisians that are already in the excursion.

## 2.5 Valuing Parisians that are already in the excursion

Here we value a Parisian option at time  $t > 0$ . Suppose we are interested in the  $PDIC$  with some barrier  $L$ . In the case  $S_t < L$ , the excursion of the stock path below  $L$  has already started and this effects its value. Define  $d$  as the time the stock already spent below  $L$  by

$$d := t - \gamma_t.$$

Here we are interested in the case where  $d < D$  and another excursion longer than  $D$  did not happen yet. It is clear that we have two possibilities now. Either we return to the level  $L$  too early to knock in, i.e. we are in the set  $\{T_L \leq D - d\}$ , or, we are in the complement of this set, and so stay long enough to knock in. Here we abuse the notation  $T_L$  for the amount of time we have to wait after time  $t$  to hit the level  $L$ , that we should write as  $T_L^t$  given by

$$T_L^t = \inf_{s>0} \{S_{s+t} = L\}.$$

In the same way we will abuse the notation of  $T_{D,L}^-$ . Considering these two cases we could be in, the value of a PDIC is given by

$$V_{PDIC}(d) = e^{-r(T-t)} \mathbb{E} \left[ (S_T - X)^+ 1_{\{T_L > D-d\}} | \mathcal{F}_t \right] + e^{-r(T-t)} \mathbb{E} \left[ (S_T - X)^+ 1_{\{T_{D,L}^- < T-t\}} 1_{\{T_L \leq D-d\}} | \mathcal{F}_t \right].$$

So, in the case that we stay long enough below  $L$  we get a standard call, otherwise we get a fresh  $PDIC$  for the remaining time to expiry. If we write  $1_{\{T_L > D-d\}} = 1 - 1_{\{T_L \leq D-d\}}$ , we find for  $V_{PDIC}(d)$

$$V_{PDIC}(d) = V_{BSC} - e^{-rT'} \mathbb{E} \left[ (S_t e^{(r-\sigma^2/2)T' + \sigma B_{T'}} - X)^+ 1_{\{T_{D,L}^- > T'\}} 1_{\{T_L \leq D-d\}} \right].$$

Here  $V_{BSC}$  is the value of a standard call with time to expiration  $T' := T - t$  and we used the Markov property to remove the conditioning. Now we change our measure to  $\mathbb{Q}$  in the same way as above. Conditioning on  $\mathcal{F}_{T_L}$  gives

$$V_{PDIC}(d) = V_{BSC} - e^{-\tilde{r}T'} \mathbb{E}_{\mathbb{Q}} \left[ 1_{\{T_L \leq D-d\}} \mathbb{E}_{\mathbb{Q}} \left[ e^{mZ_{T'}} (S_t e^{\sigma Z_{T'}} - X)^+ 1_{\{T_{D,L}^- > T'\}} | \mathcal{F}_{T_L} \right] \right],$$

where  $\tilde{r}$  is defined by  $\tilde{r} := r - 0.5m^2$ . Using the Markov property again, we recognize  $V_{PDOC}(T' - T_L)$  apart from the proper discounting, so we get

$$V_{PDIC}(d) := V_{BSC} - e^{ml} \mathbb{E}_{\mathbb{Q}} \left[ 1_{\{T_L \leq D-d\}} e^{-\tilde{r}T_L} V_{PDOC}(T' - T_L) \right],$$

where  $l$  is defined by  $l = \sigma^{-1} \ln \frac{L}{S_t}$ . Using the distribution of the hitting time [31] we can calculate the expectation. If we furthermore approximate  $V_{PDOC}(T' - T_L)$  by  $V_{DOC}(\tilde{L}^*, T' - T_L)$  we obtain

$$V_{PDIC}(d) := V_{BSC} - \int_0^{D-d} V_{DOC}(\tilde{L}^*, T' - u) \frac{|l| e^{ml - \tilde{r}u - \frac{l^2}{2u}}}{\sqrt{2\pi u^3}} du.$$

This integral should be computed numerically. In the example later on we will show that a relatively small number of steps is sufficient to obtain a value close to the true Parisian price. The same way of reasoning could be used to derive prices for the other types of Parisian contracts.

## 2.6 Numerical examples

As we presented our method as one that can be very useful in practice, we will give some numerical results. Table 2.1 contains a comparison between implied barrier prices and Laplace prices.

Table 2.1: Prices for PDIC at  $t = 0$ 

$S_0=100, L=90$		D = 10/365				D = 20/365				D=200/365			
		Laplace		Imp Bar		Laplace		Imp Bar		Laplace		Imp Bar	
X		T=1	T=2	T=1	T=2	T=1	T=2	T=1	T=2	T=1	T=2	T=1	T=2
80	r=4.5%	6.54	11.36	6.55	11.36	4.97	9.42	4.99	9.43	0.26	1.68	0.35	1.77
90	$\sigma=30\%$	3.84	8.23	3.84	8.23	2.79	6.69	2.80	6.69	0.08	0.99	0.14	1.06
100		2.18	5.92	2.18	5.92	1.52	4.72	1.52	4.72	0.02	0.58	0.05	0.64
110		1.21	4.25	1.21	4.25	0.81	3.32	0.81	3.32	0.01	0.34	0.02	0.39
	ImpBar			84.57	84.57			82.42	82.42			68.13	68.13
<hr/>													
80	r=2.5%	8.53	14.38	8.54	14.38	6.51	11.98	6.53	11.99	0.35	2.21	0.48	2.35
90	$\sigma=40\%$	5.74	11.30	5.75	11.31	4.24	9.27	4.25	9.28	0.15	1.48	0.24	1.60
100		3.84	8.91	3.84	8.91	2.74	7.20	2.75	7.20	0.06	1.00	0.12	1.10
110		2.55	7.04	2.56	7.04	1.77	5.61	1.78	5.62	0.03	0.68	0.06	0.77
	ImpBar			85.45	85.45			80.04	80.04			62.22	62.22

Table 2.2: Deltas for PDIC at  $t = 0$ 

$S_0=100, L=90$		D = 10/365				D = 20/365				D=200/365			
		Laplace		Imp Bar		Laplace		Imp Bar		Laplace		Imp Bar	
X		T=1	T=2	T=1	T=2	T=1	T=2	T=1	T=2	T=1	T=2	T=1	T=2
80	r=4.5%	-0.34	-0.40	-0.34	-0.40	-0.27	-0.35	-0.27	-0.35	-0.03	-0.09	-0.03	-0.09
90	$\sigma=30\%$	-0.23	-0.32	-0.23	-0.32	-0.18	-0.28	-0.18	-0.27	-0.01	-0.06	-0.01	-0.06
100		-0.15	-0.26	-0.15	-0.25	-0.11	-0.21	-0.11	-0.21	0.00	-0.04	0.00	-0.04
110		-0.09	-0.20	-0.09	-0.20	-0.06	-0.16	-0.06	-0.16	0.00	-0.02	0.00	-0.02
	ImpBar			84.57	84.57			82.42	82.42			68.13	68.13
<hr/>													
80	r=4.5%	-0.29	-0.32	-0.29	-0.32	-0.24	-0.28	-0.24	-0.28	-0.03	-0.08	-0.03	-0.08
90	$\sigma=30\%$	-0.23	-0.28	-0.22	-0.28	-0.18	-0.24	-0.18	-0.24	-0.01	-0.06	-0.02	-0.06
100		-0.17	-0.24	-0.17	-0.24	-0.13	-0.20	-0.13	-0.20	-0.01	-0.04	-0.01	-0.04
110		-0.12	-0.20	-0.12	-0.20	-0.09	-0.17	-0.09	-0.17	0.00	-0.03	0.00	-0.03
	ImpBar			85.45	85.45			80.04	80.04			62.22	62.22

Here we see that prices are close to the inverse Laplace prices for  $D$  relatively small compared to  $T$ . Furthermore we see that the implied barrier that is found in the upper left corner (i.e. 84.57), is recognized in the implied barrier graph in figure 2.1 for the same case as shown above. As we would like to use the prices for relatively small  $D$ , we also need deltas for  $D$  relatively large compared to  $T$ . Table 2.2 shows that the error in the deltas is much less than that in the prices.

We also computed prices for Parisians based on a stock path that is already in the excursion. Table 2.3 lists these prices.

As these computations involved numerical integration we have to choose a number of integration steps. In this numerical approximation the interval is divided into 25 steps for  $D = 10/365$  and  $D = 20/365$ . We divided it into 250 steps for  $D = 200/365$ . The results are analogous to the former price

Table 2.3: Price for PDIC at  $t > 0$  and  $d > 0$ 

r=4.5%, $\sigma=30\%$		D = 10/365				D = 20/365				D=200/365			
$S_0=100, L=90$		Laplace		Imp Bar		Laplace		Imp Bar		Laplace		Imp Bar	
X	d	T=1	T=2	T=1	T=2	T=1	T=2	T=1	T=2	T=1	T=2	T=1	T=2
80	0.2D	13.04	18.56	13.04	18.56	11.02	16.40	11.02	16.41	1.40	4.16	1.51	4.24
100	0.2D	5.44	10.77	5.45	10.77	4.34	9.26	4.35	9.26	0.27	1.75	0.31	1.81
80	0.6D	13.98	19.52	13.97	19.52	12.59	18.05	12.59	18.05	2.79	5.92	2.95	5.99
100	0.6D	5.99	11.46	5.99	11.46	5.22	10.43	5.22	10.43	0.82	2.82	0.86	2.88
ImpBar				84.57	84.57			82.42	82.42			68.13	68.13

Table 2.4: Deltas for PDIC at  $t > 0$  and  $d > 0$ 

r=4.5%, $\sigma=30\%$		D = 10/365				D = 20/365				D=200/365			
$S_0=100, L=90$		Laplace		Imp Bar		Laplace		Imp Bar		Laplace		Imp Bar	
X	d	T=1	T=2	T=1	T=2	T=1	T=2	T=1	T=2	T=1	T=2	T=1	T=2
80	0.2D	0.03	0.02	0.02	0.02	-0.25	-0.28	-0.25	-0.28	-0.15	-0.26	-0.14	-0.26
100	0.2D	0.02	0.02	0.02	0.02	-0.12	-0.19	-0.12	-0.19	-0.04	-0.13	-0.03	-0.13
80	0.6D	0.28	0.29	0.28	0.29	-0.19	-0.21	-0.19	-0.21	-0.40	-0.58	-0.39	-0.57
100	0.6D	0.16	0.21	0.16	0.21	-0.09	-0.14	-0.09	-0.14	-0.14	-0.33	-0.13	-0.32
ImpBar				84.57	84.57			82.42	82.42			68.13	68.13

table. The prices are quite good for  $D$  relative small compared to  $T$ . Again we will compute for this particular case the deltas to show that they do not differ that much, as is shown in table 2.4.

## 2.7 Conclusion

Valuation of Parisian options is important as popular investment tools like convertible bonds exhibit the Parisian option feature. Well known methods for calculating its price are either computationally slow (PDE method) or inflexible (Laplace method). Here we provide a way to use standard barrier models with an implied barrier for calculating prices. The advantages of this method for trading firms are threefold. First, no new model has to be implemented. Moreover it is possible to value the American options with a Parisian constraint, by using the implied barrier in the standard American barrier option. Discrete dividends can be taken into account. Finally a lot has been done pricing barriers in a non-constant volatility environment. Using the implied barrier concept again might yield an approximation of the Parisian price in such an environment.

## Chapter 3

# Double-sided Parisian options

In this paper we derive Fourier transforms for double-sided Parisian option contracts. The double-sided Parisian option contract is triggered by the stock price process spending some time above an upper level or below some lower level. The double-sided Parisian knock-in call contract is the general type of Parisian contract from which also the single-sided contract types follow. We also discuss the Fourier inversion in the paper and conclude with a series of numerical examples, explaining the Parisian optionality by studying price behavior and peculiar behavior of the Greeks.

### 3.1 Introduction

The Parisian option is a kind of a barrier option with the difference that the contract is not specified in terms of touching a barrier, but in terms of staying above or below the barrier for a certain period of time. The interest in these options is motivated by the study of structured products, insurance and investment problems. Convertible bonds and problems in real options contain Parisian optionality; the Parisian option contract itself is at present time not exchange traded. Details about the practical differences between standard barrier options and Parisian options are discussed in [30], the first paper on Parisian options. The way Parisian options turn up in real option problems is treated in [43], for an application in the direction of convertible bonds see [61]. For applications in credit risk and life insurance see [66] and [27] respectively. The authors in [30] derived Laplace transforms for the single-sided version, which is extended in [43] to a Parisian type of contract that is triggered by staying a period of time above the barrier or hitting a level exceeding this barrier. Chesney and Gauthier treat American Parisian

options in [28]. Here we treat the pricing of the double-sided Parisian option and, like the papers previously mentioned, we use Fourier (or Laplace) transforms to achieve this. The calculation of Fourier transforms instead of Laplace transforms is motivated by the fact that a lot of numerical Laplace inversion algorithms are using the complex continuation of Laplace transforms to Fourier transforms for the actual inversion, see e.g. [53]. As we want to conclude our paper by a section on numerical examples, we have to invert the Fourier transforms we will calculate. In [49] the authors treat a PDE method approach to solve the Parisian option pricing problem, but convergence turns out to be rather slow, which is a result of the local behavior of Brownian motion.

The reason to treat double-sided Parisian options, apart from that there may be practical applications to this type of optionality, is that this contract type is rather general. After analyzing the double-sided Parisian knock-in call contract, we are able to give prices for the single-sided versions as well. We do not need to derive separate formulas for Parisian down-and-out calls, Parisian up-and-in puts and so on. Prices for all of these contract types can be computed from the Fourier transform of the double-sided Parisian knock-in call. The concluding numerical examples will show the reader how the various Parisian option types, that can be constructed from the double-sided Parisian knock-in call, behave. The double-sided Parisian option treated by [60] differs from the one treated here as will be pointed out in the next section.

The paper is organized as follows. In the first section we introduce the double-sided Parisian option and the relevant notation. In order to price the contract, we rewrite the pricing problem into the problem of calculating a probability. In the second section we derive Laplace transforms for the double-sided Parisian stopping time and the value of the standard Brownian motion at that stopping time. The third section treats the actual Fourier transform calculation, where some technical details are deferred to the appendix. The next section treats the case where the life of the option has been started and we are possibly for some time period already below the lower barrier or above the upper barrier. The author in [78] has extended the results of the original paper of [30] to incorporate this case. Section 3.6 discusses the Parisian put contract type, and section 3.7 summarizes all the contract types that can be derived from the double-sided Parisian knock-in call. In this section we touch upon the double-sided barrier option, of which pricing by transforms has been done in [44]. More on the relation between double-sided barrier and standard barrier options can be found in [58], where we use the algorithm in [73] to obtain double-sided barrier prices in our numerical examples. In section 3.8 we discuss the Fourier inversion and propose an alternative algorithm. We conclude by a section on numerical examples showing various features of the double-sided Parisian option price and Greeks.

### 3.2 The Parisian contract

Let  $(\Omega, \mathcal{F}, \mathbb{P})$  be a probability space with filtration  $\{\mathcal{F}_t\}$  and  $(W_t)_{t \geq 0}$  be a standard Brownian motion with respect to this filtration. By  $(S_t)_{t \geq 0}$  we denote the risk-neutral stock price process, given by the classical geometric Brownian motion,

$$S_t = S_0 e^{(r - \frac{1}{2}\sigma^2)t + \sigma W_t},$$

where  $r$  and  $\sigma$  are the risk-free interest rate and the volatility respectively. In this setup  $\mathbb{P}$  is the risk-neutral measure or, equivalently, the pricing measure and not the physical measure. Assuming that there exists a bank-account that pays the risk-free interest rate  $r$  in a continuously compounded way, the price of an option with a (random) pay-off is given by the discounted expectation of that pay-off under the pricing measure. The random time  $\gamma_T^L(S)$  measures the last time before  $T$  that a process  $S$  has been equal to  $L$  and is given by,

$$\gamma_T^L(S) := \begin{cases} \sup\{0 \leq t \leq T | S_t = L\} & T_L(S) \leq T, \\ 0 & T_L(S) > T. \end{cases} \quad (3.1)$$

Here  $T_L(S)$  denotes the hitting time of the level  $L$  by the process  $S$ . Note that  $\gamma_T^L$  is not a stopping time. In case the process is a standard Brownian motion, we suppress the  $W$  between brackets that you would expect to appear in (3.1). Now we define the double-sided Parisian stopping time  $T_{D_1, D_2}^{L_1^-, L_2^+}(S)$  for the levels  $L_1 < L_2$  by,

$$T_{D_1, D_2}^{L_1^-, L_2^+}(S) := \min\left(T_{D_1}^{L_1^-}, T_{D_2}^{L_2^+}\right), \quad (3.2)$$

where the single-sided Parisian stopping time  $T_D^{L^\pm}$  is given by,

$$T_D^{L^\pm} = \inf\left\{t > 0 \mid (t - \gamma_t^L(S))1_{\{S_t \gtrless L\}} > D\right\}.$$

The stopping time  $T_{D_1, D_2}^{L_1^-, L_2^+}(S)$  is the first time that the process  $S$  stays longer than time  $D_1$  below level  $L_1$  *or*<sup>1</sup> longer than time  $D_2$  above level  $L_2$ . The double-sided Parisian knock-in call is a contract that pays off like a standard call only in the scenarios where the double-sided Parisian stopping time occurs before the time of expiry. The value  $V_{DPIC}$  of this double-sided Parisian knock-in call can be computed by,

$$V_{DPIC} = e^{-rT} \mathbb{E} \left[ (S_T - K)^+ 1_{\{T_{D_1, D_2}^{L_1^-, L_2^+}(S) \leq T\}} \right]. \quad (3.3)$$

---

<sup>1</sup>In [60] the double-sided contract type is treated where the process  $S$  should stay longer than time  $D_1$  below level  $L_1$  *and* longer than time  $D_2$  above level  $L_2$ .

As in [24] we are going to split this expectation into two probabilities, where we use the Girsanov transform to obtain the result. In order to shorten the notation, we replace the indicator by a functional  $I$  that maps the paths on the time interval  $[0, T]$  of  $S$  into either the value 0 or 1, so we write,

$$\begin{aligned} \mathbb{E} [(S_T - K)^+ I(S)] &= \\ \mathbb{E} [S_T I(S) 1_{\{S_T > K\}}] - K \mathbb{P} [I(S) = 1; S_T > K]. \end{aligned} \quad (3.4)$$

Transforming the expectation on the right-hand side into a probability is the step based on the Girsanov theorem. If we construct a new measure  $\mathbb{Q}$  by,

$$\left. \frac{d\mathbb{Q}}{d\mathbb{P}} \right|_{\mathcal{F}_T} = \frac{S_T}{S_0 e^{rT}} = e^{-\frac{1}{2}\sigma^2 T + \sigma W_T},$$

then the process  $W_t - \sigma t$  is a Brownian motion under  $\mathbb{Q}$  and therefore  $S$  rewritten by,

$$S_t = S_0 e^{(r + \sigma^2 - \frac{1}{2}\sigma^2)t + \sigma(W_t - \sigma t)},$$

is a GBM under  $\mathbb{Q}$  with drift  $r + \sigma^2$  instead of  $r$ . We recognize the stochastic part of the Radon-Nikodým derivative in (3.4) and rewrite it into,

$$\mathbb{E} [(S_T - K)^+ I(S)] = S_0 e^{rT} \mathbb{Q} [I(S) = 1; S_T > K] - K \mathbb{P} [I(S) = 1; S_T > K].$$

The last equation states that the double-sided Parisian knock-in call can be priced in terms of the following probability,

$$P_\mu(T) = \mathbb{P}_\mu \left[ S_T \geq K; T_{D_1^-, D_2^+}^{L_1^-, L_2^+}(S) \leq T \right], \quad \mu \in \mathbb{R}, \quad (3.5)$$

where  $\mu$  stands for the drift of the geometric Brownian motion  $S$ . By (3.5) we obtain for  $V_{DPIC}$  the following expression,

$$V_{DPIC} = S_0 P_{r+\sigma^2}(T) - K e^{-rT} P_r(T). \quad (3.6)$$

The problem of pricing this double-sided Parisian knock-in call is equivalent to computing the probability as given in (3.5). The stochastic properties of the stock price process  $S$  are entirely determined by the behavior of the underlying Brownian motion, so it is a natural choice to solve the problem in terms of the Brownian motion. If we introduce the process  $(\tilde{W}_t)_{t \geq 0}$  by,

$$\tilde{W}_t := \frac{r - \frac{1}{2}\sigma^2}{\sigma} t + W_t = mt + W_t, \quad (3.7)$$

then we can write  $S_t$  the stock price at  $t$  as  $S_0 e^{\sigma \tilde{W}_t}$ . The events in terms of  $S$  can be rewritten into events in terms of  $\tilde{W}$  like,

$$\{S_T > K\} = \{\tilde{W}_T > k\} \quad \text{where} \quad k = \frac{1}{\sigma} \ln \left( \frac{K}{S_0} \right).$$

In the same manner for  $i = 1, 2$  the levels  $L_i$  transform into  $l_i$  resulting in  $\gamma_T^{L_i}(S) = \gamma_T^{l_i}(\tilde{W})$ . A change of measure allows us to compute the quantity  $P_r(T)$  by,

$$P_r(T) = e^{-\frac{1}{2}m^2T} \mathbb{E} [e^{mW_T} \mathbf{1}_{\{W_T > k\}} \mathbf{1}_{\{\tau \leq T\}}], \quad (3.8)$$

where we used  $\tau$  as a shorthand notation for  $T_{D_1, D_2}^{l_1^-, l_2^+}(W)$ . The same kind of notation we introduce for  $\tau^+$  and  $\tau^-$  abbreviating respectively  $T_{D_2}^{l_2^+}(W)$  and  $T_{D_1}^{l_1^-}(W)$ . By replacing  $r$  by  $r + \frac{1}{2}\sigma^2$  we have to change  $m$  in (3.7) to turn (3.8) into a formula for  $P_{r+\frac{1}{2}\sigma^2}(T)$ , which we need in the pricing formula (3.6). In the next section we derive formulas for the Laplace transforms of the double-sided Parisian stopping times for a standard Brownian motion.

### 3.3 The Laplace transform of the double-sided hitting times

We start recalling the Brownian meander from the Appendix in [30]. The process  $(m_u^{(t)})_{0 \leq u \leq 1}$  can be defined for every  $t > 0$  by

$$m_u^{(t)} = \frac{1}{\sqrt{t - \gamma_t}} |W_{\gamma_t + u(t - \gamma_t)}|, \quad u \leq 1,$$

where we suppressed the 0 in the notation of  $\gamma_t^0$ . For  $t = 1$  this process is the Brownian meander. Here we are only interested in  $m_1^{(t)}$ , the final value of the meander which we denote by  $n_t$  given by,

$$n_t = \frac{1}{\sqrt{t - \gamma_t}} |W_t|.$$

The  $\sigma$ -algebra  $\mathcal{F}_{\gamma_t}^+$  is generated by the random variable  $\text{sgn}(W_t)$  and the variables  $\xi_{\gamma_t}$ , where  $\xi$  is a predictable process w.r.t. the natural Brownian filtration. As pointed out in [30],  $n_t$  is for every  $t > 0$  independent of  $\mathcal{F}_{\gamma_t}^+$  and therefore independent of the pair  $(\gamma_t, \text{sgn}(W_t))$ . Moreover,  $n_t \stackrel{d}{=} N$ , where  $N$  has the following density,

$$\mathbb{P}[N \in dx] = x e^{-\frac{x^2}{2}} \mathbf{1}_{\{x \geq 0\}} dx, \quad (3.9)$$

and for later on it is useful to define the function  $\Psi_c$  for  $c \geq 0$  by

$$\Psi_c(z) := \mathbb{E} [e^{zN} \mathbf{1}_{\{N \geq c\}}] = e^{-\frac{c^2}{2} + zc} + z\sqrt{2\pi} e^{\frac{z^2}{2}} \mathcal{N}(z - c), \quad (3.10)$$

where  $\mathcal{N}$  is the CDF of the standard normal distribution. We will abbreviate  $\Psi_0$  by  $\Psi$  and  $\Psi - \Psi_c$  by  $\tilde{\Psi}_c$ . Now consider the meander at time  $t$  away from level  $l$  and denote its final value by  $n_t^l$  given by

$$n_t^l = \frac{\mathbf{1}_{\{T_l < t\}}}{\sqrt{t - \gamma_t^l}} |W_t - l|,$$

where  $T_l$  denotes the first hitting time of the level  $l$  by the Brownian motion. It follows from the strong Markov property and the independence of  $n_t$  and the pair  $(\text{sgn}(W_t), \gamma_t)$  that for all bounded, measurable functions  $f$  and  $g$ ,

$$\begin{aligned}
& \mathbb{E} \left[ f(n_t^l) g(\text{sgn}(W_t - l), \gamma_t^l) 1_{\{T_l < t\}} \middle| \mathcal{F}_{T_l} \right] \\
&= 1_{\{T_l < t\}} \mathbb{E}^l \left[ f \left( \frac{|W_{t-s} - l|}{\sqrt{t - \gamma_{t-s}^l}} \right) g(\text{sgn}(W_{t-s} - l), \gamma_{t-s}^l) \right]_{s=T_l} \\
&= 1_{\{T_l < t\}} \mathbb{E} \left[ f \left( \frac{|W_{t-s}|}{\sqrt{t - \gamma_{t-s}}} \right) g(\text{sgn}(W_{t-s}), \gamma_{t-s}) \right]_{s=T_l} \\
&= 1_{\{T_l < t\}} \mathbb{E} [f(N)] \mathbb{E} [g(\text{sgn}(W_{t-s}), \gamma_{t-s})]_{s=T_l}. \tag{3.11}
\end{aligned}$$

Here  $\mathbb{E}^l$  denotes the expectation under the measure under which the Brownian motion  $W$  starts from level  $l$ . Hence, conditional on hitting level  $l$  before time  $t$ ,  $n_t^l$  has the same distribution as  $N$  and  $n_t^l$  is independent of the pair  $(\text{sgn}(W_t - l), \gamma_t^l)$ . Now we can construct another process  $\mu_t^l$  by,

$$\mu_t^l = 1_{\{T_l < t\}} \text{sgn}(W_t - l) \sqrt{t - \gamma_t^l},$$

which is, given  $T_l < t$  conditionally independent of  $n_t^l$ , so we can use it to decompose the Brownian motion into two independent parts,

$$1_{\{T_l < t\}}(W_t - l) = n_t^l \mu_t^l. \tag{3.12}$$

Now we construct the  $\sigma$ -algebra  $\mathcal{H}_\tau$  that contains the information of the processes  $\mu^{l_i}$  and  $\gamma^{l_i}$  for  $i = 1, 2$  at the random time  $\tau$  by,

$$\mathcal{H}_\tau = \sigma(\mu_\tau^{l_1}, \mu_\tau^{l_2}, \gamma_\tau^{l_1}, \gamma_\tau^{l_2}).$$

Note that the events  $\{\tau^+ < \tau^-\}$  and  $\{\tau^- < \tau^+\}$  can be constructed from these random variables in the following way,

$$\{\tau^- < \tau^+\} = \{\mu_\tau^{l_1} < 0\}, \quad \{\tau^+ < \tau^-\} = \{\mu_\tau^{l_2} > 0\}, \tag{3.13}$$

and therefore they are  $\mathcal{H}_\tau$  measurable. The equation

$$\tau = (\gamma_\tau^{l_1} + D_1) 1_{\{\tau^- < \tau^+\}} + (\gamma_\tau^{l_2} + D_2) 1_{\{\tau^+ < \tau^-\}},$$

shows that  $\tau$  is also  $\mathcal{H}_\tau$  measurable. The following lemma states conditional independence between  $n_\tau^{l_2}$  and  $\mathcal{H}_\tau$ .

**Lemma 3.3.1.** *The following equation holds for any bounded measurable function  $f$ ,*

$$\mathbb{E} \left[ 1_{\{\tau^+ < \tau^-\}} f(n_\tau^{l_2}) \middle| \mathcal{H}_\tau \right] = 1_{\{\tau^+ < \tau^-\}} \mathbb{E} [f(N)] \quad a.s. \tag{3.14}$$

*Proof.* We have to show that for any  $H \in \mathcal{H}_\tau$  we have

$$\int_H 1_{\{\tau^+ < \tau^-\}} f(n_\tau^{l_2}) d\mathbb{P} = \mathbb{E}[f(N)] \mathbb{P}[H; \tau^+ < \tau^-], \quad (3.15)$$

and directly following from the construction of  $\mathcal{H}_\tau$  this is equivalent to showing that for any bounded measurable function  $g$  we have,

$$\begin{aligned} \mathbb{E} \left[ 1_{\{\tau^+ < \tau^-\}} f(n_\tau^{l_2}) g(\gamma_\tau^{l_1}, \gamma_\tau^{l_2}, \mu_\tau^{l_1}, \mu_\tau^{l_2}) \right] = \\ \mathbb{E}[f(N)] \mathbb{E} \left[ 1_{\{\tau^+ < \tau^-\}} g(\gamma_\tau^{l_1}, \gamma_\tau^{l_2}, \mu_\tau^{l_1}, \mu_\tau^{l_2}) \right]. \end{aligned}$$

On the set  $\{\tau^+ < \tau^-\}$  we have  $\mu_\tau^{l_2} = \sqrt{D_2}$  and  $\mu_\tau^{l_1}$  can be expressed in terms of  $\gamma_\tau^{l_1,2}$  in the following way

$$\mu_\tau^{l_1} = \sqrt{D_2 + (\gamma_\tau^{l_2} - \gamma_\tau^{l_1})}.$$

So we can rewrite the function  $g$  as function  $\tilde{g}$  of  $\gamma_\tau^{l_1,2}$  only. After replacing  $\{\tau^+ < \tau^-\}$  by  $\{\mu_\tau^{l_2} > 0\}$  as in (3.13) it remains to show,

$$\mathbb{E} \left[ 1_{\{\mu_\tau^{l_2} > 0\}} f(n_\tau^{l_2}) \tilde{g}(\gamma_\tau^{l_1}, \gamma_\tau^{l_2}) \right] = \mathbb{E}[f(N)] \mathbb{E} \left[ 1_{\{\mu_\tau^{l_2} > 0\}} \tilde{g}(\gamma_\tau^{l_1}, \gamma_\tau^{l_2}) \right]. \quad (3.16)$$

Now by (3.11) both  $\mu_\tau^{l_2}$  and  $\gamma_\tau^{l_2}$  are conditionally independent of  $n_\tau^{l_2}$ , so (3.16) would hold if  $\tilde{g}$  had been a function of  $\gamma_\tau^{l_2}$  only. Therefore it remains to prove that on the set  $\{\mu_\tau^{l_2} > 0\}$  also  $\gamma_\tau^{l_1}$  is independent of  $n_\tau^{l_2}$ . Define the following sequence of stopping times  $T^{(n)}$ ,  $n = 0, 1, \dots$  by  $T^{(0)} = 0$  and

$$T^{(n+1)} = \inf \left\{ t > T^{(n)} \mid W_t = 0 \text{ and } W_s \in \{l_1, l_2\} \text{ for some } T^{(n)} \leq s \leq t \right\},$$

then  $\tau^+$  is always in between two of these stopping times  $T^{(n)}$  and  $T^{(n+1)}$ . Moreover  $\tau^-$  cannot be in between the same two stopping times as  $\tau^+$  is, so we can write for any bounded measurable functions  $f$  and  $h$

$$\begin{aligned} \mathbb{E} \left[ 1_{\{\mu_\tau^{l_2} > 0\}} f(n_\tau^{l_2}) h(\gamma_\tau^{l_1}) \right] \\ = \sum_{n=0}^{\infty} \mathbb{E} \left[ 1_{\{T^{(n)} < \tau\}} h(\gamma_{T^{(n)}}^{l_1}) \mathbb{E} \left[ 1_{\{\tau < T^{(n+1)}\}} 1_{\{\mu_\tau^{l_2} > 0\}} f(n_\tau^{l_2}) \mid \mathcal{F}_{T^{(n)}} \right] \right], \end{aligned}$$

where we used that on the set  $\{\tau^+ < \tau^-\} \cap \{T^{(n)} < \tau < T^{(n+1)}\}$  we have  $\gamma_\tau^{l_1} < T^{(n)}$  and therefore  $\gamma_\tau^{l_1} = \gamma_{T^{(n)}}^{l_1}$ . Now we can use the strong Markov property to restart the Brownian motion in zero at time  $T^{(n)}$ ,

$$\begin{aligned} \sum_{n=0}^{\infty} \mathbb{E} \left[ 1_{\{T^{(n)} < \tau\}} h(\gamma_{T^{(n)}}^{l_1}) \mathbb{E} \left[ 1_{\{\tau < T^{(n+1)}\}} 1_{\{\mu_\tau^{l_2} > 0\}} f(n_\tau^{l_2}) \mid \mathcal{F}_{T^{(n)}} \right] \right] \\ = \sum_{n=0}^{\infty} \mathbb{E} \left[ 1_{\{T^{(n)} < \tau\}} h(\gamma_{T^{(n)}}^{l_1}) \mathbb{E} \left[ 1_{\{\tau < T^{(1)}\}} 1_{\{\mu_\tau^{l_2} > 0\}} f(n_\tau^{l_2}) \right] \right] \\ = \sum_{n=0}^{\infty} \mathbb{E} \left[ 1_{\{T^{(n)} < \tau\}} h(\gamma_{T^{(n)}}^{l_1}) \mathbb{E} \left[ 1_{\{\tau^+ < T^{(1)}\}} f(n_{\tau^+}^{l_2}) \right] \right], \end{aligned}$$

where we used in the last equality that the event  $\{\tau^+ < T^{(1)}\}$  equals the intersection of the events  $\{\tau < T^{(1)}\}$  and  $\{\tau^+ < \tau^-\}$ . By (3.11) we can get the expectation of  $n_{\tau^+}^{l_2}$  out of the sum,

$$\begin{aligned} & \sum_{n=0}^{\infty} \mathbb{E} \left[ \mathbb{1}_{\{T^{(n)} < \tau\}} h(\gamma_{T^{(n)}}^{l_1}) \mathbb{E} \left[ \mathbb{1}_{\{\tau^+ < T^{(1)}\}} f(n_{\tau^+}^{l_2}) \right] \right] \\ &= \mathbb{E} [f(N)] \sum_{n=0}^{\infty} \mathbb{E} \left[ \mathbb{1}_{\{T^{(n)} < \tau\}} h(\gamma_{T^{(n)}}^{l_1}) \mathbb{E} \left[ \mathbb{1}_{\{\tau^+ < T^{(1)}\}} \right] \right] \\ &= \mathbb{E} [f(N)] \sum_{n=0}^{\infty} \mathbb{E} \left[ \mathbb{1}_{\{T^{(n)} < \tau\}} h(\gamma_{T^{(n)}}^{l_1}) \mathbb{1}_{\{\tau^+ < T^{(n+1)}\}} \right], \end{aligned}$$

where the equality of the last two lines can be established by conditioning the expectation on the last line on  $\mathcal{F}_T^{(n)}$ . In the final step we use that set  $\{T^{(n)} < \tau\} \cap \{\tau^+ < T^{(n+1)}\}$  is equal to  $\{T^{(n)} < \tau < T^{(n+1)}\} \cap \{\tau^+ < \tau^-\}$ . Moreover, on this set the level  $l_1$  is not touched within the time interval  $(T^{(n)}, T^{(n+1)})$ . Therefore we can replace  $\gamma_{T^{(n)}}^{l_1}$  by  $\gamma_{\tau}^{l_1}$ , altogether resulting in

$$\begin{aligned} & \mathbb{E} [f(N)] \sum_{n=0}^{\infty} \mathbb{E} \left[ \mathbb{1}_{\{T^{(n)} < \tau\}} h(\gamma_{T^{(n)}}^{l_1}) \mathbb{1}_{\{\tau^+ < T^{(n+1)}\}} \right] \\ &= \mathbb{E} [f(N)] \mathbb{E} \left[ h(\gamma_{\tau}^{l_1}) \mathbb{1}_{\{\mu_{\tau}^{l_2} > 0\}} \right], \end{aligned}$$

which yields the desired independence result.  $\square$

We are interested in the Laplace transforms of  $\tau$  and we have the following theorem on  $\mathbb{E}_+(\lambda)$  and  $\mathbb{E}_-(\lambda)$ , the restricted Laplace transforms of  $\tau$  denoted by,

$$\mathbb{E}_+(\lambda) := \mathbb{E} \left[ e^{-\frac{1}{2}\lambda^2\tau} \mathbb{1}_{\{\tau^+ < \tau^-\}} \right] \quad \text{and} \quad \mathbb{E}_-(\lambda) := \mathbb{E} \left[ e^{-\frac{1}{2}\lambda^2\tau} \mathbb{1}_{\{\tau^- < \tau^+\}} \right].$$

**Theorem 3.3.2.** *For the restricted Laplace transforms  $\mathbb{E}_+(\lambda)$  and  $\mathbb{E}_-(\lambda)$  of  $\tau$  the following holds,*

$$\mathbb{E}_+(\lambda) = \frac{e^{\lambda l_1} \Psi(-\lambda_1) - e^{-\lambda l_1} \Psi(\lambda_1)}{e^{\lambda(l_1-l_2)} \Psi(-\lambda_1) \Psi(-\lambda_2) - e^{\lambda(l_2-l_1)} \Psi(\lambda_1) \Psi(\lambda_2)} \quad (3.17)$$

$$\mathbb{E}_-(\lambda) = \frac{e^{-\lambda l_2} \Psi(-\lambda_2) - e^{\lambda l_2} \Psi(\lambda_2)}{e^{\lambda(l_1-l_2)} \Psi(-\lambda_1) \Psi(-\lambda_2) - e^{\lambda(l_2-l_1)} \Psi(\lambda_1) \Psi(\lambda_2)}, \quad (3.18)$$

where we used  $\lambda_i = \lambda\sqrt{D_i}$  for  $i = 1, 2$  to shorten the notation.

*Proof.* The first step of proof consists of the following application of the optional sampling theorem to the martingale  $M$  defined by  $M_t = e^{-\frac{1}{2}\lambda^2 t + \lambda W_t}$ ,

$$\begin{aligned} 1 &= \mathbb{E} \left[ e^{-\frac{1}{2}\lambda^2\tau + \lambda W_{\tau}} \right] \\ &= \mathbb{E} \left[ e^{-\frac{1}{2}\lambda^2\tau + \lambda W_{\tau}} \mathbb{1}_{\{\tau^+ < \tau^-\}} \right] + \mathbb{E} \left[ e^{-\frac{1}{2}\lambda^2\tau + \lambda W_{\tau}} \mathbb{1}_{\{\tau^- < \tau^+\}} \right], \end{aligned} \quad (3.19)$$

where the optional sampling theorem holds because by the appendix 3.11.3  $M_t^\tau$ , the  $\tau$ -stopped version of the martingale  $M$  is an uniformly integrable martingale. The expectation in (3.19) on the left-hand side can be computed as follows,

$$\begin{aligned} \mathbb{E} \left[ e^{-\frac{1}{2}\lambda^2\tau + \lambda W_\tau} 1_{\{\tau^+ < \tau^-\}} \right] &= \mathbb{E} \left[ e^{-\frac{1}{2}\lambda^2\tau + \lambda(\mu_\tau^2 n_\tau^2 + l_2)} 1_{\{\tau^+ < \tau^-\}} \right] \\ &= e^{\lambda l_2} \mathbb{E} \left[ e^{-\frac{1}{2}\lambda^2\tau} 1_{\{\tau^+ < \tau^-\}} \mathbb{E} \left[ e^{\lambda\sqrt{D_2}n_\tau} \middle| \mathcal{H}_\tau \right] \right] \\ &= e^{\lambda l_2} \mathbb{E} \left[ e^{\lambda\sqrt{D_2}N} \right] \mathbb{E} \left[ e^{-\frac{1}{2}\lambda^2\tau} 1_{\{\tau^+ < \tau^-\}} \right] = e^{\lambda l_2} \Psi(\lambda\sqrt{D_2})\mathbb{E}_+(\lambda), \end{aligned} \quad (3.20)$$

where lemma 3.3.1 is used to obtain the third line from the second. By the symmetry of Brownian motion the following expression can be found for the right-hand side expectation in (3.19),

$$\begin{aligned} \mathbb{E} \left[ e^{-\frac{1}{2}\lambda^2\tau + \lambda W_\tau} 1_{\{\tau^+ > \tau^-\}} \right] &= \mathbb{E} \left[ e^{-\frac{1}{2}\lambda^2\tau + \lambda(l_1 - \sqrt{D_1}n_\tau^1)} 1_{\{\tau^+ > \tau^-\}} \right] \\ &= e^{\lambda l_1} \Psi(-\lambda\sqrt{D_1})\mathbb{E}_-(\lambda). \end{aligned} \quad (3.21)$$

Note that  $\mathbb{E}_+(\lambda)$  and  $\mathbb{E}_-(\lambda)$  are even functions of  $\lambda$  and the theorem is proved by solving the set of equations obtained by plugging (3.20) and (3.21) into (3.19) for  $\pm\lambda$ .  $\square$

By taking the limit for  $\lambda \rightarrow 0$  in (3.18), we can derive the following corollary from the theorem.

**Corollary 3.3.3.** *The probability that a Brownian motion will spend time  $D_1$  below level  $l_1$  before it spends  $D_2$  above level  $l_2$  is given by the following formula,*

$$\mathbb{P} [\tau^- < \tau^+] = \frac{l_2\sqrt{\frac{2}{\pi}} + \sqrt{D_2}}{(l_2 - l_1)\sqrt{\frac{2}{\pi}} + \sqrt{D_1} + \sqrt{D_2}} \quad l_1 < 0 < l_2. \quad (3.22)$$

**Remark 3.3.4.** *By taking the limits  $l_2 \downarrow 0$  and  $l_1 \uparrow 0$  in (3.22), we get for a Brownian motion that the probability that a positive excursion of length  $D_2$  happens before a negative excursion of length  $D_1$  is equal to*

$$\frac{\sqrt{D_1}}{\sqrt{D_1} + \sqrt{D_2}},$$

*which is a remarkably simple expression. In the same way as in [77] one could use excursion theory as another way to obtain this probability.*

Now we have computed the Laplace transforms of the Parisian stopping times for a standard Brownian motion, we return in the next section to the original problem of deriving Fourier transforms for the probabilities related to the double-sided Parisian knock-in call option contract.

### 3.4 Calculating the Fourier transform

We recall that the relevant quantity to compute in order to price Parisian options maturing at time  $T$  is the probability  $P_r(T)$  given by (3.5). Also note, that formulas for  $P_{r+\frac{1}{2}\sigma^2}(T)$  appear to be similar, except that a different value for  $m$  is needed. Here we calculate its Fourier transform  $\phi$  in the parameter  $T$  and actual numbers can be obtained by numerical inversion. In this section we assume  $L_1 \leq S_0 \leq L_2$  or, stated in terms of the standard Brownian motion,  $l_1 \leq 0 \leq l_2$ . The case where the initial stock price  $S_0$  is above  $L_2$  or below  $L_1$  is treated in section 3.5. As a function of time, the probability  $P_r(T)$  is non-decreasing, and in order to assure integrability we introduce an exponential damping factor  $a > 0$ . We have for  $\phi$ ,

$$\phi(v) = \int_0^\infty e^{ivT} e^{-aT} P_r(T) dT. \quad (3.23)$$

Now we can substitute (3.8) for  $P_r$ , use  $\alpha = a + \frac{1}{2}m^2$  and split up the event  $\{\tau \leq T\}$  in the parts where the Parisian constraint is fulfilled above the upper level or below the lower level,

$$\begin{aligned} \phi(v) &= \int e^{(iv-\alpha)T} \mathbb{E} \left[ e^{mW_T} 1_{\{W_T > k\}} 1_{\{\tau \leq T\}} (1_{\{\tau^+ < \tau^-\}} + 1_{\{\tau^- < \tau^+\}}) \right] dT \\ &=: \phi_+(v) + \phi_-(v). \end{aligned} \quad (3.24)$$

Of course  $\phi$  depends on the value of the strike, the barriers and the times that have to be spent below or above these barriers, so a more precise notation would be  $\phi(v; k, l_1, D_1, l_2, D_2)$ . Here we try to keep the notation as simple as possible without being ambiguous. The following lemma links the results from the previous section to  $\phi_+$  and  $\phi_-$ .

**Lemma 3.4.1.** *The Fourier transforms  $\phi_+$  and  $\phi_-$  can be written as,*

$$\phi_+(v) = \mathbb{E}_+(\tilde{v}_\alpha) \mathbb{E} \left[ \int_0^\infty e^{(iv-\alpha)\rho} h(\rho, l_2 + \sqrt{D_2}N) d\rho \right], \quad (3.25)$$

$$\phi_-(v) = \mathbb{E}_-(\tilde{v}_\alpha) \mathbb{E} \left[ \int_0^\infty e^{(iv-\alpha)\rho} h(\rho, l_1 - \sqrt{D_1}N) d\rho \right], \quad (3.26)$$

where  $N$  is the random variable with density (3.9) and

$$h(\rho, w) = \mathbb{E} \left[ e^{m(W_\rho+w)} 1_{\{W_\rho+w > k\}} \right] \quad \text{and} \quad \tilde{v}_\alpha = \sqrt{2(\alpha - iv)}.$$

*Proof.* We give the proof for  $\phi_+$ , which, after an application of Fubini, the substitution  $\rho = T - \tau$  and the strong Markov property of Brownian motion

can be written as,

$$\begin{aligned}
\phi_+(v) &= \int_0^\infty e^{(iv-\alpha)T} \mathbb{E} \left[ e^{mW_T} \mathbf{1}_{\{W_T > k\}} \mathbf{1}_{\{\tau^+ < \tau^-\}} \mathbf{1}_{\{\tau \leq T\}} \right] dT \\
&= \int_0^\infty e^{(iv-\alpha)T} \mathbb{E} \left[ \mathbf{1}_{\{\tau^+ < \tau^-\}} \mathbf{1}_{\{\tau \leq T\}} \mathbb{E} \left[ e^{mW_T} \mathbf{1}_{\{W_T > k\}} \mid \mathcal{F}_\tau \right] \right] dT \\
&= \mathbb{E} \left[ \mathbf{1}_{\{\tau^+ < \tau^-\}} \int_\tau^\infty e^{(iv-\alpha)T} \mathbb{E}^{W_\tau} \left[ e^{mW_t} \mathbf{1}_{\{W_t > k\}} \right]_{t=T-\tau} dT \right] \\
&= \mathbb{E} \left[ \mathbf{1}_{\{\tau^+ < \tau^-\}} \int_0^\infty e^{(iv-\alpha)(\rho+\tau)} \mathbb{E} \left[ e^{m(W_\rho+w)} \mathbf{1}_{\{W_\rho+w > k\}} \right]_{w=W_\tau} d\rho \right]
\end{aligned}$$

Given  $\tau^+ < \tau^-$ , by lemma 3.3.1, the stopping time  $\tau$  and the value of the Brownian motion  $W_\tau$  are independent and, moreover,  $W_\tau \stackrel{d}{=} l_2 + \sqrt{D_2}N$ , which proves the lemma for  $\phi_+$ . By symmetry of the Brownian motion, the proof for equation for  $\phi_-$  proceeds along the same lines, where we remark that now  $W_\tau \stackrel{d}{=} l_1 - \sqrt{D_1}N$ , given  $\tau^- < \tau^+$ .  $\square$

The quantities  $\mathbb{E}_+$  and  $\mathbb{E}_-$  in equations (3.25) and (3.26) are given by theorem 3.3.2, so we proceed to calculate the remaining expectations. Let  $c_1$  and  $c_2$  be real numbers and denote by  $E(c_1, c_2)$  the for lemma 3.4.1 relevant expectation,

$$E(c_1, c_2) = \mathbb{E} \left[ \int_0^\infty e^{(iv-\alpha)\rho} h(\rho, c_1 + c_2 N) d\rho \right], \quad (3.27)$$

The following lemma computes this expectation for special case of  $c_1$  and  $c_2$ .

**Lemma 3.4.2.** *The following holds for the expectation  $E(c_1, c_2)$ ,*

$$E(c_1, c_2) = \begin{cases} \frac{e^{(m-\tilde{v}_\alpha)k + \tilde{v}_\alpha c_1}}{\tilde{v}_\alpha(\tilde{v}_\alpha - m)} \mathbb{E} \left[ e^{\tilde{v}_\alpha c_2 N} \right], & k > c_1; c_2 < 0 \\ \frac{2e^{m c_1}}{\tilde{v}_\alpha^2 - m^2} \mathbb{E} \left[ e^{m c_2 N} \right] - \frac{e^{k(m+\tilde{v}_\alpha) - c_1 \tilde{v}_\alpha}}{\tilde{v}_\alpha(m+\tilde{v}_\alpha)} \mathbb{E} \left[ e^{-\tilde{v}_\alpha c_2 N} \right], & k < c_1; c_2 > 0 \end{cases}$$

*Proof.* The expectation  $E(c_1, c_2)$  can be written out as follows,

$$\begin{aligned}
E(c_1, c_2) &= \int_0^\infty u e^{-\frac{u^2}{2}} \int_0^\infty e^{(iv-\alpha)\rho} \frac{1}{\sqrt{2\pi\rho}} \int_{k-c_1-c_2u}^\infty e^{m(x+c_2u+c_1)} e^{-\frac{x^2}{2\rho}} dx d\rho du \\
&= \int_0^\infty u e^{-\frac{u^2}{2}} \int_{k-c_1-c_2u}^\infty e^{m(x+c_2u+c_1)} \int_0^\infty \frac{e^{(iv-\alpha)\rho}}{\sqrt{2\pi\rho}} e^{-\frac{x^2}{2\rho}} d\rho dx du,
\end{aligned}$$

where we integrate over the densities of  $W_\rho$  and  $N$  and change the order of integration with Fubini. Calculation of the inner  $\rho$ -integral yields,

$$\begin{aligned}
\int_0^\infty e^{(iv-\alpha)\rho} \frac{1}{\sqrt{2\pi\rho}} e^{-\frac{x^2}{2\rho}} d\rho &= \int_0^\infty e^{(iv-\alpha)\rho} \int_{|x|}^\infty \frac{y}{\sqrt{2\pi\rho^3}} e^{-\frac{y^2}{2\rho}} dy d\rho \\
&= \int_{|x|}^\infty e^{-y\sqrt{2(\alpha-iv)}} dy = \frac{e^{-|x|\tilde{v}_\alpha}}{\tilde{v}_\alpha}. \quad (3.28)
\end{aligned}$$

Here we used the complex continuation of the Laplace transform of the first hitting time of  $y$  by a standard Brownian motion, see [55] for example. Now we combine the previous two equations to arrive at

$$E(c_1, c_2) = \frac{e^{mc_1}}{\tilde{v}_\alpha} \int_0^\infty u e^{-\frac{u^2}{2} + c_2 mu} \int_{k-c_1-c_2u}^\infty e^{mx - \tilde{v}_\alpha |x|} dx du. \quad (3.29)$$

The inner integral of (3.29) converges as a result of the definition of  $\alpha$  just below equation (3.23) and must be computed for each of the cases  $k > c_1, c_2 < 0$  and  $k < c_1, c_2 > 0$  separately. For the case  $k > c_1, c_2 < 0$  we have that  $k - c_1 - c_2u \geq 0$  for every  $u \geq 0$  resulting in

$$\int_{k-c_1-c_2u}^\infty e^{mx - \tilde{v}_\alpha |x|} dx = \frac{e^{(m-\tilde{v}_\alpha)(k-c_1-c_2u)}}{\tilde{v}_\alpha - m},$$

which plugged back into (3.29) gives

$$E(c_1, c_2) = \frac{e^{(m-\tilde{v}_\alpha)k + \tilde{v}_\alpha c_1}}{\tilde{v}_\alpha(\tilde{v}_\alpha - m)} \int_0^\infty e^{c_2 \tilde{v}_\alpha u} u e^{-\frac{u^2}{2}} du,$$

where the integral contains the density of  $N$  as given in (3.9) and therefore equals the expectation as stated in the lemma. For the case  $k < c_1, c_2 > 0$  we have that  $k - c_1 - c_2u \leq 0$  for every  $u \geq 0$  resulting in

$$\int_{k-c_1-c_2u}^\infty e^{mx - \tilde{v}_\alpha |x|} dx = \frac{2\tilde{v}_\alpha}{\tilde{v}_\alpha^2 - m^2} - \frac{e^{(m+\tilde{v}_\alpha)(k-c_1-c_2u)}}{\tilde{v}_\alpha + m},$$

which again by plugging back into (3.29) proves the lemma.  $\square$

We have now all the ingredients we need to calculate  $\psi_+$  and  $\psi_-$  in the following special cases.

**Corollary 3.4.3.** *The following expressions hold for  $\psi_+$  and  $\psi_-$  in case  $l_1 \leq 0 \leq l_2$  and  $l_1 \leq k \leq l_2$ ,*

$$\phi_+(v) = \mathbb{E}_+(\tilde{v}_\alpha) \left( \frac{2e^{ml_2} \Psi(m\sqrt{D_2})}{\tilde{v}_\alpha^2 - m^2} - \frac{e^{k(m+\tilde{v}_\alpha) - l_2 \tilde{v}_\alpha} \Psi(-\tilde{v}_\alpha \sqrt{D_2})}{\tilde{v}_\alpha(m + \tilde{v}_\alpha)} \right), \quad (3.30)$$

$$\phi_-(v) = \mathbb{E}_-(\tilde{v}_\alpha) \frac{e^{(m-\tilde{v}_\alpha)k + \tilde{v}_\alpha l_1} \Psi(-\tilde{v}_\alpha \sqrt{D_1})}{\tilde{v}_\alpha(\tilde{v}_\alpha - m)}. \quad (3.31)$$

*Proof.* The corollary directly follows by plugging the result of lemma 3.4.2 into lemma 3.4.1 and using the special function  $\Psi$  defined in (3.10) for the expectation in lemma 3.4.2.  $\square$

Adding  $\phi_-$  and  $\phi_+$  gives an expression for  $\phi$ . We remark that the expressions are only valid for  $L_1 \leq K, S_0 \leq L_2$ . In order to get expressions for the general case, we need a formula for  $\phi_+$  in case  $k > l_2$  and a formula for  $\phi_-$  in case

$k < l_1$ . In order to get there, we need to extend lemma 3.4.2 to the cases  $k < c_1, c_2 < 0$  and  $k > c_1, c_2 > 0$ , which is rather involved and therefore deferred to the appendix. Here we just state the results as they follow from lemma 3.11.1 in appendix 3.11.1 for  $\phi_+$ ,

$$\phi_+(v) = \mathbb{E}_+(\tilde{v}_\alpha) \left( \frac{e^{(m-\tilde{v}_\alpha)k+l_2\tilde{v}_\alpha} \tilde{\Psi}_{u_2^*}(\tilde{v}_\alpha\sqrt{D_2})}{\tilde{v}_\alpha(\tilde{v}_\alpha - m)} + \frac{2e^{ml_2} \Psi_{u_2^*}(m\sqrt{D_2})}{\tilde{v}_\alpha^2 - m^2} - \frac{e^{(\tilde{v}_\alpha+m)k-l_2\tilde{v}_\alpha} \tilde{\Psi}_{u_2^*}(-\tilde{v}_\alpha\sqrt{D_2})}{\tilde{v}_\alpha(\tilde{v}_\alpha + m)} \right) \quad k > l_2, \quad (3.32)$$

and for  $\phi_-$ ,

$$\phi_-(v) = \mathbb{E}_-(\tilde{v}_\alpha) \left( \frac{e^{(m-\tilde{v}_\alpha)k+l_1\tilde{v}_\alpha} \tilde{\Psi}_{u_1^*}(-\tilde{v}_\alpha\sqrt{D_1})}{\tilde{v}_\alpha(\tilde{v}_\alpha - m)} + \frac{2e^{ml_1} \tilde{\Psi}_{u_1^*}(-m\sqrt{D_1})}{\tilde{v}_\alpha^2 - m^2} - \frac{e^{(m+\tilde{v}_\alpha)k-l_1\tilde{v}_\alpha} \tilde{\Psi}_{u_1^*}(\tilde{v}_\alpha\sqrt{D_1})}{\tilde{v}_\alpha(m + \tilde{v}_\alpha)} \right) \quad k < l_1, \quad (3.33)$$

where the constants  $u_1^*$  and  $u_2^*$  are given by,

$$u_1^* = \frac{l_1 - k}{\sqrt{D_1}} \quad \text{and} \quad u_2^* = \frac{k - l_2}{\sqrt{D_2}},$$

based on the constant  $u^*$  in (3.39). The Fourier transforms we have computed so far are valid in case the stock price process starts in between the two barriers. We do not derive transforms for the Greeks, because their transforms are already rather complicated for the single-sided Parisian options as given in [30]. For the double-sided Parisian option the derivation will be very confusing because the Fourier transform is a product of  $\mathbb{E}_\pm$  and  $E(c_1, c_2)$ , where both terms have dependencies on  $l_1, l_2$  and  $k$ . The alternative of numerical differentiation of the inverted Fourier transform delivers accurate Greeks as is shown in the section on numerical examples. The next section treats the case in which the stock price process is already above the upper or below the lower barrier for some time, i.e., the stock price process is "already in the excursion".

### 3.5 Already in the excursion

Suppose the stock is already trading above level  $L_2$  for a couple of days and it will only take an extra period of length  $d$  for the Parisian to knock in. Denoting the remaining time to expiry by  $T$ , the option knocks in if the stock price process  $S$  stays above level  $L_2$  longer than this time  $d$ . If the stock price process hits level  $L_2$  before time  $d$  has gone by, the contract

knocks in as soon as the stock spends either time  $D_2$  above  $L_2$  or time  $D_1$  below  $L_1$ . So it knocks in if  $\tau_d \leq T$ , where,

$$\tau_d = d1_{\{T_{L_2} > d\}} + \tau 1_{\{T_{L_2} \leq d\}},$$

Now the probability we are interested in becomes for  $T > d$ ,

$$\mathbb{P}[S_T > K; \tau_d \leq T] = \mathbb{P}[S_T > K; T_{L_2} > d] + \mathbb{P}[S_T > K; T_{L_2} \leq d; \tau \leq T].$$

We remark that in the first probability on the right-hand side we should add the constraint that  $T > d$ , otherwise the Parisian knock-in has not taken place. The reason for leaving this out here, is that we know the value of the Parisian knock-in contract to be zero in case of  $T < d$  and we would not invert the Fourier transform in this situation. First, we restate the problem in terms of the standard Brownian motion and recognize that the stock trading above level  $L_2$  translates into the case  $l_1 < l_2 < 0$ . We start calculating the Fourier transform  $\phi_1$  of the first probability on the right-hand side and after that we will compute  $\phi_2$ , the Fourier transform of the second probability on the right-hand side. We want to use the strong Markov property later on, so we have to rewrite the probability and split the Fourier transform into two parts,

$$\begin{aligned} \phi_1(v) &= \int_0^\infty e^{(iv-\alpha)T} \mathbb{E} \left[ e^{mW_T} 1_{\{W_T > k\}} (1 - 1_{\{T_{l_2} \leq d\}}) \right] dT \\ &=: \phi_{1,1}(v; k) - \phi_{1,2}(v; k), \end{aligned}$$

where we explicitly add the  $k$  to the notation of  $\phi_{1,1}$  and  $\phi_{1,2}$ , because we want to use  $k$  as a parameter. The first part  $\phi_{1,1}$  can be computed as follows,

$$\begin{aligned} \phi_{1,1}(v; k) &= \int_0^\infty e^{(iv-\alpha)T} \frac{1}{\sqrt{2\pi T}} \int_k^\infty e^{mx} e^{-\frac{x^2}{2T}} dx dT = \\ &= \frac{1}{\tilde{v}_\alpha} \int_k^\infty e^{mx - |x|\tilde{v}_\alpha} dx = \begin{cases} \frac{e^{(m-\tilde{v}_\alpha)k}}{\tilde{v}_\alpha(\tilde{v}_\alpha - m)}, & k \geq 0, \\ \frac{2}{(\tilde{v}_\alpha^2 - m^2)} - \frac{e^{(m+\tilde{v}_\alpha)k}}{\tilde{v}_\alpha(m+\tilde{v}_\alpha)}, & k < 0. \end{cases} \end{aligned}$$

Where we used the same type of arguments as in (3.28). Now for  $\phi_{1,2}$  we get after conditioning on  $\mathcal{F}_{T_{l_2}}$  and multiple applications of Fubini,

$$\begin{aligned} \phi_{1,2}(v) &= \\ &e^{ml_2} \mathbb{E} \left[ e^{(iv-\alpha)T_{l_2}} 1_{\{T_{l_2} \leq d\}} \right] \int_0^\infty e^{(iv-\alpha)T} \mathbb{E} \left[ e^{mW_T} 1_{\{W_T > k-l_2\}} \right] dT. \quad (3.34) \end{aligned}$$

The integral on the right-hand side of this equation equals  $\phi_{1,1}(v; k-l_2)$ . In Appendix 3.11.2 we compute the expectation on the right-hand side given in (3.42). Adding the results gives,

$$\phi_1(v) = \phi_{1,1}(v; k) - \left( e^{l_2(m+\tilde{v}_\alpha)} \mathcal{N}(c_+^{up}) + e^{l_2(m-\tilde{v}_\alpha)} \mathcal{N}(c_-^{up}) \right) \phi_{1,1}(v; k-l_2),$$

where,

$$c_{\pm}^{up} = \frac{l_2 \pm \tilde{v}_{\alpha} d}{\sqrt{d}},$$

and the superscript  $up$  is used in this notation to denote that the initial stock price is above both barriers. We still have to compute  $\phi_2$ , which we can re-write by conditioning on  $\mathcal{F}_{T_{l_2}}$ . We use the complete, rather elaborate, notation for the Parisian stopping time to explain the strong Markov property in more detail,

$$\begin{aligned} \phi_2(v) &= \int_0^{\infty} e^{(iv-\alpha)T} \mathbb{E} \left[ e^{mW_T} 1_{\{W_T > k\}} 1_{\{T_{l_2} \leq d\}} 1_{\{\tau \leq T\}} \right] dT \\ &= e^{ml_2} \int_0^{\infty} e^{(iv-\alpha)T} \mathbb{E} \left[ 1_{\{T_{l_2} \leq d\}} \mathbb{E} \left[ e^{mW_{\tau}} 1_{\{W_{\tau} > k-l_2\}} 1_{\{\tilde{\tau} \leq t\}} \right]_{t=T-T_{l_2}} \right] dT, \end{aligned}$$

where

$$\tau = T_{D_1, D_2}^{l_1-, l_2+} \quad \text{and} \quad \tilde{\tau} = T_{D_1, D_2}^{(l_1-l_2)-, 0+}.$$

Again by substitution and multiple Fubini we get an equation for  $\phi_2$  like (3.34),

$$\begin{aligned} \phi_2(v) &= \\ &e^{ml_2} \mathbb{E} \left[ e^{(iv-\alpha)T_{l_2}} 1_{\{T_{l_2} \leq d\}} \right] \int_0^{\infty} e^{(iv-\alpha)T} \mathbb{E} \left[ e^{mW_T} 1_{\{W_T > k-l_2\}} 1_{\{\tilde{\tau} \leq T\}} \right] dT. \end{aligned}$$

We recognize immediately the first part of  $\phi_{1,2}$  given in (3.34) in this equation. The integral on the right-hand side is in fact nothing else than the original problem we are solving for different barriers. So finally we have,

$$\begin{aligned} \phi(v) &= \phi_{1,1}(v; k) + \left( e^{l_2(m+\tilde{v}_{\alpha})} \mathcal{N}(c_{+}^{up}) + e^{l_2(m-\tilde{v}_{\alpha})} \mathcal{N}(c_{-}^{up}) \right) \times \\ &\quad (\phi(v; k-l_2, l_1-l_2, 0) - \phi_{1,1}(v; k-l_2)), \quad l_1 \leq l_2 < 0, \end{aligned}$$

where  $\phi(v; k-l_2, l_1-l_2, 0)$  denotes the Fourier transform as defined in the previous section for the strike  $k-l_2$ , lower level  $l_1-l_2$  and upper level 0. For the case where the initial stock price is below both levels, i.e.,  $0 < l_1 < l_2$  we introduce the *down* version of the  $c$  constants,

$$c_{\pm}^{down} = \frac{-l_1 \pm \tilde{v}_{\alpha} d}{\sqrt{d}}.$$

Following the same steps we can derive the Fourier transform for this case is given by,

$$\begin{aligned} \phi(v) &= \phi_{1,1}(v; k) + \left( e^{l_1(m-\tilde{v}_{\alpha})} \mathcal{N}(c_{+}^{down}) + e^{l_1(m+\tilde{v}_{\alpha})} \mathcal{N}(c_{-}^{down}) \right) \times \\ &\quad (\phi(v; k-l_1, 0, l_2-l_1) - \phi_{1,1}(v; k-l_1)), \quad 0 < l_1 \leq l_2. \end{aligned}$$

For now, we are able to price the double-sided Parisian knock-in call for all combination of initial stock price value, strike and barriers. The next section relates the Fourier transforms computed so far to the double-sided Parisian knock-in put.

### 3.6 The Parisian put

For the put option, we need in analogy with (3.5) to calculate the following probability,

$$\mathbb{P}_r \left[ S_T \leq K; T_{D_1, D_2}^{L_1^-, L_2^+} \leq T \right].$$

In [30] the authors use an alternative type of put-call parity. Here we suggest the approach taken in [12], i.e. writing the probability as the difference of two probabilities,

$$\mathbb{P}_r \left[ T_{D_1, D_2}^{L_1^-, L_2^+} \leq T \right] - \mathbb{P}_r \left[ S_T \geq K; T_{D_1, D_2}^{L_1^-, L_2^+} \leq T \right],$$

where the right-hand side probability is exactly the probability given in (3.5) and the left-hand side probability can be obtained by taking the limit of (3.5) for  $K \downarrow 0$ . So we have to take  $k \rightarrow -\infty$  in equations (3.30) and (3.33) resulting in,

$$\phi(v) = \frac{2e^{ml_2} \Psi(m\sqrt{D_2})}{\tilde{v}_\alpha^2 - m^2} \mathbb{E}_+(\tilde{v}_\alpha) + \frac{2e^{ml_1} \Psi(-m\sqrt{D_1})}{\tilde{v}_\alpha^2 - m^2} \mathbb{E}_-(\tilde{v}_\alpha) \quad \text{for } k \rightarrow -\infty.$$

Note that we used the equation for  $\phi$  in which we assume that  $L_1 \leq S_0 \leq L_2$ . Prices for the Parisian put option for the case where it is already in the excursion can be obtained by taking  $k \rightarrow -\infty$  in the formulas for  $\phi$  as given in section 3.5. Now we have Fourier transforms for double-sided Parisian knock-in options, both put and call, we continue discussing the other types of Parisian contract types we can construct from the double-sided Parisian contract.

### 3.7 Other types of Parisian contracts

Recall the way we defined  $\phi_+$  and  $\phi_-$  in (3.24), where  $\phi_+$  is the Fourier transform w.r.t. the parameter  $T$  of the probability of the intersection of the following events:

- the event that the stock price at time  $T$  exceeds the strike price;
- the event  $\{\tau^+ \leq T\}$ , which states that the stock price made an excursion of length  $D_2$  above level  $L_2$  at some time before  $T$ ;
- the event  $\{\tau^+ < \tau^-\}$ , which represents the stock price process paths that spend time  $D_2$  above level  $L_2$  before spending time  $D_1$  below level  $L_1$ .

For  $\phi_-$  the last two events are replaced by  $\{\tau^- \leq T\}$  and  $\{\tau^- < \tau^+\}$  respectively, with analogue interpretation. Now we can construct different types of contracts, like the single-sided Parisian option, by different selections of  $\phi_+$ ,  $\phi_-$  and parameter sets in the following way:

- *Type 1.*  $\phi = \phi_+ + \phi_-$ . The double-sided Parisian contract that is paying off when  $S$  stays longer than consecutive time  $D_1$  below level  $L_1$  or  $D_2$  above level  $L_2$ .
- *Type 2a.*  $\phi = \phi_+ + \phi_-$  and  $l_1 \rightarrow -\infty$  or  $D_1 \rightarrow \infty$ . The single-sided Parisian up-and-in call. Taking these limits in the equations for  $\phi$  gives the formulas in [30], where we remark that we compute transforms of the probabilities needed to calculate the Parisian option value, where the authors of [30] compute transforms of the non discounted pay-off.
- *Type 2b.*  $\phi = \phi_+ + \phi_-$  and  $l_2 \rightarrow \infty$  or  $D_2 \rightarrow \infty$ . Analogously to the previous case, this is the single-sided down-and-in call.
- *Type 3a.*  $\phi = \phi_+$  The Parisian contract that pays off when  $S$  stays above level  $L_2$  for a consecutive period of length  $D_2$ , without having been below  $L_1$  for a period  $D_1$  before. This contract type is called the double-sided Parisian up-before-down-in call.
- *Type 3b.*  $\phi = \phi_-$  The Parisian contract that pays off when  $S$  stays below level  $L_1$  for a consecutive period of length  $D_1$ , without having been above  $L_2$  for a period  $D_2$  before, denoted by the double-sided Parisian down-before-up-in call.

A very rough upper bound for the prices of the specified contract types is the plain vanilla call. A less rough upper bound is given by the double-sided knock-in barrier call. We continue discussing the price ordering of the contracts above. For double-sided barriers this has already been done in [58]. We remark that for given levels  $L_1, L_2$  and periods  $D_1, D_2$  the contract type 1 is strictly most expensive, because given one of the contract types 2a, 2b, 3a or 3b there exist stock price paths that do trigger contract type 1 without knocking in the given contract type. Less expensive are the single-sided Parisian options denoted by contract types 2a and 2b. For the one sided Parisians there is only one level for the stock price process that can cause a knock-in of the contract. However, the behavior of the stock price above the other level cannot cause the Parisian option to knock out, which is the case for the cheapest contract types 3a and 3b. This type of double-sided Parisians do not only have just one stock price level that can cause a knock-in, but it also contains another level for the stock price process that knocks out the contract if the stock price process spends a certain time above or below this level. Note that it is possible to obtain (numerical) values for the single-sided Parisian contract without actually taking the limits as proposed in the description of types 2a and 2b. For a given time to expiry  $T$  the value of the single-sided Parisian down-and-in call can be obtained by inverting the Fourier transform of the double-sided Parisian contract for some  $L_2$  and  $D_2 > T$ . Similarly we get the value of the single-sided up-and-in by inverting the transform for some  $L_1$  and  $D_1 > T$ . We will illustrate these remarks in

the section on numerical examples. Figure 3.1 shows the relations between the double-sided and single-sided Parisian contracts, where we abbreviate the double-sided Parisian in call by DPIC and the out call by DPOC. The single-sided contracts are either up (PU..) or down (PD..) and either in (P.I.) or out (P.O.) contracts. The same type of scheme could be drawn for the Parisian put contracts. Now we have computed and discussed various types of Parisian contracts, we discuss the Fourier inversion in the next section.

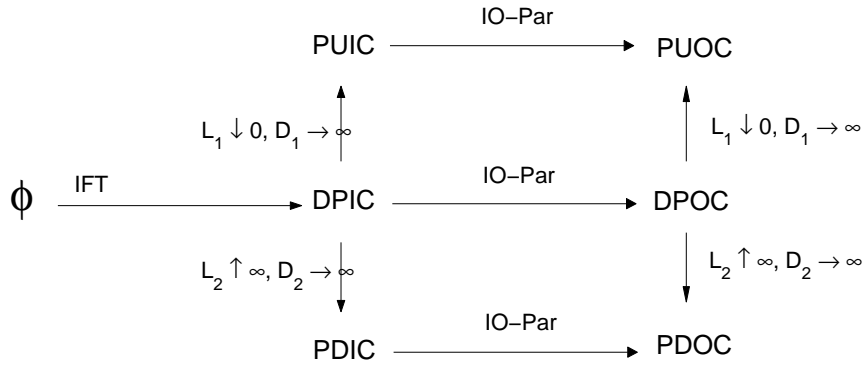


Figure 3.1: Relations between different types of Parisian contracts

## 3.8 Fourier inversion algorithm

### 3.8.1 General Fourier inversion

Apart from deriving Fourier transforms for the relevant probabilities for the double-sided Parisian option contracts, we are also interested in numerical values for these options. We have to obtain these values by inversion of the Fourier transform for the probabilities we need to construct the contract, where we recall formula (3.6). In (3.23) the definition of  $\phi$ , the Fourier transform of the probability  $P_r(T)$  is stated and values for  $P_r(T)$  can be obtained by the following standard Fourier inversion formula,

$$P_r(T) = \frac{e^{aT}}{2\pi} \int_{-\infty}^{\infty} e^{ivT} \phi(v) dv = \frac{2e^{aT}}{\pi} \int_0^{\infty} \cos(vT) \Re\{\phi(v)\} dv,$$

where  $\Re\{\phi(v)\}$  denotes the real part of  $\phi(v)$ . We recall that  $a$  is the damping factor to assure integrability in (3.23) and the  $\alpha$  we are using in all the derivations is given by  $\alpha = a - \frac{1}{2}m^2$ , where  $m$  is a constant coming from the Girsanov transform, implicitly defined in (3.7). To arrive at the integral over the positive real line on the right-hand side we refer to [4], where the key idea is that from  $P_r(T)$  with domain on the positive real line a symmetric function  $f$  on the whole real line can be constructed by  $f(t) := P_r(|t|)$ . Now

it is straightforward to obtain numerical values for  $P_r$  by discretizing and truncating the integral,

$$P_r(T) = \frac{2he^{aT}}{\pi} \sum_{j=0}^N \cos(v_j T) \Re\{\phi(v_j)\} + \epsilon_t + \epsilon_d, \quad (3.35)$$

where  $h$  is the stepsize,  $Nh$  the level of truncation and  $\epsilon_d$  and  $\epsilon_t$  respectively the discretization and the truncation error. Following [4], we analyse the discretization error  $\epsilon_d$  using the Poisson summation formula which assumes an Euler approximation for the integral in (3.35). In appendix 3.11.4 we derive for the discretization error,

$$\epsilon_d \leq \frac{2e^{-a(\frac{2\pi}{h}-T)}}{1 - e^{-\alpha\frac{2\pi}{hT}}} \quad \text{for } h < \frac{2\pi}{T}.$$

In appendix 3.11.5 we analyze the truncation error and find,

$$\epsilon_t \leq \arctan\left(\frac{a}{h(N-1)}\right), \quad (3.36)$$

which is very slowly going to zero. Experiments show that the number of terms needed for a given accuracy is much less than indicated by the bound on  $\epsilon_t$ . This suggests that the bound presented in (3.36) is not strong enough. The next section elaborates on the truncation error bound in order to come up with a better estimate for the accuracy.

### 3.8.2 Remarks on the truncation bound

The  $\arctan(\cdot)$ -term in (3.36) is very slowly going to zero, resulting in an impractical number of terms we have to compute in the truncated sum of (3.35) in case we want to obtain a reasonable error of e.g. 1%. We could try to solve this by using alternative inversion algorithms as Euler summation, which is proposed by [4], or approximation of the Fourier transform by polynomial-like functions of which the inverse is known as has been done by [10] instead of the standard FFT. Here we introduce a slightly modified version of the Euler summation, the average summation, because it seems to fit better to limiting the properties of the Fourier transform, but it has the same drawback as the other methods, which is that it is not possible to give a reasonable bound for the truncation error, without using heuristics. In [2] the authors conclude that it is often difficult to provide reasonable error bounds and therefore they suggest to use two "good" methods and compare the results for an error estimate. By numerically studying the behaviour of the sum in (3.35) it appears that this sum as a function of  $N$  oscillates for  $N$  big enough around its limiting value with a double frequency. A high frequency determined by  $T$  and a low frequency determined by  $D$ , which is

the smallest number divisible by both  $D_1$  and  $D_2$ . For the Fourier transform of a single-sided Parisian contract one can actually show this by making a Taylor expansion of the Fourier transform. For the double-sided Parisian option it is very complicated to obtain this Taylor expansion and here we just assume it to be true. In order to get rid of the high-frequency oscillation, we propose to average the sum over the last  $M$  terms as follows,

$$\sum_{j=0}^{\infty} \cos(v_j T) \Re\{\phi(v_j)\} \approx S_{N,M} := \frac{1}{M} \sum_{k=1}^M S_{N+k}, \quad \text{where } M = \frac{2\pi}{Dh},$$

and  $S_N$  is the partial sum of the first  $N$  terms. Now, for  $n$  large enough, also the partial averaged sums  $S_{n,M}$  will oscillate around the limiting value but with a much smaller amplitude. In the following algorithm we use this oscillating behavior to come up with an estimate for the error, because we know that the local maxima and minima are all above respectively below the limit we are interested in. If  $y$  is a  $N$ -dimensional vector containing the partial averaged sums, i.e.,  $y[k] = S_{k,M}$  for  $0 \leq k \leq N$ , the local extrema are defined by,

$$\begin{aligned} y[i] \text{ is a local max} &\Leftrightarrow y[i-1] < y[i] > y[i+1] \\ y[i] \text{ is a local min} &\Leftrightarrow y[i-1] > y[i] < y[i+1], \end{aligned}$$

for  $i \in \{1, \dots, N-1\}$ . The inversion algorithm now becomes,

- $n = 2$ ,  $y[0] = 0$ ,  $y[1] = 1$ .
- Choose  $\alpha$  and  $h$  such that the discretization error is  $\epsilon_d$ .
- Determine  $M$ .
- Repeat
  - $y[n] = S_{n,M}$
  - $P_{max} = \min\{y[i], 0 \leq i \leq n \mid y[i] \text{ is a local max}\}$
  - $P_{min} = \max\{y[i], 0 \leq i \leq n \mid y[i] \text{ is a local min}\}$
- Until  $P_{max} - P_{min} < 2\epsilon_d$
- $P = (P_{max} + P_{min})/2$  with truncation error  $\epsilon_t < \epsilon_d$ .

Experiments show that by using this algorithm we obtain a given accuracy much quicker than the truncation bound in (3.36) suggests. They even show that averaging over  $M$  terms diminishes the amplitude of the sum drastically compared both to plain summation and Euler summation. As we are now able to obtain numerical values from the Fourier transforms we previously calculated, we will conclude the paper with a section on numerical examples.

### 3.9 Numerical examples

In this section we illustrate the inversion of the Parisian option prices. Throughout the examples we use, if not mentioned otherwise,  $S_0 = K = 100$ ,  $L_1 = 90$ ,  $L_2 = 110$ ,  $D_1 = D_2 = 10/250$ ,  $T = 1$ ,  $r = 3.5\%$ ,  $\sigma = 25\%$  and  $h = 0.2$ , which for  $\alpha \geq 0.65$  will give a discretization error less than  $10^{-8}$ . If we denote quantities in units of days, then  $n$  days correspond to  $n/250$  years. We use Fourier inversion as described in the previous section and obtain prices typically within one second. Simulation of Parisian options usually is much slower, like the order of minutes for the same accuracy, because one needs to choose a really fine grid in order to capture the local behavior of the underlying Brownian motion.

#### 3.9.1 Double-sided Parisian prices

In this example we show how the double-sided Parisian knock-in option price behaves. First we vary the time that should be spend by the stock price process below or above the respective barriers  $L_1$  and  $L_2$ .

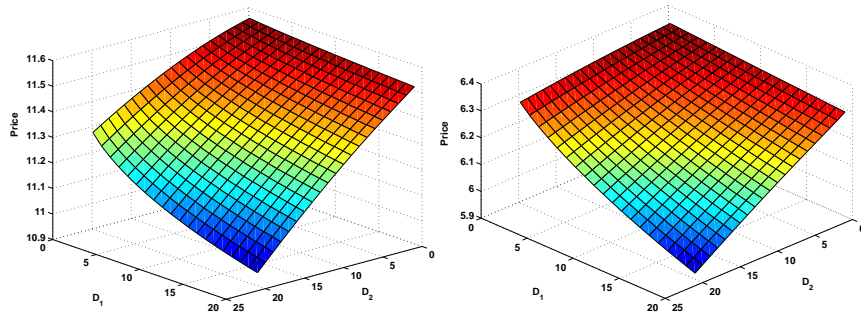


Figure 3.2: Double-sided Parisian knock-in call option prices for various times  $D_1$  and  $D_2$  with  $S_0 = 100$  (left) and  $S_0 = 90$  (right).

Figure 3.2 shows that the prices of the Parisian knock-in call decrease as the time  $D_1$  to spend below  $L_1$  or  $D_2$  to spend above  $L_2$  increase. The graph on the left-hand side shows that in case the stock price is exactly in between the levels  $L_1$  and  $L_2$  the time  $D_2$  has more influence on the price than  $D_1$ . This is a result of the fact that knocking in via the upper level and ending up above the strike is more likely than knocking in via the lower level and ending up above the strike. In the right-hand graph we changed the initial stock price to  $S_0 = 90$ . As we are now more in the neighborhood of the lower level  $L_1$ , the influence of  $D_1$  in comparison to  $D_2$  increases, which clearly follows from the graph.

Instead of computing pricing for various  $D_1$  and  $D_2$ , we can also vary the barriers  $L_1$  and  $L_2$ . The graph in figure 3.3 shows the behavior of the double-sided Parisian knock-in call for different levels. Just like the previous

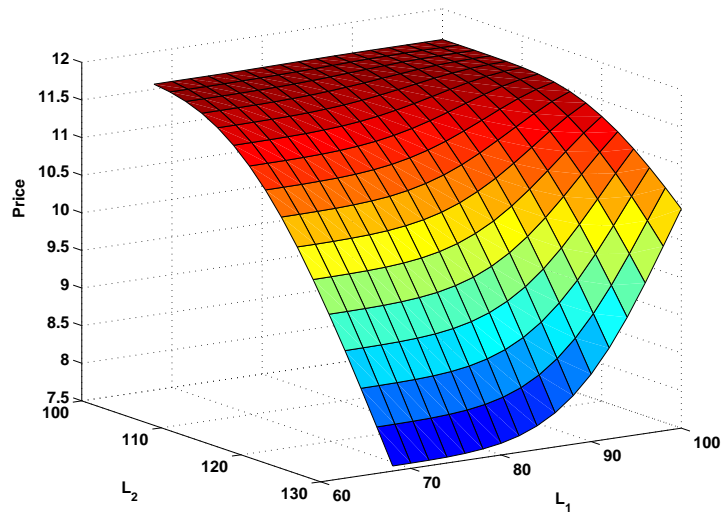


Figure 3.3: Double-sided Parisian knock-in call option prices for various barriers  $L_1$  and  $L_2$  with  $S_0 = 100$ .

example, the Parisian option price is much more sensitive to the upper level  $L_2$  than the lower level  $L_1$ .

### 3.9.2 Delta

As mentioned at the end of section 3.4 the most practical way to obtain the Greeks is by numerical differentiation. Here we give an example of the delta, the partial derivative of the double-sided Parisian knock-in call price with respect to the initial stock price value  $S_0$ . The left-hand side surface plot in figure 3.4 shows the delta for different times  $D_1 = D_2$  that should the stock price spend below  $L_1$  or above  $L_2$  to knock in. The notation on the  $D_1 = D_2$ -axis is in days. The surface plot shows that increasing periods  $D$  sharpen the shape of the delta curve w.r.t. the initial stock price value.

The delta in the surface plot looks still quite familiar to the plain vanilla delta. For example the gamma, i.e. the partial derivative of the delta w.r.t. the stock price, seems to be always positive. More spectacular behavior of the delta can be observed if we widen the barriers to  $L_1 = 80$  and  $L_2 = 120$  and we look at the region  $S_0 \leq L_1$ . In that case we need the formulas from section 3.5, because the stock is already in the excursion. Recall that  $d$  denotes the time that the stock price process still has to stay below  $L_1$  before the Parisian actually knocks in. The right-hand side graph of figure 3.4 shows how delta behaves for different  $d$ . Note that there actually exist values of  $d$  for which the gamma becomes negative.

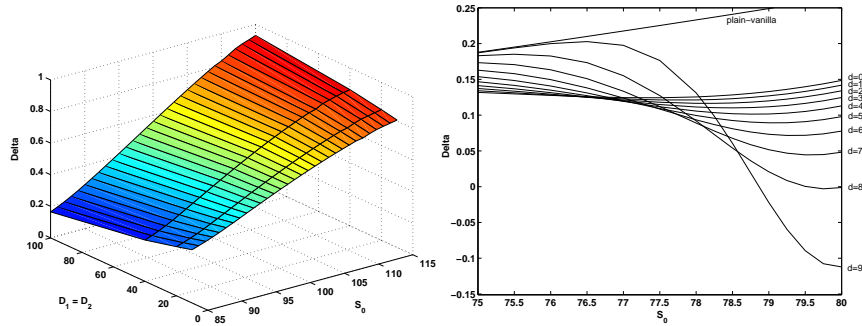


Figure 3.4: Double-sided Parisian knock-in call option deltas for various times  $D_1 = D_2$  and  $S_0$  (left) and for various  $d$  and  $S_0$  in case the barriers are set to  $L_1 = 80$  and  $L_2 = 120$  (right).

### 3.9.3 Various contract types

In this numerical example we compare the prices of the double-sided Parisian contract types as listed in section 3.7. We add the double-sided barrier option to this comparison and we implement the method described in [73] to obtain the prices. Table 3.1 contains prices of the various contracts for dif-

Table 3.1: Prices of various option contracts.

Contract type	$S_0 = 90$	$S_0 = 95$	$S_0 = 100$	$S_0 = 105$	$S_0 = 110$
Plain-vanilla	6.362	8.768	11.591	14.800	18.349
Double-sided knock-in	6.362	8.767	11.591	14.799	18.349
Double-sided P knock-in (1)	6.236	8.568	11.371	14.608	18.226
Single P up-in (2a)	5.792	8.218	11.113	14.435	18.129
P up-before-down-in (3a)	3.568	6.844	10.284	13.957	17.886
Single P down-in (2b)	2.676	1.742	1.123	0.719	0.457
P down-before-up-in (3b)	2.668	1.723	1.087	0.651	0.339

ferent values of the initial stock price. The numbers refer to the contract type numbers in their description in section 3.7 and  $P$  denotes Parisian. The plain vanilla call is the most expensive contract, very closely followed by the double-sided knock-in call barrier option. The double-sided Parisian knock-in call is again cheaper than its standard version, where the price difference is determined by  $D_1$  and  $D_2$  as is shown in figure 3.2. Both the single-sided Parisian contracts are cheaper than the double-sided in version, whereas the double-sided up-before-down-in and down-before-up-in contracts are again cheaper than the single-sided up-and-in and down-and-in contracts respectively.

### 3.9.4 Theta in the tails

In this example we consider the evolution in time of the double-sided Parisian knock-in call option for values of the initial stock price  $S_0$  below the lower barrier  $L_1$  or above the upper barrier  $L_2$ , which we will denote by the lower and upper tail respectively. We need to invert the Fourier transform as given in section 3.5, which treats the case that the stock price process is already in the excursion. The partial derivative of the option price with respect to the time to maturity is called the theta. The price of plain vanilla call options on non-dividend paying stocks always decreases as the time to expiry decreases. In practice traders with a long position in an option try to make a profit from trading their hedging portfolio. This profit should compensate the theta they are loosing in the option's long position. We start calculating prices of options that expire in  $T = 1$  year. Then we let time run in steps of one day, so the remaining time the Parisian option needs to stay away from the barrier decreases by one day. In table 3.2 we give this price evolution for  $S_0 \leq L_1$  and the barriers  $L_1 = 80, L_2 = 120$ , where  $d$  is printed in days. The columns *Par* and *Plain* contain the Parisian and plain vanilla option values respectively. The table shows that for  $S_0 = 76$  and  $S_0 = 78$  the theta is negative for the Parisian option, i.e., the value of the option increases as the time to maturity decreases. This effect is the result of the stock price spending extra days below  $L_1$  which leads to an increase of the probability of knock-in. The table also shows that theta of a Parisian is not always negative for any  $S_0 < L_1$ . For  $S_0 = 74$  theta eventually becomes positive again and the Parisian option price tends to the plain vanilla prices. The reason for this behavior is that  $S_0$  is so far below  $L_1$  that the Parisian is going to knock in with high probability and therefore its price is almost equal to the plain vanilla price. For  $S_0 = 80$  the excursion has not started yet, so the Parisian option price is strictly below the plain vanilla price.

Table 3.2: Price evolution for various values of  $S_0 \leq L_1, L_1 = 80$  and  $L_2 = 120$ .

d	$S_0 = 74$		$S_0 = 76$		$S_0 = 78$		$S_0 = 80$	
	Par	Plain	Par	Plain	Par	Plain	Par	Plain
10	1.474	1.547	1.737	1.923	1.987	2.358	2.257	2.856
9	1.474	1.536	1.740	1.911	1.984	2.344	2.240	2.841
8	1.475	1.525	1.744	1.898	1.982	2.330	2.222	2.825
7	1.476	1.514	1.750	1.885	1.984	2.316	2.205	2.809
6	1.476	1.503	1.759	1.873	1.988	2.302	2.187	2.794
5	1.475	1.492	1.770	1.860	1.997	2.288	2.170	2.778
4	1.472	1.481	1.783	1.848	2.014	2.274	2.152	2.762
3	1.467	1.470	1.797	1.835	2.041	2.260	2.135	2.747
2	1.459	1.459	1.809	1.823	2.087	2.245	2.117	2.731
1	1.448	1.448	1.809	1.810	2.164	2.231	2.100	2.715

Table 3.3 shows that also in the upper tail theta can become negative. The effect is not so strong as in the lower tail, because the probability of the intersection of ending up above the strike and knocking in via the upper

Table 3.3: Price evolution for various values of  $S_0 \geq L_2$ ,  $L_1 = 80$  and  $L_2 = 120$ .

d	$S_0 = 120$		$S_0 = 122$		$S_0 = 124$		$S_0 = 126$	
	Par	Plain	Par	Plain	Par	Plain	Par	Plain
10	25.57	26.28	27.43	27.98	29.33	29.70	31.21	31.46
9	25.54	26.26	27.42	27.95	29.32	29.68	31.21	31.43
8	25.51	26.23	27.40	27.93	29.31	29.66	31.21	31.41
7	25.48	26.21	27.39	27.91	29.31	29.63	31.21	31.39
6	25.45	26.18	27.38	27.88	29.31	29.61	31.21	31.36
5	25.42	26.16	27.37	27.86	29.32	29.58	31.21	31.34
4	25.39	26.13	27.38	27.83	29.33	29.56	31.22	31.32
3	25.36	26.11	27.39	27.81	29.36	29.54	31.24	31.29
2	25.33	26.08	27.43	27.78	29.40	29.51	31.25	31.27
1	25.30	26.06	27.53	27.76	29.46	29.49	31.24	31.25

tail is much bigger than ending up above the strike and knocking in via the lower tail. Therefore the Parisian knock-in call will behave more like a plain vanilla for  $S_0 > L_2$  than it does for  $S_0 < L_1$ .

Table 3.4: Price evolution for various values of  $S_0 \leq L_1$ ,  $L_1 = 90$  and  $L_2 = 110$ .

d	$S_0 = 84$		$S_0 = 86$		$S_0 = 88$		$S_0 = 90$	
	Par	Plain	Par	Plain	Par	Plain	Par	Plain
10	4.028	4.051	4.702	4.751	5.436	5.521	6.236	6.362
9	4.012	4.032	4.686	4.731	5.416	5.500	6.212	6.340
8	3.997	4.014	4.669	4.711	5.397	5.479	6.188	6.317
7	3.981	3.995	4.653	4.691	5.378	5.457	6.164	6.295
6	3.966	3.976	4.638	4.671	5.360	5.436	6.140	6.272
5	3.950	3.958	4.623	4.651	5.343	5.415	6.116	6.250
4	3.935	3.939	4.610	4.631	5.328	5.394	6.092	6.227
3	3.919	3.920	4.597	4.611	5.315	5.372	6.068	6.205
2	3.901	3.902	4.585	4.591	5.307	5.351	6.044	6.182
1	3.883	3.883	4.570	4.571	5.308	5.329	6.019	6.160

Tables 3.4 and 3.5 contain the same information as tables 3.2 and 3.3, except that the Parisian are now calculated for narrower barriers  $L_1 = 90$  and  $L_2 = 110$ . The tables show that the negative theta effect disappears in this case. The prices of both the Parisian knock-in call option and the plain vanilla call decrease as time goes by. The Parisian is very likely to knock in for these narrow barriers and therefore it behaves much more like the plain vanilla call.

### 3.10 Conclusion

In this paper we derived the Fourier transform for the probabilities related to the double-sided Parisian in options. These Parisian options are triggered by a double-sided Parisian stopping time. In order to get the Fourier transforms of the options, we derived the Laplace transform of the Parisian stopping time, for which we used excursion theory. We also treated the case that the Parisian option already has spent some time in the excursion. The

Table 3.5: Price evolution for various values of  $S_0 \geq L_2$ ,  $L_1 = 90$  and  $L_2 = 110$ .

d	$S_0 = 110$		$S_0 = 112$		$S_0 = 114$		$S_0 = 116$	
	Par	Plain	Par	Plain	Par	Plain	Par	Plain
10	18.23	18.35	19.76	19.85	21.34	21.40	22.95	22.99
9	18.20	18.32	19.73	19.83	21.32	21.38	22.93	22.97
8	18.17	18.30	19.71	19.80	21.29	21.35	22.91	22.94
7	18.14	18.27	19.68	19.77	21.27	21.32	22.89	22.91
6	18.11	18.24	19.66	19.75	21.25	21.30	22.87	22.89
5	18.08	18.21	19.64	19.72	21.23	21.27	22.84	22.86
4	18.05	18.19	19.61	19.69	21.21	21.25	22.82	22.84
3	18.03	18.16	19.59	19.67	21.19	21.22	22.80	22.81
2	18.00	18.13	19.58	19.64	21.18	21.19	22.78	22.79
1	17.97	18.11	19.58	19.61	21.16	21.16	22.76	22.76

Fourier transform of the double-sided Parisian in call could also be used to obtain the Fourier transform of the equivalent Parisian put. Furthermore we could derive the single-sided Parisian contract types from the double-sided Parisian as well as a down-before-up contract type. The numerical example treats the behavior of the double-sided Parisian knock-in call contract. In order to obtain actual values, we use average summation as inversion technique. Apart from the prices, we show that the Greeks can behave rather peculiar, in the sense that the Parisian contract can have a negative gamma and theta.

### 3.11 Appendix

#### 3.11.1 Calculation of $\phi_+$ for $k > l_2$ and $\phi_-$ for $k < l_1$

Here we derive the expressions for  $\phi_+$  and  $\phi_-$  as given by (3.32) and (3.33). The first step is to come up with a formula for  $E(c_1, c_2)$  for the cases not covered by lemma 3.4.2, which is done in the following lemma. The equations (3.32) and (3.33) now follow as a corollary from this lemma in the same way as corollary 3.4.3 follows from lemma 3.4.2.

**Lemma 3.11.1.** *Let  $E(c_1, c_2)$  be defined by (3.27) in lemma 3.4.2 for the real numbers  $c_1$  and  $c_2$ , then the following formulas hold,*

$$E(c_1, c_2) = \frac{2e^{mc_1}}{\tilde{v}_\alpha^2 - m^2} \mathbb{E} [e^{c_2 m N} \mathbf{1}_{\{N \leq u^*\}}] - \frac{e^{(m+\tilde{v}_\alpha)k - \tilde{v}_\alpha c_1}}{\tilde{v}_\alpha(\tilde{v}_\alpha + m)} \mathbb{E} [e^{-c_2 \tilde{v}_\alpha N} \mathbf{1}_{\{N \leq u^*\}}] \\ + \frac{e^{(m-\tilde{v}_\alpha)k + \tilde{v}_\alpha c_1}}{\tilde{v}_\alpha(\tilde{v}_\alpha - m)} \mathbb{E} [e^{c_2 \tilde{v}_\alpha N} \mathbf{1}_{\{N \geq u^*\}}], \quad k < c_1, c_2 < 0, \quad (3.37)$$

and

$$E(c_1, c_2) = \frac{e^{(m-\tilde{v}_\alpha)k + \tilde{v}_\alpha c_1}}{\tilde{v}_\alpha(\tilde{v}_\alpha - m)} \mathbb{E} [e^{c_2 \tilde{v}_\alpha N} \mathbf{1}_{\{N \leq u^*\}}] + \frac{2e^{mc_1}}{\tilde{v}_\alpha^2 - m^2} \mathbb{E} [e^{c_2 m N} \mathbf{1}_{\{N \geq u^*\}}] \\ - \frac{e^{(m+\tilde{v}_\alpha)k - \tilde{v}_\alpha c_1}}{\tilde{v}_\alpha(\tilde{v}_\alpha + m)} \mathbb{E} [e^{-c_2 \tilde{v}_\alpha N} \mathbf{1}_{\{N \geq u^*\}}], \quad k > c_1, c_2 > 0, \quad (3.38)$$

where

$$u^* = \frac{k - c_1}{c_2}. \quad (3.39)$$

*Proof.* The starting point is equation (3.29) in lemma 3.4.2, which we can write as,

$$E(c_1, c_2) = \frac{e^{mc_1}}{\tilde{v}_\alpha} \int_0^\infty u e^{-\frac{u^2}{2} + c_2 m u} I_{k-c_1-c_2 u} du, \quad (3.40)$$

where  $I_a$  is for real  $a$  given by,

$$I_a = \int_a^\infty e^{mx - |x|\tilde{v}_\alpha} dx = \begin{cases} \frac{e^{(m-\tilde{v}_\alpha)a}}{\tilde{v}_\alpha - m} & a \geq 0 \\ \frac{2\tilde{v}_\alpha}{\tilde{v}_\alpha^2 - m^2} - \frac{e^{(m+\tilde{v}_\alpha)a}}{m+\tilde{v}_\alpha} & a < 0 \end{cases}.$$

Now we split up the integral in (3.40) into two parts, separated by  $u^*$  given by (3.39), resulting in

$$E(c_1, c_2) = \frac{e^{mc_1}}{\tilde{v}_\alpha} \left( \int_0^{u^*} u e^{-\frac{u^2}{2} + c_2 m u} I_{k-c_1-c_2 u} du + \int_{u^*}^\infty u e^{-\frac{u^2}{2} + c_2 m u} I_{k-c_1-c_2 u} du \right). \quad (3.41)$$

For the case  $k < c_1$  and  $c_2 < 0$  the subscript of  $I$  is negative for left-hand side integral and positive for the right-hand side integral, giving

$$E(c_1, c_2) = \frac{e^{mc_1}}{\tilde{v}_\alpha} \left( \int_0^{u^*} u e^{-\frac{u^2}{2} + c_2 m u} \left( \frac{2\tilde{v}_\alpha}{\tilde{v}_\alpha^2 - m^2} - \frac{e^{(m+\tilde{v}_\alpha)(k-c_1-c_2u)}}{\tilde{v}_\alpha + m} \right) du \right. \\ \left. + \int_{u^*}^{\infty} u e^{-\frac{u^2}{2} + c_2 m u} \frac{e^{(m+\tilde{v}_\alpha)(k-c_1-c_2u)}}{\tilde{v}_\alpha - m} du \right).$$

Now put in this equation every non- $u$  term in front of the integral and rewrite the remaining integral as an expectation using the density of  $N$  given in (3.9) to arrive at (3.37). For the case  $k > c_1$  and  $c_2 > 0$ , except that the subscript of  $I$  is positive for the left-hand side integral in (3.41) and negative for the right-hand side integral. By symmetry we arrive at the same formula, except that the indicator sets  $\{N \leq u^*\}$  and  $\{N \geq u^*\}$  are interchanged, which gives (3.38).  $\square$

### 3.11.2 The Laplace Transform of $T_l$ occurring before $d$

We define  $\psi_l(\lambda; d)$ , the Laplace transform of the distribution of the hitting time of level  $l$  by a standard Brownian motion  $W$  restricted to the set where this hitting time occurs before  $d$  by,

$$\psi_l(\lambda; d) := \mathbb{E} \left[ e^{-\lambda T_l} 1_{\{T_l \leq d\}} \right] \quad \lambda \geq 0,$$

Now we construct a stopping time  $H = T_l \wedge d$  and use the martingale  $M_t = e^{-\frac{z^2}{2}t + zW_t}$  for our computation. As  $H$  is a bounded stopping time, we can use optional sampling to arrive at,

$$1 = \mathbb{E}[M_H] = e^{zl} \mathbb{E} \left[ e^{-\frac{z^2}{2}T_l} 1_{\{T_l \leq d\}} \right] + e^{-\frac{z^2}{2}d} \mathbb{E} \left[ e^{zW_d} 1_{\{T_l > d\}} \right].$$

The second expectation on the right-hand side can explicitly be calculated as the density  $\mathbb{P}[W_d \in dx; T_l > d]$  is well-known (see e.g. [31]),

$$\mathbb{E} \left[ e^{zW_d} 1_{\{T_l > d\}} \right] = \frac{1}{\sqrt{2\pi d}} \int_{-\infty}^b e^{zx} \left( e^{-\frac{x^2}{2d}} - e^{-\frac{(x-2l)^2}{2d}} \right) dx \\ = e^{\frac{z^2 d}{2}} \left[ \mathcal{N} \left( \frac{l - zd}{\sqrt{d}} \right) - e^{2lz} \mathcal{N} \left( \frac{-l - zd}{\sqrt{d}} \right) \right].$$

Here we assumed  $l \geq 0$ . The calculations of  $l \leq 0$  proceed in the same way and we can write a general result for all  $l$  and  $\lambda \geq 0$  by,

$$\psi_l(\lambda; d) = e^{-|l|\sqrt{2\lambda}} \mathcal{N} \left( \frac{-|l| + \sqrt{2\lambda d}}{\sqrt{d}} \right) + e^{|l|\sqrt{2\lambda}} \mathcal{N} \left( \frac{-|l| - \sqrt{2\lambda d}}{\sqrt{d}} \right). \quad (3.42)$$

### 3.11.3 UI property of $e^{-\frac{1}{2}\lambda^2(t\wedge\tau)+\lambda W_{t\wedge\tau}}$

In order to prove the UI-property we need the following two lemmas, where the first one is on the distribution of the stopped Brownian motion.

**Lemma 3.11.2.** *Let  $\tau^+$  the Parisian stopping time of the upper level, then the following holds for any  $t > 0$  and  $x \geq l_2$ ,*

$$\mathbb{P}[W_{t\wedge\tau^+} > x] \leq \mathbb{P}[W_{\tau^+} > x]. \quad (3.43)$$

*Proof.* First, recall that  $W_{\tau^+} - l_2$  is distributed as  $\sqrt{D_2}N$  and by (3.9) we can compute the probability on the right-hand side

$$\mathbb{P}[W_{\tau^+} \geq x] = \int_{\frac{x-l_2}{\sqrt{D_2}}}^{\infty} ye^{-\frac{y^2}{2}} dy = e^{-\frac{(x-l_2)^2}{2D_2}}. \quad (3.44)$$

Now rewrite the left-hand side probability in (3.43) by,

$$\begin{aligned} \mathbb{P}[W_{t\wedge\tau^+} > x] &= \\ &= \mathbb{P}[W_{\tau^+} > x | t \geq \tau^+] \mathbb{P}[t \geq \tau^+] + \mathbb{P}[W_t > x | t < \tau^+] \mathbb{P}[t < \tau^+], \end{aligned}$$

so we have to find a bound for the second conditional probability on the right-hand side. Assume that  $t \geq D_2$  and let for  $s \geq 0$  the random time  $T_{l_2}^{(s)}$  be given by

$$T_{l_2}^{(s)} = \inf\{t \geq s | W_t = l_2\},$$

denoting the first time that the Brownian motion hits the level  $l_2$  after time  $s$ . We can write for the conditional probability,

$$\begin{aligned} \mathbb{P}[W_t > x | t < \tau^+] &= \mathbb{P}[W_t > x | \tau^+ \notin [0, t - D_2) \cap T_{l_2}^{(t-D_2)} \in [t - D_2, t)] \\ &= \mathbb{P}[W_t > x | T_{l_2}^{(t-D_2)} \in [t - D_2, t)] \\ &= \int_{t-D_2}^t \mathbb{P}[W_{t-\tilde{t}} > x - l_2] \mathbb{P}[T_{l_2}^{(t-D_2)} \in d\tilde{t} | T_{l_2}^{(t-D_2)} \in [t - D_2, t)] \\ &\leq \mathbb{P}[W_{D_2} > x - l_2], \end{aligned} \quad (3.45)$$

where we used the strong Markov property to restart the process after  $T_{l_2}^{(s)}$ . Now we have to show that the probability in (3.45) is smaller than that in (3.44),

$$\begin{aligned} \mathbb{P}[W_{D_2} > x - l_2] &= \frac{1}{\sqrt{2\pi D_2}} \int_x^{\infty} e^{-\frac{(y-l_2)^2}{2D_2}} dy \\ &= \frac{e^{-\frac{(x-l_2)^2}{2D_2}}}{\sqrt{2\pi D_2}} \int_x^{\infty} e^{-\frac{(y-l_2)^2 - (x-l_2)^2}{2D_2}} dy \\ &\leq \frac{e^{-\frac{(x-l_2)^2}{2D_2}}}{\sqrt{2\pi D_2}} \int_x^{\infty} e^{-\frac{(y-x)^2}{2D_2}} dy = \frac{1}{2} \mathbb{P}[W_{\tau^+} \geq x]. \end{aligned}$$

For  $t < D_2$ , we have that

$$\mathbb{P}[W_t > x | t < \tau^+] = \mathbb{P}[W_t > x] \leq \mathbb{P}[W_{D_2} > x] \leq \mathbb{P}[W_{D_2} > x - l_2].$$

For the last probability we have already shown that it satisfies the necessary inequality to prove the lemma.  $\square$

The following lemma relates the inequality of the distribution of the previous lemma to an inequality of the expectations.

**Lemma 3.11.3.** *Let  $X$  and  $Y$  be random variables for which for every  $x > x_0$  the following inequality holds,*

$$\mathbb{P}[X > x] \leq \mathbb{P}[Y > x], \quad (3.46)$$

*then the following inequality of the expectations is satisfied for any  $l > x_0$ ,*

$$\mathbb{E}[X1_{\{X>l\}}] \leq \mathbb{E}[Y1_{\{Y>l\}}].$$

*Proof.* Let  $h^{(n)} = 2^{-n}$ , then the following approximation shows the lemma,

$$\begin{aligned} \mathbb{E}[X1_{\{X>l\}}] &= \lim_{n \rightarrow \infty} \mathbb{E} \left[ l1_{\{X>l\}} + h^{(n)} \sum_{k=1}^{\infty} 1_{\{X>l+kh^{(n)}\}} \right] \\ &\leq \lim_{n \rightarrow \infty} \mathbb{E} \left[ l1_{\{Y>l\}} + h^{(n)} \sum_{k=1}^{\infty} 1_{\{Y>l+kh^{(n)}\}} \right] = \mathbb{E}[Y1_{\{Y>l\}}], \end{aligned}$$

where we get from the first to the second line by using (3.46).  $\square$

Now we have the tools to prove the UI property of the stopped martingale  $(M_t^T)_{t \geq 0}$  given by,

$$M_t^T = e^{-\frac{1}{2}\lambda^2(t \wedge \tau) + \lambda W_{t \wedge \tau}}.$$

Consider  $\lambda > 0$ , then we have

$$M_t^T \leq e^{\lambda W_{t \wedge \tau}} \quad \text{a.s.},$$

so it remains to show that  $e^{\lambda W_{t \wedge \tau}}$  is UI. By lemma 3.11.2 we have that for  $x \geq e^{\lambda l_2}$  the following inequality holds

$$\mathbb{P}[e^{\lambda W_{\tau \wedge t}} > x] \leq \mathbb{P}[e^{\lambda W_{\tau^+ \wedge t}} > x] \leq \mathbb{P}[e^{\lambda W_{\tau^+}} > x],$$

which results by lemma 3.11.3 for  $H > e^{\lambda l_2}$  and  $h = \lambda^{-1} \ln(H)$  in

$$\mathbb{E}[e^{\lambda W_{t \wedge \tau}} 1_{\{e^{\lambda W_{t \wedge \tau}} > H\}}] \leq \mathbb{E}[e^{\lambda W_{\tau^+}} 1_{\{W_{\tau^+} > h\}}].$$

The distribution of  $W_{\tau^+}$  is known, so we have for  $h' = D_2^{-\frac{1}{2}}h$

$$\mathbb{E}[e^{\lambda W_{\tau^+}} 1_{\{W_{\tau^+} > h\}}] = e^{\lambda l_2} \mathbb{E}[e^{\lambda \sqrt{D_2} N} 1_{\{N > h'\}}] = e^{\lambda l_2} \Psi_{h'}(\lambda \sqrt{D_2}).$$

The expression on the right-hand side can be made arbitrary small by increasing  $h'$ , which proves the UI property for  $\lambda > 0$ . For  $\lambda < 0$  the proof is symmetric, where have to formulate lemma 3.11.2 in terms of  $\tau_-$ .

### 3.11.4 Discretization error

If we define the function  $f$  by,

$$f(t) = e^{-at} P_r(t) 1_{\{t \geq 0\}},$$

then the Fourier transform  $\phi$  we compute throughout the paper is in fact the Fourier transform of this function  $f$ . Now define the periodic function  $f_p$  by,

$$f_p(t) := \sum_{j=-\infty}^{\infty} f\left(t + \frac{2\pi j}{h}\right). \quad (3.47)$$

This sum is uniformly bounded in  $t$  by,

$$f_p(t) \leq \sum_{j=0}^{\infty} e^{-a\frac{2\pi j}{h}} \leq \frac{h}{2\pi} \int_{-\frac{2\pi}{h}}^{\infty} e^{-ax} dx = \frac{h}{2\pi a} e^{\frac{2\pi a}{h}}.$$

Now  $f_p$  is periodic with period  $\frac{2\pi}{h}$ , so we obtain its Fourier series by,

$$f_p(t) = \sum_{n=-\infty}^{\infty} \frac{h}{2\pi} c_n e^{ihn} \quad \text{where} \quad c_n = \int_{-\pi/h}^{\pi/h} f_p(t) e^{-ihn} dt \quad (3.48)$$

Calculation of the coefficients  $c_n$  gives,

$$\begin{aligned} c_n &= \int_{-\pi/h}^{\pi/h} f_p(t) e^{-ihn} dt = \int_{-\pi/h}^{\pi/h} \sum_{j=-\infty}^{\infty} f\left(t + \frac{2\pi j}{h}\right) e^{-ihn} dt \\ &= \sum_{j=-\infty}^{\infty} \int_{-\pi/h}^{\pi/h} f\left(t + \frac{2\pi j}{h}\right) e^{-ihn} dt \\ &= \int_{-\infty}^{\infty} f(t) e^{-ihn} dt = \phi(-nh) \end{aligned} \quad (3.49)$$

The interchange of sum and integral is allowed by dominated convergence. Using the coefficients in (3.49) and the equality between (3.48) and (3.47) we obtain the Poisson summation formula,

$$\sum_{j=-\infty}^{\infty} f\left(t + \frac{2\pi j}{h}\right) = \frac{h}{2\pi} \sum_{n=-\infty}^{\infty} \phi(-nh) e^{ihn}. \quad (3.50)$$

We can derive the same result for the symmetric function  $g$  defined by  $g(t) = f(|t|)$ . For a fixed  $t > 0$  we can set  $h = \frac{\delta}{t}$  and obtain,

$$\begin{aligned} \sum_{j=-\infty}^{\infty} g\left(t\left(1 + \frac{2\pi j}{\delta}\right)\right) &= \frac{\delta}{2\pi t} \sum_{n=-\infty}^{\infty} \phi_g(-nh) e^{ihn} \\ &= \frac{\delta}{\pi t} \Re\{\phi(0)\} + \frac{2\delta}{\pi t} \sum_{n=1}^{\infty} \Re\left\{\phi\left(\frac{n\delta}{t}\right)\right\} \cos(n\delta). \end{aligned}$$

Using  $f(t) = g(t)$  for  $t > 0$  we have,

$$f(t) = g(t) = \frac{\delta}{\pi t} \Re\{\phi(0)\} + \frac{2\delta}{\pi t} \sum_{n=1}^{\infty} \Re\left\{\phi\left(\frac{n\delta}{t}\right)\right\} \cos(n\delta) - \sum_{|j|>0} g\left(t\left(1 + \frac{2\pi}{\delta}j\right)\right). \quad (3.51)$$

In order to get an estimate for the error, we need to control the last sum term. Suppose we choose  $\delta < 2\pi$ , then we have for this error term  $\epsilon$ ,

$$\begin{aligned} \epsilon &= \sum_{|j|>0} g\left(t\left(1 + \frac{2\pi}{\delta}j\right)\right) \leq \sum_{|j|>0} \exp\left(-at\left|1 + \frac{2\pi}{\delta}j\right|\right) \\ &\leq 2 \sum_{j=1}^{\infty} \exp\left(-at\left(\frac{2\pi}{\delta}j - 1\right)\right) \leq \frac{2e^{-a\left(\frac{2\pi}{\delta}-1\right)t}}{1 - e^{-a\frac{2\pi}{\delta}t}} \end{aligned} \quad (3.52)$$

### 3.11.5 Truncation error

If we approximate the integral by a sum, we have

$$\int_0^{\infty} \cos(vT) \Re\{\phi(v)\} dv \approx h \sum_{j=1}^{\infty} \cos(v_j T) \Re\{\phi(v_j)\}.$$

Here  $v_j = h(j-1)$ . To get a bound on the truncation error  $\epsilon$ , we have to calculate,

$$\epsilon = \left| h \sum_{j=N+1}^{\infty} \cos(v_j T) \Re\{\phi(v_j)\} \right| \leq h \sum_{j=N+1}^{\infty} |\Re\{\phi(v_j)\}| = h \sum_{j=N+1}^{\infty} \epsilon_j$$

For the  $\epsilon_j$  we can write,

$$\begin{aligned} \epsilon_j &= \left| \Re \int_0^{\infty} e^{iv_j t} f(t) dt \right| \leq \left| \int_0^{\infty} \cos(v_j t) e^{-\alpha t} dt \right| \\ &= e^{-\alpha t} \frac{v_j \sin(v_j t) - \alpha \cos(v_j t)}{\alpha^2 + v_j^2} \Bigg|_{t=0}^{t=\infty} = \frac{\alpha}{\alpha^2 + v_j^2}. \end{aligned}$$

As the term  $\frac{\alpha}{\alpha^2 + v_j^2}$  is decreasing in  $v_j$  we can write,

$$\epsilon \leq h \sum_{j=N+1}^{\infty} \frac{\alpha}{\alpha^2 + v_j^2} \leq \int_{v_N}^{\infty} \frac{\alpha}{\alpha^2 + v^2} dv = \arctan\left(\frac{\alpha}{h(N-1)}\right) \quad (3.53)$$

## Chapter 4

# Pricing Parisians and barriers by hitting time simulation

Parisian options are not exchange traded, but there are various applications of Parisian optionality in the fields of real option theory, convertible bond valuation and credit risk. Especially the valuation of consecutive Parisian options is complicated and there exist no explicit formulas for these contracts. So far valuation can be done by numerically inverting Laplace transforms or by PDE methods. This paper develops a Monte Carlo method by exploiting the Markovian nature of the underlying value process. As a result, the Parisian option value can be written as an expression that can be solved by Monte Carlo integration, where the Parisian times are the random variables that need to be simulated. The Parisian times cannot be simulated directly as there exists no explicit distribution function. Therefore these times are approximated by the simulation of hitting times in a special way. The quality of this approximation can be controlled and is a trade-off between accuracy and computation time.

### 4.1 Introduction

The Parisian option is a path-dependent option that is triggered by the first time the underlying value process spends a given time period below or above some level. The additional stay-above-or-below feature extends the notion of a standard barrier option, for which just hitting a level is enough to trigger the contract. The standard barrier is governed by the hitting time and we denote the time that governs the Parisian contract by the Parisian time. This time can be measured in a consecutive or a cumulative way. In

the consecutive case the measurement of the time period below or above the barriers starts from zero each time the barrier is crossed, whereas these periods are added up in the cumulative case. Although Parisian options are nowadays not exchange traded, there are a number of applications of Parisian optionality in mathematical finance. They turn up in real option problems as treated in [43]. Parisians are the building block of the soft-call constraint in convertible bonds as in [61]. For applications in credit risk and life insurance see [66] and [27] respectively. As a result of this variety of applications, the valuation problem of Parisian options is of interest to a broad range of financial fields, where risk-management, investment theory and credit risk are just a few that we mention.

The valuation of cumulative Parisian options has to do with occupation time densities and there are useful results in [35], [65] and [72]. The valuation of the consecutive Parisian option is more complicated and it has been initiated by [30]. These authors did derive Laplace transforms for various consecutive Parisian contracts. We will use their Laplace transforms and the numerical inversion techniques in [4] to obtain reference prices for our numerical examples. In [10] the authors use polynomial approximation of the Laplace transforms of [30] to obtain prices. The authors in [49] use a PDE approach to value Parisians, but convergence appears to be very slow. In [6] the authors also formulate a PDE and construct a trinomial lattice from it. The author in [33] constructs a clever combinatorial approach to count the paths in a binomial tree that satisfy the Parisian constraint. For all of these lattice methods the local behavior of Brownian motion makes it necessary to choose the step size of the lattice carefully. In this paper, we are going to develop a Monte Carlo method for Parisian option pricing, as this method seems to be missing in the literature. The reason to consider Monte Carlo valuation for Parisian options is in the flexibility of Monte Carlo methods. Once a Monte Carlo has been developed it might be possible to modify it for the cases of a more complicated pay-off or more sophisticated underlying value model. Note, that the literature on Parisian options we cite here only deals with the classical geometric Brownian motion as model for the underlying value process.

As a result of the local behavior of Brownian motion, the main ingredient of the underlying value process, straightforward path-simulation of this process will not result in a Monte Carlo method that converges within reasonable time. Therefore we construct an alternative Monte Carlo algorithm, which we base on hitting time simulation. Using the Markovian structure of the underlying process, we can write the valuation of a Parisian option as an expression that can be solved by Monte Carlo integration, where the Parisian time is the random variable that needs to be simulated. A similar expression for standard barrier options has already been derived in [82]. We obtain approximations of samples of the Parisian time by an algorithm that simulates hitting times in a special way. The algorithm contains a parameter  $\epsilon$  that

determines the quality of the approximation. As always, there is a trade-off between the quality of the approximation and the computation time.

In this paper we start with the explanation of the idea of hitting time simulation. We will use the standard barrier option in a particular case to explain the method and show the accuracy of it. Once the concept is presented, the hitting time simulation algorithm will be extended to the valuation of a general barrier, which is in fact an application of Girsanov's theorem. After that we show that we can value both the cumulative and the consecutive Parisian option using this concept and also illustrate the presented recipe with an example. Finally we make some numerical remarks about the parameter  $\epsilon$  that is important in the approximation of the Parisian time.

## 4.2 Model of the economy

The economy we are going to use for option pricing consists of a bank-account and an asset price process. Assume that on the bank-account the interest rate  $r$  is calculated in the continuously compounded way and equal for positive and negative amounts of money. Let  $\{S_t; t \geq 0\}$  be the asset price process defined on the filtered probability space  $(\Omega, \mathcal{F}, \mathcal{F}_t, \mathbb{P})$ . We assume the price process  $S$  to be given by a geometric Brownian motion as it is within the Black-Scholes model. It is well-known that, in case a set conditions is fulfilled, this economy is complete, which means that for every pay-off  $\Psi$  at time  $T$  that can be expressed in terms of the asset price path up to time  $T$ , there exists a replicating self-financing trading strategy. A self-financing trading strategy is called replicating for a pay-off  $\Psi$  if at time  $T$  the (random) value of the portfolio constructed by this strategy equals the pay-off  $\Psi$ . It is also well-known that this economy is arbitrage-free, i.e., it is not possible to have a positive probability of a return on your money bigger than the risk-free interest rate  $r$  without having a positive probability of a return less than  $r$ . If an economy is complete and arbitrage-free, the replicating strategy should be unique and the price of a derivative should be given by the initial investment of the replicating strategy. In order to calculate this initial investment, we introduce the risk-neutral asset price process given by

$$S_t = s_0 \exp \left\{ \left( r - \frac{1}{2} \sigma^2 \right) t + \sigma W_t \right\},$$

where  $\{W_t; t \geq 0\}$  denotes a standard Brownian motion,  $s_0$  the initial value of the stock,  $r$  the risk-free interest rate and  $\sigma$  the volatility of the asset. The initial investment of the replicating strategy, which is the price  $V_\Psi$  of a derivative with pay-off  $\Psi((S_t)_{0 \leq t \leq T})$  and maturity  $T$  can be computed by,

$$V_\Psi = e^{-rT} \mathbb{E} [\Psi((S_t)_{0 \leq t \leq T})]. \quad (4.1)$$

The previously mentioned conditions that ensure arbitrage-freeness and completeness of an economy are conditions like the ability of short-selling, continuous trading and absence of transaction costs. In the equity markets for example, these conditions are almost fulfilled. Professional institutions are allowed short-selling, they can trade continuously around the globe and their transaction costs are negligible in comparison to the size of their trades. An intuitive discussion on these conditions can be found in [52] and a more formal treatment is given in [12].

A standard barrier option is an option that pays off like a standard call or put with strike  $X$  in cases where a predefined barrier  $L$  is hit or not. Barriers that do not pay off once the barrier  $L$  is hit, are called knock-out barriers and their counterparts are denoted by knock-ins. In the sequel we look at the value  $DIC$  of a down-and-in call, this is a knock-in contract, where the barrier  $L$  is below the initial asset price  $s_0$ . The value  $DIC$  is calculated by,

$$DIC = e^{-rT} \mathbb{E} [(S_T - X)^+ 1_{\{T_L \leq T\}}], \quad (4.2)$$

where  $T_L$  denotes the hitting time of the level  $L$  by the process  $S$ :

$$T_L := \inf\{t \geq 0; S_t = L\}. \quad (4.3)$$

There is a closed form solution to (4.2), for example in [12]. In the next section we will show how we can use samples of (4.3) and Monte Carlo integration to calculate the barrier price.

### 4.3 Hitting time simulation for the standard barrier option

In this section we show how we obtain a Monte Carlo integration method for a special parameter set of the standard down-and-in call by using the strong Markov property for Brownian motion. For a general introduction on Monte Carlo methods in finance, see [46]. The approach we take here of integrating over the hitting time density has been followed by [56] and [82]. Thereafter we rely on Girsanov's theorem to generalize the method for all parameter sets. First we start with the special case  $r = 0.5\sigma^2$ , which gives,

$$S_t = L \quad \Leftrightarrow \quad W_t = \sigma^{-1} \ln \frac{L}{s_0} =: l.$$

Defining  $\tau_l$  as the hitting time of  $l$  by the Brownian motion  $W$  in the same way as in (4.3), we have  $T_L = \tau_l$ . Let  $BSC(s_0, T)$  be the value of a vanilla call with time to maturity  $T$  and initial asset price  $s_0$ . Now we use conditioning

and the strong Markov property of Brownian motion to obtain,

$$\begin{aligned}
DIC &= e^{-rT} \mathbb{E} [(S_T - X)^+ 1_{\{T_L \leq T\}}] \\
&= e^{-rT} \mathbb{E} [1_{\{\tau_l \leq T\}} \mathbb{E} [(s_0 e^{\sigma W_T} - X)^+ | \mathcal{F}_{\tau_l}]] \\
&= \mathbb{E} [1_{\{\tau_l \leq T\}} e^{-r\tau_l} e^{-r(T-\tau_l)} \mathbb{E} [(L e^{\sigma W_s} - X)^+ ]_{s=T-\tau_l}] \\
&= \mathbb{E} [1_{\{\tau_l \leq T\}} e^{-r\tau_l} BSC(L, T - \tau_l)]. \tag{4.4}
\end{aligned}$$

From (4.4) we have that, once we can simulate  $\tau_l$ , we immediately have a Monte Carlo algorithm for the valuation of the standard barrier price. In fact, solving (4.4) by Monte Carlo is called Monte Carlo integration. In order to speed up the algorithm, we write

$$\begin{aligned}
DIC &= \int_0^T e^{-rt} BSC(L, T - t) \mathbb{P}[\tau_l \in dt] \\
&= \mathbb{P}[\tau_l \leq T] \int_0^\infty e^{-rt} BSC(L, T - t) \mathbb{P}[\tau_l \in dt | \tau_l \leq T]. \tag{4.5}
\end{aligned}$$

We use the reflection principle (see e.g. [55]) to obtain  $F_{\tau_l}$ , the distribution function of  $\tau_l$  and obtain:

$$F_{\tau_l}(t) = \mathbb{P}[\tau_l \leq t] = 2\mathbb{P}[W_t \leq l] = 2\Phi\left(\frac{l}{\sqrt{t}}\right), \tag{4.6}$$

where  $\Phi$  is the standard normal distribution function. Note, that (4.6) is actually a distribution function as for the case  $L \leq s_0$  we have  $l \leq 0$ . In order to draw the samples, we need the inverse distribution function  $F_{\tau_l}^{-1}$ ,

$$F_{\tau_l}^{-1}(y) = \left(\frac{l}{\Phi^{-1}\left(\frac{y}{2}\right)}\right)^2. \tag{4.7}$$

Now we compute the expectation (4.4) by constructing a Monte Carlo integration algorithm for (4.5). So, we have to sample random variables from the distribution of the hitting time, conditional on the event that this hitting time does happen before  $T$ . We use the hitting time distribution and its inverse to do so and construct the following algorithm.

ALGORITHM 1 (SIMPLE DIC)

- Take  $\alpha = F_{\tau_l}(T)$ ,  $Res = 0$ .
- Repeat  $N$  times :
  - Sample  $u$  from  $\mathcal{U}[0, \alpha]$ .
  - Obtain the sample  $\tau$  by  $\tau = F_{\tau_l}^{-1}(u)$
  - $Res = Res + e^{-r\tau} BSC(L, T - \tau)$
- $Res = N^{-1} \cdot \alpha \cdot Res$

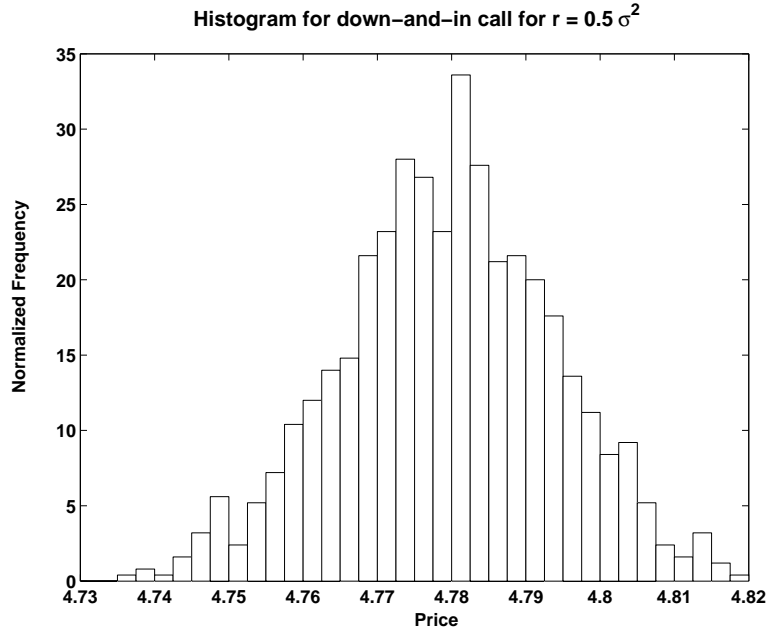


Figure 4.1: Normalized histogram generated by 1000 runs of the algorithm for the ( $r = \frac{1}{2}\sigma^2$ )-case of the down-and-in call. Each individual run consists of  $10^4$  samples and the reference price is 4.7792

Here we used  $\alpha$  to obtain only relevant samples in the region  $T_L \leq T$ . We implemented the algorithm for a *DIC* with  $L = 90$ ,  $s_0 = 100$ ,  $X = 100$ ,  $T = 1$ ,  $r = 4.5\%$  and  $\sigma = 30\%$ . The exact price of this contract up to 4 digits is 4.7792. Figure 4.1 gives the distribution of the Monte Carlo values around this exact value for  $N = 10^4$ , where we used 1000 runs of the algorithm to obtain the histogram. Note that the frequencies are normalized, such that the total area below the histograms equals one. The rate of convergence is shown in figure 4.2, where we did run the algorithm 1000 times and plot the 95%, 90% and 50% empirical quantiles of the absolute error distribution.

In algorithm 1, we are only able to simulate prices in case  $r = 0.5\sigma^2$ . We can extend this to general values for  $r$  and  $\sigma$  using the Girsanov transformation, without that it is necessary to sample values from a Brownian hitting time with drift. We define a process  $\{Z_t, t \geq 0\}$  and a constant  $m$  by,

$$Z_t := \frac{r - 0.5\sigma^2}{\sigma}t + W_t =: mt + \sigma W_t \quad (4.8)$$

Now we denote by  $\tau_l$  the hitting time of the level  $l$  by the process  $Z$ . We know from Girsanov's theorem that there exists an equivalent measure  $\mathbb{Q}$  such that  $Z$  is a standard Brownian motion under  $\mathbb{Q}$ . Furthermore this theorem gives the Radon-Nikodým derivative connecting  $\mathbb{P}$  and  $\mathbb{Q}$ , so we

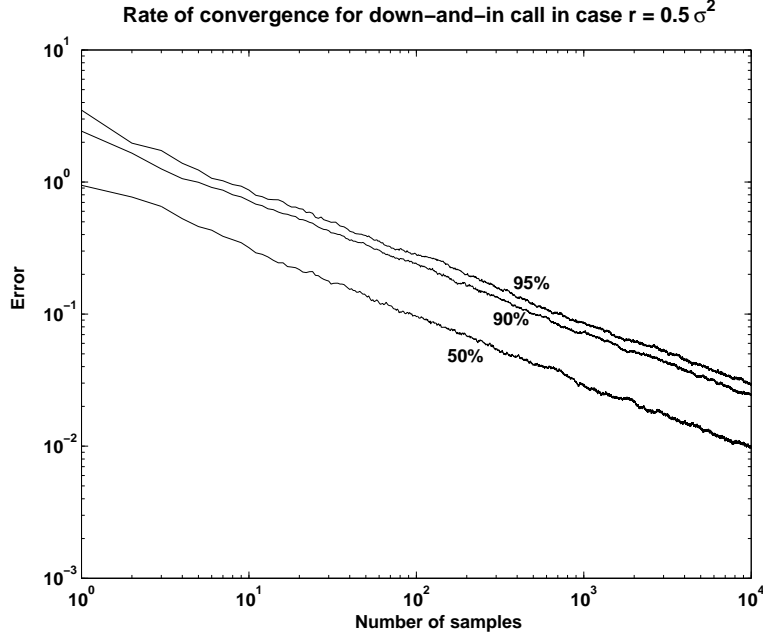


Figure 4.2: Rate of convergence graph containing plots of the 95%, 90% and 50% empirical quantiles of absolute error distribution versus number of hitting time simulations, generated by 1000 runs of the algorithm for the ( $r = \frac{1}{2}\sigma^2$ )-case of the down-and-in call. Each individual run consists of  $10^4$  samples.

can value a claim  $\Psi$  as in (4.1) by,

$$\begin{aligned}
 V_{\Psi} &= e^{-rT} \mathbb{E} \left[ \Psi((s_0 e^{(r-0.5\sigma^2)t + \sigma W_t})_{0 \leq t \leq T}) \right] \\
 &= e^{-rT} \mathbb{E} \left[ \Psi((s_0 e^{\sigma Z_t})_{0 \leq t \leq T}) \right] \\
 &= e^{-rT} e^{-\frac{m^2}{2}T} \mathbb{E}_{\mathbb{Q}} \left[ e^{mZ_T} \Psi((s_0 e^{\sigma Z_t})_{0 \leq t \leq T}) \right]. \quad (4.9)
 \end{aligned}$$

Here we used the definition in (4.8) of the process  $Z$  and the change-of-measure to get rid of the drift part of the Brownian motion. It is possible to obtain directly the distribution of  $\tau_l$  under  $\mathbb{P}$ , see e.g. [12]. As we are also interested in the inverse of the hitting time distribution, we will simulate under  $\mathbb{Q}$ , using the fact that we know the connecting Radon-Nikodým derivative. If we proceed along the same lines as we did for the derivation of (4.4), we find:

$$\begin{aligned}
 DIC &= e^{-rT} e^{-\frac{m^2}{2}T} \mathbb{E}_{\mathbb{Q}} \left[ e^{mZ_{\tau}} 1_{\{\tau \leq T\}} \mathbb{E}_{\mathbb{Q}} \left[ e^{m(Z_T - Z_{\tau})} (s_0 e^{\sigma Z_T} - X)^+ \middle| \mathcal{F}_{\tau} \right] \right] \\
 &= e^{ml} \mathbb{E}_{\mathbb{Q}} \left[ e^{-(r + \frac{m^2}{2})\tau} 1_{\{\tau \leq T\}} e^{-(r + \frac{m^2}{2})(T - \tau)} \mathbb{E}_{\mathbb{Q}} \left[ e^{mZ_t} (L e^{\sigma Z_t} - X)^+ \middle|_{t=T-\tau} \right] \right] \\
 &= e^{ml} \mathbb{E}_{\mathbb{Q}} \left[ e^{-(r + \frac{m^2}{2})\tau} 1_{\{\tau \leq T\}} BSC(L, T - \tau) \right]. \quad (4.10)
 \end{aligned}$$

Here we used  $Z_{\tau_l} = l$ . Now we can use the distribution of  $\tau_l$  we already computed for the algorithm, because under  $\mathbb{Q}$  the process  $Z$  is a standard Brownian motion, just as  $W$  is under  $\mathbb{P}$  and it is therefore not necessary to sample from the distribution of the hitting time of a Brownian motion with drift. Also in this case it is possible to draw conditional samples, like we showed by deriving (4.5) from (4.4). The modified algorithm is given below.

ALGORITHM 2 (DIC)

- Take  $\alpha = F_{\tau_l}(T)$ ,  $Res = 0$ .
- Repeat  $N$  times :
  - Sample  $u$  from  $\mathcal{U}[0, \alpha]$ .
  - Obtain the sample  $\tau$  by  $\tau = F_{\tau_l}^{-1}(u)$
  - $Res = Res + e^{-(r+0.5m^2)\tau} BSC(L, T - \tau)$
- $Res = N^{-1} \cdot e^{ml} \cdot \alpha \cdot Res$

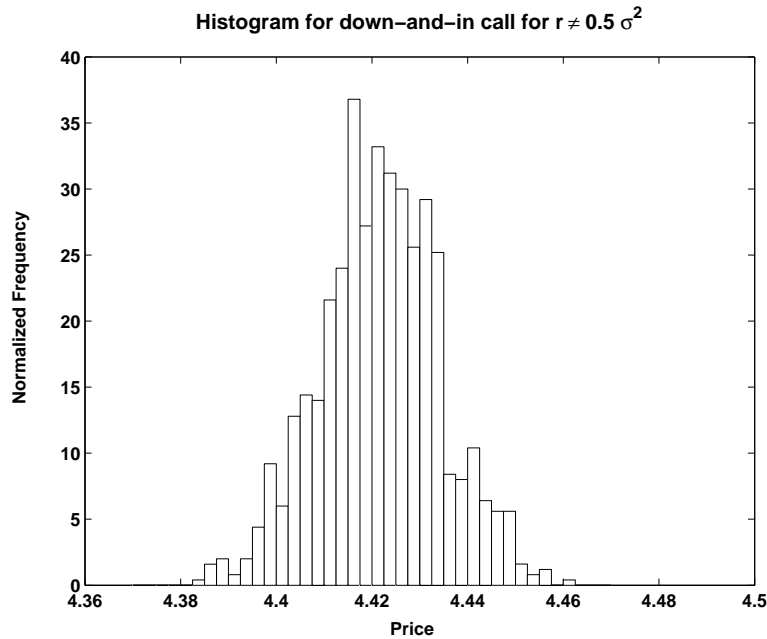


Figure 4.3: Normalized histogram generated by 1000 runs of the algorithm for the  $(r < \frac{1}{2}\sigma^2)$ -case of the down-and-in call. Each individual run consists of  $10^4$  samples and the reference price is 4.4213

We implemented the algorithm for a *DIC* with  $L = 90$ ,  $s_0 = 100$ ,  $X = 100$ ,  $T = 1$ ,  $r = 1.5\%$  and  $\sigma = 30\%$ . The exact price of this contract up to 4 digits is 4.4213. Figure 4.3 gives the distribution of the Monte Carlo values

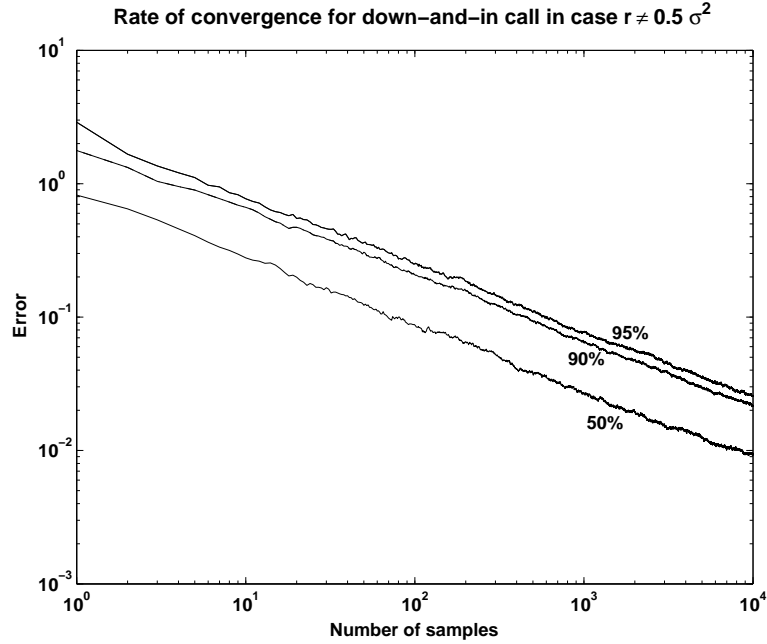


Figure 4.4: Rate of convergence graph containing plots of the 95%, 90% and 50% empirical quantiles of absolute error distribution versus number of hitting time simulations, generated by 1000 runs of the algorithm for the ( $r < \frac{1}{2}\sigma^2$ )-case of the down-and-in call. Each individual run consists of  $10^4$  samples.

around this exact value for  $N = 10^4$ . Figure 4.4 gives insight in the rate of convergence by estimating the quantiles of the absolute error distribution in the same way as in the previous example.

#### 4.4 The consecutive Parisian contract

In the previous section we used Monte Carlo integration for barrier option pricing and, as the distribution of the relevant hitting time is explicitly known, we could directly sample from this distribution to perform the Monte Carlo integration as described in the algorithms 1 and 2. Here we are going to consider a Parisian option and the stopping time that determines the Parisian pay-off does not have an explicit density or distribution. So again we can use the strong Markov property as in (4.4) and (4.10), but we have to do extra work to obtain samples from the stopping time distribution.

The consecutive Parisian option contract is very much like a barrier contract, except that it does not only need to touch the barrier, but it also needs to stay above or below this barrier for some consecutive period  $H$ . Define  $\Gamma_t^L$  to be the last time before  $t$  that  $S$  equals  $L$ ,

$$\Gamma_t^L = \sup\{s \leq t; S_s = L\}.$$

Then, using the process  $S$  again, we can define  $\gamma_t^l$  as the last time before  $t$  that the process  $Z$  hits the level  $l$  and we have  $\gamma_t^l = \Gamma_t^L$ . Let us consider  $PDIC$ , the Parisian down-and-in call, for which we can write,

$$PDIC = e^{-rT} \mathbb{E}[(S_T - X)^+ 1_{\{T_H^{L,-} \leq T\}}],$$

where  $T_H^{L,-}$  is given by,

$$\begin{aligned} T_H^{L,-} &= \inf \{t > 0; S_t < L \wedge (t - \Gamma_t^L) \geq H\} \\ &= \inf \{t > 0; Z_t < l \wedge (t - \gamma_t^l) \geq H\}. \end{aligned}$$

We are now looking for a way to obtain samples for  $T_H^{L,-}$ . There are theoretical results on this stopping time, see for example [30] and [43], but these results are in terms of Laplace transforms, explicit distributions are not given. A first intuition would be to simulate a hitting time for the barrier  $L$ , then simulate the length of the excursion below  $L$  and repeat this until the length of the excursion is larger than  $H$ . Unfortunately the first excursion after hitting the level  $L$  is not properly defined as a consequence of the local behavior of Brownian motion. Here we suppose the strike  $X$  above the barrier  $L$ , such that we can define  $\tau_H^{l,-}$  the first time after  $T_H^{L,-}$  the process  $Z$  hits the level  $l$  again by,

$$\tau_H^{l,-} := \inf \{t > T_H^{L,-} : Z_t = l\}.$$

The idea is now to approximate  $\tau_H^{l,-}$ , because using the strong Markov property and Girsanov again we can derive,

$$\begin{aligned} PDIC &= e^{-rT} \mathbb{E} \left[ (S_T - X)^+ 1_{\{T_H^{L,-} \leq T\}} \right] \\ &= e^{ml} \mathbb{E}_{\mathbb{Q}} \left[ e^{-(r + \frac{m^2}{2})\tau_H^{l,-}} 1_{\{\tau_H^{l,-} \leq T\}} BSC \left( L, T - \tau_H^{l,-} \right) \right]. \end{aligned} \quad (4.11)$$

Here we exploited the fact that  $X > L$  and the continuity of the asset price process that gives,

$$\{S_T > X\} \cap \{T_H^{L,-} \leq T\} = \{S_T > X\} \cap \{\tau_H^{l,-} \leq T\} \quad \text{a.s.} \quad (4.12)$$

The approximation of  $\tau_H^{l,-}$  will be done in the following way. We fix an  $\epsilon > 0$  and take  $l'(\epsilon)$  such that hitting the level  $L - \epsilon$  by  $S$  is equivalent to hitting the level  $l'(\epsilon)$  by  $Z$ . In the sequel we will write  $l'$  whenever it is clear that  $\epsilon$  is fixed. Now we simulate  $\tau_1$  from  $F_{0,l'}$ , the distribution of hitting times of  $Z$  hitting  $l'$  starting in 0. Then we simulate  $\tau_2$  from  $F_{l',l}$  the distribution of hitting times of  $Z$  hitting  $l$ , starting in  $l'$ . Now we have three possibilities:

- If  $\tau_1 + \tau_2 \geq T$ , then the asset price path does not exceed the barrier within the interval  $[\tau_1, T]$  and therefore at time  $T$  it is certainly below the strike. For this sample the PDIC expires worthless and we throw it away.
- In case of  $\tau_2 > H$  we have a sample of  $\tau_H^{l,-}$  and we stop, keeping the sample.
- If case of  $\tau_2 < H$  we are at  $l$  and need to get back to  $l'$  again in order to fulfill the Parisian constraint. So we simulate  $\tau_3$  from  $F_{l,l'}$ , the distribution of hitting times of  $Z$  hitting  $l'$ , starting in  $l$ . Now we start again as if we simulated a hitting time  $\tau_1$  of  $\tau_1 = \tau_1 + \tau_2 + \tau_3$ . We keep on repeating this until we either have to throw away the sample (the first bullet) or we can keep it (the second bullet).

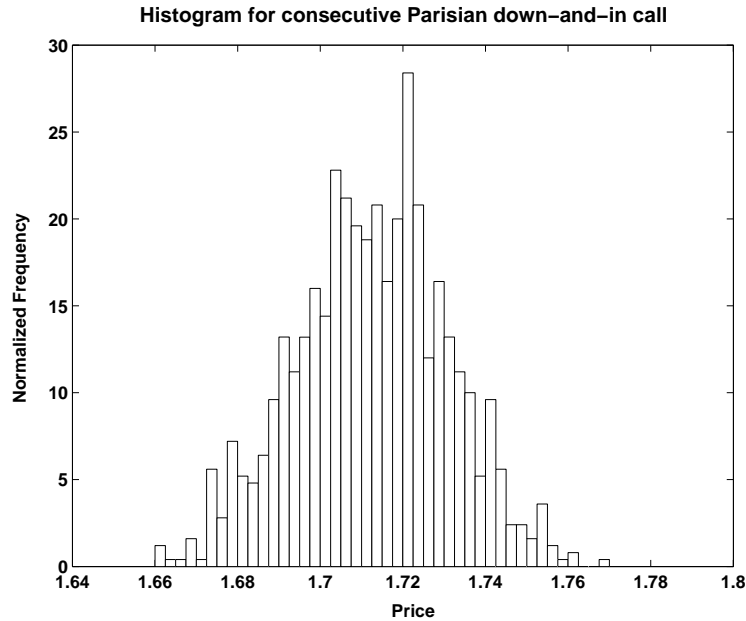


Figure 4.5: Normalized histogram generated by 1000 runs of the algorithm for the consecutive Parisian down-and-in call. Each individual run consists of  $10^4$  samples and the reference price is 1.712.

We need to know the distribution  $F_{l,l'}$  and  $F_{l',l}$ . We recall that we are simulating under  $\mathbb{Q}$ . So we know that  $Z$  is a standard Brownian motion and the symmetry of this object ensures that  $F_{l,l'} = F_{l',l}$ . Furthermore we can use the stationarity to obtain that  $F_{l',l} = F_{0,(l'-l)}$ , where the last one we can derive from (4.6) by,

$$F_{0,(l'-l)} = F_{\tau_{(l'-l)}}$$

Transforming this in an Monte Carlo algorithm we obtain the algorithm on the next page for the Parisian down-and-in call. Within the while loop, we

simulate time periods that the asset price process needs to travel from  $L - \epsilon$  to  $L$  and back. We keep on doing this until either the cumulative time is larger than expiry or we have stayed below  $L$  long enough. The first case corresponds to a sample path that did not manage to fulfill the Parisian condition and we have  $\tau_H^{l,-} > T$ . In the second case we have an approximation of  $\tau_H^{l,-}$ . If the simulated hitting time of level  $L$  is too small, we did not spend enough time below the barrier and we have to go back to the level  $L - \epsilon$  to start over again.

ALGORITHM 3 (CONSECUTIVE PDIC WITH  $X \geq L$ )

- Take  $\alpha = F_{\tau_l}(T)$ ,  $Res = 0$ .
- Repeat  $N$  times :
  - Sample  $u$  from  $\mathcal{U}[0, \alpha]$ .
  - Obtain the sample  $\tau$  by  $\tau = F_{\tau_l}^{-1}(u)$
  - $h = 0$
  - While  $\tau < T$  AND  $h < H$ ,
    - Sample  $w$  from  $\mathcal{U}[0, 1]$ .
    - Obtain the sample  $h$  by  $h = F_{\tau_{(l-l)}}^{-1}(w)$
    - $\tau = \tau + h$
    - If  $h < H$ ,
      - Sample  $w$  from  $\mathcal{U}[0, 1]$ .
      - Obtain the sample  $h'$  by  $h' = F_{\tau_{(l-l)}}^{-1}(w)$
      - $\tau = \tau + h'$ .
    - end If
  - end While
  - If  $\tau < T$ ,
    - $Res = Res + e^{-(r+0.5m^2)\tau} BSC(L, T - \tau)$
- $Res = N^{-1} \cdot e^{ml} \cdot \alpha \cdot Res$

We implemented the algorithm and simulated for a *PDIC* with  $L = 90$ ,  $\epsilon = 0.5$ ,  $H = 10/250$ ,  $s_0 = 100$ ,  $X = 100$ ,  $T = 1$ ,  $r = 1.5\%$  and  $\sigma = 30\%$ . We use a reference price for this Parisian option denoted by the Laplace price, which is obtained by numerical Laplace inversion using a method of [4] of the Laplace transforms given in [30]. The Laplace price of this contract - significant up to 3 digits - is 1.712. Figure 4.5 gives the distribution of the Monte Carlo value around this Laplace price for  $N = 10^4$ , where figure 4.6 shows the rate of convergence.

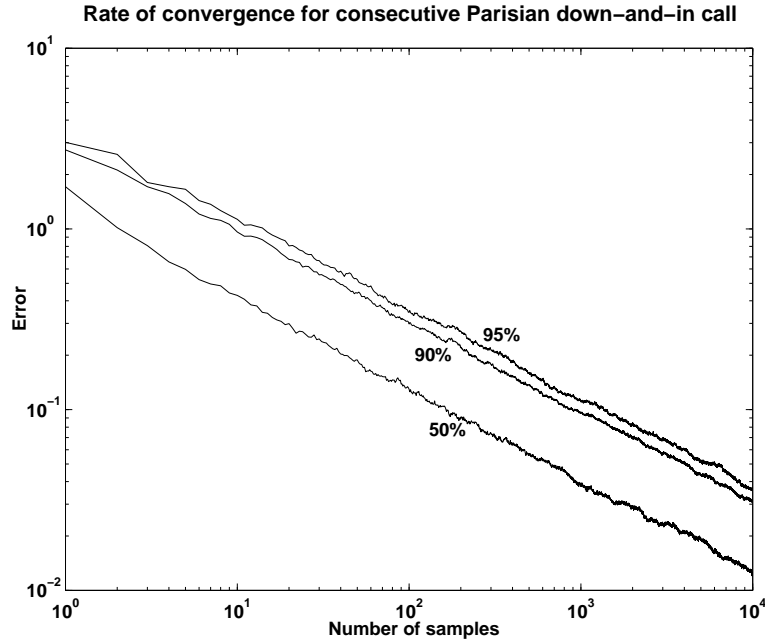


Figure 4.6: Rate of convergence graph containing plots of the 95%, 90% and 50% empirical quantiles of absolute error distribution versus number of hitting time simulations, generated by 1000 runs of the algorithm for the consecutive Parisian down-and-in call. Each individual run consists of  $10^4$  samples.

## 4.5 The cumulative Parisian contract

In analogy to the consecutive Parisian option contract, we can define the cumulative contract. Here the asset price process  $S$  should also stay below or above some barrier for a certain period  $H$ , but this period need not to be a consecutive period of time. Again we are interested in the cumulative Parisian down-and-in call (CPDIC), so we look at  $T_H^{L,c-}$  the first time that the cumulative time spent by the asset price process  $S$  below the barrier  $L$  is of length  $H$ ,

$$\begin{aligned} T_H^{L,c-} &:= \inf \left\{ t > 0; \int_0^t 1_{\{S_u \leq L\}} du = H \right\} \\ &= \inf \left\{ t > 0; \int_0^t 1_{\{Z_u \leq l\}} du = H \right\}. \end{aligned} \quad (4.13)$$

The second equality shows that we can define  $T_H^{L,c-}$  also in terms of  $Z$ . The integrals in (4.13) represent the occupation time of a Brownian motion. Cumulative Parisian option pricing is therefore linked to occupation time density problems. A representation of the cumulative Parisian option in terms of these occupation time densities can be found in [30] or [35]. More on the application of occupation time densities in finance can be found in

[72]. Here we proceed pricing the cumulative Parisian options in the same way we priced the consecutive contracts, although other methods might perform better. Like the consecutive Parisian case, we assume the strike  $X$  to be above the barrier  $L$ , so it makes sense to define  $\tau_H^{l,c-}$  by,

$$\tau_H^{l,c-} := \inf\{t > T_H^{L,c-}; Z_t = l\}.$$

Using again the continuity of the asset price process and  $X > L$  we have an equality similar to (4.12),

$$\{S_T > X\} \cap \{T_H^{L,c-} \leq T\} = \{S_T > X\} \cap \{\tau_H^{l,c-} \leq T\} \quad \text{a.s.}$$

The computation of the cumulative Parisian down-and-in call *CPDIC* is by the same arguments we used to derive (4.11) given by,

$$CPDIC = e^{ml} \mathbb{E}_{\mathbb{Q}} \left[ e^{-(r + \frac{m^2}{2})\tau_H^{l,c-}} 1_{\{\tau_H^{l,c-} \leq T\}} BSC \left( L, T - \tau_H^{l,c-} \right) \right].$$

From this expectation we can construct a Monte Carlo algorithm, where the key ingredient is a recipe for simulation of  $\tau_H^{l,c-}$ . We still are using the same notation as in the previous section where we developed the recipe for simulating  $\tau_H^{l,-}$ . We also introduce the extra variable  $\tau^*$ , that is initially zero. Like in the previous section, we initially simulate  $\tau_1$  from  $F_{0,l'}$  and then simulate  $\tau_2$  from  $F_{l',l}$ . In addition we set  $\tau^* = \tau^* + \tau_2$  and consider the following three possibilities:

- If  $\tau_1 + \tau_2 \geq T$  the PDIC expires without pay-off, we throw away the sample.
- In case of  $\tau^* > H$  we have a sample of  $\tau_H^{l,c-}$  and we stop, keeping the sample.
- If case of  $\tau^* < H$  we need to get back at  $l$  again in order to fulfill the Parisian constraint. So we simulate  $\tau_3$  from  $F_{l',l'}$ , the distribution of hitting times of  $Z$  hitting  $l'$ , starting in  $l$ . Now we start again as if we simulated a hitting time  $\tau_1$  of  $\tau_1 = \tau_1 + \tau_2 + \tau_3$ . We keep on repeating this until we either have to throw away the sample (the first bullet) or we can keep it (the second bullet).

The recipe given here is only slightly different from the recipe in the previous section and the corresponding Monte Carlo algorithm of the CPDIC given below is just a slightly modified version of that of the PDIC. In figure 4.7 we show the distribution of Monte Carlo prices for number of samples  $N = 10^4$ . The contract we are pricing is the CPDIC with  $L = 90$ ,  $\epsilon = 0.5$ ,  $H = 10/250$ ,  $s_0 = 100$ ,  $X = 100$ ,  $T = 1$ ,  $r = 1.5\%$  and  $\sigma = 30\%$ . Here we generated a Monte Carlo price of 2.305 as reference price using  $10^8$  samples giving enough precision up to 4 digits.

ALGORITHM 4 (CUMULATIVE PDIC WITH  $X \geq L$ )

- Take  $\alpha = F_{\tau_l}(T)$ ,  $Res = 0$ .
- Repeat  $N$  times :
  - Sample  $u$  from  $\mathcal{U}[0, \alpha]$ .
  - Obtain the sample  $\tau$  by  $\tau = F_{\tau_l}^{-1}(u)$
  - $h^* = 0$
  - While  $\tau < T$  AND  $h^* < H$ ,
    - Sample  $w$  from  $\mathcal{U}[0, 1]$ .
    - Obtain the sample  $h$  by  $h = F_{\tau(u-l)}^{-1}(w)$
    - $\tau = \tau + h$
    - $h^* = h^* + h$
    - If  $h^* < H$ ,
      - Sample  $w$  from  $\mathcal{U}[0, 1]$ .
      - Obtain the sample  $h'$  by  $h' = F_{\tau(u-l)}^{-1}(w)$
      - $\tau = \tau + h'$ .
  - end If
  - end While
  - If  $\tau < T$ ,
    - $Res = Res + e^{-(r+0.5m^2)\tau} BSC(L, T - \tau)$
- $Res = N^{-1} \cdot e^{ml} \cdot \alpha \cdot Res$

Here we keep track of the cumulative time spend below the barrier  $L$  by the extra variable  $h^*$  which is represented in the recipe by the variable  $\tau^*$ .

## 4.6 Numerical remarks

Calculating (cumulative) Parisian prices with the recipe presented here involves the choice of a value for  $\epsilon$ . In the first part of this section we treat the effects of taking different values for  $\epsilon$ . In the second part we give a numerical example of the relationship between the standard barrier, the consecutive Parisian and the cumulative Parisian.

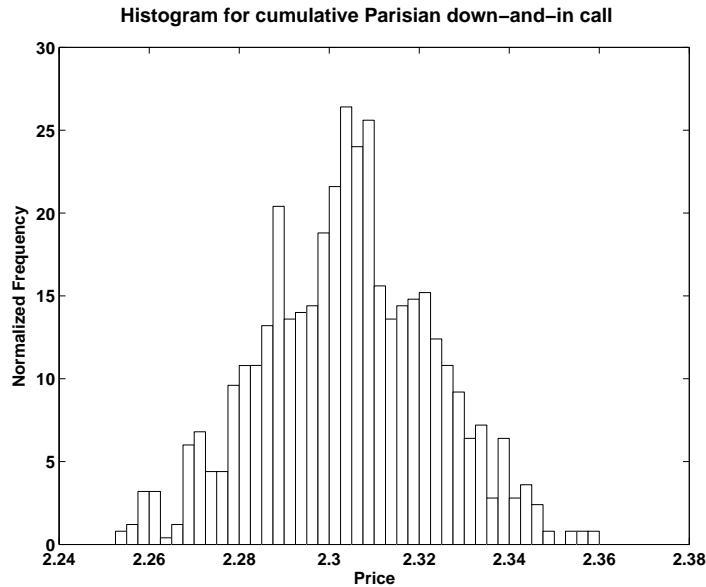


Figure 4.7: Normalized histogram generated by 1000 runs of the algorithm for the cumulative Parisian down-and-in call. Each individual run consists of  $10^4$  samples and the reference price is 2.305.

#### 4.6.1 The parameter $\epsilon$

From the construction according to the recipe of both  $\tau_H^{l,-}$  and  $\tau_H^{l,c-}$  by hitting a barrier of level  $L - \epsilon$  it is clear that this recipe results in an approximation for the true random variable. Suppose we are considering a barrier of level 90 and  $\epsilon = 10$ , here we take  $\epsilon$  rather large for the sake of argument. Then, as a result of the procedure of simulation, we are considering excursions below the barrier of level 90 with length bigger than  $H$  that also touch the level 80, so every sample path with an excursion of length  $H$  that does not hit 80 will be ignored by the recipe. Furthermore we measure the length  $H$  as the time the excursion needs to reach 90 again after hitting 80, ignoring the time that has already been spent in the excursion since the last exit of 90. Taking these properties of the recipe into account, the values of the times of interest we are simulating are upper bounds for the true values. These upper bounds become worse as epsilon becomes larger. An upper bound for the hitting time, transfers into a lower bound for the (cumulative) Parisian down-and-in call price. Figure 4.9 shows on the left axis the dependency of the PDIC price on the value of  $\epsilon$  and exhibits the relationship of larger epsilon resulting in lower PDIC prices. We use the same values as in the former Parisian examples and  $N = 10^6$ .

The larger the value of  $\epsilon$ , the more asset price paths that actually fulfill the knock-in condition are ignored by the simulation recipe, so we should take  $\epsilon$  reasonably small. Taking  $\epsilon$  too small results in very lengthy computer times.

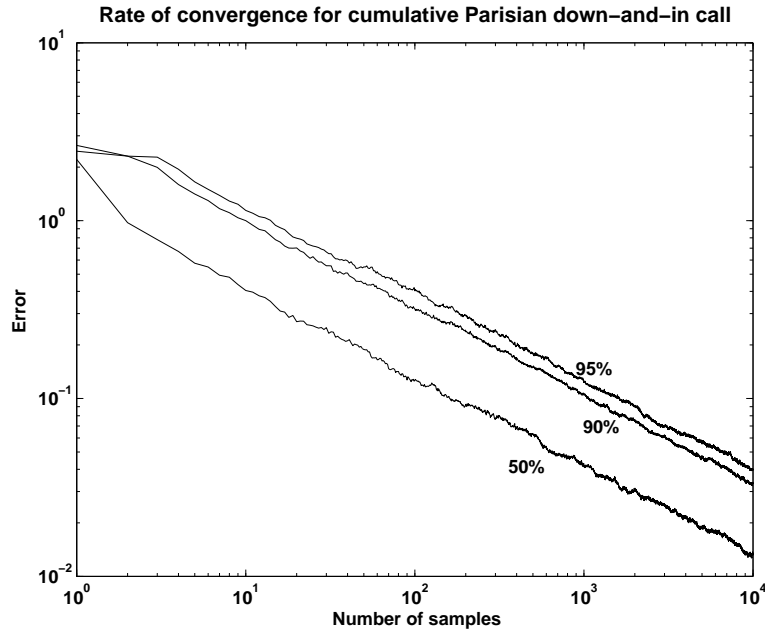


Figure 4.8: Rate of convergence graph containing plots of the 95%, 90% and 50% empirical quantiles of absolute error distribution versus number of hitting time simulations, generated by 1000 runs of the algorithm for the cumulative Parisian down-and-in call. Each individual run consists of  $10^4$  samples.

The right-hand axis of the figure above illustrates that property. For small  $\epsilon$  the probability that the simulated  $\tau_2$ , the first hitting time of the asset price process of  $L$  starting in  $L - \epsilon$  exceeds  $H$  is smaller than for larger  $\epsilon$ . Using formulas we have,

$$l'(\epsilon_1) < l'(\epsilon_2) \Rightarrow 1 - F_{l'(\epsilon_1),l}(H) > 1 - F_{l'(\epsilon_2),l}(H) \quad \text{for } \epsilon_1 > \epsilon_2.$$

This results into more "new starts" of the algorithm, taking more computation time. Moreover the algorithm terminates as soon as either the knock-in condition becomes true or the sum of simulated times exceeds the time to maturity of the option. Taking  $\epsilon$  smaller results on average in smaller simulated times, so it will also take more "new starts" before a sample is thrown away.

Summarizing, the value of  $\epsilon$  affects the price in two ways:

- Sample paths that stay long enough below the barrier  $L$  not hitting the level  $L - \epsilon$  are thrown away.
- The time from the last exit of the level  $L$  up to the first hitting of level  $L - \epsilon$  is not taken into account.

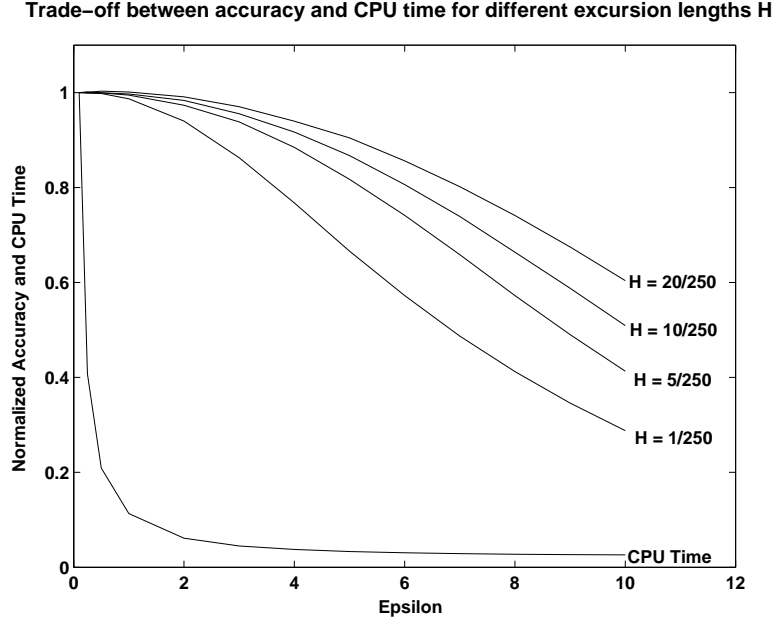


Figure 4.9: Normalized prices for consecutive Parisian down-and-in call options vs the parameter  $\epsilon$ . The behavior clearly differs for different  $H$ , the time that the asset price process should spend below the barrier before the contract knocks in. The normalized CPU time shows that one has to pay for increasing accuracy.

From [31] we use the distribution of the minimum value of a Brownian motion in an excursion given the length of the excursion. The probability that we are throwing away a sample path that actually is paying off is smaller than the probability that an excursion of length  $H$  has a minimum bigger than  $L - \epsilon$ . If we denote the minimum of an excursion of length  $H$  by  $M^H$ , the probability distribution is given by,

$$\begin{aligned} \mathbb{P}[M^H > L - \epsilon] = \\ 1 + 2 \sum_{n=1}^{\infty} \left( 1 + \frac{4n^2 \ln^2 \left( \frac{L-\epsilon}{L} \right)}{\sigma^2 H} \right) \exp \left( \frac{2n^2 \ln^2 \left( \frac{L-\epsilon}{L} \right)}{\sigma^2 H} \right) \end{aligned} \quad (4.14)$$

If we keep this probability below  $10^{-4} S_0^{-1}$  we are sure that the error is (very roughly) bounded by  $10^{-4}$ , so precision up to 4 decimals. Here we use that the option price is bounded by the asset price, a smaller bound could be obtained using that the Parisian price is bounded by the price of the standard call. Computing (4.14) for the examples throughout the text, we have that it is smaller than  $10^{-15}$ , so the error introduced to this particular choice of epsilon is negligible.

The time described in the second item we denote by  $\gamma_{T_L^\epsilon}$  and is defined by,

$$\gamma_{T_L^\epsilon} = \sup\{0 \leq t < T_{L-\epsilon}; S_t = L\}.$$

We can compute its expected value, using (4.20) from the appendix, by

$$\mathbb{E}[\gamma_{T_L^\epsilon}] = \frac{1}{3} \left( \frac{\ln \frac{L-\epsilon}{L}}{\sigma} \right)^2$$

As we are averaging over the sample paths, we are valuing Parisians with excursions of length  $H + \mathbb{E}[\gamma_{T_L^\epsilon}]$ . If we want this to be a small fraction  $\alpha$  of  $H$  we have an upper bound for epsilon by,

$$\epsilon \leq L \left( 1 - \exp(-\sigma \sqrt{3\alpha H}) \right). \quad (4.15)$$

Here we choose  $\alpha$  to be 5 promille, so for the 10 days examples we used throughout the text, we are in fact valuing Parisians of 10 days and 70 minutes.

#### 4.6.2 Standard barrier versus cumulative and consecutive Parisian

We can argue that each sample path that fulfills the consecutive Parisian knock-in condition also fulfills the cumulative one, where the other way around is not true. Moreover it is clear that each sample path for which the cumulative knock-in condition is satisfied also hits the barrier  $L$  and here again the other way around is not true. So we have the obvious inequality,

$$PDIC \leq CPDIC \leq DIC \leq BSC.$$

Furthermore both the price of the cumulative and the consecutive Parisian down-and-in call are increasing for decreasing  $H$ , where we have that in the limit for  $H \rightarrow 0$  the Parisians should equal the standard barrier price. This is illustrated in figure 4.10. The prices computed for this figure are all with initial asset price  $S_0 = 100$ , strike  $X = 100$ , barrier  $L = 90$ , volatility  $\sigma = 30\%$ , interest rate  $r = 1.5\%$  and time to maturity  $T = 1$ . Here we used  $10^6$  simulations and for  $\epsilon$  we used the bound as given in (4.15) for  $\alpha = 0.001$ , where we verified that the relevant error probability as given in (4.14) does not introduce an error bigger than  $10^{-4}$ . We recall that the standard barrier price for these contract specifications is 4.4213.

## 4.7 Conclusion

In this paper we developed a Monte Carlo algorithm for pricing Parisian options, which are options that are triggered by the Parisian time which occurs as soon as the stock price process spends a given time below or above some barrier. A standard Monte Carlo procedure that simulates the

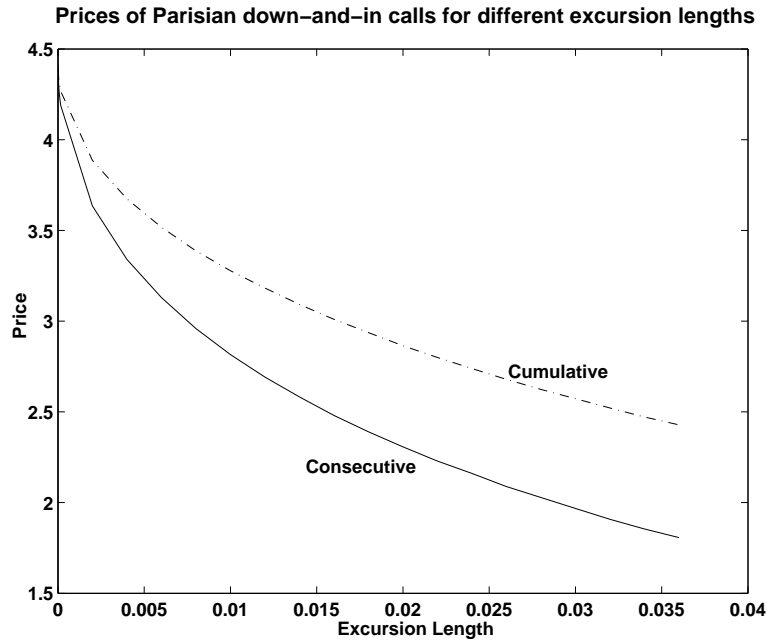


Figure 4.10: Prices for cumulative and consecutive Parisian down-and-in call options for different lengths of the excursion, i.e., the time that the underlying value should spend below the barrier before the contract knocks in.

underlying stock price path in a straightforward way does not result into a method that converges within acceptable time. The method we propose here, consists of two steps. First the Markovian nature of the underlying value process is used to arrive at an expression that can be computed by Monte Carlo integration. The random variable that needs to be simulated is the Parisian time. Unfortunately there exists no explicit distribution formula for the Parisian time. Therefore we approximate it by simulating hitting times in a special way, where the accuracy of the approximation can be controlled, where increasing accuracy results in increasing computation times.

The reason to come up with a Monte Carlo algorithm for Parisian options is the flexibility of Monte Carlo methods. There are various applications of Parisian optionality and if one wants to change the pay-off structure or the model of the underlying value process the flexibility of the Monte Carlo method is very useful. For example, this method can serve as a starting point for the valuation of Parisian options in the case where the underlying value process is given by a variance gamma process. This can be done as soon as one is able to compute vanilla options in the variance gamma model and simulate variance gamma based hitting times.

## 4.8 Appendix

### 4.8.1 The average of $\gamma_{\tau_\delta}$

We recall that the simulation procedure of the relevant hitting times for the Parisian contracts consists of the simulation of a hitting time of the level  $L - \epsilon$ . As discussed in the numerical remarks paragraph hitting the level  $L - \epsilon$  by an asset price path  $S_t(\omega)$  implies that this sample path did already spend some time in the excursion away from the level  $L$ . If we translate this into the sample path of the underlying Brownian motion  $Z$ , we can express distributional properties of the time that is already spent in the excursion in terms of the time that a standard Brownian motion  $B$  on a probability space  $(\Omega, \mathcal{F}, \mathbb{P}^0)$  is already traveling in the excursion below 0 at the moment it hits the level  $-\delta$ , where we can compute  $\delta$  by,

$$\delta = \frac{1}{\sigma} \ln \frac{L}{L - \epsilon}.$$

By the symmetry of the standard Brownian motion the distributional properties of hitting  $-\delta$  are similar to those of hitting  $\delta$ . By  $\tau_\delta$  we denote the first time that  $B$  hits  $\delta$  and by  $\gamma_{\tau_\delta}$  the last time the process  $B$  was zero before it hit  $\delta$ ,

$$\gamma_{\tau_\delta} = \sup\{0 \leq s < \tau_\delta; B_s = 0\}.$$

So  $\tau_\delta - \gamma_{\tau_\delta}$  is the time that the  $B$  is away from zero, which is in distribution equal to the time that  $S$  is already below  $L$  when it hits  $L - \epsilon$ . We use the notation as in [55] and denote by  $\mathbb{P}^x$  the probability measure for which  $B - x$  is a standard Brownian motion, i.e.  $B$  is with respect to  $\mathbb{P}^x$  a standard Brownian motion that starts in  $x$ . For the density of  $\tau_\delta - \gamma_{\tau_\delta}$  we have,

$$\begin{aligned} \mathbb{P}[\tau_\delta - \gamma_{\tau_\delta} \in dt] &= \lim_{x \downarrow 0} \mathbb{P}^x[\tau_\delta \in dt | \tau_\delta < \tau_0] \\ &= \lim_{x \downarrow 0} \frac{\delta}{x\sqrt{2\pi t^3}} \sum_{n=-\infty}^{\infty} ((2n+1)\delta - x) \exp\left(-\frac{(2n\delta + \delta - x)^2}{2t}\right) dt. \end{aligned}$$

Here the first equality states that the time already spent in the excursion is time it takes for  $B$  just after leaving zero to reach  $\delta$  before reaching zero again. The second inequality is the result of the combination of (8.26) and exercise 8.13 on page 100 of [55]. Now we calculate the distribution of  $\tau_\delta - \gamma_{\tau_\delta}$  by,

$$\mathbb{P}[\tau_\delta - \gamma_{\tau_\delta} \leq T] = \lim_{x \downarrow 0} \frac{\delta}{x} \sum_{n=-\infty}^{\infty} \int_0^T \frac{(2n+1)\delta - x}{\sqrt{2\pi t^3}} e^{\left(-\frac{(2n\delta + \delta - x)^2}{2t}\right)} dt. \quad (4.16)$$

The first interchange of limit and integral is because for every  $0 < x < \delta$  the part of the equation on the right of the limit is a positive function (because it

is a density) that is integrable for every  $x$  and can be bounded for  $x < 0.5\delta$ . For the second interchange, we define the constants  $c_n(x)$  by,

$$c_n(x) = (2n + 1)\delta - x.$$

Then we have for each  $0 \leq x \leq \delta$  the inequality,

$$c_{-n}(x) > -c_n(x).$$

Now we define a sequence of functions  $f_m$  that converges for  $m \rightarrow \infty$  to the probability density we want to integrate by,

$$f_m(t, x) = \frac{\delta}{x} \sum_{n=-m}^m \frac{(2n + 1)\delta - x}{\sqrt{2\pi t^3}} e^{-\frac{(2n\delta + \delta - x)^2}{2t}}.$$

Now we can compute the  $m$ -th term of the sum for  $m > 1$ ,  $0 \leq x \leq \delta$  and  $0 \leq t \leq T$  by,

$$\begin{aligned} f_m(t, x) - f_{m-1}(t, x) &= \frac{c_m(x)}{\sqrt{2\pi t^3}} e^{-\frac{c_m(x)^2}{2t}} + \frac{c_{-m}(x)}{\sqrt{2\pi t^3}} e^{-\frac{c_{-m}(x)^2}{2t}} \\ &\geq \frac{c_m(x)}{\sqrt{2\pi t^3}} e^{-\frac{c_m(x)^2}{2t}} - \frac{c_m(x)}{\sqrt{2\pi t^3}} e^{-\frac{(c_m(x))^2}{2t}} \geq 0. \end{aligned}$$

So we have an increasing sequence of positive functions  $f_m$  that for fixed  $x$  converges to the probability density we are interested in. By monotone convergence we can interchange sum and integral. The integral in (4.16) is apart from the sign similar to the calculation of the probability distribution of the hitting time of the level  $|c_n|$  by a standard Brownian motion, see (8.5) on page 96 of [55]. Using (4.6) we can rewrite (4.16) by,

$$\begin{aligned} \mathbb{P}[\tau_\delta - \gamma_{\tau_\delta} \leq T] &= \lim_{x \downarrow 0} \frac{2\delta}{x} \sum_{n=-\infty}^{\infty} \text{sign}((2n + 1)\delta - x) \Phi\left(-\frac{|(2n + 1)\delta - x|}{\sqrt{T}}\right) \\ &= \lim_{x \downarrow 0} \frac{2\delta}{x} \sum_{n=0}^{\infty} \Phi\left(\frac{(2n + 1)\delta + x}{\sqrt{T}}\right) - \Phi\left(\frac{(2n + 1)\delta - x}{\sqrt{T}}\right). \\ &= \lim_{x \downarrow 0} \frac{2\delta}{x} \sum_{n=0}^{\infty} \frac{2x}{\sqrt{2\pi T}} \exp\left(-\frac{((2n + 1)\delta)^2}{2T}\right). \end{aligned}$$

In the last step we approximate the probability that a standard normal r.v.  $X$  is in the interval  $[(2n + 1)\delta - x, (2n + 1)\delta + x]$  by  $2xf((2n + 1)\delta)$ , where  $f$  is the density of a standard normal random variable. Using the property that this density  $f(u)$  is decreasing for  $u > 0$  it is easy to derive upper and lower bounds for the approximation given that  $x$  is smaller than some constant. It can be shown that the approximation becomes exact for  $x \rightarrow 0$ . So we end up with,

$$\mathbb{P}[\tau_\delta - \gamma_{\tau_\delta} \leq T] = 2\delta \sqrt{\frac{2}{\pi T}} \sum_{n=0}^{\infty} \exp\left(-\frac{((2n + 1)\delta)^2}{2T}\right). \quad (4.17)$$

We are interested in the average time of the excursion of the asset price process. Computing the average  $\mathbb{E}[\tau_\delta - \gamma_{\tau_\delta}]$  gives,

$$\begin{aligned}\mathbb{E}[\tau_\delta - \gamma_{\tau_\delta}] &= \int_0^\infty \mathbb{P}[\tau_\delta - \gamma_{\tau_\delta} > t] dt \\ &= \int_0^\infty \left( 1 - 2\delta \sqrt{\frac{2}{\pi t}} \sum_{n=0}^\infty \exp\left(-\frac{((2n+1)\delta)^2}{2t}\right) \right) dt.\end{aligned}$$

Here arises the problem of interchange of limit (the sum to infinity) and integral. If we just cut of the sum at the  $M$ -th term we are allowed to interchange. However, the computation of the integral is op to a constant similar to the computation of the expectation of the hitting time for a standard Brownian motion, which is infinite. So the reason that just cutting of the sum at the  $M$ -th term does not work is due to the fact that (4.17) becomes very inaccurate for large  $T$ . Now we use the fact that in our Monte Carlo recipe we throw away all simulated hitting times bigger than the expiry, so the expected time we have to add to our excursion length is bounded by  $\mathbb{E}[(\tau_\delta - \gamma_{\tau_\delta})1_{\{\tau_\delta - \gamma_{\tau_\delta} \leq T\}}]$  which we will denote hereafter by  $\mu_\delta(T)$ , where  $T$  is the time to maturity of the option. Now we can use this fixed  $T$  to estimate the error we make in the summation by truncating at  $M$  and interchange limit and integral to obtain,

$$\begin{aligned}\mu_\delta(T) &\approx T - 2\delta \sum_{n=0}^M \int_0^T \sqrt{\frac{2}{\pi t}} \exp\left(-\frac{((2n+1)\delta)^2}{2t}\right) dt \\ &= T - 4\delta \sum_{n=0}^M \sqrt{\frac{2T}{\pi}} e^{-\frac{((2n+1)\delta)^2}{2T}} - 2((2n+1)\delta)\Phi\left(-\frac{(2n+1)\delta}{\sqrt{T}}\right).\end{aligned}\quad (4.18)$$

Now we continue giving heuristic arguments, in the sense that we do not precisely give error bounds for all statements. So for the first part of the sum we have for large  $T$  and  $M$ ,

$$\begin{aligned}4\delta \sum_{n=0}^M \sqrt{\frac{2T}{\pi}} e^{-\frac{((2n+1)\delta)^2}{2T}} &= 4T \sum_{n=0}^M \frac{1}{\sqrt{2\pi}} \frac{2\delta}{\sqrt{T}} e^{-\frac{((2n+1)\frac{\delta}{\sqrt{T}})^2}{2}} \\ &\approx 4T \frac{1}{\sqrt{2\pi}} \int_0^\infty e^{-\frac{x^2}{2}} dx = 2T.\end{aligned}$$

Furthermore we expect that we have chosen  $T$  large, such that the expression (4.18) is independent of  $T$ . Considering the second part of the sum as a function of  $T$ , its derivative with respect to  $T$  should be equal to one as can be shown,

$$\begin{aligned}\frac{\partial}{\partial T} \sum_{n=0}^M 8\delta((2n+1)\delta)\Phi\left(-\frac{(2n+1)\delta}{\sqrt{T}}\right) &= \frac{2}{T} \sum_{n=0}^M 2\delta \frac{((2n+1)\delta)^2}{\sqrt{2\pi T}} e^{-\frac{((2n+1)\delta)^2}{2T}} \\ &\approx \frac{2}{T} \frac{1}{\sqrt{2\pi T}} \int_0^\infty x^2 e^{-\frac{x^2}{2T}} dx = 1\end{aligned}$$

So we can write for (4.18),

$$\mu_\delta(T) \approx -T + 8\delta^2 \sum_{n=0}^M (2n+1) \Phi\left(-\frac{(2n+1)\delta}{\sqrt{T}}\right). \quad (4.19)$$

Suppose we want to calculate the expectation for  $\delta' = c\delta$ , where  $c > 0$ . We have,

$$\begin{aligned} \mu_{\delta'}(T) &\approx -T + 8c^2\delta^2 \sum_{n=0}^M (2n+1) \Phi\left(-\frac{(2n+1)c\delta}{\sqrt{T}}\right) \\ &= c^2 \left\{ -T' + 8\delta^2 \sum_{n=0}^M (2n+1) \Phi\left(-\frac{(2n+1)\delta}{\sqrt{T'}}\right) \right\} \approx c^2 \mu_\delta(T'). \end{aligned}$$

Here  $T' = Tc^{-2}$  and as we expect  $T$  large enough, we have the relation,

$$\mu_{c\delta} = c^2 \mu_\delta.$$

Moreover it is obvious that for  $\delta = 0$  we have  $\mu_\delta = 0$ , so there should exist a constant  $\alpha$  such that,

$$\mu_\delta = \alpha\delta^2. \quad (4.20)$$

In order to determine this constant, we compute numerically (4.19) for  $\delta = 1$  and sufficiently large  $T$  and  $M$  and obtain  $\alpha = 1/3$ .

## Chapter 5

# Double-sided knock-in calls in an exponential compound Poisson framework

In the present paper we consider the exponential compound Poisson process with exponential jumps to model the stock price process. We will determine the Laplace transforms for the plain vanilla call option and the double-sided knock-in call option and then we will numerically invert them to generate actual prices. Several numerical examples will be given, which show the calibration of the exponential compound Poisson model to the market, the behavior of prices of the double-sided knock-in call. We will also discuss the implied volatility smile that is produced by the model.

### 5.1 Introduction

A well-known problem of the Black-Scholes framework in option pricing, i.e., the use of the geometric Brownian motion for modeling the stock price process, is the inability to calibrate this model to the volatility smile in the option market. In practice this is solved by allowing different volatilities for each strike, which in turn leads to the problem of pricing exotic options consistently with this smile. In this paper we address this problem for the double-barrier knock-in call options, options that become plain vanilla calls as soon as a lower or upper level has been reached by the stock price process. We model the stock price by an exponential compound Poisson process and numerically invert a Laplace transform to obtain plain vanilla option prices and, furthermore, even a two-dimensional Laplace transform to obtain the double-sided knock-in call prices. After calibrating the exponential compound Poisson model to the market we compute implied volatilities for

the double-sided knock-in calls to show that there can exist a substantial difference between the implied volatility in the plain vanilla option market and the implied volatility of an exotic option that is priced in a to this market calibrated non-GBM model for the stock price process. The exponential compound Poisson process is one of the simplest processes in the class of exponential Lévy processes, which are popular for modeling the underlying value process in option markets that exhibit the volatility smile and term structure. The well-known examples are the variance gamma process in [63] or the Kou's jump-diffusion model as in [59], where the exponential compound Poisson model is a special version of the Kou's model. Our model serves as a toy model, because it does not meet the standards people usually set for a realistic model, see for a discussion on these standards Rama and Cont [32].

Lipton treats in [62] the case of pricing a derivative with a single barrier, where the logarithm of underlying is modeled by a double exponential jump-diffusion model. He also uses fluctuation theory to derive transforms, which he inverts to obtain prices. Our work is close to Lipton's work, except that we look at double-sided exit problems and therefore at double-sided barrier options instead of standard barrier options. See also [7] for an application of fluctuation theory to single barrier option pricing. The Laplace transforms of first passage times can be very natural in case one considers problems in credit risk. For example, in [34] the Laplace transform is part of the explicit solution of the debt value the authors want to price. In [18] the authors use methods like pseudodifferential operators, which are much more complicated than fluctuation theory, but allow for more general processes like Feller processes.

The reason for us to use the toy model, is that it is very tractable, without losing the capability of calibrating to the actual option market. The computation of the various Laplace transforms involves the computation of zeros of an expression of the Laplace exponent of the process. In our model the computation of these zeros is straightforward, whereas complicating the model may eventually create a need for a numerical procedure to determine these zeros. The technique we use to compute prices is the Laplace transform. For the double barrier options in the GBM case this approach has been taken by Geman and Yor in [44]. The difference is that they can, using the density of Brownian motion, explicitly compute a certain expectation which results in the one-dimensional Laplace transform. For Lévy processes this density does not need to have an explicit formula and that is why we end up with a two dimensional Laplace transform. We use the results of Kadankov and Kadankova for general Lévy processes in [54] relying on fluctuation theory and Wiener-Hopf factorization to incorporate the information of the double-sided passage times into the Laplace transform. The authors in [67] show how prices of exotic options can be expressed in terms of the Wiener-Hopf factors of the underlying Lévy process. We actually compute these factors

to come up with numerical examples. In order to produce these numerical examples, we use the algorithm of Den Iseger in [53] to numerically invert one and two-dimensional Laplace transforms. The paper shows how to use the Laplace transform to price exotic options in the exponential Lévy setting and this approach will work if the exponential compound Poisson model is replaced by a more sophisticated model, however then some numerical effort will be needed because the explicit roots do not exist anymore. In [81], the author takes a less probabilistic approach by using the method of partial integro-differential equations of which he computes Laplace transforms w.r.t. time. He considers a double-exponential jump diffusion and has therefore to deal with an equivalent numerical problem as the root-finding problem we discussed earlier.

The paper is organized as follows. We start with a section that describes the exponential compound Poisson model, followed by a section on the theoretical background. The theoretical section is rather brief and the details can be found in the Appendix. Section 3 derives the Laplace transforms needed to price plain vanilla calls and double-sided knock-in calls. In Section 4 we use the computed transforms of section 3 to calculate Laplace transforms for the option prices. The final section contains three numerical examples showing the calibration of the exponential compound Poisson model to the market, the behavior of prices of the double-sided knock-in call and finally the implied volatility smile that is produced by the model.

## 5.2 Description of the model

Let  $(\Omega, \mathcal{F}, \mathbb{P})$  be a probability space equipped with a filtration  $\{\mathcal{F}_t\}_{t \geq 0}$  that satisfies the usual conditions of right-continuity and completion. We assume that all random variables and stochastic processes are defined on this probability space. Furthermore we assume that  $\mathbb{P}$  is the pricing measure. The toy model for the stock price process  $\{S_t; t \geq 0\}$  we use throughout the paper is given by

$$S_t = S_0 e^{-\alpha X_t}, \quad (5.1)$$

where  $X = \{X_t; t \geq 0\}$  is given by

$$X_t = \sum_{k=1}^{N_t} Y_k - t, \quad (5.2)$$

where  $\{N_t; t \geq 0\}$  is the Poisson process with intensity  $\lambda$  and the jump sizes  $Y_k$  for  $k = 1, 2, \dots$  are independent, exponentially distributed random variables with parameter  $\mu$ . This model is in fact a special version of the Kou's model in [59], which has exponential jumps in both negative and positive directions. The reason for simplifying the Kou's model in this way is that the formulas for the Laplace transform of the double-sided passage

times are much more tractable in case the Lévy process is spectrally one-sided, i.e., it has either positive or negative jumps. The sample paths of  $S$  will not look like the sample paths of a stock price process in reality, however, as we are modeling directly under the pricing measure we do not care so much whether the structure of the paths resembles reality. We do care whether the plain vanilla option prices can be calibrated to the market prices, which is essentially the ability of the model to describe the volatility smile and term structure. Numerical example 5.5.1 elaborates on calibrating the model to the actual option market. The Laplace transform of  $X_t$  can be written in terms of the Laplace exponent  $k(p)$  of the process  $X$ ,

$$\mathbb{E} [e^{-pX_t}] = e^{tk(p)}, \quad \Re\{p\} \geq 0,$$

where the Laplace exponent is given by,

$$k(p) = p + \lambda (\mathbb{E} [e^{-pY_1}] - 1) = p - \frac{\lambda p}{p + \mu}. \quad (5.3)$$

Define for every  $s$  the numbers  $c_1(s), c_2(s) > 0$  such that  $c_1(s)$  and  $-c_2(s)$  are the roots of the equation

$$k(p) - s = 0, \quad (5.4)$$

which gives for  $k(p)$  given by (5.3)

$$\begin{aligned} c_1(s) &= \frac{\lambda + s - \mu + \sqrt{(\lambda + s - \mu)^2 + 4s\mu}}{2}, \\ c_2(s) &= -\frac{\lambda + s - \mu - \sqrt{(\lambda + s - \mu)^2 + 4s\mu}}{2}. \end{aligned} \quad (5.5)$$

In the general theory that is used as a base for the theoretical background we present in the next chapter, these  $c_{1,2}(s)$  play an important role. It is a merit from the exponential compound Poisson model that the explicit expression (5.5) for the roots exist. This property is lost as soon as one complicates the model, and numerical techniques are needed to obtain values for  $c_{1,2}(s)$ . Note, that the stock price process is an exponential Lévy process since the underlying  $X$  in (5.2) is a Lévy process. As we model the stock price by an exponential Lévy process with jumps, the market is not complete, i.e. there exists no replicating portfolio, and hence we avoid the term risk-neutral measure and assume  $\mathbb{P}$  to be the pricing measure instead. Under the pricing measure  $\mathbb{P}$  the market should be arbitrage-free, see section 1.3.2, and thus for every  $t \geq 0$  the following equation should hold

$$\mathbb{E} [S_t] = S_0 e^{rt}. \quad (5.6)$$

Once the parameters  $\mu$  and  $\lambda$  of the process  $X$  are determined, the parameter  $\alpha$  in the stock price process  $S$  needs to be chosen such that (5.6) holds. This can be achieved by setting  $\alpha = c_1(r)$ . Finally, note that  $S_T$  the stock price

process at time  $T$  is a random variable taking values in  $(0, S_0 e^{\alpha T}]$  with one atom given by

$$\mathbb{P}[S_T = S_0 e^{\alpha T}] = \mathbb{P}[N_T = 0] = e^{-\lambda T}, \quad (5.7)$$

whereas  $S_T$  has a density on  $(0, S_0 e^{\alpha T})$ , or equivalently,  $X_T$  has the density  $f_X(x)$  for  $x \in (-T, \infty)$ .

### 5.3 Theoretical background

In this section we will study the two-boundary characteristics of the process  $X$  as given in (5.2), which is in fact a study of the two-sided exit problem from an interval  $[-y, x]$  by the process  $X$  for  $x, y > 0$ . The solution for this problem will enable us to price double-barrier options on a stock modeled by the stock price process defined in the previous section. The results of this section are derived from the results for more general Lévy processes presented in the paper of Kadankov and Kadankova [54], which are based on fluctuation theory, probabilistic methods and Wiener-Hopf factorization. Denote the first time that the process  $X$  leaves the interval  $[-y, x]$  for  $x, y > 0$  by  $\tau$  given by

$$\tau = \inf\{t > 0 : X_t \notin [-y, x]\}.$$

Then  $\tau$  is equivalent to the minimum of the first passage times  $T_y^- = \inf\{t > 0 : X_t < -y\}$  and  $T_x^+ = \inf\{t > 0 : X_t > x\}$  of the lower level  $-y$  and upper level  $x$  by the process  $X$ . Define the following events

$$A^x = \{X_\tau > x\} \quad \text{and} \quad A_y = \{X_\tau < -y\},$$

where  $A^x$  and  $A_y$  denote an exit through respectively the upper and lower boundary. Since  $\tau < \infty$  a.s. we have  $\mathbb{P}[A^x \cup A_y] = 1$ . Now we have the following theorem on Laplace transforms of the first exit time.

**Theorem 5.3.1.** *Let  $\{X_t; t \geq 0\}$ ,  $X_0 = 0$  be the compound Poisson process with drift as given in (5.2) and  $x, y > 0$ . Then for  $s > 0$  the Laplace transforms of the distribution of  $\tau$  satisfy the following equalities*

$$\begin{aligned} \mathbb{E}[e^{-s\tau}; A^x] &= e^{-xc_2(s)} \left(1 - \frac{c_2(s)}{\mu}\right) \frac{1 - e^{-yc(s)}}{1 - K(s, B)}, \\ \mathbb{E}[e^{-s\tau}; A_y] &= \frac{1 - K(s, x)}{1 - K(s, B)} e^{-yc_1(s)}, \end{aligned} \quad (5.8)$$

where  $B = x + y$ ,  $c_{1,2}(s)$  are the roots of  $k(p) - s = 0$  as given in (5.5),  $c(s) = c_1(s) + c_2(s)$  and  $K(s, x)$  is given by

$$K(s, x) = \frac{\mu - c_2(s)}{\mu + c_1(s)} e^{-xc(s)}, \quad x \geq 0. \quad (5.9)$$

**Remark 5.3.2.** *The proof of Theorem 5.3.1 follows from the general theorem on the first exit time for Lévy processes [54] and is given in the Appendix.*

**Corollary 5.3.3.** *The probability that the first exit from the interval  $[-y, x]$  by the compound Poisson process with drift given in (5.2) happens through the upper boundary is given by,*

$$\mathbb{P}[A^x] = \begin{cases} (1 - e^{-y(\lambda-\mu)}) \left(1 - \frac{\mu}{\lambda} e^{-B(\lambda-\mu)}\right)^{-1}, & \lambda > \mu; \\ 1 - \left(1 - \frac{\lambda}{\mu} e^{-x(\mu-\lambda)}\right) \left(1 - \frac{\lambda}{\mu} e^{-B(\mu-\lambda)}\right)^{-1}, & \mu > \lambda; \\ \mu y (1 + \mu B)^{-1}, & \lambda = \mu, \end{cases} \quad (5.10)$$

*Proof.* Take the limit  $s \rightarrow 0$  in the expressions of theorem 5.3.1.  $\square$

For the double-barrier option pricing problem, we are interested in the following two-dimensional Laplace transform

$$l(s, p) = \int_0^\infty e^{-sT} \mathbb{E} \left[ e^{-pX_T} 1_{\{\tau \leq T\}} 1_{\{X_T > -T\}} \right] dT. \quad (5.11)$$

In view of the general results in [54], it is more convenient to derive  $B(s, p)$  given by,

$$\begin{aligned} B(s, p) &= \int_0^\infty e^{-sT} \mathbb{E} \left[ e^{-pX_T} 1_{\{\tau > T\}} \right] dT \\ &= \int_0^\infty e^{-sT} \mathbb{E} \left[ e^{-pX_T} 1_{\{X_T^- > -y\}} 1_{\{X_T^+ < x\}} \right] dT, \end{aligned}$$

where  $X_T^-$  and  $X_T^+$  are the infimum respectively supremum of the process  $X$  up to time  $T$ . The following theorem leads to the result for  $B(s, p)$ .

**Theorem 5.3.4.** *Let  $\{X_t; t \geq 0\}$ ,  $X_0 = 0$  be the Poisson process with a drift as in (5.2). Then the integral transform  $Q^s(p) = \int_0^\infty s e^{-st} \mathbb{E} [e^{-pX_t}; -y < X_t^-, X_t^+ < x] dt$  is given by the following formula*

$$\begin{aligned} Q^s(p) &= \frac{Cs}{c(s)} \left[ \frac{\mu + c_1(s)}{p - c_1(s)} [1 - e^{-B(p-c_1(s))}] - \frac{\mu - c_2(s)}{p + c_2(s)} [1 - e^{-B(p+c_2(s))}] \right] - \\ &\frac{s}{c(s)} \left[ \frac{\mu + c_1(s)}{p - c_1(s)} [1 - e^{-x(p-c_1(s))}] - \frac{\mu - c_2(s)}{p + c_2(s)} [1 - e^{-x(p+c_2(s))}] \right], \end{aligned} \quad (5.12)$$

where  $C$  is given by

$$C = e^{py} \frac{(\mu + c_1(s))e^{xc_1(s)} - (\mu - c_2(s))e^{-xc_2(s)}}{(\mu + c_1(s))e^{Bc_1(s)} - (\mu - c_2(s))e^{-Bc_2(s)}}.$$

**Remark 5.3.5.** *The proof of this theorem is based on applying the general result from [54] and it can be found in the Appendix.*

The expression for the integral transform  $Q^s(p)$  from the theorem is everything we need to derive an expression for  $l(s, p)$  in the following corollary.

**Corollary 5.3.6.** *The two-dimensional Laplace transform  $l(s, p)$  as defined in (5.11) is for  $\Re\{s\} > \Re\{p\}$  given by,*

$$l(s, p) = \frac{1}{s - k(p)} - \frac{1}{s} Q^s(p) - \frac{1}{s + \lambda - p} e^{-(s+\lambda-p)y}. \quad (5.13)$$

*Proof.* We can write

$$l(s, p) = \int_0^\infty e^{-sT} \mathbb{E} [e^{-pX_T} 1_{\{\tau \leq T\}}] dT - \int_0^\infty e^{-sT} \mathbb{E} [e^{-pX_T} 1_{\{\tau \leq T\}} 1_{\{X_T = -T\}}] dT.$$

Note that for the first integral on the right-hand side we can write

$$\begin{aligned} \int_0^\infty e^{-sT} \mathbb{E} [e^{-pX_T} 1_{\{\tau \leq T\}}] dT &= \int_0^\infty e^{-sT} \mathbb{E} [e^{-pX_T}] dT - B(s, p) \\ &= \frac{1}{s - k(p)} - \frac{1}{s} Q^s(p), \end{aligned}$$

and for the right-hand side integral we use the following equation to complete the proof,

$$\mathbb{E} [e^{-pX_T} 1_{\{\tau \leq T\}} 1_{\{X_T = -T\}}] = 1_{\{-T < -y\}} e^{pT} e^{-\lambda T}.$$

□

## 5.4 Option Pricing

Here we will show how we use Laplace transforms for option pricing. First we focus on the standard  $T$ -maturing European call option with strike  $K$  and value  $V_C(T)$  given by,

$$V_C(T) = e^{-rT} \mathbb{E} [(S_T - K)^+] = S_0 e^{-rT} \mathbb{E} \left[ \left( e^{-\alpha X_T} - e^{-k} \right)^+ \right], \quad (5.14)$$

where  $k = \ln(S_0/K)$ . The option price  $V_C(T)$  is only bigger than zero for  $K \leq S_0 e^{\alpha T}$  or equivalently  $k \geq -\alpha T$ . In the end we need to invert the Laplace transforms to obtain actual option prices. The numerical inversion method we are going to use works well for smooth functions, so we have to be careful if the random variables of interest have atoms. Recall (5.7), that

shows that the stock price process has an atom. Denote the expectation on the right-hand side of (5.14) by  $E_T(k)$ , where for  $k \geq -\alpha T$  this expectation can be computed as follows,

$$\begin{aligned} E_T(k) &= \mathbb{E} \left[ \left( e^{-\alpha X_T} - e^{-k} \right)^+ \right] \\ &= \int_{-T}^{k/\alpha} (e^{-\alpha y} - e^{-k}) f_X(y) dy + e^{-\lambda T} (e^{\alpha T} - e^{-k}) \\ &=: \tilde{E}_T(k) + e^{-\lambda T} (e^{\alpha T} - e^{-k}). \end{aligned}$$

Define the Laplace transform of  $X_T$  restricted to values where it has the density  $f_X$  by

$$\begin{aligned} l_T(p) &:= \mathbb{E} \left[ e^{-pX_T} 1_{\{X_T > -T\}} \right] \\ &= \mathbb{E} \left[ e^{-pX_T} \right] - e^{pT} \mathbb{P} [X_T = -T] = e^{Tk(p)} - e^{(p-\lambda)T}. \end{aligned}$$

We note that  $\tilde{E}_T(k)$  is positive and bounded for all  $k$ . The Laplace transform of  $\tilde{E}_T(k - \alpha T)$  can be computed in the following way,

$$\begin{aligned} \phi_T(p) &= \int_0^\infty e^{-pk} \tilde{E}_T(k - \alpha T) dk \\ &= \int_0^\infty e^{-pk} \int_{-T}^{(k-\alpha T)/\alpha} (e^{-\alpha x} - e^{-(k-\alpha T)}) f_X(x) dx dk \\ &= \int_{-T}^\infty \int_{\alpha(x+T)}^\infty e^{-pk} \left( e^{-\alpha x} - e^{-(k-\alpha T)} \right) dk f_X(x) dx \\ &= \left( \frac{1}{p} - \frac{1}{p+1} \right) e^{-\alpha p T} \int_{-T}^\infty e^{-\alpha(1+p)x} f_X(x) dx \\ &= \left( \frac{1}{p} - \frac{1}{p+1} \right) e^{-\alpha p T} l_T(\alpha(1+p)). \end{aligned}$$

If we now want to compute a standard  $T$ -maturing call option price with strike  $K$ , we first compute  $k$ , then numerically invert  $\phi_T$  to obtain  $\tilde{E}_T(k)$ , calculate  $E_T(k)$  and finally use the result in (5.14) to obtain  $V_C(T)$ . Numerical example 5.5.1 follows this procedure.

The next step is to consider double-barrier options, for which we need to introduce the double-sided passage time  $T_{L_1, L_2}$  given by

$$T_{L_1, L_2} = T_{L_1} \wedge T_{L_2}, \quad (5.15)$$

where  $T_{L_i}$ ,  $i = 1, 2$ , is the first passage time of level  $L_i$  of the stock price process  $S$ . The definition of  $T_{L_1, L_2}$  only makes sense if there is no a.s. strict ordering between  $T_{L_1}$  and  $T_{L_2}$ , that is,  $S_0$  is in between  $L_1$  and  $L_2$ . The value  $V_{DBIC}$  of a double-barrier in call option can be computed by,

$$\begin{aligned} V_{DBIC} &= e^{-rT} \mathbb{E} \left[ (S_T - K)^+ 1_{\{T_{L_1, L_2} \leq T\}} \right] \\ &= S_0 e^{-rT} \mathbb{E} \left[ (e^{-\alpha X_T} - e^{-k})^+ 1_{\{\tau \leq T\}} \right] =: S_0 e^{-rT} E(k, T), \end{aligned}$$

where  $\tau$  is a shorthand notation for  $\tau_{1,l_2}$ , which is given analogously to (5.15),  $\tau_i$ ,  $i = 1, 2$  is the first crossing time of the level  $l_i$  by the process  $X$ , and the levels  $l_i$  are given by  $l_i = \alpha^{-1} \ln(S_0/L_i)$ . Again we have to deal with the atom of the stock price process,

$$\begin{aligned} E(k, T) &= \mathbb{E} \left[ \left( e^{-\alpha X_T} - e^{-k} \right)^+ 1_{\{\tau \leq T\}} 1_{\{X_T > -T\}} \right] + \\ &\quad \left( e^{\alpha T} - e^{-k} \right) \mathbb{P}[\tau \leq T; X_T = -T] \\ &:= \tilde{E}(k, T) + 1_{\{-T \leq l_-\}} \left( e^{\alpha T} - e^{-k} \right) e^{-\lambda T}, \end{aligned}$$

where  $l_- = \min(l_1, l_2)$  and we assume  $k \geq -\alpha T$ . We derive the two-dimensional Laplace transform of  $\tilde{E}(k - \alpha T, T)$  in the following way,

$$\begin{aligned} \phi_{DBIC}(p, s) &= \int_0^\infty \int_0^\infty e^{-pk - sT} \tilde{E}(k - \alpha T, T) dk dT \\ &= \int_0^\infty \int_0^\infty e^{-pk - sT} \mathbb{E} \left[ \left( e^{-\alpha X_T} - e^{-(k - \alpha T)} \right)^+ 1_{\{\tau \leq T\}} 1_{\{X_T > -T\}} \right] dk dT \\ &= \int_0^\infty e^{-sT} \mathbb{E} \left[ 1_{\{\tau \leq T\}} 1_{\{X_T > -T\}} \int_{\alpha(X_T + T)}^\infty e^{-pk} \left( e^{-\alpha X_T} - e^{-(k - \alpha T)} \right) dk \right] dT \\ &= \left( \frac{1}{p} - \frac{1}{p+1} \right) \int_0^\infty e^{-(s + \alpha p)T} \mathbb{E} \left[ e^{-(p+1)\alpha X_T} 1_{\{\tau \leq T\}} 1_{\{X_T > -T\}} \right] dT \\ &= \left( \frac{1}{p} - \frac{1}{p+1} \right) l(s + \alpha p, (p+1)\alpha), \end{aligned}$$

where  $l(s, p)$  is the two-dimensional Laplace transform given by corollary 5.3.6 in the formula (5.13). Actual prices can again be obtained via numerical Laplace inversion of this two dimensional transform. The numerical inversion method we use in our examples has been treated in detail in section 1.4 of the introduction.

## 5.5 Numerical Examples

The first numerical example shows that the exponential compound Poisson model with drift can be calibrated to the real-life option market. The calibration result is shown in terms of the implied volatility smile for a fixed expiry date and there is also a plot of the density resulting from the calibrated parameter values. The second numerical example shows option price behavior of the double-barrier option for different barriers. The last numerical example focuses on the implied volatility of the double-barrier options for both different barriers and different strikes.

### 5.5.1 Calibration of the model

As the first numerical example, we calibrate our toy model to the real-life option market. The reason for doing this is to show that, although the model is very simple, it is possible to capture the volatility smile in the real-life market. We choose the Amsterdam option market with options on the Dutch AEX index and use data of 20th of October 2006 for options that expire on 19th of October 2007, so we use  $T = 1$ . We use an interest rate  $r = 0.035$  and a dividend yield of  $q = 0.03$ . The option price formulas we presented so far, do not deal with a dividend yield. Therefore we set in these formulas the interest rate to  $r - q$  and multiply our final option price by  $e^{-qT}$ .

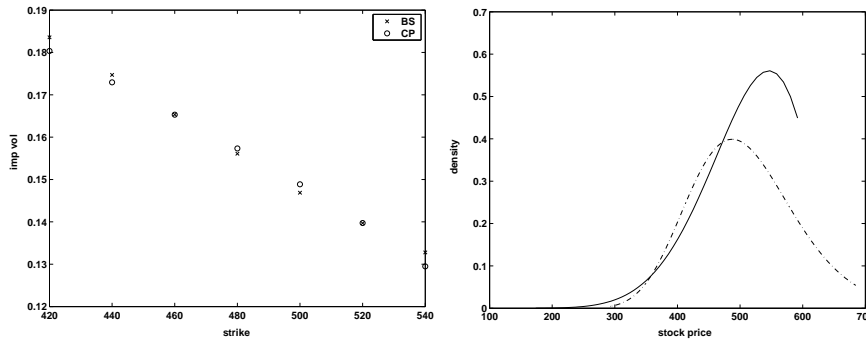


Figure 5.1: Calibration of the toy model to the Amsterdam option market with volatility smile (left) and resulting density (right)

The value of the AEX index at the moment of calibration was 492.19. As a result we did obtain  $\lambda = 3.101$  and  $\mu = 2.9883$  and from (5.6) follows that  $\alpha = 0.1945$ . In figure 5.1 we show on the left-hand side the implied volatility smile of the market and the calibrated model and remark that the model fits the smile quite well. On the right-hand side of the figure we show by the solid line the density for the parameters  $\lambda$  and  $\mu$  as they result from the calibration. The dotted line is the density of a stock modeled by a standard GBM with volatility set to the at-the-money level of 0.15. The picture shows that the toy model has fatter tails than the GBM model, which one expects of a model that matches the volatility smile. Finally, we remark that our stock price toy model has an atom at  $S_T = 492.19e^{0.1945} \approx 597$  and no support for the values above 597, which is also shown in the figure. The probability that corresponds to that atom is  $e^{-3.101} = 0.045$ .

### 5.5.2 Price behavior for double-sided barrier options

Now we use the parameters we found in the previous example to get an idea about behavior of the double-barrier prices. In this example we use the double-sided knock-in call, for which we derived two-dimensional Laplace

transforms in Section 5.4. In figure 5.2 we show the prices of a double-

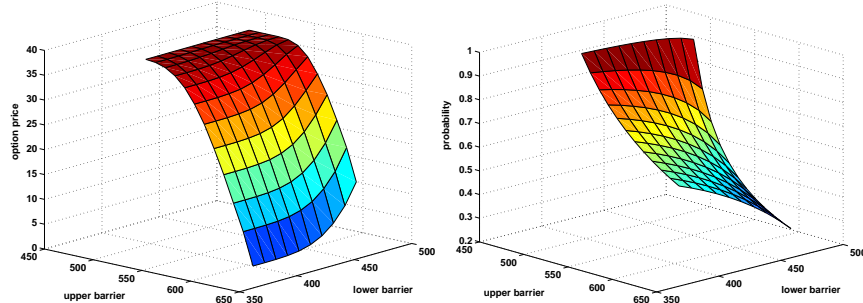


Figure 5.2: Behavior of the prices of double barrier options for different values of the lower and the upper barrier(left) and probability of exit through the upper barrier (right).

sided knock-in call with strike 480. The lower barrier seems to have less effect on the price than the upper barrier. This suggests that knocking in happens much more often continuously by hitting the upper level, than with a jump crossing the lower level. We use equation (5.10) in Corollary 5.3.3 to calculate the probability of exiting through the upper level and plot the results in the right-hand side graph confirming that it is more likely to exit via the upper barrier.

### 5.5.3 Implied volatility for double-sided barrier options

In the final numerical example we will calculate implied volatilities for the double-sided knock-in call. Suppose you are going to price this kind of double barrier option in the classical Black-Scholes framework and you want to do it consistently with the volatility smile in the market. Immediately the problem of choosing a volatility arises; do you have to let your volatility depend on the strike or the barriers? In this numerical example we price the double barrier using the exponential compound Poisson model and obtain the implied volatility from these prices. We show in fact the implied volatilities that follow from the GBM model for prices produced by the exponential compound Poisson model. Again, we use the calibrated parameters from the first numerical example. The prices and implied volatilities for the double-sided knock-in call options in case the underlying is modeled by a geometric Brownian motion are obtained after implementing the method of Pelsser as discussed in [73]. The implied volatility does exist as the double-sided knock-in call price is an increasing function of the volatility. In the left-hand graph of figure 5.3 we show a plot for the double-sided knock-in call with strike 480 and the different values of both the upper and the lower barrier. This graph is very similar to the surface graph of the previous numerical example, only it shows implied volatilities instead of prices now.

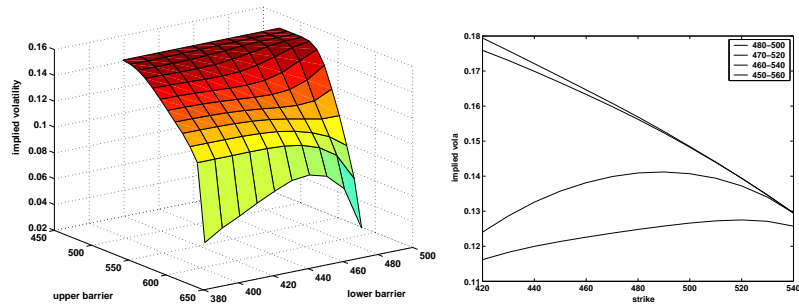


Figure 5.3: Implied volatility for double-sided knock-in call options for fixed strike and different barriers (left) and for fixed barriers and different strikes (right).

This graph reveals that the prices produced by the exponential compound Poisson model are structurally below the prices produced by the geometric Brownian motion with the volatility set to the implied volatility that belongs to the 480 strike according to the market as given in the left-hand side of figure 5.1. The right-hand side of figure 5.3 shows the volatility smile for the double-sided knock-in calls and the fixed barriers as produced by the exponential compound Poisson model. It is remarkable that by widening the barriers the smile changes from its original form to a parabolic form, something you do not expect. This example illustrates that although it is a toy model that is calibrated to the option market, the implied volatility of the double-sided barrier option can be really far from the implied volatility of the plain vanilla options.

## 5.6 Conclusions

In this paper we use the exponential compound Poisson process with exponential jumps to model the stock price process. For this stock price model we derived the Laplace transforms for the plain vanilla call option and the double-sided knock-in call option, which we numerically invert to generate actual prices. The numerical examples show that it is actually possible to calibrate even this toy model to the plain vanilla options market, and that the implied volatility for double-barrier options generated by this toy model is not trivial. As pointed out, the results still hold for a more sophisticated model and it is future work to solve the numerical problems that will arise in equation (5.4).

## 5.7 Appendix

### 5.7.1 One-boundary characteristics

Before we are able to give a proof of theorem 5.3.1 we will compute the one-boundary characteristics of the compound Poisson process  $X$  given in (5.2). For  $x > 0$  we define the following quantities

$$\begin{aligned} X_t^+ &= \sup_{s \leq t} X_s, & T_x^+ &= \inf\{t > 0 : X_t \geq x\}, & O_x^+ &= X_{T_x^+} - x \\ X_t^- &= \inf_{s \leq t} X_s, & T_x^- &= \inf\{t > 0 : X_t \leq -x\}, & O_x^- &= -X_{T_x^-} - x, \end{aligned}$$

where  $X_t^\pm$  denotes the supremum or infimum up to time  $t$ ,  $T_x^\pm$  the first passage time of the level  $\pm x$  and  $O_x^\pm$  the overshoot through this level. Let  $\nu_s$  be a random time which is exponentially distributed with parameter  $s$ . The Wiener-Hopf factorization, see [11] states that the characteristic function of  $X_{\nu_s}$  can be uniquely decomposed as the product of two characteristic functions, one supported on  $(-\infty, 0]$  and one on  $[0, \infty)$  of infinitely divisible distributions with zero drift. This factorization allows us to write

$$\mathbb{E}[e^{-pX_{\nu_s}}] = \mathbb{E}[e^{-p(X_{\nu_s}^+ - X_{\nu_s})}] \mathbb{E}[e^{-pX_{\nu_s}^+}], \quad \Re\{p\} = 0,$$

as in [11] it is shown that the distributions of  $X_{\nu_s}^+$  and  $X_{\nu_s}^+ - X_{\nu_s}$  are infinitely divisible with zero drift and the right support to fit into the Wiener-Hopf factorization. The process  $-X$  is also a Lévy process and therefore we have from the Wiener-Hopf factorization

$$\mathbb{E}[e^{-pX_{\nu_s}}] = \mathbb{E}[e^{-pX_{\nu_s}^-}] \mathbb{E}[e^{-pX_{\nu_s}^+}], \quad \Re\{p\} = 0. \quad (5.16)$$

Now we can compute the left-hand side of (5.16) and refactor it to the product of two characteristic functions that fulfill the conditions as follows

$$\begin{aligned} \mathbb{E}[e^{-pX_{\nu_s}}] &= \frac{s}{s - k(p)} = -\frac{s(\mu + p)}{p^2 + p(\mu - s - \lambda) - s\mu} \\ &= \frac{s(\mu + p)}{(c_1(s) - p)(p + c_2(s))} = \frac{c_1(s)}{c_1(s) - p} \times \frac{c_2(s)}{\mu} \frac{\mu + p}{p + c_2(s)}. \end{aligned} \quad (5.17)$$

Recall that  $c_1(s)$  and  $-c_2(s)$  are the roots of the equation  $k(p) - s = 0$  from which it follows that  $c_1(s)c_2(s) = s\mu$  and  $c_2(s) > \mu$  for  $\lambda > 0$ . Combining (5.16) and (5.17) results in the following expressions for the Wiener-Hopf factors

$$\begin{aligned} \mathbb{E}[e^{-pX_{\nu_s}^-}] &= \frac{c_1(s)}{c_1(s) - p}, \quad \Re\{p\} \leq 0, \\ \mathbb{E}[e^{-pX_{\nu_s}^+}] &= \frac{c_2(s)}{\mu} \frac{\mu + p}{p + c_2(s)}, \quad \Re\{p\} \geq 0. \end{aligned}$$

So,  $-X_{\nu_s}^-$  is exponentially distributed with parameter  $c_1(s)$  and by partial integration we have

$$\mathbb{E} \left[ e^{-sT_x^-} \right] = \mathbb{P} \left[ X_{\nu_s}^- < -x \right] = e^{-xc_1(s)}.$$

We are not interested in  $O_x^-$  as the crossing of the lower level will happen continuously. The Spitzer-Rogozin identity, see [71], relates the triple Laplace transform of the level, the first passage time and the overshoot to the Wiener-Hopf factors, giving the following equation for  $\Re\{p\} > 0$  and  $\Re\{s\}, \Re\{z\} \geq 0$

$$\begin{aligned} \int_0^\infty e^{-px} \mathbb{E} \left[ e^{-sT_x^+ - zO_x^+} \right] dx &= \frac{1}{p-z} \left( 1 - \mathbb{E}[e^{-pX_{\nu_s}^+}] / \mathbb{E}[e^{-zX_{\nu_s}^+}] \right) \\ &= \frac{\mu - c_2(s)}{(p + c_2(s))(\mu + z)}. \end{aligned} \quad (5.18)$$

Now invert this transform with respect to  $p$  to obtain for  $\Re\{s\}, \Re\{z\} \geq 0$

$$\mathbb{E} \left[ e^{-sT_x^+ - zO_x^+} \right] = e^{-xc_2(s)} \frac{\mu - c_2(s)}{\mu + z}.$$

Inverting once more, this time with respect to  $z$  yields for  $\Re\{s\} \geq 0$ ,

$$\mathbb{E} \left[ e^{-sT_x^+}; O_x^+ \in du \right] = e^{-xc_2(s)} \left( 1 - \frac{c_2(s)}{\mu} \right) \mu e^{-\mu u} du,$$

which, after integrating out the overshoot  $O_x^+$ , finally results in

$$\mathbb{E} \left[ e^{-sT_x^+} \right] = e^{-xc_2(s)} \left( 1 - \frac{c_2(s)}{\mu} \right).$$

### 5.7.2 Proof of Theorem 5.3.1

First, we state the theorem for a general Lévy process and then derive the specific results for the Poisson process with a drift we are considering. We introduce the following notation

$$F^x(du, s) = \mathbb{E} \left[ e^{-sT_x^+}; O_x^+ \in du \right] - \int_0^\infty \mathbb{E} \left[ e^{-sT_y^-}; O_y^- \in dv \right] \mathbb{E} \left[ e^{-sT_{v+B}^+}; O_{v+B}^+ \in du \right],$$

and

$$F_y(du, s) = \mathbb{E} \left[ e^{-sT_y^-}; O_y^- \in du \right] - \int_0^\infty \mathbb{E} \left[ e^{-sT_x^+}; O_x^+ \in dv \right] \mathbb{E} \left[ e^{-sT_{v+B}^-}; O_{v+B}^- \in du \right].$$

Recall that the events  $A^x$  and  $A_y$  denote an exit from the interval  $[-y, x]$  through the upper and lower boundary respectively. The following theorem is theorem 1 in [54].

**Theorem 5.7.1.** *Let  $\{X_t; t \geq 0\}$  be a Lévy process,  $B \geq 0$ ,  $x \in [0, B], y = B - x$ ,  $X_0 = 0$ , and*

$$\tau = \inf\{t > 0 : X_t \notin [-y, x]\}, \quad \mathcal{O} = (X_\tau - x) 1_{\{A_x\}} + (-X_\tau - y) 1_{\{A_y\}}$$

*the first exit time from the interval  $[-y, x]$  by the process  $X_t$  and the value of the overshoot through one of the boundaries at the moment of the exit. Then the Laplace transforms of the joint distribution of  $\{\tau, \mathcal{O}\}$  for  $s > 0$  satisfy the following equalities*

$$\begin{aligned} \mathbb{E}[e^{-s\tau}; \mathcal{O} \in du, A_x] &= F^x(du, s) + \int_0^\infty F^x(dv, s) \mathfrak{K}_+^s(v, du), \\ \mathbb{E}[e^{-s\tau}; \mathcal{O} \in du, A_y] &= F_y(du, s) + \int_0^\infty F_y(dv, s) \mathfrak{K}_-^s(v, du), \end{aligned} \quad (5.19)$$

where

$$\mathfrak{K}_\pm^s(v, du) = \sum_{n \in \mathbb{N}} K_\pm^{(n)}(v, du, s), \quad v, u > 0, \quad \mathbb{N} = \{1, 2, \dots\} \quad (5.20)$$

are the series of the successive iterations and

$$\begin{aligned} K_\pm^{(1)}(v, du, s) &= K_\pm(v, du, s), \\ K_\pm^{(n+1)}(v, du, s) &= \int_0^\infty K_\pm^{(n)}(v, dl, s) K_\pm(l, du, s) \end{aligned} \quad (5.21)$$

are the successive iterations ( $n \in \mathbb{N}$ ) of the kernels  $K_\pm(v, du, s)$ , which are given by the defining equalities

$$\begin{aligned} K_+(v, du, s) &= \int_0^\infty \mathbb{E}[e^{-sT_{v+B}^-}; O_{v+B}^- \in dl] \mathbb{E}[e^{-sT_{l+B}^+}; O_{l+B}^+ \in du], \\ K_-(v, du, s) &= \int_0^\infty \mathbb{E}[e^{-sT_{v+B}^+}; O_{v+B}^+ \in dl] \mathbb{E}[e^{-sT_{l+B}^-}; O_{l+B}^- \in du]. \end{aligned} \quad (5.22)$$

We apply now the formulas of theorem 5.7.1 to the exponential compound Poisson model with drift that we are considering. This application should result in theorem 5.3.1. We start with the first formula in (5.19) and calculate the kernels (5.22) and the iterations (5.21) for this process, where we recall that  $c(s) = c_1(s) + c_2(s)$  and we use the one-boundary characteristics from the previous section,

$$\begin{aligned} K_+(v, du, s) &= \int_0^\infty e^{-(v+B)c_1(s)} \delta(l) dl e^{-(l+B)c_2(s)} \left(1 - \frac{c_2(s)}{\mu}\right) \mu e^{-\mu u} du \\ &= e^{-vc_1(s)} \left(1 - \frac{c_2(s)}{\mu}\right) e^{-Bc(s)} \mu e^{-\mu u} du, \end{aligned}$$

so that

$$\begin{aligned} K_+^{(2)}(v, du, s) &= \int_0^\infty K_+(v, dl, s)K_+(l, du, s) \\ &= \int_0^\infty \mu e^{-\mu l} e^{-lc_1(s)} dl e^{-vc_1(s)} \left(1 - \frac{c_2(s)}{\mu}\right)^2 e^{-2Bc(s)} \mu e^{-\mu u} du \\ &= K(s, B)K_+(v, du, s), \end{aligned}$$

where we recall that  $K(s, B)$  is given by (5.9). From the recursion relation it is now clear that for  $n \in \mathbb{N}$

$$K_+^{(n)}(v, du, s) = K(s, B)^{n-1}K_+(v, du, s).$$

As  $c_{1,2}(s) > 0$  it follows that  $0 < K(s, B) < 1$  and therefore

$$\mathfrak{R}_+^s(v, du) = \sum_{n \in \mathbb{N}} K_+^{(n)}(v, du, s) = \frac{K_+(v, du, s)}{1 - K(s, B)}.$$

The next step is to compute the  $F^x(du, s)$ , again by using the one-boundary results from the previous section,

$$\begin{aligned} F^x(du, s) &= e^{-xc_2(s)} \left(1 - \frac{c_2(s)}{\mu}\right) \mu e^{-\mu u} du - \\ &\quad \int_0^\infty e^{-yc_1(s)} \delta(v) dv e^{-(v+B)c_2(s)} \left(1 - \frac{c_2(s)}{\mu}\right) \mu e^{-\mu u} du \\ &= (\mu - c_2(s)) e^{-xc_2(s)} \left[1 - e^{-yc(s)}\right] e^{-\mu u} du. \end{aligned}$$

It remains to calculate the integral in the first formula of (5.19) for which we have now all the ingredients,

$$\begin{aligned} \int_0^\infty F^x(dv, s) \mathfrak{R}_+^s(v, du) &= \frac{1}{1 - K(s, B)} \int_0^\infty F^x(dv, s) K_+(v, du, s) \\ &= e^{-xc_2(s)} \left(1 - \frac{c_2(s)}{\mu}\right) \left[1 - e^{-yc(s)}\right] \frac{K(s, B)}{1 - K(s, B)} \mu e^{-\mu u} du \\ &= F^x(du, s) \frac{K(s, B)}{1 - K(s, B)}, \end{aligned}$$

so that we can add up the results to arrive at

$$\begin{aligned} \mathbb{E}[e^{-s\tau}; \mathcal{O} \in du, A^x] &= F^x(du, s) \left(1 + \frac{K(s, B)}{1 - K(s, B)}\right) \\ &= e^{-xc_2(s)} \left(1 - \frac{c_2(s)}{\mu}\right) \frac{1 - e^{-yc(s)}}{1 - K(s, B)} \mu e^{-\mu u} du. \end{aligned}$$

Integrating out the overshoot  $\mathcal{O}$  gives the first formula of (5.8) in theorem 5.3.1.

In order to calculate the quantities in the second formula of (5.19) we start calculating  $K_-(v, du, s)$  and  $K_-^{(2)}(v, du, s)$  to arrive at  $K_-^{(n)}(v, du, s)$ . Using the one-boundary characteristics from the previous section we get analogous results to the  $K_+^{(\cdot)}$  case,

$$\begin{aligned} K_-(v, du, s) &= \int_0^\infty e^{-(v+B)c_2(s)} \left(1 - \frac{c_2(s)}{\mu}\right) \mu e^{-\mu l} dl e^{-(l+B)c_1(s)} \delta(u) du \\ &= e^{-vc_2(s)} K(s, B) \delta(u) du \end{aligned}$$

$$K_-^{(n)}(v, du, s) = K(s, B)^{n-1} K_-(v, du, s),$$

and, also analogously,

$$\mathfrak{K}_-^s(v, du) = \sum_{n \in \mathbb{N}} K_-^{(n)}(v, du, s) = \frac{K_-(v, du, s)}{1 - K(s, B)}.$$

Now compute  $F_y(du, s)$ ,

$$\begin{aligned} F_y(du, s) &= e^{-yc_1(s)} \delta(u) du \\ &\quad - \int_0^\infty e^{-xc_2(s)} (\mu - c_2(s)) e^{-\mu v} dv e^{-(v+B)c_1(s)} \delta(u) du \\ &= e^{-yc_1(s)} [1 - K(s, x)] \delta(u) du. \end{aligned}$$

For the integral we get a similar expression as for the first formula,

$$\begin{aligned} &\int_0^\infty F_y(dv, s) \mathfrak{K}_-^s(v, du) \\ &= \int_0^\infty e^{-yc_1(s)} [1 - K(s, x)] \delta(v) dv e^{-vc_2(s)} \frac{K(s, B)}{1 - K(s, B)} \delta(u) du \\ &= F_y(du, s) \frac{K(s, B)}{1 - K(s, B)}. \end{aligned}$$

Thus, the second formula of (5.19) becomes

$$\begin{aligned} \mathbb{E} [e^{-s\tau}; \mathcal{O} \in du, A_y] &= F_y(du, s) \left(1 + \frac{K(s, B)}{1 - K(s, B)}\right) \\ &= e^{-yc_1(s)} \frac{1 - K(s, x)}{1 - K(s, B)} \delta(u) du. \end{aligned}$$

It is again by integrating out the overshoot  $\mathcal{O}$  that we obtain the second formula of (5.8) in theorem 5.3.1.

### 5.7.3 Proof of Theorem 5.3.4

We first state a theorem for a spectrally positive Lévy process, i.e. a Lévy process with positive jumps only and then derive the formulas of theorem 5.3.4 given in (5.12) by computing the quantities in the stated theorem for our process. The following theorem is lemma 2 and equation (23) of [54].

**Theorem 5.7.2.** *Let  $\{X_t; t \geq 0\}, X_0 = 0$  be a spectrally positive Lévy process. Then the integral transform*

$$Q^s(p) = \int_0^{\infty} s e^{-st} \mathbb{E}[e^{-pX_t}; -y < X_t^-, X_t^+ < x] dt$$

obeys the following representation

$$\frac{1}{s} Q^s(p) = e^{yp} \frac{R_s(x)}{R_s(B)} \int_0^B e^{-up} R_s(u) du - \int_0^x e^{-up} R_s(u) du, \quad (5.23)$$

where

$$R_s(x) = \frac{1}{2\pi i} \int_{\gamma-i\infty}^{\gamma+i\infty} e^{xp} \frac{1}{k(p) - s} dp, \quad \gamma > c(s) \quad (5.24)$$

is the scale function of the spectrally positive Lévy process as in [11].

The process (5.2) has only upward jumps, so it is a spectrally positive Lévy process and the theorem applies. The scale function of the process (5.2) follows by calculating the residuals and is given by

$$R_s(x) = \frac{1}{c(s)} \left[ (\mu + c_1(s)) e^{xc_1(s)} - (\mu - c_2(s)) e^{-xc_2(s)} \right], \quad R_s(0) = 1.$$

Now we calculate the integral over the interval  $[0, B]$  in (5.23)

$$\begin{aligned} & \int_0^B e^{-pu} R_s(u) du \\ &= \frac{1}{c(s)} \int_0^B \left[ (\mu + c_1(s)) e^{uc_1(s)} - (\mu - c_2(s)) e^{-uc_2(s)} \right] e^{-pu} du \\ &= \frac{1}{c(s)} \left[ \frac{\mu + c_1(s)}{p - c_1(s)} [1 - e^{-B(p-c_1(s))}] - \frac{\mu - c_2(s)}{p + c_2(s)} [1 - e^{-B(p+c_2(s))}] \right], \end{aligned}$$

immediately resulting in an expression for the integral over the interval  $[0, x]$ . Denote the multiplier in front of the first integral in (5.23) by  $C$  for which we can compute

$$C = e^{yp} \frac{R_s(x)}{R_s(B)} = e^{py} \frac{(\mu + c_1(s)) e^{xc_1(s)} - (\mu - c_2(s)) e^{-xc_2(s)}}{(\mu + c_1(s)) e^{Bc_1(s)} - (\mu - c_2(s)) e^{-Bc_2(s)}}.$$

Now we can compute (5.23) as follows

$$\begin{aligned} & \frac{1}{s} Q^s(p) \\ &= C \times \frac{1}{c(s)} \left[ \frac{\mu + c_1(s)}{p - c_1(s)} [1 - e^{-B(p-c_1(s))}] - \frac{\mu - c_2(s)}{p + c_2(s)} [1 - e^{-B(p+c_2(s))}] \right] - \\ & \quad \frac{1}{c(s)} \left[ \frac{\mu + c_1(s)}{p - c_1(s)} [1 - e^{-x(p-c_1(s))}] - \frac{\mu - c_2(s)}{p + c_2(s)} [1 - e^{-x(p+c_2(s))}] \right], \end{aligned}$$

which is, after multiplication of both sides by  $s$  the formula (5.12) of theorem 5.3.4.

## Chapter 6

# Commodity volatility modeling and option pricing with a potential function approach

We consider a novel approach to modeling of commodity prices and apply it to commodity option pricing and volatility estimation. This approach is particularly suited for prices with multiple attraction regions: such as crude oil and other energy and agricultural commodities. The price is modeled as a diffusion process governed by a potential function with minima at the attraction points. When applied to crude oil prices, the method captures characteristic behavior of the prices remarkably well. Pricing of European options on spot and futures commodity contracts is developed within the potential model, and compared to the Black-Scholes framework. The approach provides a new way of estimating the volatility, which is particularly useful when option prices (and hence implied volatilities) are not readily available; this is often the case for commodity markets. European options on physical commodities and commodity futures are priced using the volatility forecasts obtained from the model. The performance of the model is evaluated on the basis of the hedging costs of an option. For options on crude oil, the method outperforms - in terms of hedge costs - the Black-Scholes approach with historical volatility.

## 6.1 Introduction

Commodity markets have experienced dramatic growth recently, in terms of the volumes and variety of traded contracts, the number of exchanges and market participants. The most dramatic expansion in the last decade has been in the trading of commodity options. Exchanges such as London International Petroleum Exchange (IPE) and New York Mercantile Exchange (NYMEX) continuously introduce options on various commodity contracts. At the same time, over-the-counter trading in physical commodity options and sophisticated option-like contracts is growing rapidly. However, the special characteristics of commodity prices require new tools to efficiently deal with this increased flow of traded derivatives. The existing pricing, hedging and volatility modeling techniques are not always directly applicable to commodities. Hence, analytical and modeling tools that take into account specific features of commodity prices are needed.

One such characteristic feature is the tendency of many commodity prices to concentrate in a number of attraction regions, preferring some values over others. A striking example is the series of daily prices of crude oil. The left-hand side graph in figure 6.1 shows the plot of daily spot prices for Brent North Sea oil, for the period from 1994 to 1999. The phenomenon of price clustering (around approximately 12, 18 and 23 dollars per barrel in this period) can be seen on the histogram of daily oil prices on the right-hand side of the same figure. Such price clustering is a well-known phenomenon in commodity markets and traders know which price levels are more persistent than others.

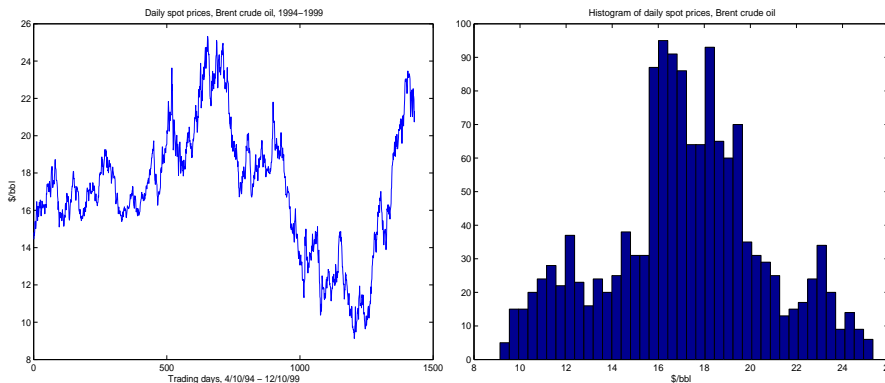


Figure 6.1: Daily spot oil prices plot (left) and histogram (right), 1994-1999.

Spot as well as futures prices of several other energy commodities (heating oil, gasoline) and agricultural commodities (coffee, cocoa, soybean) exhibit similar behavior. Figure 6.2 shows histograms of heating oil prices and cocoa prices, both clearly exhibiting price clustering. Commodity market participants are well aware of this price clustering phenomenon. For agricultural

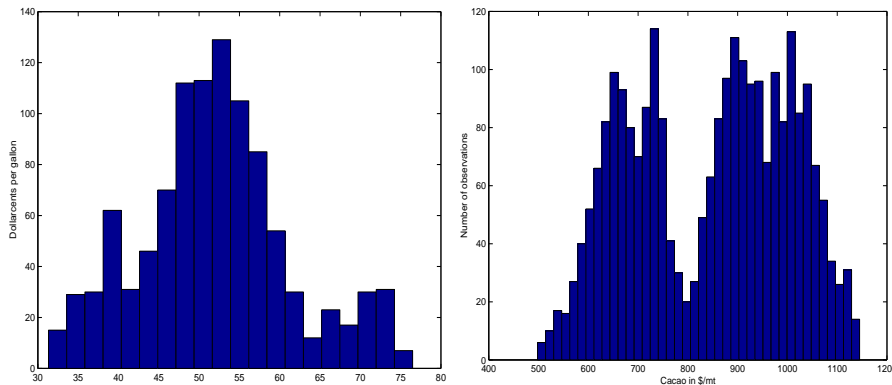


Figure 6.2: Histograms of heating oil prices (left) and cocoa prices (right).

commodities, the explanation for the peaks in the histogram of prices is straightforward: these correspond to good and bad harvest years (whose occurrence is not periodic). For energy commodities, the explanation is not as simple, and there is a significant body of research in economic literature concerned with this issue. Possible explanations involve such factors as the global balance of oil supply and demand, OPEC quotas and target price bands, economic planning in the petroleum industry, the cyclic development of new exploration technologies and the strategic importance of oil. Economists are searching for theoretical explanation of oil price multistability in terms of macroeconomic factors, and there is a vast literature on the subject (see e.g. [25], [74], [5], [22],[68]). Another, more empirical approach, adopted by some econometricians, is to build mathematical nonlinear models of price dynamics with two or more attracting regions. Brock and Hommes analyze in [20], [21] and [51] how the assumption of heterogeneous beliefs can lead to complicated (chaotic) dynamics of prices with strange attractors and multiple attracting regions.

For the commodities mentioned above, prices regularly move between attraction regions, although the time spent at a given region can be long (and unpredictable). This relates to the well-known property of *mean-reversion*. Mean-reverting diffusion models have been widely used to model commodity prices, see [19] and [79]. However, mean-reverting models postulate the existence of just one (possibly time-varying) mean, and hence cannot generate processes with multiple attraction regions. Standard time series analysis techniques (linear AR and ARMA models with Gaussian innovations) or (G)ARCH models are also unable to model the phenomenon of multiple attraction regions. Thus, an alternative model to mean-reversion is needed to preserve a multimodal invariant distribution that reflects multiple attracting regions.

The approach suggested by the author in [50] employs a nonlinear model

that admits the possibility of changes in regime, i.e. occasional discrete shifts in the parameters governing the behavior of the time series. A novel approach to modeling continuous as well as discrete time processes that exhibit "preferred" regions was introduced in [16]. In this approach the price is governed by a potential function with (local) minima at the attracting values with perturbation by random fluctuations. This gives rise to a process with a multimodal invariant distribution, such as an observed price series. The resulting model is as simple and tractable for estimation and option pricing purposes as traditional mean-reverting models. However, it is more versatile, as it allows modeling of multiple stable price levels (attracting regions) and encompasses a mean-reverting model as a special case.

Here we explore the pricing of European options on commodities whose prices behave as the diffusion governed by the potential function. We focus in particular on the stochastic part of the price process, which characterizes the volatility. The volatility estimated from the potential function model can then be used as an alternative to the historical or GARCH volatility for option pricing and other applications.

The paper is organized as follows. First, we describe the potential function model in more detail, discuss its economic motivation and statistical estimation. Then we introduce the volatility estimation within the potential model. Section 6.3 is devoted to pricing options on spot and futures commodity contracts. Section 6.4 describes the model application to oil markets and addresses the robustness of the model with respect to the potential function specification. Section 6.5 briefly outlines the multivariate extension and section 6.6 concludes.

## 6.2 Volatility and the potential function model

### 6.2.1 The potential function model

A detailed treatment of the potential function approach, of which this section is a summary, is given in [16]. Let  $(p_t)_{t \geq 0}$  be a continuous-time price process in  $\mathbb{R}$  (the observed price series is its realization at discrete time points). We postulate that  $p_t$  evolves according to the stochastic differential equation

$$dp_t = -U'(p_t) dt + \sigma dW_t, \quad (6.1)$$

where  $U : \mathbb{R} \rightarrow \mathbb{R}$  is a potential function, i.e., it is twice continuously differentiable. The process  $W_t$  is a standard Brownian motion, and  $\sigma$  is the scalar factor that measures the magnitude of random fluctuations, i.e., the influence of the Brownian motion on the evolution of the process. We assume that the potential function and the parameter  $\sigma$  are constant, and we interpret  $\sigma$  as the *average*, or *long-term volatility*.

Equation (6.1) is an example of a diffusion process with drift. If the potential is a quadratic function, then the drift term is linear in  $p_t$  and (6.1) becomes the Langevin equation and  $(p_t)$  the well-known Ornstein-Uhlenbeck process. The following, by the Euler scheme discretized, version of the continuous-time model (6.1)

$$p_{i+h} - p_i = -U'(p_i)h + \epsilon_i, \quad (6.2)$$

provides some insight. In this discrete model  $h$  is the discretization step and the  $(\epsilon_i)$  are the increments of the process  $\sigma dW_t$ , so they are independent normally distributed random variables with mean 0 and variance  $h\sigma^2$ . Since here we analyze daily prices and volatilities, we take the discretization step  $h = 1$  (one day). In words, the next value of the series tends to move in the direction of the nearest minimum of the potential function with respect to the current value. The random fluctuations  $(\epsilon_n)$  ensure that the series is not trapped in a local minimum but continues to move between minima.

This evolution is illustrated in figure 6.3. Here a one-dimensional "bowl" plays the role of the potential function with dips at local minima, and the observed process is the horizontal coordinate of a ball moving along the bowl's walls, subject to gravity and some random impulses. The ball has a natural tendency to move downhill into the dips, but random shocks prevent it from settling there and force it up the walls and move it from one dip to another. Note that the deeper a minimum (i.e. a dip), the longer the process spends there. So in a series of observations on such a process, there are more observations near the minima of the potential than at other locations.

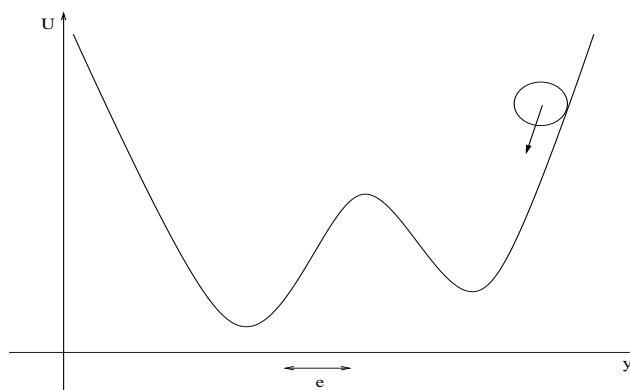


Figure 6.3: Evolution governed by a potential function

We mention in passing that this model has been inspired by the application of diffusions to global optimization as in [45], which in turn are related to an optimization technique called *simulated annealing*.

For an observed price series, neither the potential function  $U$  nor the long-term volatility  $\sigma$  are known. However, the following distributional result

from [64] allows us to estimate the potential (and subsequently  $\sigma$ ) from the historical data. If  $p_t$  evolves according to (6.1), then, under suitable conditions on  $U$ , the distribution of  $p_t$  approaches (weakly) an equilibrium, which is a *Gibbs distribution* with density

$$\pi_\sigma(p) = \frac{1}{Z_\sigma} \exp(-2U(p)/\sigma^2), \quad (6.3)$$

where  $Z_\sigma$  is the normalization constant. As pointed out in [16] for every potential function  $U$  there exists a potential function  $\tilde{U}$  such that the equilibrium distribution is the same as for  $U$  and the normalization constant  $Z_\sigma = 1$ , so we will consider  $Z_\sigma = 1$  in the sequel. Inverting (6.3), we find that the potential function can be expressed via the density of the invariant distribution as

$$U(p) = -\frac{\sigma^2}{2} \log(\pi_\sigma(p)). \quad (6.4)$$

We can estimate the density of the invariant distribution from the observed prices in numerous ways, e.g. by using a kernel density estimator, fitting a mixture of Gaussian densities or a high-degree polynomial to the histogram. This alone does not give us the estimate of the potential yet, since (6.4) also involves the unknown parameter  $\sigma$ . So we first estimate the *scaled potential*

$$G_\sigma(p) = \frac{2}{\sigma^2} U(p) = -\log(\pi_\sigma(p))$$

by  $\hat{G}_\sigma(p) = -\log(\hat{\pi}_\sigma(p))$ , where  $\hat{\pi}_\sigma$  is the estimated density of the observations. Then  $\sigma^2$  can be estimated by the least-squares procedure, observing that

$$p_{i+1} - p_i = -\frac{\sigma^2}{2} \hat{G}'_\sigma(p_i) + \epsilon_i, \quad (6.5)$$

i.e.  $\sigma^2$  is the parameter of a linear regression of the price increments ( $p_{i+1} - p_i$ ) on  $(-\hat{G}'_\sigma(p_i)/2)$  without an intercept term. The variance of the  $(\epsilon_i)$  should also equal  $\sigma$ , which should be taken into account if one wants to enhance the estimation procedure.

We estimated the model parameters for historical daily prices of Brent oil from 1994 to 1999. The potential function is estimated by taking the log of a fit to the histogram of prices fitted 10th degree polynomial. Figure 6.4 shows the resulting potential function on the left. The estimated value of  $\sigma$  is 0.22 (recall that this is the estimate of the average volatility of daily price increments). This corresponds to an annualized volatility of daily price returns of approximately 20% (for an average price level of 18\$/bbl), which is indicative of the average volatility in oil markets in that period. Figure 6.5 shows in the left-hand side graph the autocorrelation function of the model residuals, which confirms that the residuals are uncorrelated. In the middle it shows the histogram of the residuals, which has a slightly more peaked shape than the normal density.

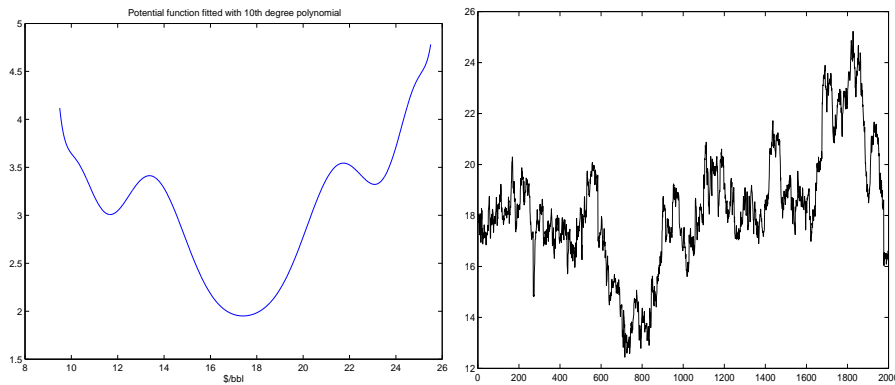


Figure 6.4: Potential function estimate (left) and copy of the oil prices series (right).

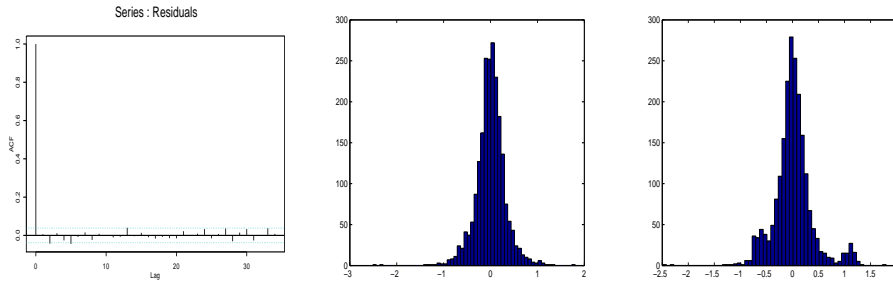


Figure 6.5: Autocorrelation function (left) and histogram (middle) of the model residuals of the potential model and histogram of the residuals of the mean-reversion model (right).

Possible applications of the potential model are forecasting the next day's price move or its direction and generating copies of the observed price series with the same invariant distribution. A copy of the oil price series generated with the model is shown in the right-hand side graph in figure 6.4, which indeed resembles the actual observed price path seen in figure 6.1; distributional characteristics such as skewness and kurtosis are also close to those for the real data. Forecasting the direction of the next day's price move with the potential model leads to correct forecasts in 57 % of days (for historical dataset), outperforming a simple delta-method (correct forecasts in 51% of days) or neural networks (53%), where a detailed description of these study can be found in [16].

Here we fitted a polynomial of a high degree (10) to the histogram of oil prices, and the potential function was obtained by taking the log-inverse of the fitted polynomial (i.e. by using the distributional result (6.3)). The choice of the polynomial degree is a matter left to the model builder, as is the bin size of the histogram to which it has to be fitted. We believe this degree

should be high enough to model significant peaks in the histogram (here the bin size is important), but not too high, so as not to model features of the histogram caused by noise, i.e., those that have no meaningful significance. For example, the histogram in figure 6.1 has three peaks, these correspond to three stable price levels well-known to oil traders. So in this case, the minimal polynomial degree should be 6; using a polynomial of lower degree would lead to missing one (or more) peaks. For example, if we fit a standard mean-reversion model with a constant mean (i.e. a quadratic polynomial) to the data in figure 6.1, the histogram of the model residuals still contains three peaks (figure 6.5), since the mean-reverting model is unable to extract these from the price distribution. We shall investigate further the influence of the polynomial degree on our results in the section on option pricing and show that the model is robust to the choice of the polynomial degree, as long as it is high enough.

Other methods of fitting the histogram or the potential function are feasible. For example, one can postulate some parametric form of the invariant price distribution or of the potential function, e.g. a mixture of Gaussian kernels, and fit the model by means of the maximum likelihood method. The latter way of fitting the model is particularly useful in multivariate extension of the model, briefly addressed in section 6.5. Fitting a mixture of three Gaussian densities to the distribution in figure 6.1 provided a potential function undistinguishable from that in figure 6.4. However, we found that, in univariate case, the method we described in this section is the easiest to implement, fastest and though rather accurate way to apply the model, since it allows for fast calculation of the potential's derivative. It is also possible to start from a polynomial with given degree and use the maximum likelihood method to obtain the coefficients from the historical data. The rather indirect method we use here has the advantage that the elements of the implementation are readily available. Nonparametric methods such as kernel density estimation can be slow and do not provide the expression for the derivative of the potential, which needs to be quickly and accurately evaluated.

The characteristic features of the modeled process (such as multiple attraction points and the long-term volatility) are learned from historical data. So the question arises, how well the potential reflects the current state of the market. The model remains valid as long as attraction points and the overall volatility do not change in time. However, shifts in market fundamentals can lead to the formation of new attraction points and to different volatility levels, which happened in the oil market in the past few years. The resulting non-stationarity of price series can seriously limit the applicability of the approach. In practice, the non-stationarity can be dealt with by regularly re-fitting the model, incorporating new price levels within the new fitted potential and new volatility levels within the parameter  $\sigma$ .

### 6.2.2 Volatility estimation in the potential function model

We assumed that the parameter  $\sigma$  is constant and interpreted is as a long-term average volatility of daily price moves. This parameter, together with the potential function, can be estimated from historical data, using the procedure outlined above. Like in the Black-Scholes case, we made a model with a constant volatility but suspect the actual volatility to be non-constant. Suppose that we apply the procedure of the previous section once and after that consider the potential function  $U$  as given. We can now construct the *daily estimate of the volatility* as follows

$$\hat{\sigma}_i^2 = (p_i - p_{i-1} + U'(p_{i-1}))^2, \quad (6.6)$$

where  $p_i$  is the price on day  $i$ . Recall that this is a measure of variability of daily price moves, rather than of daily returns which we are used to in the Black-Scholes case. It can be easily translated into a daily volatility of returns by means of re-scaling:  $\sigma_i^{ret} = \sigma_i/p_i$ . However, in the next section we shall see the benefits of using the volatility of price increments, rather than of returns, for option pricing.

The volatility estimate (6.6) can be used for derivatives pricing (which is addressed in the next section), risk management (Value-at-Risk in particular), portfolio management and other applications, as an alternative to the historical or GARCH volatility (see [15]).

We applied this approach to estimating the volatility of daily oil prices. Figure 6.6 shows the series of the realized volatility of daily returns on the left-hand side and on the right-hand side it shows the series of daily price moves volatility estimated by (6.6). Recall that the difference in scale between the graphs in figure 6.6 is due to considering daily price increments for the potential function volatility rather than daily returns. For option pricing one usually considers a series of data points, representing a time period equivalent to the time to expiry of the option, to estimate the historical volatility as has been done in figure 6.9.

According to the discrete-time model (6.2), the magnitude of the daily price increments (and hence, the spread of their distribution) is partly determined by the derivative of the potential and partly by random fluctuations. The presence of a deterministic component, given by the potential's derivative, is what distinguishes the daily volatility measure (6.6) from the historical volatility. The deterministic component explains a part of the daily price increments' variability, while another part is due to stochastic fluctuations. The deterministic component plays a more significant role if the current price is far from one of the attracting points (i.e. the local minima, where the derivative of the potential is higher in absolute value). Near the attraction points the derivative of the potential is close to zero, so the random fluctuations are predominantly responsible for price movements. This is in good

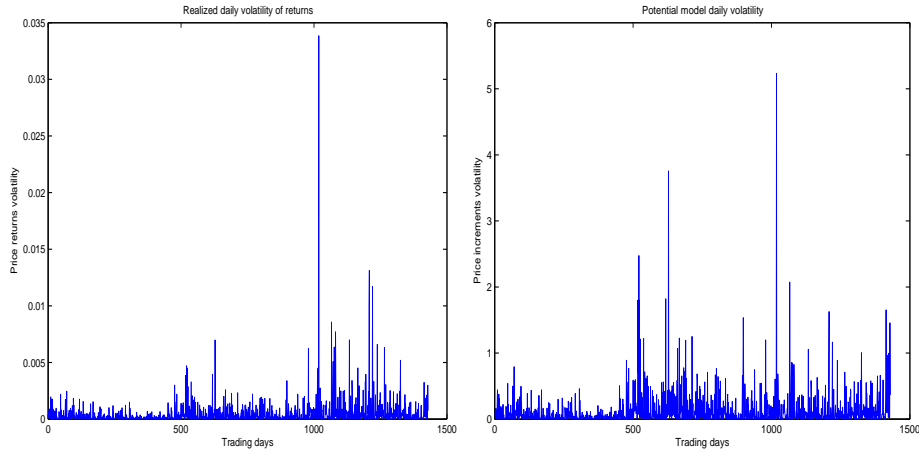


Figure 6.6: Historical (left) and potential function (right) daily volatility.

agreement with economic arguments (such as convergence to an equilibrium price) and with the market's perceptions.

Recall that, for constant parameter  $\sigma$ , the invariant distribution of the process (6.1) is given by the Gibbs distribution. An interesting theoretical question is whether the result on convergence of the distribution of  $p_t$  to the Gibbs distribution continues to hold, if the volatility  $\sigma = \sigma_t(\omega)$  is a stationary stochastic process (such as stationary GARCH process or a process arising from most of stochastic volatility models).

## 6.3 Option pricing within the potential function framework

### 6.3.1 Potential versus Black-Scholes models

Recall that in the Black-Scholes framework, a general model for the underlying value  $(p_t)_{t \geq 0}$  is given by

$$dp_t = \mu(p_t, t) dt + \sigma_{BS} p_t dW_t,$$

where the function  $\mu : \mathbb{R}^+ \times \mathbb{R}^+ \rightarrow \mathbb{R}$  is a deterministic drift and  $\sigma_{BS}$  is the Black-Scholes volatility. The Black-Scholes model is characterized by the normality of price (log)returns. On the other hand, the potential function model belongs to the class of models of the general form

$$dp_t = \nu(p_t) dt + \sigma_{pot} dW_t, \quad (6.7)$$

with the specific drift term  $\nu(p) = -U'(p)$  (where  $U : \mathbb{R} \rightarrow \mathbb{R}$  is the potential function and  $\sigma_{pot}$  is the potential model volatility). This class of

models is characterized by the normality of the price increments (and not of the log-returns, as in Black-Scholes' model).

Models of the type (6.7) are often suggested for commodity prices as an alternative to the Black-Scholes model. For instance, mean-reversion price models often belong to this class. The main criticism of such models is that they allow zero or even negative prices. However, in the potential function model, the potential function is chosen in such a way that the price regions which have never been observed are assigned almost zero probabilities. This is the consequence of the fact that the invariant distribution of the price process is determined by the potential function and vice versa.

The model (6.7) has some nice and intuitive volatility properties. In the Black-Scholes model, the diffusion term coefficient  $\sigma_{BS}p_t$  varies proportionately to the underlying value  $p_t$ . This is not the case in for the model (6.7). If we assume the equivalence between the magnitude of the fluctuations in both models and let  $\sigma_{pot}$  be constant, we see that it corresponds to increasing of  $\sigma_{BS}$  if the underlying value  $p_t$  decreases and to decreasing of  $\sigma_{BS}$  if  $p_t$  increases. Consequently, the model (6.7) satisfies the well-known option market's rule of thumb:

- An increase in the underlying value leads to a decrease in the Black-Scholes volatility  $\sigma_{BS}$ . (In traders' terms: "The volatility floats out of the market").
- A decrease in the underlying value leads to an increase in the Black-Scholes volatility  $\sigma_{BS}$ . (In traders' terms: "The volatility shoots into the market").

This rule of thumb is reflected in the so-called "volatility smile" observed in the market, which is intrinsically embedded in the model (6.7).

In derivatives pricing, the volatility is an important parameter, and often the only one not directly observable in the market. In fact, the value of volatility used to price an option should be a forecast of the volatility over the entire period from the present time until the option's expiry. The implied volatility is often used, i.e. market option prices are observed and the volatility is calculated by inverting the expression for the option price (for a discussion of the implied volatility surface in oil markets see e.g. [17]). Unfortunately, this approach is not always feasible, especially for commodities options. Commodities option markets are not as developed and as liquid as stock option markets. Moreover, over-the-counter (OTC) options constitute a large part of traded commodities options. So in this case the observed option prices are often either not reliable or not available.

One way to deal with this is to use the historic (i.e. realized) or the GARCH volatility, averaged over a certain past period. The duration of the averaging period usually equals to the time to the option's expiry. For example, if we price an option expiring in 3 months, the historical data of the past 3

months is used to forecast the next-3-months average volatility. We shall use the same principle for option pricing in the potential model framework: estimate the daily volatility by (6.6) and then average these estimates over a past period of the same length as the option's time to expiry.

### 6.3.2 hedge costs

In the next section we compare option pricing in the potential model and in the Black-Scholes framework. For the comparison criterion we use the hedge cost of an option. This is one of the most important practical consequences of how well options are priced and how good the volatility forecast is. If option prices are not very liquid (as it is the case for many commodity options), option traders calculate their hedge costs and, by comparing them to quoted option prices, they decide whether to take a position in a particular option. Let  $p_t$  be the underlying value at time  $t$ ,  $K$  the strike price of a European option and  $T$  the time to option's expiry. The replication argument of option pricing assures that there exists a hedging strategy that allows the option's seller to replicate the option. The seller's portfolio at expiry will consist of one unit of the underlying in case of  $p_T > K$  and it will be empty in case of  $p_T \leq K$ . The costs involved in hedging are the same for every possible path of the underlying. Therefore, by the no-arbitrage argument, the option price should be equal to the discounted hedge costs. The hedging strategy consists of buying an amount of underlying and borrowing the money at the current interest rate to do so. The amount of underlying in the portfolio at time  $t$  is given by the option's delta ( $\Delta$ ) which is the partial derivative of the option price at time  $t$  with respect to the underlying value  $p_t$ .

Ideally, the portfolio should be re-balanced continuously. In practice this cannot be satisfied, as it would lead to high transaction costs. So we assume the portfolio is re-balanced daily (which is often the case in practice). If the expiration time  $T$  of the option is  $N$  days ahead, the portfolio is re-balanced at the time points  $0 = t_0 < t_1 < \dots < t_N = N/365$ . The discounted hedging costs  $H$  then are

$$H((\Delta_t)_{t=t_0, t_1, \dots, t_N}) = \Delta_{t_0} p_{t_0} + \sum_{k=1}^N e^{-kr\delta} p_{t_k} (\Delta_{t_k} - \Delta_{t_{k-1}}) - \Delta_{t_N} K, \quad (6.8)$$

where  $\delta = 1/365$ . The equation (6.8) summarizes the following hedging strategy: at time  $t_0$  buy  $\Delta_{t_0}$  of the underlying for the price  $p_{t_0}$ , then re-balance the portfolio at every time instant  $t_k$  by buying  $(\Delta_{t_k} - \Delta_{t_{k-1}})$  at the price  $p_{t_k}$  and discount the costs back for  $k$  days. In the end, we have either  $\Delta_{t_N} = 0$  or  $\Delta_{t_N} = 1$ , the later meaning that the option is in the money at expiration. In that case we have to sell the underlying to the option holder for the strike  $K$ .

By the replication argument, the total hedge costs  $H$  should be equal to the option price. In practice, this is not the case for several reasons. First, the

hedging portfolio is not re-balanced continuously. Most importantly though, the model for the underlying and the volatility forecast used to calculate the option price are inaccurate. So the difference between the option price and the hedge costs (the so-called the *hedging error*) is a good measure of both the model performance and the volatility forecast.

### 6.3.3 Options on physical commodity

Theory of option pricing relies heavily on the ability of an investor to hedge a contingent claim with the underlying asset, i.e. to construct a riskless portfolio which replicates the claim's pay-off. If the underlying asset is a commodity, many hedging arguments are not valid anymore. See [41] for a detailed treatment on commodity options. For instance, it might be impossible to take an arbitrary long or short position in the underlying commodity, or a long position might involve significant storage costs. Some commodities (such as electricity) cannot be stored at all, and others (such as agricultural commodities) can lose their value if stored. Moreover, complicated delivery issues can arise. In such cases a contingent claim cannot be hedged with the underlying asset, so we then speak of an *incomplete market*. When it is impossible to construct a riskless portfolio replicating a claim's pay-off, the risk associated with the underlying cannot be hedged away. As a consequence, the so-called *market price of risk* enters all pricing and hedging equations.

To avoid dealing with the market price of risk (which is essentially an unknown model parameter), here we shall assume that the underlying commodity closely resembles a traded asset in the usual sense, i.e. that we can hedge (some) contingent claims with the underlying. More precisely, we make the following assumptions:

- A commodity can be stored without quality loss, for a period up to the option's expiration.
- Storing a commodity leads to storage costs  $u$ , expressed in dollars per unit of commodity, per time unit. We assume that these storage costs are constant during the lifetime of an option.

These assumptions are quite realistic for commodities such as crude oil, metals (and, more recently, for natural gas), while clearly inappropriate for e.g. electricity and some agricultural commodities. We also assume that we cannot take short positions on a physical commodity. This means that we can only hedge two types of claims: short calls and long puts. Here we deal with pricing and hedging of short European call options. For simplicity, we assume everywhere that the risk-free interest rate  $r$  is constant.

The way to calculate the option price is to first find the expression for the dynamics of the underlying  $(p_t)_{t \geq 0}$  under the risk-neutral probability

measure. Using standard financial calculus arguments as in [12] and the above assumptions, we find that the risk-neutral process for the underlying value is given by

$$dp_t = (rp_t + u) dt + \sigma_{BS} p_t dW_t^* \quad (6.9)$$

in the Black-Scholes framework, and by

$$dp_t^{pot} = (rp_t^{pot} + u) dt + \sigma_{pot} dW_t^* \quad (6.10)$$

in the potential model framework. Here  $(W_t^*)_{t \geq 0}$  is the Brownian motion under the risk-neutral probability measure and  $u$  is the storage cost per unit of commodity.

Note that the deterministic drift of the price dynamic under the real probability measure is replaced in both cases by  $(rp_t + u)$  under the risk-neutral measure. Hence, the potential function does not explicitly enter the risk-free dynamic of the underlying. However, when pricing an option,  $\sigma_{pot}$  is calculated using the potential model. So the potential function is implicitly contained in the risk-free dynamics via the corresponding volatility measure. For risk-neutral process evolving according to (6.10) the explicit solution is

$$p_t^{pot} = e^{rt} \left\{ p_0 + u \frac{1 - e^{-rt}}{r} + \sigma_{pot} \int_0^t e^{-rs} dW_s^* \right\}.$$

Hence,  $p_t^{pot}$  is normally distributed with mean  $m_t$  and standard deviation  $s_t$  given by

$$\begin{aligned} m_t &= e^{rt} \left( p_0 + \frac{1 - e^{-rt}}{r} u \right) \\ s_t &= e^{rt} \sigma_{pot} \sqrt{\frac{1 - e^{-2rt}}{2r}}. \end{aligned}$$

Evaluating the expected discounted pay-off under the risk-neutral measure, we get that the European call option price is

$$\begin{aligned} &C^{(pot)}(T, K, p_0, \sigma_{pot}, r, u) \\ &= e^{-rT} \left\{ \frac{s_T}{\sqrt{2\pi}} e^{-\frac{(m_T - K)^2}{2s_T^2}} - (K - m_T) \Phi \left( \frac{m_T - K}{s_T} \right) \right\}, \quad (6.11) \end{aligned}$$

where  $\Phi$  is the cumulative distribution function of the standard normal distribution. Differentiating (6.11) with respect to the underlying value, we get the delta:

$$\Delta_t^{(pot)} = \frac{\partial C^{(pot)}}{\partial p} = \Phi \left( \frac{m_{T-t} - K}{s_{T-t}} \right).$$

In the Black-Scholes framework, the solution of (6.9) is

$$p_t = e^{(r - 0.5\sigma^2)t + \sigma W_t} \left\{ p_0 + u \int_0^t e^{-(r - 0.5\sigma^2)s - \sigma W_s} ds \right\}, \quad (6.12)$$

and it is not clear what the distribution of  $p_t$  is. The expression (6.12) simplifies considerably if instead of  $u$  (storage costs per unit of commodity) we use a "storage cost rate"  $\tilde{u}$  (storage costs per dollar of the spot price). In that case the risk-neutral dynamic (6.9) becomes

$$dp_t = (r + \tilde{u})p_t dt + \sigma_{BS}p_t dW_t^*,$$

which is the Black-Scholes equation for a stock paying dividend at the rate  $-\tilde{u}$ . The European call option price is then the well-known expression

$$C^{(BS)}(T, K, p_0, \sigma_{BS}, r, \tilde{u}) = p_0 e^{\tilde{u}T} \Phi(d_1) - K e^{-rT} \Phi(d_2),$$

where

$$d_1 = \frac{\ln(p_0/K) + (r + \tilde{u} + 0.5\sigma_{BS}^2)T}{\sigma_{BS}\sqrt{T}} \quad \text{and} \quad d_2 = d_1 - \sigma_{BS}\sqrt{T},$$

and the corresponding delta is

$$\begin{aligned} \Delta_t^{(BS)} &= \frac{\partial C^{(BS)}}{\partial p} \\ &= e^{\tilde{u}(T-t)} \Phi \left( \frac{\ln(p_t/K) + (r + \tilde{u} + 0.5\sigma_{BS}^2)(T-t)}{\sigma_{BS}\sqrt{T-t}} \right). \end{aligned} \quad (6.13)$$

Figure 6.7 shows the option's deltas versus the spot price, computed from Black-Scholes and potential models, for a 1-year European call option with the strike price of 20.

Note that, in contrary to stock options,  $\Delta^{(BS)}$  can now become greater than one. This is the consequence of the storage costs proportional to the spot price. In absence of storage costs, rising spot price leads to the rise in the call option price, but proportionately, this rise cannot exceed one. In presence of storage costs rate  $\tilde{u}$ , it becomes more expensive to reproduce the call: in addition to the "regular" delta, the amount that has to be paid to store the commodity also increases. This leads to an extra rise in call option price (expressed by the exponent in (6.13)) and hence can lead to  $\Delta > 1$ .

Defining storage costs as a "rate" is very common; however, it has a major drawback: in the real world commodity storage costs are quoted per unit of commodity and not per dollar of the spot price. Moreover, while it is realistic to assume that  $u$  is constant during the lifetime of an option, it is certainly not true for  $\tilde{u}$  as it changes together with the spot price:  $\tilde{u} = u/p_t$ . Note that another advantage of the potential function framework is that we can use the real storage costs  $u$  directly in the pricing formula instead of the storage cost rate  $\tilde{u}$ .

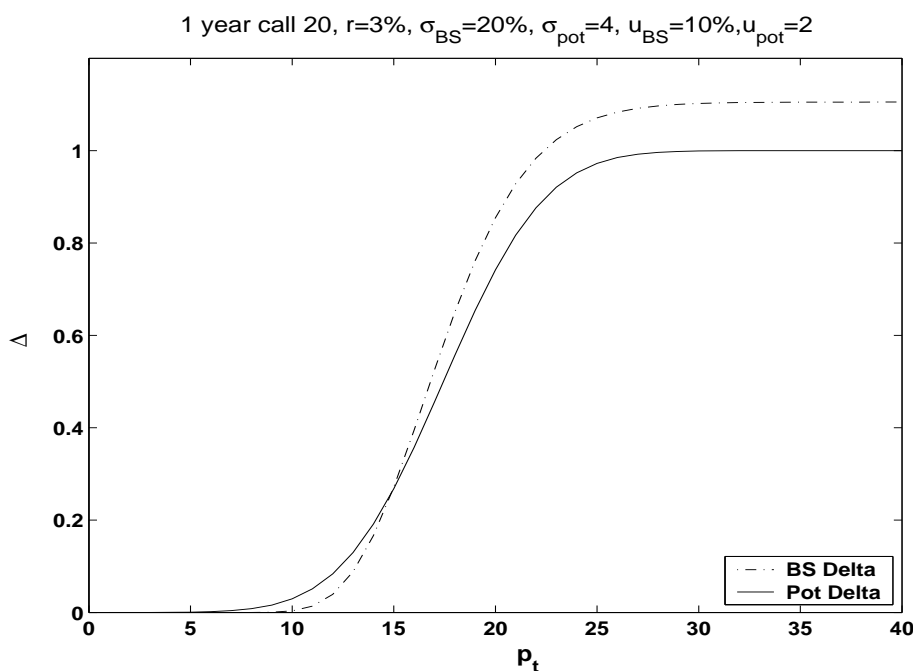


Figure 6.7: Option's delta vs. spot price in BS and potential models.

### 6.3.4 Options on futures

Options on commodity futures are easier to price and hedge than options on physical commodity, since futures are the same type of assets as stocks: they are liquid "paper" contracts traded on exchanges. So all storage and delivery problems encountered for physical commodities are not relevant for futures. This is the main reason why options on commodity futures are more popular than options on a physical commodity.

A common approach to pricing of futures is to assume some dynamic for the spot price (e.g. mean-reverting diffusion process) and derive from it the futures price dynamic by traditional risk-neutral pricing arguments (e.g. by using the fact that futures price is the expected spot price under the risk-neutral probability measure), or by a cost-of-carry relationship. Here we shall not use the spot-futures prices relationship and model futures prices directly. We postulate that the futures contract is itself an underlying traded asset. This approach is particularly suited for commodities, where futures price is not closely related to the spot price, and for markets where is no good proxy for the spot price. This is the case in e.g. electricity markets, where the quoted spot prices are often unreliable (or non-existent), and there may be a large discrepancy between the futures and the spot prices. So when pricing futures options in the framework of the potential model, we shall not pay attention to the spot price but instead assume that, for a

fixed expiry date, the futures price evolves as the diffusion governed by the potential function.

The fundamental difference between futures and stocks is that entering a futures contract does not require an initial investment. A futures contract behaves as a stock paying continuous dividend yield at the rate equal to the risk-free interest rate (for discussion on this general result see e.g. [52]). Since it costs nothing to enter a futures contract, the expected growth rate of a futures price is zero, and Black's model (see [13]) for the risk-free dynamics of a futures contract is given by

$$dp_t = \sigma_B p_t dW_t^*, \quad (6.14)$$

where  $\sigma_B$  denotes the volatility within Black's model. By the same arguments, for the potential model the futures price dynamic under the risk-neutral probability measure is

$$dp_t^{pot} = \sigma_{pot} dW_t^*, \quad (6.15)$$

where  $\sigma_{pot}$  is the potential model volatility. The explicit solution of (6.15) is

$$p_t^{pot} = p_0 + \sigma_{pot} W_t.$$

Again, the difference between (6.14) and (6.15) is in the volatility term. Standard risk-neutral valuation leads then to the following European call option price:

$$\begin{aligned} & C^{(pot)}(T, K, p_0, \sigma_{pot}, r) \\ &= e^{-rT} \left\{ \sqrt{\frac{\sigma_{pot}^2 T}{2\pi}} e^{-\frac{(K-p_0)^2}{2\sigma_{pot}^2 T}} - (K-p_0) \Phi\left(\frac{p_0-K}{\sigma_{pot}\sqrt{T}}\right) \right\}, \end{aligned} \quad (6.16)$$

and the corresponding delta is given by

$$\Delta_t^{(pot)} = e^{-rT} \Phi\left(\frac{p_t - K}{\sigma_{pot}\sqrt{T-t}}\right). \quad (6.17)$$

Compare (6.16) to the Black model's European call option price:

$$C^{(B)}(T, K, p_0, \sigma_B, r) = e^{-rT} [p_0 \Phi(d_1) - K \Phi(d_2)],$$

where

$$d_1 = \frac{\ln(p_0/K) + 0.5\sigma_B^2 T}{\sigma_B \sqrt{T}} \quad \text{and} \quad d_2 = d_1 - \sigma_B \sqrt{T};$$

and (6.17) to the corresponding delta:

$$\Delta_t^{(B)} = e^{-rT} \Phi\left(\frac{\ln(p_t/K) + 0.5\sigma_B^2(T-t)}{\sigma_B \sqrt{T-t}}\right).$$

## 6.4 Applications to oil spot and futures markets

### 6.4.1 Option pricing and hedging

We apply the above approach to options on crude oil for physical delivery (i.e. the spot market oil) and on oil futures. We price and hedge the European call option with  $N = 60$  days to expiry and the at-the-money strike,  $K = p_0$  (in order to reduce skew effects).

In our simulation study, we use historical price series of Dated Brent and IPE Brent futures, front month expiry (both from 1994 to 1999). For every day in the dataset starting with the 61st observation, we calculate the Black-Scholes and the potential model option prices. For the potential model, we use the potential model volatility estimates (6.6), and for Black-Scholes model - the realized volatility, both averaged over the preceding 60 observations. The call options are hedged daily for 60 days (until expiry), using the corresponding deltas. This setup is schematically shown in figure 6.8.

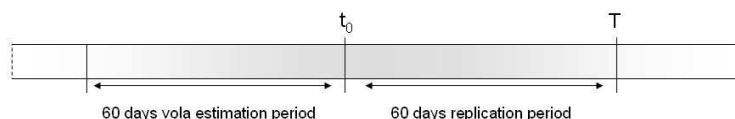


Figure 6.8: The setup of the simulation study.

In the end, we obtain samples of hedge errors (differences between the hedge costs and the corresponding option prices) for options priced on each day in the dataset. The distribution and, in particular, the average hedge error measure the model's performance and the volatility forecast's accuracy.

For spot prices, figure 6.9 shows the 60-days annualized averaged historical volatility of daily returns in the left-hand side graph and the 60-days averaged potential function volatility on the right-hand side graph. These are the volatilities that we used for option pricing.

For simulations, we take storage costs  $u = 2$  \$/bbl per year (this is a realistic number in oil industry), and to compute the Black-Scholes option price on day  $t$ , we take  $\tilde{u}_t = u/p_t$ . Figure 6.10 shows the histograms of the hedge error in both cases.

The histograms of the hedge costs are quite similar and both skewed to the left. In both cases, hedge errors are very small, so the hedge is almost perfect. The average hedge error is smaller for the potential function model: at 0.007 it is below 0.009 for the Black-Scholes model with historical volatility. The variance of the hedge errors is also smaller for the potential model: 0.08 vs. 0.1 for Black-Scholes. For further comparison, we also show the histogram of the differences in hedge costs between the Black-Scholes with historical volatility and potential models (right-hand side graph of figure 6.10).

For options on oil futures, the results are quite similar. The average hedge

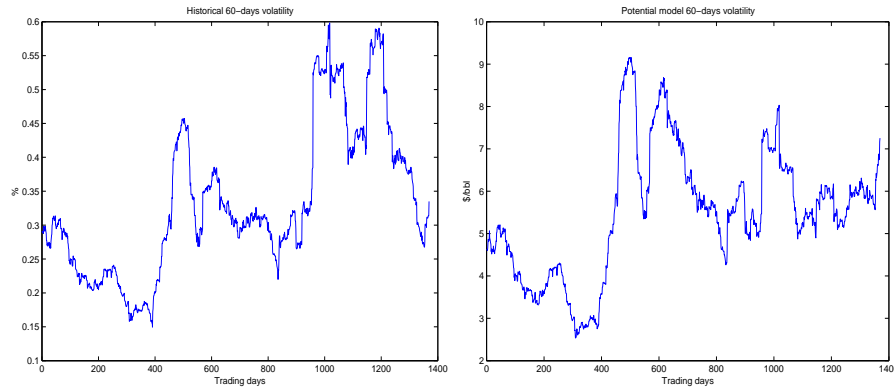


Figure 6.9: 60-days historical (left) and potential (right) volatility.

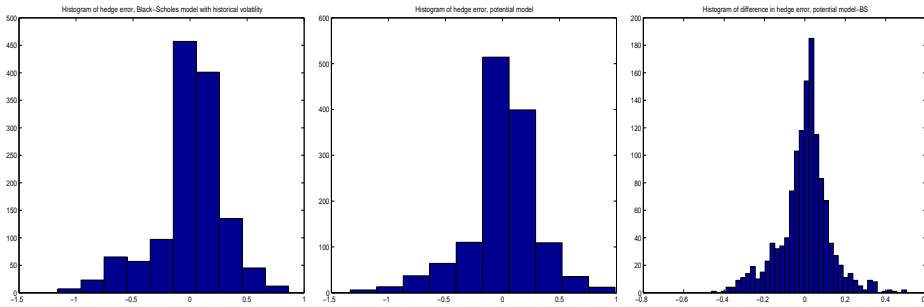


Figure 6.10: Histogram of Black-Scholes (left) and potential function (middle) hedge error and difference in hedge error (right).

errors are at 0.01 for the Black's and 0.009 for the potential models, and the variances of the hedge errors are respectively 0.11 and 0.09. The histograms of the hedge errors are shown in figure 6.11.

The simulation results show that for options on physical oil, in terms of hedge costs, the potential model outperforms the Black-Scholes model with historical volatility. For options on oil futures the results are comparable.

#### 6.4.2 Robustness of option prices in the potential framework

When deriving the option price formula in the potential model framework, we pointed out that the potential function does not directly enter the expression for the option price. However, given (an estimate of) the potential function, one is able to estimate the daily volatility by the equation (6.6). Here we want to consider the robustness of the potential model from the option pricing point of view. For that we only have to study the impact of changes in the potential function specification on the estimated volatility. We assumed that the potential function  $U$  is approximated by a polynomial of some degree  $k$ , so it is interesting to investigate whether different

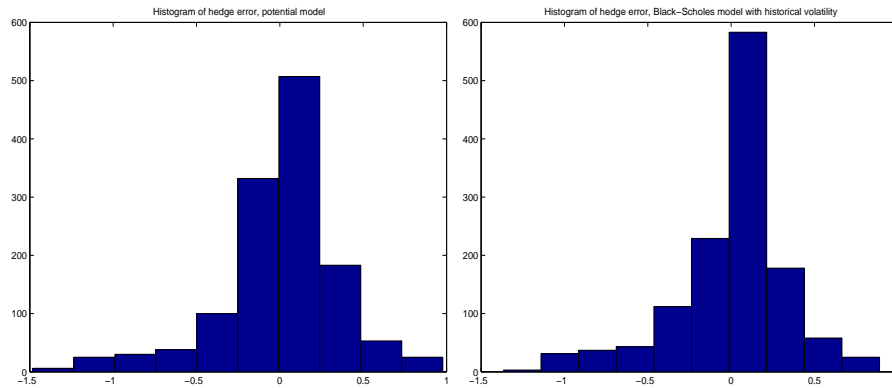


Figure 6.11: Histogram of future hedge error for potential model (left) and Black's model (right).

values for  $k$  significantly affect the volatility estimates. We are interested in whether changes in the polynomial degree affect 60-days volatility estimates shown in the right-hand side graph of figure (6.9). Let  $\hat{\sigma}_i^{(k)}$  be the 60-days volatility estimate on the day  $i$  obtained by the potential model with the potential function being a polynomial of degree  $k$ . In order to compare volatility estimates corresponding to degrees  $k$  and  $j$ , we introduce the average absolute difference measure  $\delta(k, j)$  given by

$$\delta(k, j) = \frac{1}{N} \sum_{i=1}^N |\hat{\sigma}_i^{(k)} - \hat{\sigma}_i^{(j)}|.$$

We computed  $\delta(k, k-1)$  for polynomial degrees  $k = 4, 5, \dots, 12$ , for Brent crude oil spot prices during 1994-1999, and plotted it against  $k$  in figure 6.12. This figure shows that increasing the polynomial degree of the potential function by one changes the volatility estimate by less than 0.2 (i.e. under 10%) on average. Hence the volatility estimate is not very sensitive to the degree of the potential function, as long as this degree is higher than 3, i.e. the polynomial degree allows for more than one attracting region.

Changes in the volatility estimate affect the option prices via the so-called vega, the measure of the option price sensitivity with respect to the volatility. Although vega depends on other parameters such as the time to maturity and the strike price, we argue that the changes in volatility estimates are so small that option prices are almost unaffected. This strongly indicates that the model is very robust with respect to the potential function specification.

## 6.5 Multivariate extension

The potential function approach naturally extends to the case of multivariate time series (price series of related commodities, such as crude oil and

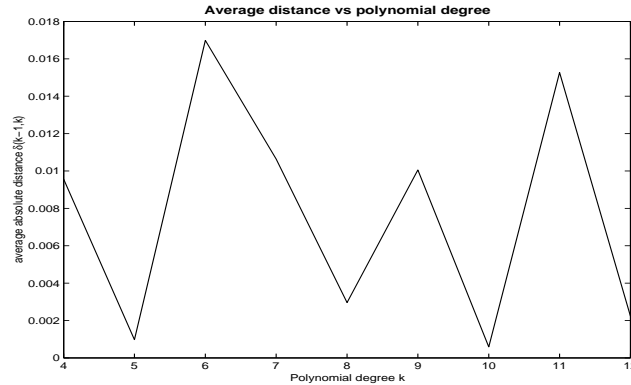


Figure 6.12: Average absolute distance  $\delta(k, k - 1)$  vs. polynomial degree  $k$ .

gasoline). For this we replace the potential function by a potential field in  $\mathbb{R}^k$ . If  $(\mathbf{p}_t)_{t \geq 0}$  is a continuous time process in  $\mathbb{R}^k$ , then the potential field model is

$$d\mathbf{p}_t = -\nabla U(\mathbf{p}_t) dt + B d\mathbf{W}_t, \quad (6.18)$$

where  $U : \mathbb{R}^k \rightarrow \mathbb{R}$  is a potential field,  $\mathbf{W}_t$  is the  $k$ -variate standard Brownian motion, and  $B = (\beta_{ij})_{k \times k}$  - a  $k$ -by- $k$  matrix describing the effect of the multivariate Brownian motion on the process.  $B$  can be interpreted as the (right-triangular) Choleski root of the covariance matrix  $\Sigma$ , so that  $\Sigma = B'B$ .

This model can be estimated from historical data in a way similar to that for the univariate model. We can assume some parametric form of the potential (e.g. a weighted sum of multivariate Gaussian kernels). Then we obtain a discrete-time model from (6.18) using the Euler scheme, and estimate the parameters of the potential field and the matrix  $\Sigma$  directly from observations by the maximum likelihood method. For an application of a bivariate potential field model to oil market data see [16]. However, as with all multivariate methods, some computational difficulties can arise, especially if  $k > 2$ .

The particular usefulness of the multivariate model is that the covariances between the price series, as well as individual volatilities, are in part accounted for by the potential field and in part by the matrix  $B$ . Hence, after the potential field and long-term covariance matrix  $B$  are estimated from the historical data, the model can be used to estimate daily volatilities and covariances, just as in the one-dimensional case. These estimates are useful for applications such as portfolio and risk management, e.g. the computation of Value-at-Risk for commodity portfolios. Also, these estimates can be used when pricing options on inter-commodity spreads, since there the correlations are needed, together with the volatilities.

This extension to multivariate models and their application to real-life data

seem rather straightforward. However, it raises some interesting computational issues which require more attention and will be investigated further.

## 6.6 Conclusions and future work

We have applied the potential function model to commodity prices exhibiting multiple attraction regions and used it to develop a new volatility estimate. We priced and hedged European options on commodity spot and futures contracts within the model's framework. For the application to crude oil, we have demonstrated that the resulting hedge costs are lower than those within the Black-Scholes model with the historical volatility. We have also shown that the model is robust with respect to the potential function specification. It would be interesting to compare option prices and the volatility forecasts obtained by the potential function model with the market option prices and the implied volatilities (which are widely considered the best volatility forecasts in practice). However, for many commodities, options trading (especially in options on physical commodities) is only done over-the-counter, if at all. Options on futures are traded on exchanges such as IPE and NYMEX, hence they are more liquid and transparent than those on physical commodities. However, it is still difficult to obtain historical option prices in commodity markets.

In addition to derivatives pricing, other applications of the model's volatility estimate include risk management (in particular, Value-at-Risk), portfolio management and other areas where volatility estimation and forecasting is required.

The potential function approach extends naturally to multivariate series, allowing for incorporation of correlations between price series within the model. This is useful for applications such as VaR computation and risk management of commodity portfolios.

An underlying assumption of the model is that the potential function and the long-term volatility do not change with time. The non-stationarity of price series can seriously limit the applicability of the approach. We applied the model to oil prices up to 1999. Significant changes affected the oil market after 1999: the oil price reached high levels rarely observed before. In such cases new attraction regions can form, changing the shape of the potential. Also the long-term volatility can change in new market conditions. In practice, the non-stationarity can be dealt with by regularly re-fitting the model, for instance, every six to twelve months. It will be interesting to investigate changes of the potential function for oil prices over a longer observation interval, e.g. from 1970's until today. This is an issue which we will address in the future.

# Bibliography

- [1] J. Abate, G. Choudhury, and W. Whitt, *An introduction to numerical transform inversion and its application to probability models*, W.Grassman (ed.) Computational Probability, Kluwer, Boston (1999), 257–323.
- [2] J. Abate and P. Valkó, *Multi-precision laplace transform inversion*, International Journal for Numerical Methods in Engineering **60** (2004), 979–993.
- [3] J. Abate and W. Whitt, *Numerical inversion of probability generating functions*, Operations Research Letters **12** (1992), 245–251.
- [4] ———, *Numerical inversion of laplace transforms of probability distributions*, ORSA Journal on computing **7** (1995), no. 1, 36–43.
- [5] M. Adelman, *World oil production and prices*, The Quarterly Review of Economics and Finance **42** (2002).
- [6] M. Avellaneda and L. Wu, *Pricing Parisian-style options with a lattice method*, IJTAF **2** (1999), no. 1, 1–16.
- [7] F. Avram, T. Chan, and M. Usabel, *On the valuation of constant barrier options under spectrally negative exponential Lévy models*, Stochastic Processes and Appl. **100** (2002), 75–107.
- [8] L. Bachelier, *Théorie de la speculation*, Ann. Ecole Norm. Sup. **17** (1900), 21–87.
- [9] N. Bellamy and M. Jeanblanc, *Incompleteness of markets driven by a mixed diffusion*, Finance and Stochastics **4** (2000), 209–222.
- [10] C. Bernard, O. Le Courtois, and F. Quittard-Pinon, *A new procedure for pricing Parisian options*, Journal of Derivatives **12** (2005), no. 4, 45–53.
- [11] J. Bertoin, *Lévy processes*, Cambridge University Press, 1996.

- [12] T. Björk, *Arbitrage theory in continuous time*, Oxford University Press, Oxford, 1998.
- [13] F. Black, *The pricing of commodity contracts*, Journal of Financial Economy **3** (1976), 167–179.
- [14] F. Black and M. Scholes, *The pricing of options and corporate liabilities*, Journal of Political Economy **81** (1973), 637–659.
- [15] T. Bollerslev, *Generalized autoregressive conditional heteroskedasticity*, Journal of Econometrics **31** (1986), 307–327.
- [16] S. Borovkova, H. Dehling, J. Renkema, and H. Tulleken, *A potential function approach to commodity prices modeling*, Computational Economics **22** (2003), no. 2/3, 139–161.
- [17] S. Borovkova, F. Permana, and J. van der Weide, *Empirical analysis of analytic approximation approaches for pricing and hedging of spread options*, Proceedings of the 4th Actuarial and Financial mathematics day in Brussels (2006), 45–54.
- [18] S.I. Boyarchenko and S.Z. Levendorskii, *Barrier options and touch-and-out options under regular Lévy processes of exponential type*, The Annals of Applied Prob. **12** (2002), 1261–1298.
- [19] M.J. Brennan and E.S. Schwartz, *Evaluating natural resource investment*, Journal of Business **58** (1985), 135–157.
- [20] W.A. Brock and C.H. Hommes, *Models of complexity in economics and finance*, in: Hey, c., schumacher, j.m., hanson, b., praagman, c. (eds.), System Dynamics in Economic and Financial Models, Wiley Publ. (1997).
- [21] ———, *Heterogeneous beliefs and routes to chaos in a simple asset pricing model*, Journal of Economic Dynamics and Control **22** (1998), 1235–1274.
- [22] A. Brook, R. Price, D. Sutherland, N. Westerlund, and C. Andre, *Oil price developments: drivers, economic consequences and policy responses*, OECD Economics Department Working Papers Organization for Economic Cooperation and Development, Paris (2004).
- [23] P. Carr, *Formulating a revolution*, Bloomberg markets **6** (2006), 142–144.
- [24] P. Carr and D. Madan, *Option valuation using the fast Fourier transform*, Journal of Computational Finance **2** (1999), 61–79.

- [25] P.C. Cashin, J. J. McDermott, and A. Scott, *Booms and slumps in world commodity prices*, IMF Working Paper (1999), no. 99/155.
- [26] U. Cetin, R. Jarrow, P. Protter, and Y. Yildirim, *Modeling credit risk with partial information*, Ann. Appl. Prob. **14** (2004), 1167–1178.
- [27] A. Chen and M. Suchaneki, *Default risk, bankruptcy procedures and the market value of life insurance liabilities*, Insurance:Mathematics and Economics **40** (2007), no. 2, 231–255.
- [28] M. Chesney and L. Gauthier, *American Parisian options*, Finance and Stochastics **10** (2006), 475–506.
- [29] M. Chesney, H. Geman, M. Jeanblanc-Picqué, and M. Yor, *Some combinations of Asian, Parisian and barrier options*, Mathematics of Derivative securities (1997), 61–87.
- [30] M. Chesney, M. Jeanblanc-Picqué, and M. Yor, *Brownian excursions and Parisian barrier options*, Adv. Appl. Prob. **29** (1997), 165–184.
- [31] K.L. Chung, *Excursions in Brownian motion*, Adv. Appl. Prob. **14** (1976), 155–177.
- [32] R. Cont and P. Tankov, *Financial modelling with jump processes*, Chapman & Hall, 2004.
- [33] M. Costabile, *A combinatorial approach for pricing Parisian options*, Decisions in Economics and Finance **25** (2002), 111–125.
- [34] B. Dao and M. Jeanblanc, *Double exponential jump diffusion process: A structural model of endogenous default barrier with roll-over debt structure*, www.defaultrisk.com (2006).
- [35] A Dassios, *The distribution of the quantiles of a Brownian motion with drift*, Ann. Appl. Prob. **5** (1995), 389–398.
- [36] A. Deitmar, *A first course in harmonic analysis*, 2. ed., Springer Verlag, New York, 2005.
- [37] F. Delbaen and W. Schachermayer, *Non-arbitrage and the fundamental theorem of asset pricing : summary of main results*, Proceedings in applied mathematics (1997).
- [38] A.K. Dixit and R.S. Pindyck, *Investment under uncertainty*, Princeton University Press, New Jersey, 1994.
- [39] R. Durrett and D. Iglehart, *Functionals of Brownian meander and Brownian excursions*, Ann. Probability **5** (1977), 130–135.

- [40] E. Eberlein and J. Jacod, *On the range of option prices*, Finance and Stochastics **1** (1997), 131–140.
- [41] A. Eydeland and K. Wolyniec, *Energy and power risk management*, Wiley Finance, New Jersey, 2003.
- [42] H. Föllmer and A. Schied, *Stochastic finance*, de Gruyter, Berlin New York, 2002.
- [43] L. Gauthier, *Excursions height- and length-related stopping times and application to finance*, Adv. Appl. Prob. **34** (2002), 846–868.
- [44] H. Geman and M. Yor, *Pricing and hedging double-barrier options : a probabilistic approach.*, Mathematical Finance **6** (1996), no. 4, 365–378.
- [45] S. Geman and C.R. Hwang, *Diffusions for global optimization*, SIAM Journal on Control and Optimization **24** (1986), 1031–1043.
- [46] P. Glasserman, *Monte carlo methods in financial engineering*, Springer Verlag, New York, 2004.
- [47] A. Grau, *Moving windows - master thesis at school of computer science*, University of Waterloo, Canada, 2003.
- [48] A.J. Grau, P.A. Forsyth, and K.R. Vetzal, *Convertible bonds with call notice periods*, Proceedings of Financial Engineering and Applications, Banff Canada (2003).
- [49] R. Haber, P.J. Schönbucher, and P. Wilmott, *Pricing Parisian options*, Journal of Derivatives **16** (1999), 71–79.
- [50] J.D. Hamilton, *Analysis of time series subject to changes in regime*, Journal of Econometrics **45** (1990), no. 1/2, 39–70.
- [51] C.H. Hommes, *Financial markets as nonlinear adaptive evolutionary systems*, Quantitative Finance **1** (2001), 149–167.
- [52] J. Hull, *Option, futures and other derivatives*, 4. ed., Wiley, New York, 2000.
- [53] P. Den Iseger, *Numerical transform inversion*, PEIS **20** (2006), 1–44.
- [54] V.F. Kadankov and T. Kadankova, *On the distribution of the first exit time from an interval and the value of overshoot through the boundaries for processes with independent increments and random walks*, Ukr. Math. J. **10** (2005), no. 57, 1359–1384.
- [55] I. Karatzas and S. Shreve, *Brownian motion and stochastic calculus*, 2. ed., Springer Verlag, Berlin, 1991.

- [56] N. El Karoui and M. Jeanblanc, *Options exotiques*, Finance **20** (1999), no. 2, 49–67.
- [57] P. Kennedy and J. Hunt, *Financial derivatives in theory and practice*, Wiley, 2001.
- [58] A.W. Kolkiewicz, *Pricing and hedging more general double-barrier options*, Journal of Computational Finance **5** (2002), no. 3, 1–26.
- [59] S. Kou, *A jump-diffusion model for option pricing*, Management Science **48** (2002), 1086–1101.
- [60] C. Labart and J. Lelong, *Pricing double barrier Parisian options using Laplace transforms*, CERMICS technical report on <http://cermics.enpc.fr/reports/CERMICS-2006/CERMICS-2006-328.pdf> (2006).
- [61] K.W. Lau and Y.K. Kwok, *Optimal calling policies in convertible bonds*, Proceedings of International Conference on Computational Intelligence for Financial Engineering (March 2003), 109–114.
- [62] A. Lipton, *Assets with jumps*, RISK magazine **September** (2002), 149–153.
- [63] D. Madan, P. Carr, and E. Chang, *The variance gamma process and option pricing*, European Finance Review **2** (1998), 79–105.
- [64] B.J. Matkovsky and Z. Schuss, *Eigenvalues of the Fokker-Planck operator and the approach to equilibrium for diffusions in potential fields*, SIAM Journal on Applied Mathematics **40** (1981), 242–254.
- [65] F. Moraux, *On cumulative Parisian options*, Finance **23** (2002), 127–132.
- [66] F. Moraux, *Valuing corporate liabilities when the default threshold is not an absorbing barrier*, Working paper Université de Rennes (2007).
- [67] L. Nguyen-Ngoc and M. Yor, *Wiener-Hopf factorization and the pricing of barrier and lookback options under general Lévy processes*, Handbook of Financial Econometrics (Y. Ait-Sahalia and L-P. Hansen, eds.), 2004.
- [68] OECD, *Economic outlook no. 76*, Organization for Economic Cooperation and Development, Paris (2005).
- [69] B. Oksendal, *Stochastic differential equations, an introduction with applications*, 5. ed., Springer Verlag, Berlin, Heidelberg, 1998.
- [70] A. Ralstom P. Rabonowitz, *A first course in numerical analysis*, 2. ed., McGraw-Hill, New York, 1978.

- [71] E.A. Pecherskii and B.A. Rogozin, *On joint distributions of random variables associated with fluctuations of a process with independent increments*, Theor. Prob. and its Appl. **14** (1969), 410–423.
- [72] A. Pechtl, *Some applications of occupation times of Brownian motion with drift in mathematical finance*, J. of Appl. Math. & Dec. Sci. **3** (1999), no. 1, 63–73.
- [73] A. Pelsser, *Pricing double barrier options using laplace transforms*, Finance and Stochastics **4** (2000), no. 1, 95–104.
- [74] R. Pindyk, *The dynamics of commodity spot and futures markets: a primer*, The Energy Journal **22** (2001), no. 3.
- [75] P. Protter, *Stochastic integration and differential equations*, 2. ed., Springer, New York, 2005.
- [76] W. Rudin, *Real and complex analysis*, 3. ed., McGraw-Hill, New York, 1987.
- [77] C. Scheffer, *The rank of the present excursion*, Stochastic processes and their applications **55** (1995), 101–118.
- [78] M. Schröder, *Brownian excursions and Parisian barrier options: a note*, Journal of Applied Prob. **40** (2003), 855–864.
- [79] E.S. Schwartz, *The stochastic behavior of commodity prices: Implications for valuation and hedging*, Journal of Finance **53** (1997), no. 3, 923–973.
- [80] M. Schweizer, *A guided tour through quadratic hedging approaches*, Jouini, Cvitanic and Musiela (eds.), “Option prices, interest rates and risk management” (2001), 538–574.
- [81] A. Sepp, *Analytical pricing of double-barrier options under a double-exponential jump diffusion process: Applications of Laplace transform*, IJTAF **7** (2004), 151–176.
- [82] M. Suchanecki, *On an alternative approach to pricing general barrier options*, University of Bonn, discussion paper **27** (2004).
- [83] K. Yosida, *Functional analysis*, 3. ed., Springer Verlag, New York, 1971.

# Samenvatting

## Methodes uit de kansrekening voor het prijzen van exotische opties

J.H.M. Anderluh

Moderne investeerders beleggen niet alleen in obligaties, aandelen of grondstoffen, maar zoeken ook naar mogelijkheden op de derivatenmarkten. Op deze derivatenmarkten worden contracten verhandeld waarvan de uitbetaling gespecificeerd is in termen van één of meer onderliggende waarden. De meest bekende derivaten zijn de opties. Dit zijn contracten waar de onderliggende waarde uit een aandeel of een index bestaat. De meest bekende opties zijn de puts en calls zoals die bijvoorbeeld verhandeld worden op LIFFE, hier worden o.a. de opties op de AEX index verhandeld. De tegenwoordige populariteit van opties is mede het gevolg van de ideeën van Black en Scholes. Zij hebben een methode bedacht volgens welke het mogelijk is de prijs van een optie nauwkeurig te bepalen. De prijs wordt bepaald door het construeren en onderhouden van een risicoloze portefeuille bestaande uit een steeds veranderende hoeveelheid onderliggende aandelen en één optie. Risicoloos betekent hier dat een infinitesimale (heel kleine) verandering van de waarde van het gedeelte belegd in aandelen te niet wordt gedaan door een gelijke verandering van de waarde van de optie. Aangezien de portefeuille alleen risicoloos is voor kleine veranderingen van de waarde van het aandeel, moet de portefeuille voortdurend, namelijk na iedere verandering van de waarde van het aandeel, worden bijgesteld. Het bijstellen van deze portefeuille betekent handelen in het onderliggende aandeel. Black en Scholes hebben in hun paper van 1973 laten zien, dat onafhankelijk van de manier waarop de koers van het aandeel zich binnen het door hen gekozen kansmodel ontwikkelt, de kosten voor het onderhouden van de portefeuille hetzelfde zijn. Deze kosten leggen de optieprijs vast als gevolg van de no-arbitrage veronderstelling die inhoudt dat het niet mogelijk is een groter rendement op een investering te behalen dan de rente zonder daarbij een risico te lopen. Revolutionair aan het idee van Black en Scholes is het achterliggende concept van de replicerende portefeuille. Voor ieder type optie met een eindige

looptijd en een zogenoemde meetbare uitbetaling kan de replicerende portefeuille bepaald worden en daarmee ligt de prijs van die optie vast. Een optie heeft een meetbare uitbetaling als het mogelijk is aan het eind de waarde van de optie te berekenen aan de hand van de koersontwikkeling van het onderliggende aandeel gedurende de looptijd van de optie. Exotische opties hebben een meetbare uitbetaling en kunnen dus op de Black-Scholes manier geprijsd worden. Het berekenen van deze replicerende portefeuille en de bijbehorende optieprijs kan aan de hand twee methoden. Vanuit de numerieke wiskunde is het gebruikelijk om een partiële differentiaalvergelijking op de stellen en die met numerieke technieken op te lossen. Vanuit de kansrekening wordt de verwachte waarde van de uitbetaling berekend onder de zogeheten martingaalmaat, waarbij de martingaalmaat een theoretisch concept is dat het berekenen van optiepreisen in een arbitrage-vrije omgeving vereenvoudigt. Het is de stelling van Feynman-Kac die de martingaalmaat benadering en de partiële differentiaalvergelijkingen benadering met elkaar verbindt. In dit proefschrift worden exotische opties geprijsd aan de hand van methodes in de kansrekening, hetgeen betekent dat de opties geprijsd worden door de verwachting onder de martingaalmaat te berekenen. Deze berekening leidt niet in alle gevallen tot expliciete formules en in dit proefschrift wordt gebruik gemaakt van Laplace en Fourier getransformeerden of een Monte Carlo methode om tot een daadwerkelijke prijs te komen. Zowel de getransformeerden als de Monte Carlo methode zijn gebruikelijke gereedschappen binnen de kansrekening.

De Parijse optie is een voorbeeld van een exotische optie. Deze optie heeft een vaste looptijd en betaalt alleen maar uit als de koers van het onderliggende aandeel gedurende die looptijd wel of juist niet aan de bij de optie behorende Parijse voorwaarde heeft voldaan. Aan de Parijse voorwaarde is voldaan op het moment dat het aandeel achtereenvolgens langer dan een vooraf bepaalde periode boven of onder een bepaald niveau heeft genoteerd. Neem als voorbeeld de Parijse up-and-in call met een niveau van 120, een periode van 10 dagen en een looptijd van een jaar. De optie betaalt over een jaar uit als een call indien het onderliggende aandeel 10 dagen achtereenvolgens boven de 120 genoteerd heeft ergens gedurende dat jaar. Andere varianten zijn down-and-in, down-and-out en up-and-out Parijse opties, waarbij ook nog gevarieerd kan worden met put en call. Parijse opties worden niet verhandeld op een optiebeurs, maar kennen toepassingen in het prijzen van converteerbare obligaties, het waarderen van de kredietwaardigheid van levensverzekeringsmaatschappijen en het bepalen van investeringsmogelijkheden volgens de zogenoemde real options methode. In het eerste, inleidende hoofdstuk van dit proefschrift worden de werking en de toepassingen van de Parijse optie in detail behandeld.

In dit proefschrift worden de Parijse opties op drie manieren gewaardeerd. Bij deze waarderingsmethoden wordt telkens de geometrische Brownse beweging als kansmodel voor het onderliggende aandeel gebruikt. De eerste

manier is om uit te gaan van de standaard barrier optie. Deze optie is een eenvoudige versie van de Parijse optie, want hier hoeft het onderliggende aandeel het niveau alleen maar te raken en niet een bepaalde periode eronder of erboven te noteren. In tegenstelling tot de Parijse optie zijn er voor de standaard barrier optie expliciete formules beschikbaar. Aangezien het raken van een niveau met een grotere kans voorkomt dan de combinatie van het raken en er een tijdje boven verblijven, zal bijvoorbeeld de Parijse up-and-in call minder waard zijn dan de standaard up-and-in call optie. Immers, het niveau kan eenmalig geraakt worden (de barrier optie gaat uitbetalen als een call), zonder dat het aandeel een langere tijd boven dat niveau noteert (de Parijse optie loopt waardeloos af). De eerste waarderingsmethode bepaalt de zogenoemde implied barrier. De implied barrier is het (hogere) niveau dat ingevuld moet worden in de expliciete formule van de standaard barrier optie zodat deze optie dezelfde waarde heeft als de Parijse optie. Hoofdstuk twee van dit proefschrift behandelt de hier beschreven implied barrier methode.

Een andere mogelijkheid om Parijse opties te waarderen bestaat uit het bepalen van expliciete formules voor de Laplace of Fourier getransformeerde van de waarde van Parijse optie. Om tot een daadwerkelijke prijs te komen, moet deze getransformeerde numeriek worden geïnverteerd. Details van de numerieke inversie worden in het inleidende hoofdstuk gegeven. De expliciete formules voor de getransformeerden worden berekend met behulp van excursie theorie, waarover veel literatuur bestaat op het gebied van de standaard Brownse beweging, de bouwsteen van de geometrische Brownse beweging, het proces waarmee het onderliggende aandeel gemodelleerd wordt. De kern van hoofdstuk drie vormt de uitbreiding van de getransformeerde van enkelzijdige Parijse opties naar dubbelzijdige Parijse opties. De dubbelzijdige Parijse opties betalen uit als een put of een call indien het aandeel ofwel een bepaalde tijd boven een niveau hoger dan de startwaarde, of een (andere) bepaalde tijd onder een niveau lager dan de startwaarde genoteerd heeft. In hoofdstuk drie worden bekende resultaten op het gebied van enkelzijdige Parijse opties gebruikt om expliciete formules voor getransformeerden van dubbelzijdige Parijse opties af te leiden. Numerieke voorbeelden geven inzicht in het gedrag van de (dubbelzijdige) Parijse optie. De Monte Carlo methode is de laatste methode die gebruikt wordt om Parijse opties te waarderen. Het puntsgewijs in de tijd simuleren van het onderliggende aandelen proces levert een uiterst langzame convergentie op, dit betekent dat bijzonder veel simulaties gedaan moeten worden voordat de prijs van de Parijse optie voldoende nauwkeurig bepaald is. Dit is het gevolg van het lokale, wilde gedrag van de standaard Brownse beweging. In hoofdstuk vier wordt een methode ontwikkeld waarbij raaktijden van een niveau direct gesimuleerd worden. Het simuleren van deze raaktijden wordt vervolgens gebruikt om te bepalen of een gesimuleerde koersontwikkeling van het onderliggende aandeel aan de voorwaarde van de uitbetaling van

een Parijse optie voldoet.

Voor het waarderen van Parijse opties is telkens de geometrische Brownse beweging als model voor de onderliggende waarde gebruikt. Dit is het model dat Black en Scholes ook hebben gebruikt bij de afleiding van hun optieprijs formules. In de praktijk is de zogenoemde volatility smile en de volatility term structure aanwezig in de optie markten. Beide verschijnselen zijn niet consistent met de keuze van de geometrische Brownse beweging. Als gevolg hiervan worden Lévy processen gebruikt om modellen voor het onderliggende aandeel te bouwen. De Brownse beweging behoort ook tot de Lévy processen, maar deze klasse is groter. Zo zijn er ook processen met sprongen die tot de Lévy processen behoren, terwijl de Brownse beweging een continu proces is. Als een eerste, kleine stap in de richting van het gebruik van Lévy processen bij het berekenen van een Parijse optieprijs wordt in hoofdstuk vijf een eenvoudig model met sprongen gebruikt om dubbelzijdige barrier opties te prijzen. De prijzen worden berekend via de methode van de Laplace getransformeerde. Om expliciete formules voor deze getransformeerde af te leiden, worden resultaten op het gebied van twee-zijdige exit problemen uit de theorie van Lévy processen gebruikt. De numerieke voorbeelden in het hoofdstuk laten zien hoe het model aan de volatility smile gecaliëbreerd kan worden en hoe die volatility smile er uitziet als de prijzen van de dubbelzijdige barrier opties, geprijsd aan de hand van het sprongmodel, als uitgangspunt worden genomen.

Tot slot behandelt dit proefschrift het prijzen van opties op grondstoffen en dan met name opties op olie. Olie wordt als grondstof verhandeld op de spot markt. Termijncontracten oftewel futures worden verhandeld op de termijn markt. Zowel de spot als de future kunnen als onderliggende waarde voor de optie fungeren. Hoofdstuk zes behandelt eerst het potentiaal model voor grondstofprijzen. Veranderingen van de grondstofprijzen zijn binnen dit model gedeeltelijk stochastisch en gedeeltelijk door een potentiaal functie bepaald. De potentiaal functie kan zo gekozen worden dat het prijsproces van de grondstof zich bij voorkeur binnen bepaalde intervallen bevindt, de zogeheten attractiepunten. Dit potentiaal model wordt gebruikt om optieprijs formules af te leiden, waarbij uitgebreid ingegaan wordt op de toepasbaarheid van de optieprijsprincipes uit de aandelenwereld op de grondstoffenwereld. Hierbij wordt een verschil gemaakt tussen opties op de spot of opties op de future en worden opslagkosten in de discussie betrokken.

# Summary

## Probabilistic methods in exotic option pricing

J.H.M. Anderluh

State-of-the-art investors do not only invest in bonds, stocks or commodities, they are also looking for opportunities in the derivative markets. The pay-off of the contracts traded on the derivative markets is specified in terms of one or more underlying values. Options are the most widely known derivatives. Options are contracts of which the underlying value consists of a stock or an index. The call and the put option are very well-known option types, which are for example traded on LIFFE, the derivative exchange where the AEX option series are traded. The popularity of options nowadays is mainly the consequence of the ideas of Black and Scholes. They invented a method that makes it possible to determine the price of an option accurately. The price is determined by constructing and maintaining a risk less portfolio containing a continuously changing amount of stocks and one option. In this case risk less means that an infinitesimal (very small) change in the value of the part of the portfolio invested in stock is neutralized by the change in value of the option. Since the portfolio is only risk less for very small changes in value of the underlying stock it needs to be continuously rebalanced. Rebalancing the portfolio is done by trading the stock. Black and Scholes showed in their 1973 paper that the costs of continuously rebalancing the portfolio are the same, independent of the way the stock price evolves within the probability model they choose. These rebalancing costs determine the option price uniquely as a result of the no-arbitrage assumption, which states that it is impossible to obtain an excess return over the interest rate without taking risk. This replicating portfolio is what made the ideas of Black and Scholes revolutionary. It is possible to determine this replicating portfolio and therefore the price for every option with a finite time to maturity and a measurable pay-off. An option's pay-off is measurable if it is possible to compute the value of the option at maturity by looking at the evolution of the underlying stock price process during the lifetime of the option. Exotic options do have a measurable pay-off and therefore they can be priced in the Black-Scholes setting. There are two ways of computing the replicating

portfolio and the option price. In the field of numerical mathematics people derive a partial differential equation and solve it with numerical techniques. Probabilists compute the expected value of the option's pay-off under the so-called martingale measure, which is a theoretical concept that simplifies the computation of option prices in an arbitrage-free environment. The theorem of Feynman-Kac connects the martingale measure approach and the partial differential equation approach. In this dissertation exotic option prices will be computed by using probabilistic methods, which means that the martingale measure approach will be followed. It is not always possible to arrive at explicit formulas and in this thesis Laplace and Fourier transforms or Monte Carlo methods will be used to obtain actual prices. Transforms and Monte Carlo methods are very common tools of the probabilist.

The Parisian option is an example of an exotic option. The Parisian option has a fixed time to maturity and it is paying off in case the for the option specific Parisian constraint is satisfied. In order to satisfy the Parisian constraint, the underlying stock price process has to trade for a consecutive period of time above or below some specified level. Consider for example the Parisian up-and-in call with level 120, consecutive period of 10 days and a time to expiry of 1 year. This option pays off like a call in one year if the stock has traded 10 consecutive days above 120 within that year. Other Parisian option types are the down-and-in, down-and-out and up-and-out Parisian options of which exist call and put versions. Parisian options as such are at present not exchange traded, but they can be applied to convertible bond pricing, the valuation of liabilities of life insurance companies and the real option way of solving investment problems. The first preliminary chapter of this thesis treats the pay-off structure and the applications of Parisian options in detail.

This thesis presents three ways of valuing Parisian options. All of these valuation methods take the geometric Brownian motion as model for the underlying stock price process. The first method starts from the standard barrier option. This option is a simple version of the Parisian option, as it pays off as soon as the stock price process hits some level, without the extra condition to stay above or below that level for some time. In contrast with the Parisian options, there exist explicit formulas for the standard barrier options. Whereas hitting a level happens with a higher probability than hitting a level and staying above it for some time, it follows that for example the Parisian up-and-in call will have a lower price than the standard up-and-in barrier option. It is after all possible that the stock price process hits the level once (the standard barrier will pay off as a call), without staying above that level for some time (the Parisian option expires worthless). The first valuation method determines the implied barrier. The implied barrier is the (higher) level that goes into the standard barrier option price formula such that the standard barrier option has the same value as the Parisian option. Chapter two of this dissertation treats the implied barrier method.

Another approach to Parisian option pricing consists of deriving explicit formulas for the Laplace or Fourier transform of the Parisian option value. To arrive at an actual price one needs to invert this transform numerically. Details of the numerical inversion are given in the preliminary chapter. The explicit formulas for the transforms are computed with help of excursion theory on which a big amount of literature is available for the standard Brownian motion, the building block of geometric Brownian motion which is used to model the underlying stock price process. The essence of chapter three consists of the extension of the transform of the (one-sided) Parisian option to the transform of the double-sided Parisian option. The double-sided Parisian option pays off like a put or call in case the stock trades for a given time above some level above the initial stock price or for some (other) given time below some level lower than the initial stock price. In chapter three well known results on one-sided Parisian options are used to derive explicit formulas for the transforms of double-sided Parisian options. Numerical examples show the way (double-sided) Parisian options behave. Monte Carlo simulation is the last method that is used in this thesis to value the Parisian option. Simply simulating the underlying stock price process on a discrete time grid results in a very slow convergence, which means that one needs to simulate many times before the Parisian option price is determined with sufficient accuracy. The slow convergence is a result of the local, wild behavior of standard Brownian motion. Chapter four presents a method based on direct simulation of hitting times. Simulating of hitting times is used to determine whether a simulated stock price evolution satisfies the Parisian constraint of the option.

So far the geometric Brownian motion has been used to model the underlying stock price process, like Black and Scholes did in deriving their option price formulas. In practice the option markets exhibit the so-called volatility smile or volatility term structure. Both phenomena are not consistent with a stock price process modeled by the geometric Brownian motion. In order to solve this problem, people use Lévy processes to build models for the underlying stock price. The Brownian motion actually is a Lévy process, but the class of Lévy processes is bigger. There exist for example processes with jumps that are Lévy processes, whereas the Brownian motion is a continuous process. A first, small step in using Lévy processes for Parisian option pricing is the use of a very basic jump model to price double-sided barrier options in chapter five. The method of Laplace transform inversion is used to obtain prices. In order to derive explicit formulas for this transform, results on two-sided exit problems for Lévy processes are used. Numerical examples show that the model can be calibrated to the market and what the volatility smile looks like if it is computed from the double-sided barrier prices generated by the jump model.

The last chapter of this thesis treats the valuation of options on commodities, especially on oil. Oil as a commodity is traded on the spot market and

futures are traded on the futures market. Both spot and future can serve as an underlying for a commodity option. Chapter six introduces the potential model for the commodity price process. Changes in the commodity price are partially determined by randomness and partially by a potential function. It is possible to choose the potential function in such a way that the commodity price process prefers to stay within certain intervals, which are located around the so-called attraction points. The potential model is used to derive option pricing formulas and the chapter contains a detailed treatment on the applicability of option pricing principles used in the equity world to the commodity world. Options on the spot and on the future are treated separately and storage costs are part of the discussion.

# Curriculum vitae

Jasper Anderluh was born in Heerlen on March 7th, 1978. From 1990 till 1996 he attended high school at Katholiek Gymnasium Rolduc, Kerkrade. In 1996 he went on to Delft to study electrical engineering at Delft University of Technology. In the meantime he passed in 2001 his propaedeuse business administration at Erasmus University in Rotterdam, where he also worked as a teaching assistant. Jasper Anderluh followed the first course on financial mathematics given in 1999 at Delft University. From that time on he was interested in the field of financial mathematics and he used in 2000 his Siemens World Scholarship to study financial mathematics, measure theory and insurance mathematics at TU Berlin and the Humboldt University. The scholarship was completed by a study of a probabilistic model of prototype testing of high voltage switches at Siemens Schaltwerk in Berlin. In 2001 he obtained his M.Sc. degree "cum laude" in electrical engineering, whereas his master thesis was on financial mathematics, mainly supervised by dr. J.A.M. van der Weide and motivated by an internship at AOT (Amsterdam Option Traders).

As of February 2002 he continued his research in the field of financial mathematics as a part time Ph.D. student at the Delft University of Technology under the supervision of dr. J.A.M. van der Weide and Prof.dr. F.M. Dekking. He combined his research with a job as a quantitative analyst at AOT. In 2003 AOT merged with BinckBank and Anderluh became the head of the quantitative research department. As such he developed completely automated trading strategies and was also a member of the risk committee and involved in the treasury activity of BinckBank. In 2007 he quited his job at BinckBank and founded, together with former colleagues, the fund management company HiQ Invest of which he is now general director. As a Ph.D. student Jasper Anderluh used his experience from practice in his research that has resulted in this thesis. He presented his work at the conference of computational science in Krakow, the Deloitte risk-management conferences 2004 and 2005 in Antwerp, the SIAM conference on financial mathematics in Boston and the financial winterschool in Lunteren.

# Propositions

belonging to the dissertation

## Probabilistic methods in exotic option pricing

by Jasper Anderluh

1. The computation of a Parisian option price is a nice example of the application of theoretical results in probability to the field of derivative pricing. (Chapters 2,3 and 4 of this dissertation).
2. The following result is a corollary of the computation of the Laplace transform of the double-sided Parisian stopping time.  
The probability that a standard Brownian motion  $W$  makes an excursion longer than  $D_2$  above zero before it makes an excursion longer than  $D_1$  below zero is given by

$$\frac{\sqrt{D_1}}{\sqrt{D_1} + \sqrt{D_2}}.$$

(Chapter 3 of this dissertation).

3. In general a renewal-reward process is not a Lévy process.
4. The following theorem is true for general renewal reward processes and is very similar to equation (5.18) of this thesis, which was deduced from a general result on Lévy processes.

Let  $\{X(t), t \geq 0\}$  be a renewal-reward process, and let  $\{(T_j, Y_j), j \geq 0\}$  the i.i.d. sequence of pairs of inter renewal times and rewards, where  $H$  denotes the distribution function of the pair  $(T_0, Y_0)$  and  $F$  the distribution function of the time  $T_0$ . Then, for  $u, s > 0$  and  $\tau_h$  the first passage time of level  $h$  the following equation holds

$$\int_0^\infty e^{-sh} \mathbb{E}(e^{-u\tau_h}) dh = \frac{\mathcal{L}_F(u) - \mathcal{L}_H(u, s)}{s(1 - \mathcal{L}_H(u, s))},$$

where  $\mathcal{L}_F$  and  $\mathcal{L}_H$  denote the Laplace-Stieltjes transforms of  $F$  and  $H$ , i.e

$$\mathcal{L}_F(u) = \mathbb{E}(e^{-uT}) \quad \text{and} \quad \mathcal{L}_H(u, s) = \mathbb{E}(e^{-uT - sY}),$$

for all  $u, s \geq 0$ . (J.A.M. van der Weide, J.H.M. Anderluh and M. Pandey, *Models for wear*, submitted paper.)

5. Although everybody admits that the assumptions made by Black and Scholes in deriving their formula are violated in practice, it is still the Black-Scholes way of option pricing that is used almost everywhere in that same practice.
6. Private investors taking positions in options almost always face an unrealized positive return on their investment before turning it, as a result of their greed, into a real loss.
7. Since in reality options are quoted in tick sizes of five cents, increasing the accuracy of option prices up to, e.g., 10 digits is a non-issue.
8. Unfortunately the no-arbitrage axiom prevents the financial mathematician from getting almost surely infinitely rich.
9. The enormous amount of literature on calibration stresses the fact that the market is always right.

These propositions are considered defensible and as such have been approved by the supervisor prof.dr. F.M. Dekking.

# Stellingen

behorende bij het proefschrift

## Probabilistic methods in exotic option pricing

van Jasper Anderluh

1. Het berekenen van de prijs van een Parijse optie is een mooi voorbeeld van de toepassing van theoretische resultaten uit de kansrekening op het gebied van het prijzen van derivaten. (Hoofdstukken 2,3 en 4 van dit proefschrift).
2. Het volgende resultaat is een corollarium van de berekening van de Laplace getransformeerde van de dubbelzijdige Parijse stoptijd.  
De kans dat een standaard Brownse beweging  $W$  een excursie langer dan  $D_2$  boven nul maakt voordat er een excursie langer dan  $D_1$  onder nul heeft plaatsgevonden wordt gegeven door

$$\frac{\sqrt{D_1}}{\sqrt{D_1} + \sqrt{D_2}}.$$

(Hoofdstuk 3 van dit proefschrift).

3. In het algemeen geldt dat een vernieuwings-beloningsproces geen Lévy proces is.
4. De volgende stelling geldt voor een algemeen vernieuwings-beloningsproces en is vergelijkbaar met vergelijking (5.18) van dit proefschrift die afgeleid is uit een algemeen resultaat op het gebied van Lévy processen.  
Zij  $\{X(t), t \geq 0\}$  een vernieuwings-beloningsproces en  $\{(T_j, Y_j), j \geq 0\}$  het onafhankelijk gelijkverdeelde rijtje van paren van tussentijden en aangroeiingen met  $H$  de verdelingsfunctie van het paar  $(T_0, Y_0)$  en  $F$  de verdelingsfunctie van de tijd  $T_0$ . Dan geldt voor  $u, s > 0$  en  $\tau_h$  de eerste overschrijdingstijd van niveau  $h$  de volgende vergelijking

$$\int_0^\infty e^{-sh} \mathbb{E}(e^{-u\tau_h}) dh = \frac{\mathcal{L}_F(u) - \mathcal{L}_H(u, s)}{s(1 - \mathcal{L}_H(u, s))},$$

waar  $\mathcal{L}_F$  en  $\mathcal{L}_H$  de Laplace-Stieltjes getransformeerden van  $F$  en  $H$  zijn, gegeven door

$$\mathcal{L}_F(u) = \mathbb{E}(e^{-uT}) \quad \text{en} \quad \mathcal{L}_H(u, s) = \mathbb{E}(e^{-uT-sY})$$

voor alle  $u, s \geq 0$ . (J.A.M. van der Weide, J.H.M. Anderluh and M. Pandey, *Models for wear*, submitted paper.)

5. Hoewel iedereen het erover eens is dat de aannames van Black en Scholes niet gelden in de praktijk, is het met name de Black-Scholes manier van opties prijzen die bijna overal in diezelfde praktijk gebruikt wordt.
6. Particulieren die beleggen in opties hebben bijna altijd een ongerealiseerd positief rendement voordat ze, als gevolg van hebzucht, een daadwerkelijk verlies lijden.
7. Aangezien opties in de praktijk gesteld worden in stapjes van vijf cent is het opvoeren van de nauwkeurigheid van optieprijs berekeningen tot bijvoorbeeld 10 cijfers achter de komma volkomen zinloos.
8. Helaas weerhoudt het geen-arbitrage axioma de financieel wiskundige ervan om bijna zeker oneindig rijk te worden.
9. De grote hoeveelheid literatuur op het gebied van calibratie geeft nog eens aan dat de markt altijd gelijk heeft.

Deze stellingen worden verdedigbaar geacht en zijn als zodanig goedgekeurd door de promotor prof.dr. F.M. Dekking.